1993

Host And Viral Determinants Influencing The Pathogenesis Of Coronavirus-induced Neurological Disease In Rodents

John M. Pasick

HOST AND VIRAL DETERMINANTS INFLUENCING THE PATHOGENESIS OF CORONAVIRUS-INDUCED NEUROLOGIC DISEASE IN RODENTS

by

John M. M. Pasick

Department of Microbiology and Immunology

Submitted in partial fulfilment
of the requirements for the degree of
Doctor of Philosophy

Faculty of Graduate Studies
The University of Western Ontario
London, Ontario
November 1992

ISBN 0-315-81301-6

Abstract

Host and viral determinants influencing the outcome of coronavirus JHM infections of the CNS of rodents were investigated using intact animals and primary neural cell cultures. Two problems pertinent to the process of pathogenesis were addressed. The first was concerned with elucidating host factors responsible for controlling the age dependent nature for induction of the demyelinating form of disease in suckling rats. In the second, the basis of the relative resistance exhibited by inbred SJL/J mice to JHMV was examined in relation to both host and viral determinants.

Using primary, dissociated neural cultures from perinatal rats, several interesting aspects of host cell tropism having potential significance to the process of pathogenesis were found. Neurons were identified as important targets for both wt and neuroattenuated variants of JHMV. Moreover, immunofluorescent and electron microscopic analysis of infected neurons revealed that trafficking of viral structural proteins and virions occurs into neurites, consistent with the notion that transneuronal transport of virus takes place. Assessment of JHMV tropism for oligodendrocyte-type-2 astrocyte (O-2A) lineage cells, which are responsible for

myelin formation within the CNS, revealed some provocative findings. Culture conditions that maintained these cells in a mitotically active, migratory, progenitor state correlated with virus non-permissiveness. By contrast, culture conditions that encouraged O-2A differentiation into oligodendrocytes correlated with a semi-permissive state for JHMV. These data, combined with the previous finding that JHMV does not replicate in terminally differentiated oligodendrocytes, suggest that permissiveness of O-2A cells for JHMV is restricted to a 'window' in their development. This coincides in vivo with the second and third weeks of postnatal life, when induction of demyelinating disease by this agent is optimal.

Finally, whole animals and primary neural cultures, in combination with viral spike protein variants were used to analyze virus-cell and virus-host interactions in relationship to the observed resistance of SJL/J mice to JHMV. Based on these studies, it was concluded that SJL/J resistance to JHMV-induced neurologic disease may result from the combination of inefficient cell-to-cell spread of the infection and protection by the cellular immune response.

ACKNOWLEDGEMENTS

I would like to thank the many people who have made my stay at the University of Western Ontario both exciting and enjoyable. Foremost, to my advisor Dr. Samuel Dales, I wish to extend my gratitude for the confidence, guidance and exchange of ideas he has provided during the course of this endeavor. Special thanks are also extended to Sharon Wilton and Andrea Hanington of our laboratory, not only for their technical assistance, but also for their friendship. Many thanks also go out to the many people within the department with whom I've had the pleasure of sharing company with, both in and out of work.

Finally, appreciation is extended to my family. To my, as well as my wife's parents, for their understanding and confidence, but above all, to Sandra herself and my children Miranda and Miles for their patience and support.

TABLE OF CONTENTS

LIST OF FIGURES

LIST OF TABLES

ABREVIATIONS

>	anti-
bFGF	basic fibroblastic growth factor
BSA	bovine serum albumin
BW	body weight
C°	degrees Celcius
cDNA	complementary deoxyribose nucleic acid
Ci	Curie
cm	centimeter
CNPase	2':3''cyclic nucleotide-3"-phosphohydrolase
cpm	counts per minute
CsA	cyclosporin A
D.I.V.	days in vitro
$DMEM_{10}$	Dulbecco's modified Eagle medium supplemented with 10% fetal bovine serum
DNA	deoxyribose nucleic acid
E	embryonic day
ECM	extracellular matrix
EDTA	ethylenediaminetetraacetic acid
FBS	fetal bovine serum
g	grams
GC	galactosylcerebroside
GFAP	glial fibrillary acidic protein
HE	hemagglutinin esterase
ic	intracranial
IgG	immunoglobulin G
IGF-I	insulin-like growth factor type I
ip	intraperitoneal
kDa	kilodaltons
l	liter
M	molar
mM	milimolar
μM	micromolar
MAG	myelin associated glycoprotein
MBP	myelin basic protein
μCi	micro Curies
MHV	mouse hepatitis virus
ml	mililiter
m.o.i.	multiplicity of infection
N	nucleocapsid protein
NSE	neuron-specific enolase
O1/T3	oligodendrocyte serum-free medium supplemented with tri-iodothronine
O-2A	oligodendrocyte-type-2 astrocyte
P	postnatal day
PBS	phosphate buffered saline

PDGF	platelet derived growth factor
pfu	plaque forming unit
PLP	proteolipid protein
PTU	propylthiouracil
RNA	ribonucleic acid
rpm	revolutions per minute
S	spike glycoprotein
SSC	standard sodium citrate
T_3	tri-iodothyronine
T_4	tetra-iodothyronine or thyroxine
TCA	trichoracetic acid
v/v	volume per unit volume
wt	wild type
w/v	weight per unit volume

CHAPTER 1

GENERAL OVERVIEW

1.1 Introduction.

Todate many human diseases remain obscure with regard to their etiology and pathogenic mechanisms. This quandry has fostered a number of approaches for gaining insight into such diseases, of which animal models have played a dominant role. Mouse hepatitis virus (MHV)-induced neurologic disease in rodents is one such model. JHM, a neurotropic variant of MHV was originally isolated from the CNS tissues of a paralyzed mouse in the late 1940's (Bailey et al., 1949; Cheever et al., 1949). Since then, this coronavirus and its close relatives have been extensively used in the development of a model aimed at understanding the pathogenesis of various forms of neurologic disease in both mice and rats, with particular emphasis placed on demyelinating encephalomyelitis. Understanding the pathogenic mechanisms of demyelination in this paradigm, may ultimately provide us with greater insights into the potential mechanisms of demyelinating diseases of humans, particularly multiple sclerosis (MS).

The possible association between coronaviruses and human neurologic diseases still remains unresolved. Early reports described the isolation of coronaviruses from the brains of two MS patients (Burks et al., 1980) and the identification of coronavirus-like particles in the brain of one MS patient

(Tanaka et al., 1976). However, these have not received further confirmation. Studies conducted in the 1950's demonstrated that MHV-JHM (JHMV) was able to cross species barriers and produce panencephalitis in either *Rhesus* or *Cynomlogus* monkeys (Kersting and Pette, 1956). Murray et al. (1992b) have recently re-examined these findings and demonstrated that JHMV and SD, a murine-like coronavirus putatively recovered from the brain tissue of an MS patient (Burks et al., 1980), could replicate and disseminate in the CNS of old and new world monkeys with resultant production of demyelinating lesions. Even more provocative is a recent report describing the detection of murine-like coronavirus RNA and to a lesser extent antigen in MS brain tissue (Murray et al., 1992a). It is therefore not unreasonable to consider the possibility that CNS infections with MHV may induce neurologic disease in both natural and laboratory hosts by common pathogenic mechanisms, enhancing the overall relevance of this model.

The succeeding overview serves two purposes. The first is to highlight the ways in which others have contributed to our understanding of this model through approaches that have focused on its various perspectives. The second is to introduce information relevant to the concerns of the present study.

1.2 Coronavirus Structure and Assembly.

Virus particles assist in the efficient dissemination of

the viral genome. To accomplish this, virions are composed of a number of accessory molecules which serve not only to protect the viral genome from the external environment, but in most instances also participate in a number of supplementary functions including: progeny virion assembly and release, recognition and attachment to target cell membranes, penetration, uncoating and expression of viral genes. Coronavirions in general are spherical, enveloped particles, 80 to 160 nm in diameter possessing a nucleocapsid with helical symmetry and an envelope with prominent, club-shaped peplomers forming an outer halo or corona that is characteristically observed in negatively stained preparations (McIntosh, 1974). They possess a single-stranded non-segmented RNA genome of positive polarity bearing a 5' cap and a 3' poly-A tail. By far the most remarkable feature regarding the genome of this family of viruses is their large size; 31 kb for MHV (Lee et al., 1991) and 27.6 kb for infectious bronchitis virus (IBV) (Boursnell et al., 1987). MHV virions are composed of either three or four structural proteins depending on strain. Three of these are integral membrane glycoproteins associated with the viral envelope while the fourth is a basic phoshoprotein involved in formation of the nucleocapsid. The three proteins found in all strains of MHV have been designated N or nucleocapsid protein, M or integral membrane glycoprotein and S or spike glycoprotein. Sturman et al. (1980) reported that the ratio of these three proteins in MHV virions is 8 N: 16 M: 1 S. The fourth structural protein

which appears optional is the HE or hemagglutinin-esterase glycoprotein. Properties of all four structural proteins will now be discussed proceeding from the interior of the virion outwards.

The nucleocapsid protein N is a 50 to 60 kDa basic phosphoprotein that interacts with viral genomic RNA to form the helical nucleocapsid (Skinner and Siddell, 1983). However, investigations have suggested that apart from this structural role N may have additional functions, in particular possible involvement in viral RNA synthesis. Support for this comes from the observations that 1) N specific MAbs can inhibit the in vitro replication of MHV genomic RNA (Compton et al., 1987), 2) N specific MAbs can coimmunoprecipitate MHV genomic, negative-stranded and subgenomic mRNAs (Baric et al., 1988) and 3) N binds specifically to the 3' end of leader RNA (Stohlman et al., 1988a), the significance of which will become apparent when coronavirus transcription is discussed.

M is an integral membrane glycoprotein with a relative molecular weight of between 25 and 30 kDa. Sequence analysis of the M gene of MHV-A59 revealed three potential membrane-spanning domains (Armstrong et al., 1984). This, coupled with the protein's extreme resistance to proteolysis while in the context of the intact virion (Sturman and Holmes, 1977), suggests that most of it is in fact buried within the lipid envelope. Under certain conditions, M was found to have RNA binding activity (Sturman et al., 1980) thus allowing for the potential interaction with the ribonucleoprotein particle.

Perhaps more interesting is the observation that M accumulates in the perinuclear region of infected cells (Tooze et al., 1984) and thus appears to dictate where progeny virion assembly is focused. At this site, particles bud into small, smooth vesicles and tubules located between the rough endoplasmic reticulum (RER) and the Golgi apparatus (Tooze et al., 1984, 1988). Retention of M to the Golgi region has been attributed to an intrinsic property of the protein and more specifically with information encoded within the first transmembrane domain (Machamer and Rose, 1987). Subsequent virion maturation takes place during transit through the Golgi apparatus and release to the cell exterior occurs through membrane compartments involved in constitutive exocytosis (Tooze et al., 1987).

S or the major spike glycoprotein forms the characteristic club or petal-shaped surface projections of the virion. Each peplomer or spike is an oligomeric structure composed of two or three S molecules each in turn having a molecular weight of 180 kDa (Delmas and Laude, 1990). S is the dominant surface antigen of the virion and is consequently responsible for eliciting a neutralizing antibody response. In addition, it also participates in attachment of virions to target cells and cell-to-cell fusion and thus spread of the infection (Collins et al., 1982; Sturman et al., 1985). During the infectious cycle, the 180 kDa form of S predominates intracellularly (Frana et al., 1985). During the course of virion maturation but prior to release from infected cells, S

is cleaved by host cell proteases into two non-identical 90 kDa subunits (Frana et al., 1985; Sturman et al., 1985). This cleavage event was originally thought to be necessary for activating the syncytiogenic properties of the molecule but not for the infectivity of particles (Sturman et al., 1985). More recently it was found that fusogenic activity is not absolutely dependent on this proteolytic cleavage event (Stauber et al., in press). Nucleotide sequence comparison between the S of JHM (Schmidt et al., 1987) and A59 (Luytjes et al., 1987) strains of MHV revealed an overall homology of 93%. The S2 or carboxy terminal subunit which possesses a hydrophobic heptad repeat, presumed to be involved in the formation of a coiled-coil and hence an elongated stalk structure (deGroot et al., 1987) is 96% homologous between the two strains. The homology of the S1 or amino terminal subunit, which is believed to form the globular head of the peplomer, is somewhat less, only 89%. This may suggest that the S2 subunit is more critical to S function than the S1 subunit especially from the standpoint of host membrane fusion (Keck et al., 1988a).

A third, intermediate-sized membrane glycoprotein forming less prominent projections from the surface of some coronavirions is the hemagglutinin-esterase or HE. This component is consistently found in bovine coronavirus (BCV) while its presence is inconsistent among strains of MHV. Initial reports indicated that the HE of MHV possess an acetylesterase activity but lacks a hemagglutinin (HA)

(Yokomori et al., 1989). However, when expression of adequately high levels of HE occurs, as found in delayed brain tumor (DBT) cells infected by a vaccinia virus vector encoding HE, both a receptor-destroying (esterase) and receptor-binding (HA) activities were detectable (Pfleiderer et al., 1991). Of particular interest was the discovery that the MHV HE shares significant sequence homology with the hemagglutinin of influenza C virus (Luytjes et al., 1988). This led to the hypothesis that MHV may have acquired HE sequences from influenza C virus by a process involving non-homologous recombination. Sequence analysis has demonstrated that in most strains of MHV, HE is present as a pseudogene due to the absence of associated transcriptional and translational start signals (Shieh et al., 1989), arising from insertion and deletion mutations (Yokomori et al., 1991). In the JHM strain, variable expression of HE correlated with the number of copies of the UCUAA pentanucleotide present within the 3'-end of the leader RNA (Yokomori et al., 1991). Although these studies concluded that HE may only function as an accessory protein not essential for MHV replication, involvement of HE in JHMV-induced neuropathogenesis was suggested in a recent report (Yokomori et al., 1992).

1.3 Replication of Coronaviruses.

The MHV infectious cycle begins with a receptor-ligand interaction between S and receptor molecules present on target cells. Identification of the MHV receptor was made in studies

that compared JHM and A59 virus binding to solubilized membrane preparations derived from hepatocytes and enterocytes of susceptible BALB/c and resistant SJL/J mice in a so-called virus overlay protein blot assay (VOPBA). In susceptible BALB/c cell membranes virus bound to a glycoprotein with an apparent molecular weight of approximately 110 kDa but failed to bind membranes from resistant SJL/J cells (Boyle et al., 1987). However, immunoblot analysis with an antiserum raised against the amino terminal 15 residues of this protein demonstrated that hepatocyte and intestinal brush border membranes of resistant SJL/J mice expressed a protein related to the MHV receptor that was 5 to 10 kDa smaller (Williams et al., 1990). Therefore, SJL/J cells evidently do express a related glycoprotein lacking virus binding activity. Subsequent molecular cloning of this glycoprotein gene uncovered a relationship to the carcinoembryonic antigen (CEA) family of molecules which in turn belong to the immunoglobulin superfamily (Dveksler et al., 1991). The MHV receptor, which is closely related to CEA clone mmCGM1, is found abundantly expressed in cells of liver, small intestine and colon but is absent from the CNS (Williams et al., 1991). This finding implied that an alternative receptor(s) may be involved in cells of the CNS. Yokomori and Lai (1992) recently demonstrated the presence of a second molecule, mmCGM2, expressed in detectable amounts within the CNS and possibly related to mmCGM1 by alternative splicing as a functional receptor for MHV.

Following MHV attachment, the precise mechanisms involved in penetration and uncoating remain controversial. Early ultrastructural studies indicated that internalization involves receptor-mediated endocytosis as the prinicipal pathway of viral entry (David-Ferreira and Manaker, 1965). Subsequent biophysical studies have demonstrated that S-induced fusion between the virus envelope and cell membrane has a neutral to alkaline pH optimum (Sawicki and Sawicki, 1986; Sturman et al., 1990). This is in contrast with viruses known to enter target cells via the acidic endosomal compartment, among them influenza and vesicular stomatitis viruses which employ the acidic milieu of endosomes for activating the fusogenicity of their envelope glycoproteins. By comparison, MHV infections are only partially inhibited by lysosomotropic agents which elevate the pH of endosomes (Mizzen et al., 1985; Kooi et al., 1991). Furthermore, internalization of a fraction of the viral inoculum via the endocytic pathway by both permissive and non-permissive cells, did not necessarily lead to a productive infection (Kooi et al., 1991). On the other hand, Gallagher et al. (1991) have reported the isolation of variant viruses arising from persistently infected OBL21A neural cells which have an obligatory requirement for acid pH dependent fusion and are inhibited by lysosomotropic agents. Therefore, it is quite possible that depending upon the circumstances MHV may enter cells by direct fusion with the plasma membrane as well as endocytosis. This issue will be dealt with further in a later

chapter.

Following disassembly of the virion and release of genomic RNA into the cytoplasm, the synthetic phase of the infectious cycle commences. Coronavirus genomic RNA by itself is infectious following transfection into target cells (Lominiczi, 1977; Schochet an et al., 1977). Furthermore, several studies have demonstrated that MHV genomic RNA can be directly translated using rabbit reticulocyte lysates (Denison and Perlman, 1986; Soe et al., 1987). Figure 1.1 depicts the organization of the MHV genome. Gene 1, which is directly translated from genomic RNA, is 21 kb in length and consists of two open reading frames (ORF) which overlap one another by 75 nucleotides (Lee et al., 1991). Studies have suggested that a ribosomal frameshifting mechanism allows these two ORFs to be translated by a single initiation event (Lee et al., 1991). The principal function of the products of these two ORFs is to direct RNA-dependent RNA transcription and hence constitute the viral polymerase. Analyses of the translation of proximal ORF 1a and distal ORF 1b have indicated that the potentially large polyprotein precursor is in fact rapidly processed into lower molecular weight products (Denison et al., 1991; Denison et al., 1992). Evidence suggests that processing likely proceeds by an autocatalytic cis mechanism (Denison and Perlman, 1986 and 1987; Denison et al., 1991) although cellular transacting proteases may also be involved (Denison et al., 1992). Sequence analysis localized a protease like the 3C-polypeptide domain of picornaviruses and two papain-like

Figure 1.1. Genetic map of mouse hepatitis virus. The numbers above each gene are the mRNAs that have been identified in infected cells. Due to the 3'-coterminal structure of the mRNAs, gene 1 is found on a genomic length mRNA, while gene 7 is found on the smallest subgenomic mRNA. Genes 1 and 5 contain two ORFs each. Gene 1 which encodes nonstructural proteins including the RNA-dependent RNA polymerase accounts for approximately 2/3 of the genome. It contains two overlapping ORFs, 1a and 1b. The products of genes 4 and 5 have not been identified thus far. Abreviations: L, leader; HE, hemagglutinin esterase; S, spike glycoprotein; M, integral membrane glycoprotein; N, nucleocapsid protein. [Adapted from Lai, M.M.C. (1990) Coronavirus: organization, replication and expression of genome. Ann. Rev. Microbiol. 44:303-333.]

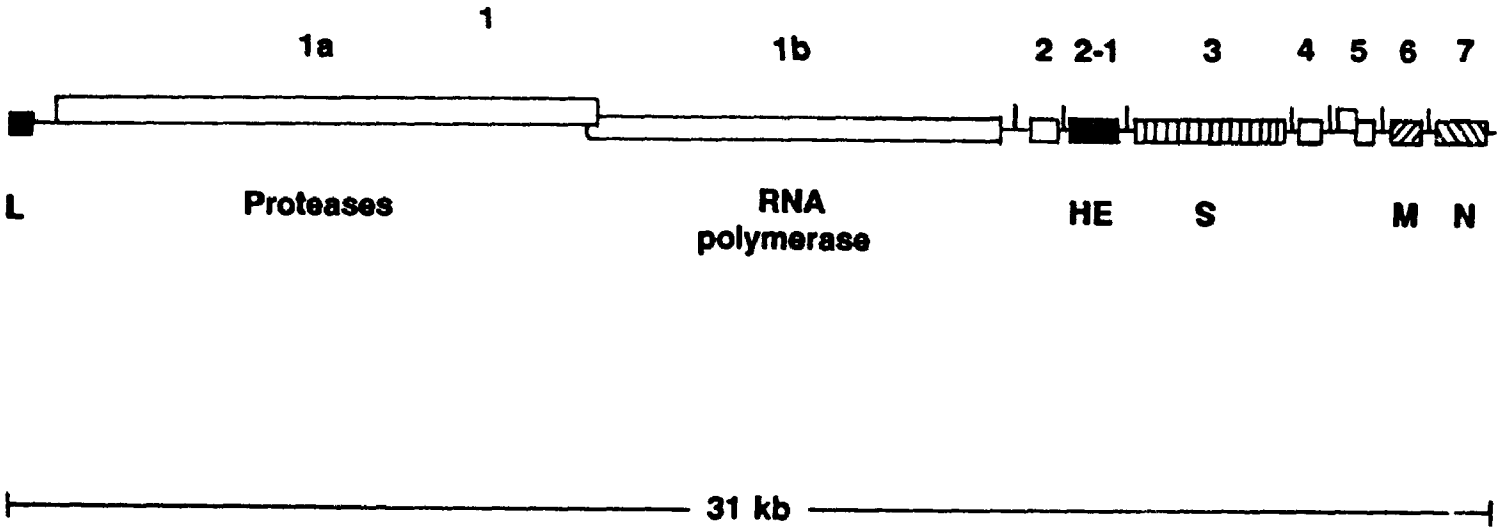

protease domains to ORF 1a, while ORF 1b was shown to contain polymerase, helicase and zinc-finger motifs (Lee et al., 1991). Synthesis and correct processing of the products of ORF's 1a and 1b are absolutely essential for virus growth since early inhibition of de novo protein synthesis (Sawicki and Sawicki, 1986) and proteolytic processing (Denison et al., in press) effectively block viral RNA synthesis.

In the presence of actinomycin-D which specifically inhibits DNA-dependent RNA transcription, synthesis of the 7 virus-specific mRNA species occurs. The largest among these is identical to the entire genomic RNA while the remaining 6 are subgenomic in size each being 3'-coterminal so as to constitute a nested set in which the sequence of each subgenomic mRNA represents a subset of the next largest member (Leibowitz et al., 1981). Only the 5' portion of each subgenomic mRNA which does not overlap sequences of the next smallest transcript is translated (Siddell, 1983); thus despite existing in a structurally polycistronic state, each mRNA is functionally monocistronic. Although details of the synthetic process by which full length and subgenomic mRNAs are transcribed from inoculum genomic RNA remain to be elucidated, the uniqueness of the process among RNA viruses is clear. Coronavirus subgenomic mRNAs were shown to possess a 72-nucleotide leader at their 5' ends (Lai et al., 1984). In view of the fact that this leader sequence is only encoded at the 5' end of genomic RNA and not within the intergenic sequences, it was postulated that a mechanism similar to

splicing, involved in the processing of nuclear mRNAs, was occurring during the transcription of viral subgenomic messages. Since coronaviruses replicate solely within the cytoplasm independent of any nuclear functions (Brayton et al., 1981) it was further hypothesized that this was under viral rather than host control. A number of key observations eventually led to the proposal that coronavirus transcription is leader-primed, discontinuous and non-processive. These included findings that 1) leader sequences could be found free in infected cells unassociated with viral mRNAs (Baric et al., 1985), 2) intergenic regions contain a common 11 nucleotide sequence which shares homology with the 3' end of leader RNA (Budzilowicz et al., 1985) and 3) during mixed infections different strains of MHV undergo recombination with one another at a relatively high frequency (Makino et al., 1986; Keck et al., 1988a and b). Minus strands which accumulate at around 3 hours postinoculation (Sawicki and Sawicki, 1986) would accordingly serve as the template for both genomic and subgenomic mRNA synthesis. However, recent evidence has strongly suggested that this is not the only mechanism for the generation of subgenomic mRNAs. In 1989, Sethna et al. reported that in transmissible gastroenteritis virus (TGEV) infected cells, genomic as well as subgenomic length minus strands could be found. Moreover, subgenomic minus strands were found in greater abundance than genomic length minus strands and were detected as double stranded replicative forms. Comparable observations were subsequently made for MHV

(Sawicki and Sawicki, 1990) and BCV (Hofmann et al., 1990). The above, along with the additional finding that all subgenomic minus strands contain a minus stranded version of the leader sequence (Sethna et al., 1991) inferred that subgenomic minus strands likely participate in the amplification of subgenomic mRNAs. This unique replication strategy was even suggested to contribute to the phenomenon of coronavirus persistence whereby subgenomic replicons could potentially behave as defective interfering RNAs (Sethna et al., 1989; Hofmann et al., 1990).

1.4 Clinical Presentation of Coronavirus-Induced Neurologic Disease in Rodents.

The clinicopathologic disease evoked by challenge with MHV is variable, reflecting the multifactorial nature of virus-host interactions involved. Challenge with virus can result in either acute encephalomyelitis, chronic panencephalitis, delayed onset demyelinating encephalomyelitis, recurrent demyelinating disease, or the total absence of disease (Weiner, 1973; Herndon et al., 1975; Nagishima et al., 1978; Sorensen et al., 1980; Stohlman and Weiner, 1981; Sorensen et al., 1982; Koga et al., 1984; Zimprich et al., 1991). The clinical signs of acute encephalitis usually develop within the first 10 days post-inoculation resulting in a rapidly fatal outcome. Affected animals initially present with hunched posture and ruffled hair coat progressing to bizzare behaviour, seizures, coma and

death. The demyelinating form of disease has a more delayed onset and chronic course. Clinical signs usually appear after 14 days post-inoculation and include para, tetra or hemiplegia progressing to a spastic paralysis and sometimes death. The outcome of viral challenge is dependent on the genotypes of virus and host, dose and route of inoculation, age of the host at the time of challenge and the host's immunologic status (Stohlman and Frelinger, 1978; Sorensen et al., 1980; Knobler et al., 1981b; Sorensen et al., 1982; Dalziel et al., 1986; Fleming et al., 1986; Perlman et al., 1987; Sorensen et al., 1987; Zimmer and Dales, 1989; Matsubara et al., 1991).

1.5 Pathology and Pathogenesis.

Understanding the pathogensis of CNS disease induced by neurotropic strains of MHV provides a formidable challenge. The reasons for this are threefold. Firstly, the mammalian brain is a complex environment for virus-cell interactions to take place within, especially from the standpoint of cellular diversity, architectonics and cell-cell interrelationships. Secondly, MHV possesses an RNA genome of 31 kb (Lee et al., 1991), the largest identified to date. Given the error-prone nature associated with RNA-dependent RNA polymerases and the rapid rate of evolution of RNA viruses in general (Steinhauer and Holland, 1987) as well as, more specifically, the high frequency with which MHV undergoes recombination during replication (Makino et al., 1986; Keck et al., 1988a and b), there is a high potential for generating variants having

altered tropism and/or virulence. Thirdly, both humoral and cellular immune responses against the virus can significantly influence the outcome of an infection. For instance, immunological selective pressures have the potential to enhance for the appearance of variants possessing altered neuropathological characteristics.

1.5.1 The CNS Environment and Neural Cell Tropism.

It has been estimated that the mammalian brain contains between 10^{11} to 10^{12} neurons which can be classified into as many as 10,000 different types based on morphologic, biochemical and biophysical criteria. In addition, there are an estimated 10 to 50 times more glial cells than neurons in the CNS, which can be broadly classified as either microglia or macroglia. Microglia are derived from blood monocytes that enter the brain during late embryonic and early postnatal periods and thus can be viewed as the resident macrophages of the brain (reviewed by Perry and Gordon, 1988). Macroglia which are of neuroectodermal origin, can be further subclassified as astrocytes or oligodendrocytes. Within each of these subclasses, evidence is accumulating for the existence of heterogeneity both in terms of developmental ancestry and unique biological properties. These various cell populations thus provide a range of potential targets for MHV to interact with, the outcome of which is dependent on each population's specific properties.

The central nervous system originates at the gastrulation

stage of embryonic development when highly integrated cell and tissue migrations result in the formation of the three germ layers - ectoderm, mesoderm and endoderm (Gilbert, 1988). At this stage the notochord, a specialized rod of mesodermal tissue, instructs the overlying ectoderm to execute the sequence of events involved in the formation of the neural tube. The latter process, referred to as neuralation, is followed by a series of regional morphogenic changes that result in the formation of the presumptive forebrain, midbrain, hindbrain and spinal cord. Within each of these specialized regions of the developing CNS, cells of the neuroepithelium proliferate and rearrange themselves. These kinetic events are accompanied by diversification of the neuroepithelial precursors generating the three major cell types found within the adult CNS. All of these events, which begin at around embryonic day 7 (E7) in the rat and continue postnatally, are precisely orchestrated to give rise to a highly ordered structure with an inconceivably complex degree of connectivity. This connectivity underlies normal CNS functions and can be classified into three major types: neuron-neuron mediated by synaptic connections resulting in the formation of neuronal networks, glia-glia mediated principally by gap junctions particularly among astrocytes and neuron-glia best exemplified by the compartmentalization of synapses by astrocytes and the formation of myelin sheaths around axons by oligodendrocytes. Hence, CNS histogenesis requires the coordination of proliferation, migration and

diversification of cells of the neuroepithelium.

The mechanisms involved in generating diversity from the germinal cells of the neural tube has been the focus of intensive efforts in recent years. From a conceptual point of view, this can arise by several means. One model proposes that diversity may be completely dependent upon the ancestry of specific precursor cells within the neuroepithelium, the products of which are strictly predetermined. A second model proposes that the fate of neuroepithelial precursors is not fixed but remain plastic and is influenced to a large extent by neighbouring cell-cell interactions. Evidence is accumulating that both cell intrinsic and cell extrinsic mechanisms are involved in the generation of neuroepithelial diversity.

The developmental potential of progenitor cells from embryonic rat cerebral cortices has been assessed both in vivo and in vitro. Price and Thurlow (1988) addressed this problem in vivo by infecting cerebral cortical progenitor cells of E16 rat fetuses with a replication-defective retrovirus carrying a reporter gene. The above phenotypic analysis of clones of cells expressing the reporter gene in adult animals led to the conclusion, now confirmed in vitro by Temple (1989), that two distinct types of progenitors populate the developing cortex at E16, one type giving rise to grey matter astrocytes and a second to both neurons and cells they tentatively identified as glia of the white matter. Temple (1989) manipulated single blast cells isolated from the septal region of E13.5 to E14.5

rat forebrain and determined the phenotype of the clones which arose from individual explanted cells. Seventy percent of the clones contained only neurons, 8% were non-neuronal and 22% contained mixtures of cell types. In a similar analysis, the majority of retrovirus-labelled precursor cells present in E16 dissociated rat cerebral cortical cultures generated clones of a single neural cell type, while 18% produced clones of mixed neuronal and oligodendrocytic phenotype (Williams et al., 1991). The above-mentioned studies thus raise questions as to the time and place within the developing CNS that neuronal and glial cell lineages diverge.

Precursor cells of the developing CNS arise from two germinal strata termed the ventricular and subventricular zones which occur in regions of the CNS possessing a laminated structure - such as the cerebrum, cerebellum and spinal cord (Figure 1.2). The ventricular zone is established first and is located at the luminal surface of the neural tube. It gives rise to all other layers including the subventricular zone by outward migration of its constituents. At a relatively early stage in development, the ventricular zone differentiates into the ependymal lining of the ventricles and central canal of the spinal cord. By contrast, cells of the subventricular zone remain mitotically active into postnatal life. Cortical neurogenesis in the rat occurs between E13 and E21 in the rat (Berry and Rogers, 1965). Neurons are thought to arise primarily from germinal cells residing within the ventricular zone. By comparison, cortical gliogenesis manifests a

Figure 1.2. Formation of mantle, intermediate and marginal zones of the cerebral cortex. Development progresses from left to right. The ventricular zone (V) contains mitotically active germinal cells which give rise to the neurons and glia that ultimately populate the other layers. Eventually some of the cells within this stratum undergo a terminal mitosis at which time they begin to migrate outward forming the intermediate (I) and marginal (M) zones. The intermediate zone contains differentiating neurons and glia that in turn give rise to the cortical plate (CP). The ventricular zone disappears early in development by differentiating into the ependymal layer (E) lining the ventricles. A second germinal stratum, referred to as the subventricular zone (S), arises from the ventricular zone and contains cells which remain mitotically active into the postnatal period. A similar histogenic pattern occurs for other laminated structures such as the cerebellum and spinal cord. [Adapted from Jacobson, M. (1978) Developmental Neurobiology (ed 2). New York, Plenum Press.]

Dalcq et al., 1982; Pasick and Dales, 1991). Though neuronal involvement generally decreases with time post-inoculation, neurons may nonetheless also participate in the pathogenesis of the more chronic demyelinating forms of disease as well. In support of this, in situ hybridization studies have demonstrated JHMV-specific RNA in hippocampal and cerebellar Purkinje neurons even during episodes of subacute, paralytic disease in Wistar Furth (WF) rats (Sorensen and Dales, 1985), suggesting that perhaps these neuronal populations may act as JHMV repositories during persistent infections. Others (Koga et al., 1984) have also observed that a clinically silent acute encephalitis precedes the appearance of subacute demyelinating encephalomyelitis. Hence, infection of neurons may be a necessary prerequisite for infection of glia, a hypothesis that has gained some support from studies conducted in vitro (Pasick and Dales, 1991). Furthermore, studies employing mice have demonstrated that JHMV as well as the less neurotropic MHV-A59 strain, utilize specific populations of neurons to invade and spread within the CNS (Lavi et al., 1988; Perlman et al., 1988, 1989, 1990). Following intranasal inoculation, both viruses spread in a temporally progressive manner to different CNS regions using well defined neuroanatomic tracts, especially olfactory, trigeminal and limbic pathways and their associated connections. This implies that virus may actually be transported interneuronally, a possibility that is examined further in this dissertation.

dichotomy with regard to the time of appearance and loci of differentiation into astrocytes and oligodendrocytes. There is convincing evidence that at least some of the CNS astrocytes of rodents originate from radial glia (LeVine and Goldman, 1988a; Misson et al., 1991) which are present commencing at the earliest stages of cortical histogenesis, coinciding with the first appearance of neurons. Early in development, the cell bodies of radial glia are confined to the ventricular zone and extend radially oriented, bipolar processes to the ventricular and pial surfaces (Misson et al., 1991). Late in gestation, the somata of these cells migrate outward and shift their location to the subventricular zone. As the cell bodies are translocated to more superficial layers of the cerebral wall, a transition from the elongated bipolar form to more process-bearing morphologies has been observed. The transformation to multi-polar forms becomes more accentuated with increasing age postnatally and is also accompanied by shifts in expression from vimentin to glial fibrillary acidic protein (GFAP) intermediate filaments (LeVine and Goldman, 1988a; Misson et al., 1991). These morphologic transformations also coincide with acquisition of new functional roles from initially providing a substrate for neuronal migration and axonal guidance, to those of trophic support for neurons, compartmentalization of synaptic connections and formation of the blood-brain barrier. Oligodendrocytes populating the cerebrum and cerebellum arise from the subventricular zone (Levine and Goldman, 1988a and b). Cells positive for the

ganglioside G_{D3} and carbonic anhydrase, an enzyme found prominently in oligodendrocytes, are already present within the subventricular zone of the forebrain in the rat at E16. They then migrate into the impending white matter beginning around the time of birth to the first weeks of postnatal life (Levine and Goldman, 1988a and b; Hardy and Reynolds, 1991). Thus, within the developing rat forebrain, the birth of neurons temporally precedes that of glia with some suggestion that their respective precursor cells may also be spatially partitioned to ventricular and subventricular zones respectively. Interestingly, the subventricular zone is retained into adult life (Privat and Leblond, 1972) although oligodendrocyte generation falls off dramatically after the third postnatal week in the rat (Levine and Goldman, 1988b).

Stemming from these observations a general question that one can ask regarding gliogenesis is: how many glial lineages within the developing CNS are there? Furthermore, does the pattern of gliogenesis for one region of the CNS, for example the spinal cord, apply equally to other regions such as the forebrain or optic nerve? Several reports using a variety of approaches on different regions of the developing CNS have suggested that oligodendrocyte and astrocyte lineages diverge during late embryonic and early postnatal periods (Raff et al., 1984; Levine and Goldman, 1988a; Vaysse and Goldman, 1990; Skoff and Knapp, 1991). Moreover, the complexity of the astrocytic lineage appears to vary from region to region within the developing CNS. This is reflected by the high

degree of phenotypic heterogeneity astrocytes possess on a regional basis for such characteristics as: expression of neurotransmitter receptors, prostaglandin synthesis and release and the ability to act as substrates for neurite outgrowth (reviewed by Wilkin et al., 1990).

In vitro studies on the gliogenesis of the rat optic nerve resulted in the identification of three populations of glial cells that were distinguished on the basis of lineage of origin and phenotype (Raff et al., 1983a and b, 1984; Raff, 1989 for review). Glial cells found in dissociated rat optic nerve cultures derived from two distinct, non-overlapping cell populations marked by the MAbs A2B5 and Ran-2 (Raff et al., 1984). The Ran-2$^+$/A2B5$^-$ population gave rise to type-1 astrocytes (Raff et al., 1983a) while the Ran-2$^-$/A2B5$^+$ population, referred to as oligodendrocyte-type-2 astrocyte (O-2A) progenitors gave rise to oligodendrocytes and type-2 astrocytes (Raff et al., 1983b). O-2A progenitors are bi-polar cells that express the surface polysialoganglioside G_{T3} (Dubois et al., 1990) recognized by the MAb A2B5 (Raff et al., 1983) and G_{D3} (Behar et al., 1988; LeVine and Goldman, 1988b; Vaysse and Goldman, 1990; Hardy and Reynolds, 1991). These cells contain vimentin but not GFAP intermediate filaments (Hardy and Reynolds, 1991), express the type A platelet-derived growth factor (PDGF) receptor (Hart et al., 1989b) and the substrate adhesion molecule cytotactin (Behar et al., 1988). Type-2 astrocytes were identified to play a possible role as perinodal astrocytes in the optic nerve. This observation,

coupled with the known function of oligodendrocytes in the formation of myelin sheaths, led ffrench-Constant and Raff (1986) to propose that cells of the O-2A lineage were specialized for CNS myelin formation. Equivalent progenitor cells were subsequently identified in the rat cerebellum (Levi et al., 1986, 1987), cerebral cortex (Behar et al., 1988; Hardy and Reynolds, 1991), brain stem (Dutly and Schwab, 1991) and spinal cord (Warf et al., 1991). Equivalence of these progenitors isolated from the above mentioned regions has been arrived at on the basis of similarities of morphology, antigenic profile, progression through their developmental pathway and response to culture conditions.

The relatively simple model invoking two types of astrocytes originally described for the rat optic nerve should be contrasted with the more complex situation recently documented for the rat forebrain (Goldman and Vaysse, 1991; Vassye and Goldman, 1992) and spinal cord (Miller and Szigeti, 1991; Fok-Seang and Miller, 1992). Astrocyte heterogeneity in these latter two regions was determined using a technique in which a retrovirus introduced marker allowed subsequent clonal identification and analysis. Based on such studies, astrocytes in the forebrain appear to originate from three or more progenitor cell types (Goldman and Vaysse, 1991; Vaysse and Goldman, 1992). Most of the established clones were morphologically and antigenically similar to type-1 astrocytes of the optic nerve, although it should be noted that this astrocyte population is probably not phenotypically

homogeneous (Lerea and McCarthy, 1989). Fewer clones were bipotential, giving rise to oligodendrocytes and GFAP$^+$ cells having a process-bearing morphology (Behar et al., 1988; Lillien et al., 1988; Vaysse and Goldman, 1990) like those of type-2 astrocytes of the optic nerve. The third lineage, comprising just under one percent of the total cell population in rat forebrain cultures, appears to be separable from both the type-1 astrocyte and O-2A lineages. These cells are GFAP$^+$/GD3$^+$/A2B5$^{+/-}$, possessing a highly spread and flat morphology with fine processes (Vaysse and Goldman, 1992). Astrocytic cell types within the rat spinal cord appear even more diverse than those in the forebrain as elucidated by single-cell and retrovirus mediated clonal analysis (Miller and Szigeti, 1991). This study identified six morphologically distinctive classes of glial clones, among which was one that was apparently equivalent to the bipotential O-2A progenitor cell population of the optic nerve and forebrain and five which were all GFAP$^+$. Only 6% of the retrovirus-marked clones contained cells with mixed morphologies suggesting that at least some of these morphologic classes may share common precursors. Curiously, one of these precursors possessed antigenic and migratory properties similar to those of bipotential O-2A progenitors but was distinct from these glial precursors by giving rise to astrocytes exclusively (Fok-Seang and Miller, 1992). The functions of these apparently diverse classes of astrocytes in the optic nerve, forebrain and spinal cord remain largely unknown at present. Within the optic

nerve, type-1 astrocytes have been reported to be part of the glial limiting membrane and the blood-brain barrier, while type-2 astrocytes have been implicated to function as perinodal astrocytes (Raff, 1989). Other functions of astrocytes include: phagocytosis (Al-Ali et al., 1988), buffering of the extracellular environment, production of growth factors (Araujo and Cotman, 1992); Gomez-Pinilla et al., 1992; Raff et al., 1988; Richardson et al., 1988; Woodward et al., 1992; Yoshida and Gage, 1991) and antigen presentation to effector cells of the immune response (Fontana et al., 1984). Presently it is not known whether all astrocyte types are capable of performing these diverse functions or whether some functions are specific to some subclasses.

Concerning the diversity of neural cell origin and function in relation to JHMV tropism, data from both in vivo and in vitro studies have provided a confusing and sometimes inconsistent picture. In general, JHMV appears to demonstrate tropism for most classes of cells of neuroectodermal origin including neurons, glia and ependymal cells. However, closer scrutinity has revealed that tropism for these classes of cells may not be absolute but conditionally dependent on various host factors. During episodes of acute encephalomyelitis, neurons have been identified as important targets (Knobler et al., 1981a; Buchmeier et al., 1984; Parham et al., 1986; Matsubara et al., 1991; Zimprich et al., 1991), an observation that has been supported by in vitro studies using primary neural cultures (Knobler et al., 1981b; Dubois-

Dalcq et al., 1982; Pasick and Dales, 1991). Though neuronal involvement generally decreases with time post-inoculation, neurons may nonetheless also participate in the pathogenesis of the more chronic demyelinating forms of disease as well. In support of this, in situ hybridization studies have demonstrated JHMV-specific RNA in hippocampal and cerebellar Purkinje neurons even during episodes of subacute, paralytic disease in Wistar Furth (WF) rats (Sorensen and Dales, 1985), suggesting that perhaps these neuronal populations may act as JHMV repositories during persistent infections. Others (Koga et al., 1984) have also observed that a clinically silent acute encephalitis precedes the appearance of subacute demyelinating encephalomyelitis. Hence, infection of neurons may be a necessary prerequisite for infection of glia, a hypothesis that has gained some support from studies conducted in vitro (Pasick and Dales, 1991). Furthermore, studies employing mice have demonstrated that JHMV as well as the less neurotropic MHV-A59 strain, utilize specific populations of neurons to invade and spread within the CNS (Lavi et al., 1988; Perlman et al., 1988, 1989, 1990). Following intranasal inoculation, both viruses spread in a temporally progressive manner to different CNS regions using well defined neuroanatomic tracts, especially olfactory, trigeminal and limbic pathways and their associated connections. This implies that virus may actually be transported interneuronally, a possibility that is examined further in this dissertation.

The delayed onset, chronic demyelinating form of disease in mice and rats is associated with viral persistence within white matter. Early work by Lampert et al. (1973) led to the conclusion that JHMV-induced demyelination in weanling Swiss-Webster mice may be the direct result of viral tropism for oligodendrocytes, a contention supported by studies using primary mouse and rat glial cultures (Beushausen and Dales, 1985; Wilson et al., 1986; Lavi et al., 1987; Pasick and Dales, 1991). In vivo and in vitro studies have also demonstrated the importance of astrocytes as targets for JHMV and MHV-A59 (Massa et al., 1986; Wilson et al., 1986; Lavi et al., 1987; Perlman and Ries, 1987; Pasick and Dales, 1991; Zimprich et al., 1991). Despite this apparently simplistic tropism of these viruses for macroglia, productive infection of both cell types is far from being unconditional. In this regard, Lavi et al. (1987) reported that even at high moi, only 10% of oligodendrocytes and 30% of astrocytes expressed viral antigens following inoculation of C57BL/6 glial cultures with MHV-A59. Beushausen and Dales (1985) had previously demonstrated that cultures enriched for flat, fibroblastic-like astrocytes present in dissociated mixed glial cultures derived from rat cerebral cortices were non-permissive hosts for JHMV. In contrast, others (Massa et al., 1986,1988) have demonstrated that brain derived rat astrocytes in culture are important targets for JHMV. In addition, astrocytes have also been identified as targets for JHMV in vivo (Zimprich et al., 1991). Thus, these discrepancies regarding astrocytic tropism

will require further clarification if we are to better understand the role in neuropathogenesis. Productive infection of oligodendrocytes also appears complicated depending intimately upon their stage of differentiation (Beushausen and Dales, 1985; Wilson et al., 1986; Beushausen et al., 1987; Pasick and Dales, 1991). In both rat and mouse oligodendrocyte-enriched cultures, JHMV replication was found to be irreversibly suppressed as a consequence of pharmacological treatments which induced the elevation of intracellular cAMP levels. Prior work by McMorris (1983) had demonstrated that the cAMP second messenger system plays an important role in the differentiation of rat oligodendrocyte precursors. Productive infection appeared to be arrested at an early stage in the infectious cycle, subsequent to virus attachment and penetration but prior to the expression of viral genes (Beushausen et al., 1987). It was hypothesized that an intermediate step, perhaps involving uncoating was being restricted which was supported by data demonstrating that the processing of the phosphorylated form of N was inhibited in differentiated oligodendrocytes. It was further hypothesized that this control by host over glial tropism may also operate in vivo and could potentially explain the age-dependent nature of induction of the demyelinating form of neurologic disease which had been documented earlier in rats (Sorensen et al., 1980, 1982). Thus, control of postnatal myelination may also be important for the development of JHMV-induced demyelinating lesions.

Two additional questions pertaining to the subject of tropism that have thus far remained incompletely resolved are: 1) does demyelination arise by direct cytolytic effects of the virus on oligodendrocytes, or are immune-mediated phenomena also involved and 2) what receptors are utilized by the virus to initiate the infectious cycle in the various classes of neural cells? To address the first question, cytopathic effects induced by MHV on glial cell populations appear to a certain extent virus strain dependent. For instance, though MHV-A59 produces non-cytolytic, non-syncytiogenic, persistent infections in mouse primary glial cultures (Lavi et al., 1987), while JHMV produces both syncytia and cytolysis (Wilson et al., 1986; Pasick et al., 1992), both viruses nevertheless induce demyelination in mice. The demyelinating form of neurologic disease has been associated with viruses possessing reduced neurovirulence and cytopathogenicity which is believed important in the establishment of persistent infections. However, the distinction between cytopathic and non-cytopathic viral strains or variants is complicated by the fact that this parameter to a large degree may be host cell dependent (Lavi et al., 1987; Massa et al., 1988). Two reports dealing with the hypothesis that JHMV-induced demyelination in mice (Wang et al., 1990) and rats (Watanabe et al., 1983) is immunologically mediated will be dealt with in a later section. In addressing the second question, two MHV receptors, mmCGM1 and mmCGM2, as outlined in section 1.3 have been identified thus far. Only the latter is expressed within the

mouse CNS (Yokomori and Lai, 1992) but the fine distribution of this protein is not yet known. The situation in rats remains even less well defined since the rat homologue of mmCGM1, an ecto-ATPase is not a functional receptor for MHV-A59 (Holmes et al., in press).

1.5.2 Viral Determinants of Pathogenesis.

Variants of JHMV and MHV-4 have provided a powerful means of identifying and analyzing viral molecular determinants associated with neurovirulence and pathogenesis. In this regard, the S peplomer, involved in attachment, syncytiogenesis and elicitation of a neutralizing antibody response (Collins et al., 1982), plays an unquestionable role. Several independently isolated variants of JHMV and MHV-4 possessing alterations involving S have been characterized. These have either been selected based on resistance to neutralization with monoclonal antibodies, or have arisen spontaneously from diseased animals or infected primary neural cultures. A partial list of important viral variants along with their molecular and biological characteristics is provided in Table 1.1.

Three topographically distinct, antigenic sites have been identified on the S peplomer protein of MHV-4 using a panel of monoclonal antibodies (MAb) (Talbot et al., 1984). Two of these sites elicited protective responses in mice in passive transfer experiments, while the third did not, in spite of mediating an in vitro virus neutralizing response.

Table 1.1

Molecular and Neuropathological Properties of JHMV/MHV-4 Variants

Variant	Basis of selection	Molecular characterization	Neuropathological properties	References
ATllf cord	spinal cord of WF rat with demyelinating encephalo-myelitis	441 nucleotide deletion in hypervariable region of S1 segment 738 nucleotide deletion in the HE gene	Neuroattenuated: Induces subacute demyelinating disease	Morris et al., 1989 La Monica et al., 1991
V5A13.1	neutralization resistance to S MAb	426 nucleotide deletion in S1 involving nucleotides 1298 to 1723	Neuroattenuated. Increased LD_{50}. Demyelination associated with moderate inflammatory cell infiltration. Apparent loss of neuronal tropism.	Dalziel et al., 1986 Parker et al., 1989 Gallagher et al., 1990
V4B11.3	"	447 nucleotide deletion in S1 involving nucleotides 1285 to 1761		
2.2-V-1	neutralization resistance to MAb 2.2	single point mutation at nucleotide 3340 in S2 segment of spike protein	Neuroattenuated: Induces subacute demyelinating disease	Fleming et al., 1986 Fleming et al., 1987 Wang et al., 1992
7.2-V-1	neutralization resistance to MAb 7.2	two point mutations at nucleotides 1766 and 1950 in S1 segment of spike protein	Retains encephalitogenic potential	"
2.2/7.2-V-2	double neutralization resistance	deletion spanning nucleotides 1523 to 1624 in S1 hypervariable region, plus point mutation at nucleotide 3340 in S2 segment	Neuroattenuated for both encephalitic and demyelinating potential	"

Variant	Basis of selection	Molecular characterization	Neuropathological properties	References
cl-2	brain of Lewis rat with acute encephalitis	15 kDa enlargement of spike protein	Enhanced neurovirulence with widespread neuronal and glial involvement in weanling Lewis rats	Taguchi et al., 1985 Matsubara et al., 1991
CNVS	isolated from cultured rat neural cells	similar enlargement of spike protein as found in cl-2	Enhanced tropism astrocytes in vitro, enhanced neurovirulence in vivo	Taguchi et al., 1976 Matsubara et al., 1991
N3	chemical mutagenesis ts mutant	RNA negative	Neuronal infection without encephalitis; Induces meningitis and demyelination	Robb et al., 1979
ts8	"	--	Neuroattenuated. Acute demyelinating disease without associated inflammatory infiltrates	Haspel et al., 1978 Knobler et al., 1982

Additionally, protection against lethal viral challenge was associated with decreased viral replication and spread of infection to neurons but not glia (Buchmeier et al., 1984). Variant viruses that had escaped neutralization with MAbs specific against two of these distinct topographical sites on S were attenuated in their neurovirulence producing subclinical demyelinating lesions rather than acute encephalitis (Dalziel et al., 1986). Multiple passaging of MHV-4 through murine delayed brain tumor (DBT) cells in the continuous presence of MAbs against either of the two antigenic sites gave rise to variants that were equally resistant to both MAbs (Dalziel et al., 1986; Gallagher et al., 1990). Molecular characterization of these variants revealed large deletions of 142 to 159 amino acids localized within the middle one-third of the S1 or amino-terminal cleavage product (Parker et al., 1989). This region of the S gene was subsequently shown to be hypervariable and subject to deletion mutations (Banner et al., 1990). These S deletion variants could be selectively amplified in cell lines sensitive to virus-induced cell fusion, a phenomenon attributed to delayed killing of the host cell (Gallagher et al., 1990). This decrease in cytopathogenicity was suggested to be the basis of their in vivo neuroattenuation. Attenuation of neurovirulence could in turn result in the sparing of critical targets within the host, particularly neurons, thereby allowing for the establishment of less pathogenic, persistent infections within alternative targets, such as

glia. It was further suggested that the pathology associated with variant virus infection of glia may be slow in onset and due to a gradual upset in cellular metabolism or be immune-mediated in nature rather than to direct cytolytic effects of the virus.

Others have used similar approaches to select for variant viruses and found comparable alterations in biological activity, but mapped changes to different sites along the S molecule. One neuroattenuated variant still capable of producing demyelinating encephalomyelitis possessed only a single point mutation within the S2 fragment, while a second variant that retained its encephalitogenic potential possessed two point mutations within the S1 fragment. A double mutant attenuated in both encephalitic and demyelinating potentials contained a point mutation within S2 plus a deletion spanning the hypervariable region of S1 (Fleming et al., 1986, 1987; Wang et al., 1992a). These studies concluded that the role of S in inducing demyelinating lesions is not due to the property of a single, unique site, but more likely to the interaction of several sites along the molecule (Wang et al., 1992a). A variant bearing a truncated S protein has also been isolated from the spinal cord of a Wistar Furth rat with demyelinating encephalomyelitis (Morris et al., 1988). It was shown to possess a large deletion involving the hypervariable region within S1, in addition to a deletion effectively knocking out the coding region of HE (La Monica et al., 1991). An obvious question that arises concerning these variants is: does the

development of viral persistence in white matter with the accompanying production of demyelinating lesions depend upon the evolution of variants during the course of an infection? This is still an unresolved issue, although Perlman et al. (1990) have reported that generation of variants was not necessary for the development of demyelinating disease in C57BL/6 mice.

In contrast to the neuroattenuated variants possessing deletions in S1 outlined above, Taguchi et al. (1985) isolated and characterized a JHMV variant from the brain of a rat undergoing acute encephalitis that possessed an S protein 15 kD larger than wt. Viruses with similar though not identical enlargements of S were also isolated from wt JHMV inoculated primary rat neural cultures (Taguchi et al., 1986). The tissue culture variant appeared to grow more selectively in primary rat astrocytes than did wt JHMV or the rat brain derived variant. The size of S was subsequently shown to play an important role in the neuropathogenic process in rats as well. Two large S protein viral variants were highly neurovirulent in weanling Lewis rats, producing widespread infections of neuronal and glial cells (Matsubara et al., 1991). Infections involved the hippocampus and cerebral cortex at 3 dpi, spreading to involve the cerebellum, pons and spinal cord in the following 3 to 10 days. In contrast, two other variants with large S proteins were of low virulence, while variants with small S proteins were avirulent.

Lastly, a number of temperature sensitive (ts) mutants of

JHMV and MHV-4 have been isolated that generally induce chronic demyelination when inoculated into animals. Mutant ts 8 for instance produces a high incidence of demyelinating disease in mice (Haspel et al., 1978), which has been attributed to its preferred tropism for oligodendrocytes in the absence of an inflammatory cell reaction (Knobler et al., 1982). Attenuation in neurovirulence however, is not always associated with concomitant changes in tropism as is evident with ts mutant N3 which still infects neurons without evoking encephalitic disease (Robb et al., 1979b). Wege et al. (1984) isolated a number of ts mutants of JHMV that produced demyelinating lesions in rats associated with mononuclear cell infiltrates. Though infectious virus was rarely recovered from these animals, the presence of a defective virus was alluded to by the ability of tissue homogenates to induce giant cell formation in a susceptible cell line. One of these mutants, ts43, could induce persistent infections of rat glial cultures characterized by the predominant involvement of astrocytes, reduced cytopathogenicity and attenuated spread (Massa et al., 1988). This altered behaviour was however glial cell specific, since ts43 and wt JHMV had similar growth curves and produced equivalent cytopathic effects when grown on susceptible Sac(-) cells. This again stresses the point that the biological properties of a variant can to some extent be host cell dependent, thus making relevance to the process of pathogenesis difficult to interpret.

1.5.3 Host Immune Response and Pathogenesis.

Both humoral and cellular immune responses have been implicated in modulating the outcome of MHV CNS infections. Passive immunization of mice with MAbs specific for any of the three viral envelope glycoproteins protects animals from acute lethal encephalitis but not the delayed demyelinating form of disease. In this regard, Fleming et al. (1989) proposed that any variable allowing animals to survive the initial encephalitis permits the subsequent development of demyelinating disease. In fact, the manifestation of the subacute demyelinating phase of disease may actually be contingent upon survival through the acute encephalitic phase with its associated neuronal involvement.

Passive immunization of BALB/c mice with MAbs specific against the S peplomer of MHV-4 is associated with a significant lowering of viral brain titers and accompanying interference of infection involving neurons but not oligodendrocytes (Buchmeier et al., 1984). The mechanism of this apparent antibody-mediated shift in tropism has been difficult to explain. Two possibilities include: the use of different domains on the S peplomer to infect the two cell populations, or the selection of neutralization resistant variants with altered tropism and/or neurovirulence. Similar results have been obtained using non-neutralizing MAbs directed against the HE glycoprotein (Yokomori et al., 1992). The suggestion was made that non-neutralizing antibodies may reduce virus growth within the brain by complement-mediated

cytolysis or antibody-dependent cell-mediated cytotoxicity. The latter mechanism is indirectly supported by the enhanced mononuclear cell infiltration observed in mice passively immunized with MAb against HE (Yokomori et al., 1992). Both neutralizing and non-neutralizing MAbs against the matrix protein M have also been reported to passively protect mice against acute encephalitis. Moreover, protection is not mechanistically dependent on a functional complement system (Fleming et al., 1989). The observed rapid rise in titre of high affinity, neutralizing IgG antibodies in the cerebrospinal fluid of JHMV infected Brown Norway rats (Schwender et al., 1991) which correlates with the resistant phenotype of this strain, further signifies the protective importance of the humoral immune response. Finally, enhanced numbers of B cells and plasma cells, as well as IgG and complement depostions have recently been documented in Lewis rats with JHMV-induced demyelinating lesions (Zimprich et al., 1991), indicating a possible role for antibody mediated cytotoxicity in lesion development. Of relevance to this was the intriguing observation that in the chronic demyelinating form of disease, S expression in infected astrocytes and oligodendrocytes appeared down-regulated as compared to the levels observed during acute disease. Parallel studies using Lewis rat glial cultures also showed that antibodies against S helped to promote establishment of persistent infections (Wege et al., 1990).

During the acute phase of JHMV infection of the murine

CNS, the T cell response appears to play an important role in halting disease progression and mediating viral clearance. Adoptively-transferred, JHMV-specific $CD4^+$, $Lyt\text{-}2^-$ T cell clones protected C57BL/6 mice from lethal, acute encephalitis by a class II MHC restricted, DTH response (Stohlman et al., 1986, 1988b). More interestingly, protection from the lethal effects of the virus was not associated with a significant reduction in viral brain titers. Moreover, these animals subsequently went on to develop demyelinating lesions and disease. Circulating levels of antiviral antibodies were not altered in DTH-inducer T cell recipients which led to the conclusion that protection was not the result of increased local synthesis of antiviral antibodies within the CNS. However, since intrathecal levels of viral specific antibodies were not measured directly, this conclusion remains uncertain. As with passive transfer of antibody, adoptive transfer of these clones also appeared to confer protection by altering virus growth within neurons (Stohlman et al., 1986).

Clearance of JHMV from the CNS is mediated by both $CD4^+$ and $CD8^+$ T cell phenotypes (Sussman et al., 1989; Williamson and Stohlman, 1990; Williamson et al., 1991; Yamaguchi et al., 1991). Protection by the adoptive transfer of nylon wool adherent $CD4^+$, $Lyt\text{-}2^-$ T cells from syngeneic, JHMV immunized mice, was associated with reduced virus replication, prevention of lethal encephalitis but not demyelination and was shown by indirect means to be mediated by $CD8^+$ T cells (Sussman et al., 1989). Though a cytotoxic T lymphocyte (CTL)

response is the implied mechanism of viral clearance, their characterization is only now being addressed. Mobley et al. (1992) were unable to identify significant CTL responses to N, M, S or p28 proteins in C57BL/6 mice, although good $CD4^+$, T helper 1 responses were elicited. Stohlman et al. (1992) have however been able to identify a CTL response to a peptide contained within the carboxy-terminal end of N in BALB/c mice. The foregoing adoptive transfer experiments have been complemented by studies using athymic nude rats and agents directed at suppressing the cellular immune response which have demonstrated an increased involvement of grey matter relative to control animals (Sorensen et al., 1982, 1987; Zimmer and Dales, 1989; Pasick et al., 1992).

Lastly, consideration must be given to whether the cellular immune response initiated by the virus may actually contribute to the production of demyelinating lesions. Support for this contention is both implicit and explicit. MHV-A59 infection of murine CNS and mixed glial cultures results in the expression of MHC class I molecules on oligodendrocytes and astrocytes, thereby allowing their participation in cell-mediated immune responses (Suzumura et al., 1986). This phenomenon required viable virus for its initiation, was found to be mediated by a heat- and trypsin-sensitive soluble factor elaborated from infected glia, most likely astrocytes (Suzumura et al., 1988) and was dependent on the continued production of virus for its maintenance (Lavi et al., 1989). Watanabe et al. (1983) reported that EAE-like lesions could be

induced in Lewis rats by adoptively transfering T cells from syngeneic animals with coronavirus-induced demyelinating encephalomyelitis. Lymphocytes from these diseased animals could be stimulated *in vitro* by exposure to myelin basic protein, an interesting finding in light of a more recent report indicating that MHV-4 increased the frequency of self-reactive, IL-2 secreting T cells (Kyuwa *et al.*, 1991). Finally, Wang *et al.* (1990) have demonstrated that JHMV-induced demyelination in C57BL/6 mice may have an immunologically mediated component. Animals inoculated with the neuroattenuated variant 2.2-V-1 (Fleming *et al.*, 1986) (see Table 1.1) and then immunosuppressed by whole body gamma irradiation at 6 dpi, developed significantly less severe demyelinating disease than controls. The reduction in severity of disease was apparently not due to the inhibition of virus growth. In fact, virus brain titers were higher and viral positive oligodendrocytes more prevalent in irradiated animals. Furthermore, transfer of T cell-enriched populations from both naive and virus inoculated donors restored disease in the irradiated recipients.

1.6 Objectives of the Present Study.

This thesis examines several aspects of JHMV-induced neuropathogenesis in rodents. One of the working hypotheses of this laboratory has been that the pathogenesis of the demyelinating form of disease, particularly in rats, is significantly influenced by the process of postnatal

myelination. In this regard, particular emphasis has been placed on further characterizing the interrelationships between determinants controlling the differentiation of cells of the oligodendrocyte-type-2 astrocyte lineage and hence CNS myelination, and permissiveness for JHMV. Virus-neuronal interactions have also been studied, especially with respect to the trafficking and/or assembly of viral structural proteins. The aim of these studies was to assess whether virus has the potential to spread interneuronally. Finally, viral variants possessing deletions within the spike glycoprotein have been used to further examine whether the basis of resistance by the inbred SJL/J strain of mouse is due to an absolute inability to establish infections with MHV or to limited spread of the infection once it has been established. In addition, the reported neuroattenuation of these variants will be analyzed with respect to possible shifts in their neural cell tropism. The results of these studies will demonstrate that the determinants influencing the outcome of CNS infections with neurotropic strains of MHV are both complex and interactive.

CHAPTER 2

JHMV NEURAL CELL TROPISM IN VITRO: INFLUENCE OF CELL INTRINSIC AND EXTRINSIC DETERMINANTS

3.1 Introduction.

Studies originally conducted by Sorensen et al. (1980, 1982) showed that the induction of demyelinating disease by JHMV in rats, was intimately dependent on the age when animals were infected. The incidence of demyelinating encephalomyelitis is highest in animals inoculated during the second and third weeks of postnatal life, coinciding with a period when myelination is also maximal. This age association still applied even when the influence of the maturing immune response was taken into consideration (Sorensen et al., 1987; Zimmer and Dales, 1989). On the basis of these characteristics, our working hypothesis has been that the state of myelination may play an important role in the pathogenesis of JHMV-induced demyelinating disease in rats.

Myelination in rodents can be influenced by many factors, among them the thyroid hormone status during the early postnatal period (see appendix for a more thorough treatment of this subject). Initial studies aimed at addressing the potential influence of thyroid hormones on the susceptibility of rats to JHMV-induced demyelinating disease were inconclusive (see appendix). This prompted the use of an alternative approach to address the possibility that

developmental determinant(s) associated with the process of myelination might be involved in regulating the apparent period of susceptibility or 'window' for induction of demyelinating disease in rats. Thus, studies were begun using primary dissociated neural cultures.

Previous studies employing cultures secondarily enriched for specific forebrain-derived macroglia demonstrated that rat cells of the lineage giving rise to oligodendrocytes could act as conditionally permissive targets for JHMV whereas type-1 astrocytes could not (Beushausen and Dales, 1985). Such specificity in glial cell tropism by JHMV was not found among murine cells (Wilson et al., 1986). Additionally, several observations indicated that the state of differentiation of rat-derived oligodendrocytes may be an important means by which the host can control virus replication within white matter, thus potentially influencing the development of demyelinating disease (Beushausen and Dales, 1985; Beushausen et al., 1987). These observations lent further support to the notion that the overlap between the periods for optimal induction of demyelinating encephalomyelitis and myelination were not merely coincidental.

Several laboratories have employed in vitro model systems to study myelinogenesis, with emphasis placed on determinants controlling the differentiation of the oligodendrocyte-type-2 astrocyte (O-2A) lineage, specialized for myelinating the CNS (ffrench-Constant and Raff, 1986). Although our understanding of this process is far from complete, the emerging picture

suggests that interactions with heterotypic cell types play an important role. Myelinogenesis has been arbitrarily divided into two phases: 1) the proliferation of oligodendrocyte precursors and 2) the synthesis of myelin sheaths by post-mitotic oligodendrocytes (Figure 2.1). Molecules that are particularly significant in mediating these events are polypeptide growth factors or cytokines. Cytokines are now generally recognized as mediators of intercellular communication important in tissue modelling, whether this occurs during normal development or unscheduled events such as wound repair. In fact, the overall process of CNS histogenesis appears to be dependent on an interacting network of cytokines whose effects are controlled temporally, spatially and contextually.

Cells with the potential to differentiate into either oligodendrocytes or astrocytes were first identified in dissociated rat optic nerve cultures by Raff et al. (1983b). These bipotential glial precursors accordingly referred to as oligodendrocyte-type-2 astrocyte (O-2A) progenitors were subsequently identified in the rat cerebellum (Levi et al., 1986; Levi et al., 1987), cerebral cortex (Behar et al., 1988; Hardy and Reynolds, 1991), brain stem (Dutly and Schwab, 1991) and spinal cord (Warf et al., 1991). Thus, the same precursor appears to give rise to oligodendrocytes in these different CNS regions.

Raff et al. (1985) originally found that when O-2A progenitors isolated from E17 rat optic nerve were cultured on

Figure 2.1. Scheme for the regulation of rat oligodendrocyte development in vitro. The current knowledge of the stages as well as factors thought to regulate the development of oligodendrocytes in vitro, are diagramatically summarized. The pathway here, is shown to begin at the mitotically active, bipotential, O-2A progenitor cell stage that in turn derives from a more immature cell found within the subventricular zone. O-2A progenitors proliferate and migrate in response to specific growth factors produced by other cells within the CNS. As development progresses, changes take place in their morphologic complexity, expression of various antigenic markers and proliferative responses to growth factors. Factors influencing progression through the pathway are listed along with whether their effects are positive (+) or negative (-). Determinants controlling differentiation along the type-2 astrocytic pathway are also shown. Abreviations: bFGF, basic fibroblastic growth factor; PDGF, platelet derived growth factor; GC, galactosylcerebroside; GFAP, glial fibrillary acidic protein; IGF-I, insulin-like growth factor type I; N-CAM, neural cell adhesion molecule; CNP, 2':3' cyclic nucleotide-3'-phosphohydrolase; MBP, myelin basic protein; MAG, myelin associated glycoprotein; PLP, proteolipid protein; CNTF, ciliary neuronotrophic factor. A2B5 and O4 are MAbs which recognize specific glycolipids.

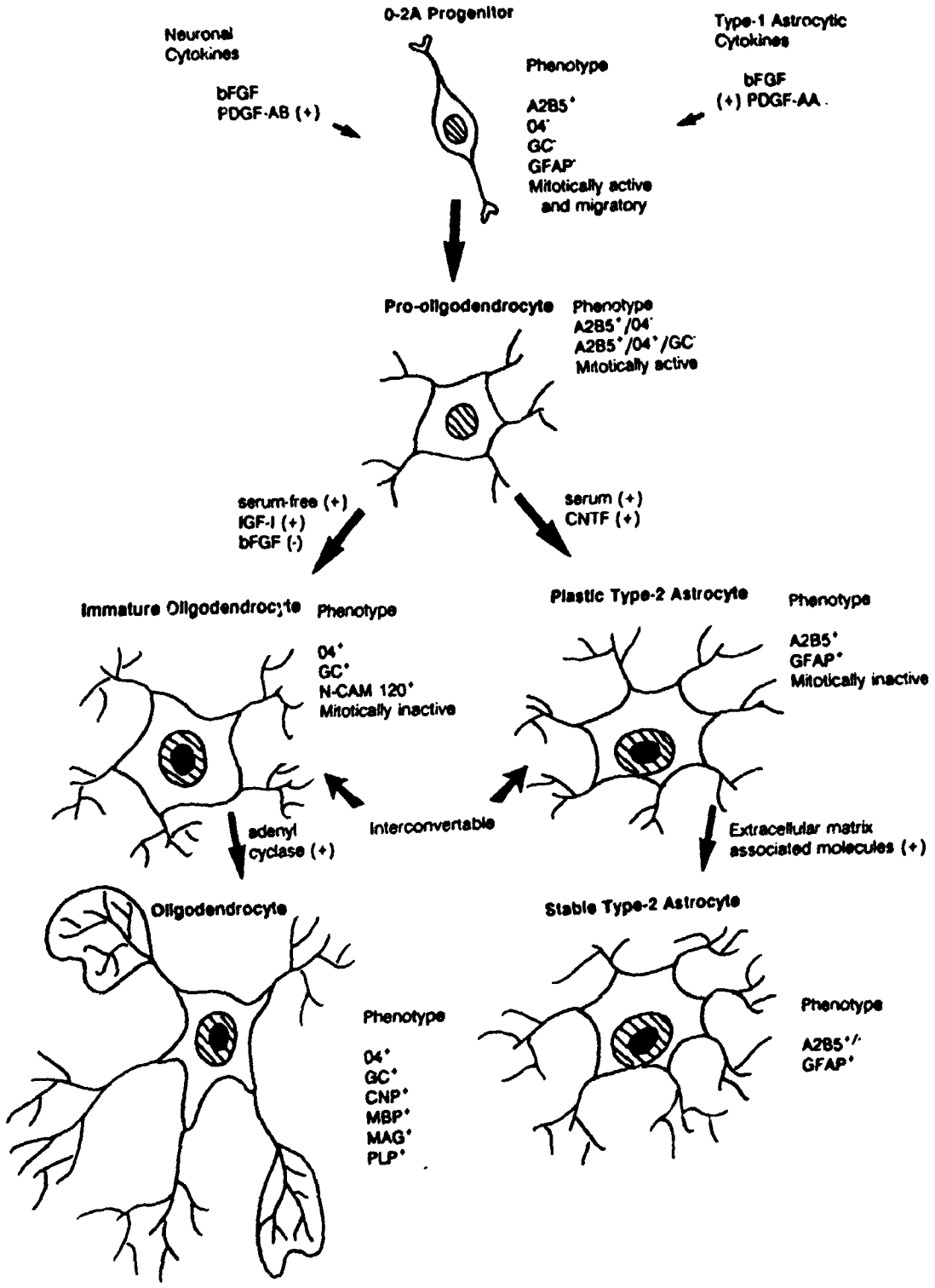
O-2A Progenitor
Neuronal Cytokines
bFGF
PDGF-AB (+)
Phenotype
A2B5+
04-
GC-
GFAP-
Mitotically active and migratory
Type-1 Astrocytic Cytokines
bFGF
(+) PDGF-AA
Pro-oligodendrocyte
Phenotype
A2B5+/04-
A2B5+/04+/GC-
Mitotically active
serum-free (+)
IGF-I (+)
bFGF (-)
serum (+)
CNTF (+)
Immature Oligodendrocyte
Phenotype
04+
GC+
N-CAM 120+
Mitotically inactive
Plastic Type-2 Astrocyte
Phenotype
A2B5+
GFAP+
Mitotically inactive
adenyl cyclase (+)
Interconvertable
Extracellular matrix associated molecules (+)
Oligodendrocyte
Phenotype
04+
GC+
CNP+
MBP+
MAG+
PLP+
Stable Type-2 Astrocyte
Phenotype
A2B5+/-
GFAP+

their own on a poly-L-lysine coated substratum in a serum-free, chemically-defined culture medium, most of the cells stopped dividing after 2 days and prematurely differentiated into oligodendrocytes. However, culturing the E17 O-2A progenitors on type-1 astrocyte monolayers prevented this from happening, providing the first evidence of the importance of cell-cell interactions in controlling O-2A differentiation. One of the molecules responsible for the observed mitogenic influence of type-1 astrocytes on O-2A progenitors was found to be platelet-derived growth factor (PDGF). The evidence for this association included: purified type-1 astrocyte cultures contain mRNA for PDGF A-chains (Richardson et al., 1988), anti-PDGF antibodies inhibit the mitogenic effect of astrocyte conditioned medium (ACM) on O-2A progenitors (Richardson et al., 1988; Noble et al., 1988) and gel filtration of ACM revealed that the fraction with mitogenic activity was the same as that containing radiolabelled PDGF (Richardson et al., 1988). More recently, neurons throughout the rodent CNS have also been shown to express the A-chain (Yeh et al., 1991) as well as the B-chain (Sasahara et al., 1991) of PDGF. In fact, A-chain expression in vivo was documented to be stronger and less variable in neurons than astrocytes (Yeh et al., 1991). Moreover, the mitogenic effect of sensory neuron conditioned medium (rat dorsal root ganglia) on the proliferation of brain stem derived O-2A progenitors was capable of being blocked completely by antibodies against PDGF (Dutly and Schwab, 1991). Studies by Hart et al. (1989b) demonstrated that O-2A

progenitors express type-A-like PDGF receptors which are capable of binding all three types of PDGF dimers (AA, AB and BB) giving further support for the direct effects of this growth factor on these cells. However, just as interesting, O-2A progenitors were shown not to divide indefinitely in the presence of type-1 astrocytes or PDGF, but rather, divided a restricted number of times before clonally related progeny synchronously became differentiated into oligodendrocytes (Temple and Raff, 1986). Furthermore, the number of cell divisions which the progeny of a particular clone underwent prior to differentiating into oligodendrocytes varied greatly. In other words, individual clones of O-2A progenitors are independently asynchronous with one another with respect to when they cease dividing and differentiate into oligodendrocytes, a finding that has been substantiated by others using retrovirus-mediated clonal analysis (Goldman and Vaysse, 1991).

In an attempt to address the intrinsic mechansims responsible for O-2A progenitor differentiation into oligodendrocytes while in the presence of PDGF, Hart et al. (1989a and b) examined PDGF receptor expression on newly formed oligodendrocytes and the effects its ligand had on intracellular signalling pathways. They found that in rat optic nerve cultures established at P0 and grown for 24 hours in a low but mitogenic concentration of PDGF, 47% ± 4 of the newly formed oligodendrocytes still bound ^{125}I-PDGF, however this dropped to 12% ± 1 after a further 48 hours in culture.

Moreover, oligodendrocytes identified on the basis of galactosylcerebroside (GC) expression did not incorporate bromodeoxyuridine (BrdU) upon exposure to the growth factor, suggesting that PDGF does not induce mitosis in these cells. PDGF was concomitantly found to induce an increase in cytosolic Ca^{++} levels in both O-2A progenitors and newly formed oligodendrocytes. Curiously, though the combination of the Ca^{++} ionophore A23187 and the phorbol ester PDB (which activates protein kinase C) was capable of stimulating DNA synthesis in O-2A progenitors and thus mimicing the effects of PDGF, similar responses were not elicited in newly formed oligodendrocytes (Hart et al., 1989a). These data led to the conclusion that O-2A progenitors become unresponsive to the mitotic effects of PDGF not because of a loss of receptors but because the signal transduction pathway becomes uncoupled at some stage distal to the receptor.

The role of PDGF and its receptor in controlling O-2A progenitor cell proliferation and differentiation has since recently become even more complicated. Two reports demonstrated the synergistic interaction between PDGF and basic fibroblastic growth factor (bFGF) in inhibiting differentiation and hence extending the proliferative capacity of O-2A progenitors (Bolger et al., 1990; McKinnon et al., 1990). McKinnon et al. (1990) likewise described the ability of bFGF to maintain high levels of type-A PDGF receptor expression on cerebral cortical O-2A progenitors, in contrast to the more differentiated stages which were associated with

lower levels of expression. This appeared to be in contradiction to the report by Hart et al. (1989a) where non-responsiveness of newly formed optic nerve oligodendrocytes did not appear to be associated with the down regulation of PDGF receptors. A recent study by Reddy and Pleasure (1992) examined the expression of PDGF A and B chains as well as type-A and -B PDGF receptors in the developing rat brain. No developmentally related changes in expression of either PDGF A or B chains were observed. In contrast however, the steady state mRNA levels encoding both forms of receptor were found to be higher at embryonic and early postnatal times than in later life, suggesting that the responsiveness to PDGF in vivo may be controlled by the level of receptor expression.

Both astrocytes and neurons have been documented as the source of bFGF within the CNS (Ferrara et al., 1988; Hatten et al., 1988; Sato et al., 1989; Torelli et al., 1990; Gomez-Pinilla et al., 1992; Woodward et al., 1992). The most recent reports (Gomez-Pinilla et al., 1992; Woodward et al., 1992) indicate however that astrocytes are likely the most prominent source of bFGF both in vivo and in vitro. bFGF distribution in neurons was found to be restricted to specific populations including: cells within the CA2 subfield of the hippocampus, the deep cerebellar nuclei, the motor and spinal subdivisions of the trigeminal and facial nerve nuclei and Purkinje neurons. Of potential importance is the existence of another 18 kDa, heparin-binding, growth-associated protein immunologically distinct from bFGF, that is expressed in rat

brain during the early postnatal growth period (Rauvala, 1989). This protein, which has been localized to neurons, reaches peak levels of expression by the the end of the first postnatal week and decreases thereafter (Rauvala, 1989). Subsequent molecular cloning of this protein (Merenmies and Rauvala, 1990) led to the demonstration that mRNA levels exhibited the same developmental kinetics as the protein. Sequence analysis revealed however that in contrast to bFGF, a signal sequence precedes the coding region of the mature molecule and that homology exists with retinoic acid-induced differentiation factor rather than bFGF (Merenmies and Rauvala, 1990). At present it is not known whether this protein plays any role in O-2A differentiation and hence CNS myelinogenesis.

The second developmental pathway of the O-2A lineage cells is that which gives rise to type-2 astrocytes. Fetal calf serum was originally shown to induce the differentiation of O-2A progenitors into type-2 astrocytes (Raff et al., 1983b). However, the factors in fetal calf serum involved in this process remain unknown. More recently, induction of type-2 astrocyte differentiation was shown to be also contingent on cell-cell interactions perhaps those related to control of development. In cultures of rat brain grown in the absence of serum, GC^+ oligodendrocytes appeared during the first week, whereas type-2 astrocytes became identifiable only during the second week (Lillien et al., 1988). The stimulus responsible for the timely appearance of type-2 astrocytes originated from

older cultures of purified type-1 astrocytes, fractionated at around 20 kDa on a gel filtration column and possessed ciliary neurotrophic factor (CNTF)-like activity. Furthermore, purified CNTF can induce premature type-2 astrocyte development in dissociated brain cultures lending credence to its involvement in this process (Lillien et al., 1988). However, CNTF by itself is incapable of promoting differentiation into a stable type-2 astrocyte phenotype, suggesting that other factors are required, which, indeed was found to be the case. One of these signals is PDGF; however, its role appeared to be principally an indirect one and involved in maintaining an undifferentiated O-2A progenitor pool capable of responding to the temporally dependent appearance of type-2 astrocyte-inducing signals (Lillien and Raff, 1990). The other signals with more direct involvement, were found to be molecules associated with the extracellular matrix (ECM) elaborated by mesenchymal cells (Lillien et al., 1990). In fact, the induction of a stable, type-2 astrocytic phenotype appeared to involve the collaborative interactions between CNTF and ECM-derived signals. Furthermore, in the absence of CNTF, the ECM-associated molecules inhibited the differentiation of O-2A progenitors along the oligodendrocytic pathway, but could not by themselves induce type-2 astrocyte differentiation (Lillien et al., 1990).

Data in this chapter pertain to the relationship between glial cell differentiation and permissiveness for JHMV. By these results I will demonstrate that culture conditions and

cell-cell interactions controlling the survival, proliferation, and differentiation of specific cell populations in rat telencephalic cultures, can influence the establishment of JHMV infections.

2.2 Materials and Methods.

2.2.1 Continuous Cells Lines.

L-2 mouse fibroblasts (Rothfells et al., 1959) were used for propagating virus stocks as well as for plaque assaying virus from inoculated neural cell cultures, as described previously (Lucas et al., 1978). The OBL21 neuronal cell line obtained from Constance Cepko of Harvard Medical School was clonally derived from CD.1 mouse olfactory bulb cultures immortalized with a replication-defective retrovirus vector carrying the avian myc gene (Ryder et al., 1990). It was routinely grown in medium DMEM supplemented with 10% (v/v) fetal bovine serum (FBS), 15 mM hepes pH 7.3 and 10 μg/ml gentamycin.

2.2.2 Viruses.

Murine hepatitis virus strain JHM originally obtained from the ATCC and the Indiana strain of vesicular stomatitis virus (VSV) were propagated and titered on murine L-2 fibroblasts as described previously by Beushausen and Dales (1985). Briefly, subconfluent L-2 monolayers grown at 37°C in Eagle's MEM (GIBCO) supplemented with 10% FBS, 100 units/ml

penicillin and 100 μg/ml streptomycin were inoculated with JHMV at a multiplicity of infection (m.o.i.) of 0.1 plaque forming unit (pfu) of virus per cell. After adsorption for 1 hour, unadsorbed virus was washed away and fresh medium added. Harvesting of membrane-associated virus was carried out 12 to 18 hours later, when virtually the entire monlayer of cells became fused into a syncytium, but cell lift off was less than 50%, by scraping the cells into the culture supernatant. The suspended cells were ruptured and fragmented by passage through 21, 26 and 30 gauge needles, thereby releasing the cell-associated virus. The lysate formed was centrifuged at 2000 x g for 20 minutes at 4°C to remove larger cellular particulates and aliquots of the clarified supernatant dispensed into tubes and stored at -70°C.

Isotopically labelled JHMV was produced following the general outline of Wilson and Dales (1988). Briefly, L-2 cultures inoculated with JHMV at an m.o.i. of 0.1 pfu/ml were incubated with $DMEM_{10}$ containing 5 μCi/ml of [5,6-^{3}H]uridine (ICN Biochemicals, Inc; 44 Ci/mmole). At 12 hours postinoculation, when 100% of the cell monolayer had been incorporated into syncytia but before the occurrence of significant cell lifting, the culture supernatant was harvested for concentration of cell-free extracellular virus. Cell debris was removed from the culture supernatant by centrifuging at 2000 rpm for 30 minutes in a Sorval RT 6000 centrifuge. The virus was then pelleted by centrifuging at 22,000 rpm for 60 minutes in a SW28 rotor. The pelleted virus

was resuspended in $DMEM_{10}$ then concentrated by centrifugation at 22,000 rpm for 60 minutes through a 20% sucrose cushion. The final virus pellet was resuspended in a small volume of $DMEM_{10}$ then stored at -70°C. This procedure generally resulted in a 10 fold concentration of cell-free virus based on titer analysis.

2.2.3 Virus Titration.

Virus titers were determined according to Lucas et al. (1978). Briefly, serial 10 fold dilutions of stock virus preparation were inoculated onto L-2 monolayers situated in either 6 or 12 well cluster dishes. An inoculum volume of 100 and 200 l was used per well in the 6 and 12 cluster well dish respectively. Adsorption was carried out for 1 hour at room temperature with continuous rocking. Cells were then overlayed with FBS supplemented MEM containing 0.5% carboxymethylcellulose and incubated for 24 hours at 37°C. The monolayers were fixed 24 hours later with a 10% formaldehyde solution, then stained with a 0.1% crystal violet solution before counting plaques.

2.2.4 Mixed Telencephalic Cultures from Neonatal Rats.

Neonatal Wistar Furth (WF) rat pups were used at least within 12 hours of birth and in most cases within 6 hours of birth for the preparation of primary dissociated telencephalic cultures. For the purpose of age assessing the cultures, this time interval was referred to as postnatal day 0 (P0). After

carefully dissecting the meninges from the surface of the cerebral hemispheres, the telencephalon was placed into ice-cold DMEM supplemented with 10% (v/v) fetal bovine serum, 15 mM hepes, and 10 μg/ml gentamycin ($DMEM_{10}$). The telencephala were then washed 3 times with cold $DMEM_{10}$ and any adherent meninges carefully removed. The tissue was minced with scalpel blades into fine pieces and washed once with cold Ca^{++} and Mg^{++} free phosphate buffered saline (PBS) pH 7.2, before digesting with 1x trypsin/EDTA (Sigma) at 37°C for 15 to 20 minutes with intermittent swirling. The tissue was washed 3 times with cold $DMEM_{10}$ and triturated gently using fire-polished Pasteur pipettes in the presence of 20 μg DNase I (Sigma) in a volume of 5 to 7 ml. The resulting cell suspension was passed by gravity through 130 and 33 m pore size nylon meshes (Nitex). The resulting filtrate was then layered over 5 ml of cold fetal bovine serum in a 15 ml conical centrifuge tube (Corning) and centrifuged at 200xg for 8 minutes. The cell pellet was resuspended in $DMEM_{10}$ and viable cell count determined based on trypan blue exclusion. The cell suspension was seeded onto either 12 mm diameter glass coverslips or 35 mm plastic petri dishes (Nunc, Roskilde, Denmark) pretreated with poly-L-lysine (Sigma) at 5 to 10 $\mu g/cm^2$. The seeding density ranged from 2.5×10^5 to 5.0×10^5 viable cells per cm^2. All cultures were grown in $DMEM_{10}$ for the first 3 days *in vitro* (D.I.V.). At this time some of the cultures were switched to a serum-free, chemically defined medium first described by Bottenstein (1986). Briefly, this medium

consisted of DMEM supplemented with 1.2 g/l $NaHCO_3$, 15 mM hepes pH 7.3, 5 µg/ml bovine insulin (Sigma), 50 µg/ml human transferrin (Sigma), 30 nM sodium selenite (Sigma), 10 ng/ml d-biotin (Sigma), and modified to include 30 nM tri-iodothyronine (Sigma), and is referred to as O1/T3. The remainder of the cultures were maintained in $DMEM_{10}$. Medium changes in either serum containing or serum-free conditions were made every 3 days, thereafter.

2.2.5 Secondary Glial Cultures Enriched for either O-2A Lineage Cells or Type-1 Astrocytes.

Enriched glial cultures of either type-1 astrocytes or cells belonging to the oligodendrocyte-type-2 astrocyte lineage (O-2A) were prepared following the outline described by McCarthy and de Vellis (1980). Briefly, complete medium changes of mixed glial cultures grown in $DMEM_{10}$ were made at 4, 6 and 8 D.I.V. At 8 to 10 D.I.V. the cultures, consisting predominantly of a bedlayer of type-1 astrocytes and top dwelling cells of the O-2A lineage at varying stages of differentiation, were washed 3 times with warm Ca^{++} and Mg^{++} free PBS pH 7.2 followed by addition of fresh $DMEM_{10}$. Cultures were placed on a rotary shaker for 15 to 30 minutes at 120 rpm to free the dead cells. The loosely attached, top dwelling O-2A lineage cells were then released into either Ca^{++} and Mg^{++} free PBS or enzyme free cell dissociation solution (Sigma) by sharply tapping the sides of the flask. The resulting cell suspension was pelleted by centrifuging at 200xg for 5

minutes, resuspended and cells deposited in 24 well dishes (Nunc) or 12 mm diameter glass coverslips at densities ranging from 1.25 x 10^5 to 3.0 x 10^5 cell per cm^2 in $DMEM_{10}$. Twenty-four hours later, the $DMEM_{10}$ was carefully removed and replaced with test medium for 48 to 72 hours followed by inoculation with virus. In some experiments process-bearing, O-2A lineage cells were shaken from mixed cultures at 5 D.I.V. instead of 8 to 10 D.I.V. This was done to enrich the percentage of cells that were still in the progenitor state. Where indicated, 10 ng/ml recombinant human basic fibroblastic growth factor (bFGF) and/or the A-B heterodimeric form of recombinant human platelet derived growth factor (PDGF), both obtained from Upstate Biotechnology Inc., Lake Placid, New York, were added to medium O1/T3 at 36 hour intervals.

Secondary cultures enriched for type-1 astrocytes were prepared from the mixed glial cultures as described by McCarthy and de Vellis (1980). After releasing any residual cells of the O-2A lineage by means of vigorous shaking, the remaining astrocyte bedlayer was passaged by lifting from the plasticware using 1x trypsin/EDTA (Sigma). Astrocytes were seeded onto poly-L-lysine coated 35 mm petri dishes and grown in either $DMEM_{10}$ or chemically defined medium O1/T3.

2.2.6 Conditioned Media Production.

Conditioned medium was prepared by exposure of chemically defined medium O1/T3 to either mixed telencephalic cultures (P3 to P12) or 75% confluent, enriched type-1 astrocyte

cultures. After washing the residual serum from cultures, 25 ml of O1/T3 was added to each 150 cm^2 culture vessel and then collected following 72 hours of conditioning. The medium was centrifuged at 2,000 rpm for 10 minutes at 0°C in a Sorval RT 6000 tabletop centrifuge to remove any cellular debris and then divided into aliquots and immediately stored in polypropylene tubes (Corning) at -70°C.

2.2.7 Inoculation of Neural Cultures and Assaying Infectivity.

Mixed, primary telencephalic cultures grown in 35 mm petri dishes were inoculated with JHMV in a volume of 350 µl at m.o.i.'s of ~ 1. Mixed, telencephalic cultures grown on 12 mm diameter glass coverslips were inoculated at m.o.i.'s ~ 5 in a 90 µl volume. The virus was adsorbed for 1 hour at 37°C in a humidified atmosphere with 5% CO_2, unbound inoculum was removed and cultures were washed twice with warm PBS before reconstituting with medium. Secondary cultures of type-1 astrocytes were grown in 35 mm petri dishes and inoculated with JHMV at m.o.i.'s from 1 to 50. Adsorption and washing of inoculum was the same as described for mixed, telencephalic cultures. Secondary O-2A lineage cultures grown in either 24 well dishes or on 12 mm diameter glass coverslips were inoculated as above with JHMV at m.o.i.'s of ~ 1 in 100 µl. The medium in all neural cultures was changed daily during the initial 48 hours post-inoculation and every second day thereafter.

2.2.8 Immunostaining of Neural Cultures.

Monoclonal antibody (MAb) A2B5 (ATCC) which recognizes the ganglioside G_{T3} (Dubois et al., 1990) present on the surface of O-2A progenitor cells (Raff et al., 1983b), type-2 astrocytes (Raff et al., 1983b), and neurons (Eisenbarth et al., 1979) was used as ascites fluid at a dilution of 1:4. MAb O4 (Sommer and Schachner, 1981) which recognizes sulfatide (Bansal et al., 1989) first expressed on the surface of cells that are transitional intermediates between O-2A progenitors and oligodendrocytes (Sommer and Schachner, 1982; Sommer and Noble, 1986) was used as tissue culture supernatant at 1:2. Rabbit> galactosyl cerebroside (GC), and rabbit antiserum to guinea pig myelin basic protein (MBP), employed previously (Beushausen and Dales, 1985) were used at 1:10 and 1:40 respectively. MAb against the 160kDa neurofilament polypeptide (Amersham) in the form of tissue culture supernatant was diluted 1:5, rabbit antibodies against rat neuron specific enolase (NSE) (Polysciences, Inc., Warrington, PA.) were at 1:900, MAb 4B6.2 specific for JHMV nucleocapsid (N) protein (a generous gift from Dr. M.J. Buchmeier, Scripps Clinic and Research Foundation) in the form of tissue culture supernatant was diluted 1:2, and rabbit antibodies against bovine glial fibrillary acidic protein (GFAP) (Dakopatts, Denmark) was used at 1:40. Primary antibodies were diluted in PBS pH 7.2 containing 3% (w/v) bovine serum albumin. The fluorochrome-conjugated secondary antibodies were used at the following dilutions, in PBS: Goat> mouse IgG-FITC (Sigma) 1:30, Goat>

mouse IgM(μ-chain specific)-FITC (Sigma) 1:30, Goat> rabbit(H and L chains)-RITC 1:40 (Cappel Laboratories), and Goat> rabbit(H and L chains)-Texas Red (Jackson Immunoresearch Laboratories) 1:50. Primary and secondary antibodies were applied at room temperature in a humidified atmosphere for 25 to 35 minutes. Staining for surface antigens was carried out on living cells. For labelling both surface and internal antigens, cells on coverslips were fixed with 4% paraformaldehyde in PBS for 5 minutes at room temperature, after completion of surface labelling reactions. Cells were then permeabilized in acid ethanol (5% glacial acetic acid/95% ethanol, v/v) for 10 minutes at -20°C, washed in PBS and again immunolabelled followed by post-fixation in 4% paraformaldehyde in PBS.

2.2.9 Electron Microscopy of Monolayer Cultures.

JHMV infected and uninfected mixed telencephalic cultures situated in 35 mm petri dishes were prepared for electron microscopy as previously described (Dales and Hanafusa, 1972). Briefly, cultures were washed with 0.1 M sodium phosphate buffer, pH 7.0 and then fixed *in situ* for 5 minutes with 1% glutaraldehyde in 0.1 M sodium phosphate buffer (v/v). Following fixation and 3 washes with 0.1 M sodium phosphate buffer, cells were post-fixed with 1% OsO_4 in 0.1 M sodium phosphate (v/v) buffer, dehydrated using a series of graded ethanol solutions and embedded in epoxy resin. Sections were cut both horizontally and vertically to the plane of the

attachment surface. After staining with uranyl acetate followed by lead citrate, specimens were viewed in a Philips EM 300 electron microscope.

2.2.10 Immune-Mediated Lysis of Selected Cell Populations in Infected Mixed Cultures.

One day postinoculation with JHMV, quadruplicate 35 mm mixed telencephalic cultures, were incubated with either MAb A2B5 diluted 1:4 in $DMEM_{10}$ or rabbit> GC antibodies diluted 1:10 in $DMEM_{10}$ as in Beushausen and Dales (1985). After incubation for 60 minutes at 20°C, unbound antibody was removed by two washes of $DMEM_{10}$. Half the antibody reacted cultures were exposed at 37°C for 30 minutes to heterologous rabbit Lo Tox complement (Cedarlane, Hornby, Ontario) diluted 1:14 in $DMEM_{10}$. Unfixed complement was removed by washing twice with 1 ml $DMEM_{10}$ before addition of medium.

2.2.11 Infectious Centers Assay.

To estimate the percentage of O-2A cells infected with JHMV within the first 24 hours postinoculation, a contact transfer or infectious centers assay was used. Process-bearing cells of the O-2A lineage were released from mixed glial cultures at 9 D.I.V. and P10 as described in section 2.2.5, and established as secondary enriched cultures. Following 96 hours in medium O1/T3, the cultures were inoculated with JHMV at an m.o.i. of 4 pfu's/cell. After adsorbing the viral inoculum for 1 hour on a rocking platform at room temperature,

the cells were washed 3 times with PBS followed by incubation in medium O1/T3 for 24 hours at 37°C. The culture medium was then removed, the cells washed 3 times with PBS and then released from the plastic surface by digesting with 1x trypsin/EDTA (Sigma). The trypsin was inactivated by the addition of FBS supplemented medium, cells were pelleted by centrifugation, then monodispersed with $DMEM_{10}$ before determination of cell count. Duplicate, serial 10 fold dilutions of O-2A cells beginning with 10^6 cells were then seeded onto L-2 cell monolayers situated in 35 mm dishes. The cell mixture was incubated at 37°C for 1 hour to allow the O-2A cells to settle onto the L-2 cell monolayer before overlaying with medium containing 0.5% carboxymethylcellulose. Plaques were counted after a further incubation period of 24 hours at 37°C.

2.2.12 Virus Adsorption Assays.

Two methods were used for assessing virus adsorption to cells. The first method which is a modification of the one described by Van Dinter and Flintoff (1987), involved inoculating cultures situated in 35 mm dishes with JHMV at an m.o.i. of ~ 2 pfu's/cell and incubating for 60 minutes at 4°C with continuous rocking. Unadsorbed inoculum was removed by 3 consecutive washes with DMEM containing 15 mM hepes pH 7.3, 10 µg/ml gentamycin, 0.5% (w/v) bovine serum albumin (BSA) and 0.05% (v/v) Tween 20. One ml of cold medium was then added to each dish and the cells gently removed from the plastic

surface with a rubber policeman. The cells were disrupted by successive passages through 26 and 30 gauge needles and 10 fold serial dilutions of the lysates titered on L-2 cell monolayers.

In the second method, virus adsorption was assayed by the method of Wilson and Dales (1988) using isotopically labelled virus. Cultures situated in 35 mm dishes were inoculated with [^{3}H]uridine-labelled JHMV at an m.o.i. of ~ 2 pfu's/cell. Adsorption was carried out for 60 minutes at 4°C on a rocking platform. Unadsorbed virus was removed by 3 consecutive washes with cold PBS pH 7.4, followed by harvesting the virus-cell complexes into 1 ml of cold PBS using a rubber policeman. An equal volume of 20% trichoroacetic acid (TCA) was added to each sample preparation and incubated on ice for 60 minutes. The resulting precipitates were filtered through Whatman GF/C fiters and successively washed 3x with 5% TCA and 1x with 95% ethanol before air drying. TCA precipitable counts were subsequently determined by liquid scintillation spectroscopy.

2.2.13 Virus Penetration Assay.

Virus penetration was assessed by the method previously described by Van Dinter and Flintoff (1987). Following removal of unadsorbed inoculum by the method described in section 3.2.12, cultures were incubated in medium $DMEM_{:0}$ at 37°C for various periods of time to allow penetration of virus to occur. At 15, 30 and 60 minute time points, non-internalized virus was removed from the cell surface by treating the

cultures with 0.5 mg/ml proteinase K in PBS for 45 minutes at 4°C. The proteinase K was inactivated by the addition of an equal volume of 6% BSA in PBS containing 2mM phenylmethylsulphonyl fluoride (PMSF). The cells were then gently scraped from the dishes and pelleted by centrifugation. All pellets were washed once in $DMEM_{10}$ before releasing proteinase K resistant or internalized virions by disrupting the cells by successive passage through 26 and 30 gauge needles. Infectious or non-uncoated virus was then assayed by titering the homogenates on L-2 cell monolayers.

2.2.14 In Situ Hybridization for JHMV Specific RNA.

Inoculated O-2A cultures were probed for JHMV specific RNA using the procedure described by Paeratakul et al. (1988). In this protocol, O-2A cultures grown in 35 mm dishes were inoculated with JHMV at an m.o.i. of ~ 5 pfu/cell. At 24, 48 and 72 hours post-inoculation, cultures were thoroughly washed with ice cold PBS and the cells gently scraped into cold PBS using a rubber policeman. After gently monodispersing the cells and determining cell concentrations, serial twofold dilutions of whole cell suspensions were spotted onto nitrocellulose previously wetted with PBS using a Schleicher & Schuell 96-well manifold filtering apparatus. The filter then was fixed in a solution of 3% (w/v) NaCl, 10 mM NaH_2PO_4/40 mM Na_2HPO_4 (pH 7.4) and 1% (v/v) glutaraldehyde for 60 minutes at 4°C. This was followed by washing the filter 3 times in proteolytic buffer consisting of 50 mM EDTA and 0.1 M Tris

hydrochloride (pH 8.0) before digesting with 20 μg/ml proteinase K in proteolytic buffer for 30 minutes at 37°C. The filter was briefly air dried before being placed into prehybridization buffer consisting of 50% (v/v) formamide, 3x SSC (1x SSC is 0.15 M NaCl plus 0.015M Na citrate), 0.01 M hepes pH 7.4, 1x Denhardt's buffer (0.02% w/v BSA, 0.02% polyvinyl pyrrolidine and 0.02% Ficoll), 1 mg/ml yeast RNA and 100 μg/ml salmon sperm DNA. The blot was prehybridized for 16 hours at 41°C then hybridized with [α-^{32}P]dATP labelled pg344 (Budzilowicz et al., 1985) for 48 hours at 41°C. The plasmid pg344 provided by Dr. S. Weiss of the University of Pennsylvania, contains an 1800 base pair MHV-A59 specific cDNA insert encoding genes 5 and 6 as well as the intergenic regions preceding genes 5,6 and 7. Following hybridization, the filter was washed sequentially 4 times with 2x SSC-0.1% SDS for 5 minutes each at room temperature, 2 times with 0.1x SSC-0.1% SDS for 15 minutes each at 50°C, and 5 times with 0.1x SSC for 1 minute each at room temperature. The filter was finally air dried and exposed to Kodak X-OMAT film at -70°C with intensifying screens.

2.3 Results.

2.3.1 Primary Mixed Telencephalic Cultures: Growth Characteristics in Serum Containing and Serum-Free Environments.

Cultures derived from neonatal rat telencephala were grown with 10% FBS supplementation during the initial 3 D.I.V. Within 24 hours of establishing the cultures, neurons began sprouting neurites, and by 3 D.I.V., cell aggregates and a complex network of processes were well established. At this time, some of the cultures were maintained in medium $DMEM_{10}$, while the remainder were switched to the serum-free, chemically defined culture medium O1/T3. Cultures grown under the two conditions remained morphologically indistinguishable up to 6 D.I.V. At this point in time, aggregates of cells in $DMEM_{10}$ began to detach from the substrate coincident with the undergrowth of flat astroglia. This cell behaviour was not observed with cultures grown in O1/T3. By 7 to 8 D.I.V. cultures in $DMEM_{10}$ took on the typical stratified appearance originally described by McCarthy and de Vellis (1980) in which phase lucent, flat, epithelioid astrocytes comprised the bedlayer, on which phase-dense, process-bearing cells, of the O-2A lineage were superimposed. In sharp contrast, cultures placed in medium O1/T3 beginning at 3 D.I.V. retained aggregates of rounded cells separated from each other by zones permeated with a network of numerous processes. Figure 2.2 illustrates the microscopic differences observed between the two culture conditions at 9 D.I.V. Phenotyping of cultures was carried out between 5 and 21 D.I.V. using monospecific and monoclonal antibodies. At 5 D.I.V./P5, neurons identified by the presence of neurofilaments and NSE, were present in both O1/T3 and $DMEM_{10}$ cultures. These same markers revealed that

Figure 2.2. Appearance at 9 D.I.V./P9 of dissociated mixed telencephalic cultures derived at P0 from WF rats. (A) Typical culture placed in O1/T3 at 3 D.I.V. S marks the soma of a large cell extending a prominent process (indicated by large straight arrows). Small straight arrows point to numerous, smaller processes and curved arrows to smaller cells typical of the O-2A lineage. (B) Typical culture in $DMEM_{10}$. Process-bearing O-2A lineage cells (curved arrows), dwell above a phase lucent bedlayer of type-1 astrocytes. A and B x 1,300.

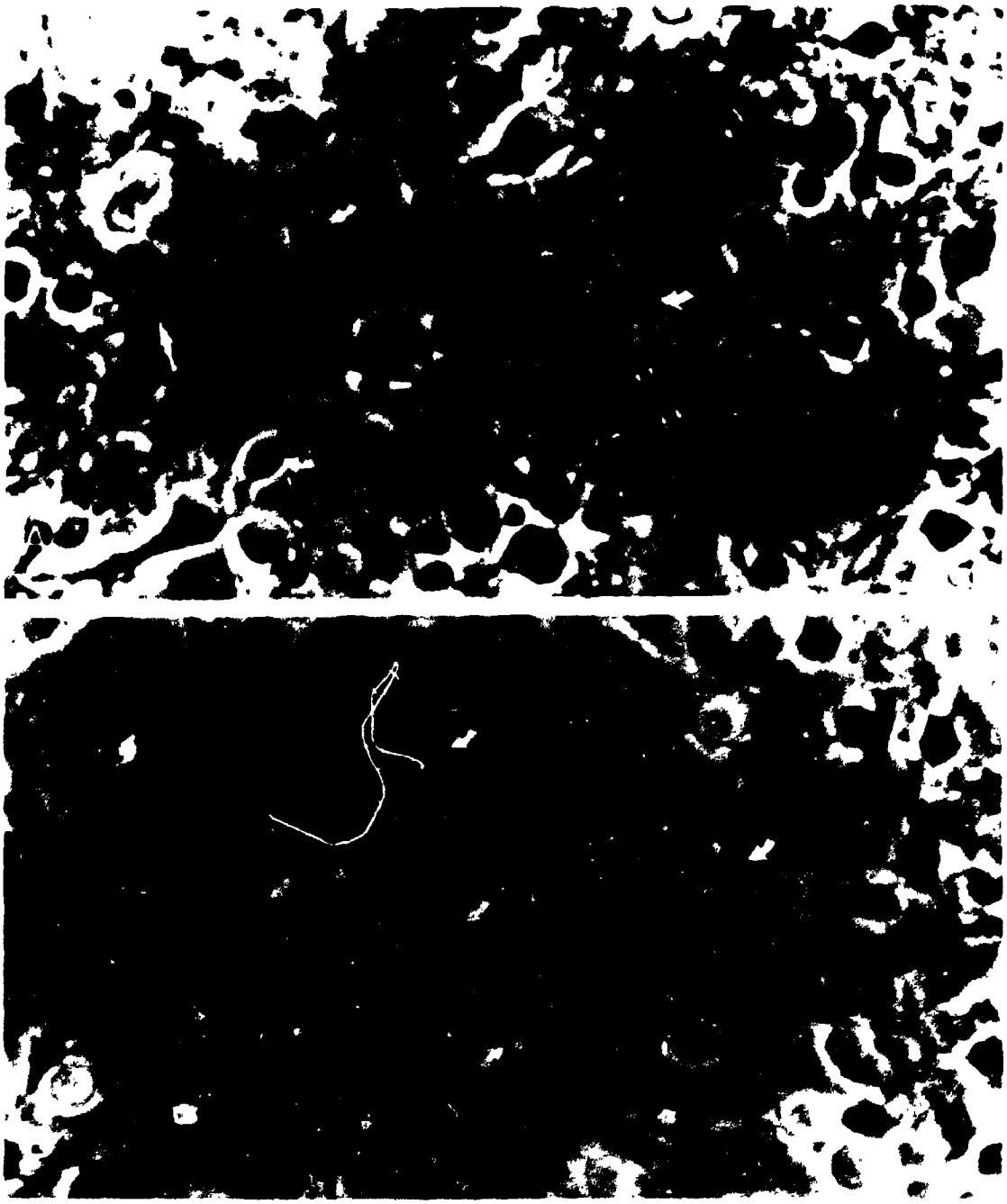

neurons were nearly totally lost from $DMEM_{10}$ cultures by 8 D.I.V. but were still numerous in cultures grown in O1/T3 until at least 21 D.I.V./P21 (Figure 2.3). The loss of neurons from cultures maintained in $DMEM_{10}$ appeared to coincide with the proliferation of epithelioid astrocytes, similar to the results reported by Gilad et al. (1990) in neonatal rat cerebellar cultures. Electron microscopic examination of O1/T3 cultures sampled at 15 D.I.V./P15 revealed the presence of cells possessing the fine structure typical of neurons and a profuse network of neurites containing numerous microtubules (Figure 2.4.A to C). $GFAP^+$ astrocytes were abundant under both growth conditions. However, astrocytes possessed a stellate morphology in O1/T3 and polygonal morphology in $DMEM_{10}$. In both $DMEM_{10}$ and O1/T3 media an abundance of bi- and tripolar A2B5+ O-2A progenitor cells was observed at 5 D.I.V./P5, along with fewer GC^+ oligodendrocytes, in agreement with previous reports (Behar et al., 1988; Gard and Pfeiffer, 1989; Hunter and Bottenstein, 1989). There was a progressive, time-related differentiation of O-2A lineage cells, detected by the loss of A2B5 immunoreactivity coupled with increased >GC and >MBP immunoreactivity (Table 2.1). This shift in antigenic phenotype was coupled with morphologic differentiation identified by the change from bipolar or simple multipolar forms, which predominated at 4 to 5 D.I.V., to more complex branching patterns evident by 10 D.I.V., consistent with previous reports (Behar et al., 1988; Gard and Pfeiffer, 1989; Hunter and Bottenstein, 1989). Morphologic differentiation of

Figure 2.3. Detection of neurons at 10 D.I.V./P10 in dissociated mixed telencephalic cultures grown in O1/T3. (A) Neuronal cell bodies (large arrows) and processes (small arrows) visualized after reaction with rabbit>NSE and TR-conjugated goat>rabbit IgG. (B) Neurites coursing over the culture surface (arrows) are revealed with MAb>160 kD neurofilament protein and FITC-conjugated goat>mouse IgG. (C) A higher magnification image demonstrating a neurofilament positive neuron. (D) A phase contrast image of C with arrows outlining the neuronal cell body. Note the prominent nucleolus. A and B x 1,000, C and D x 3,750.

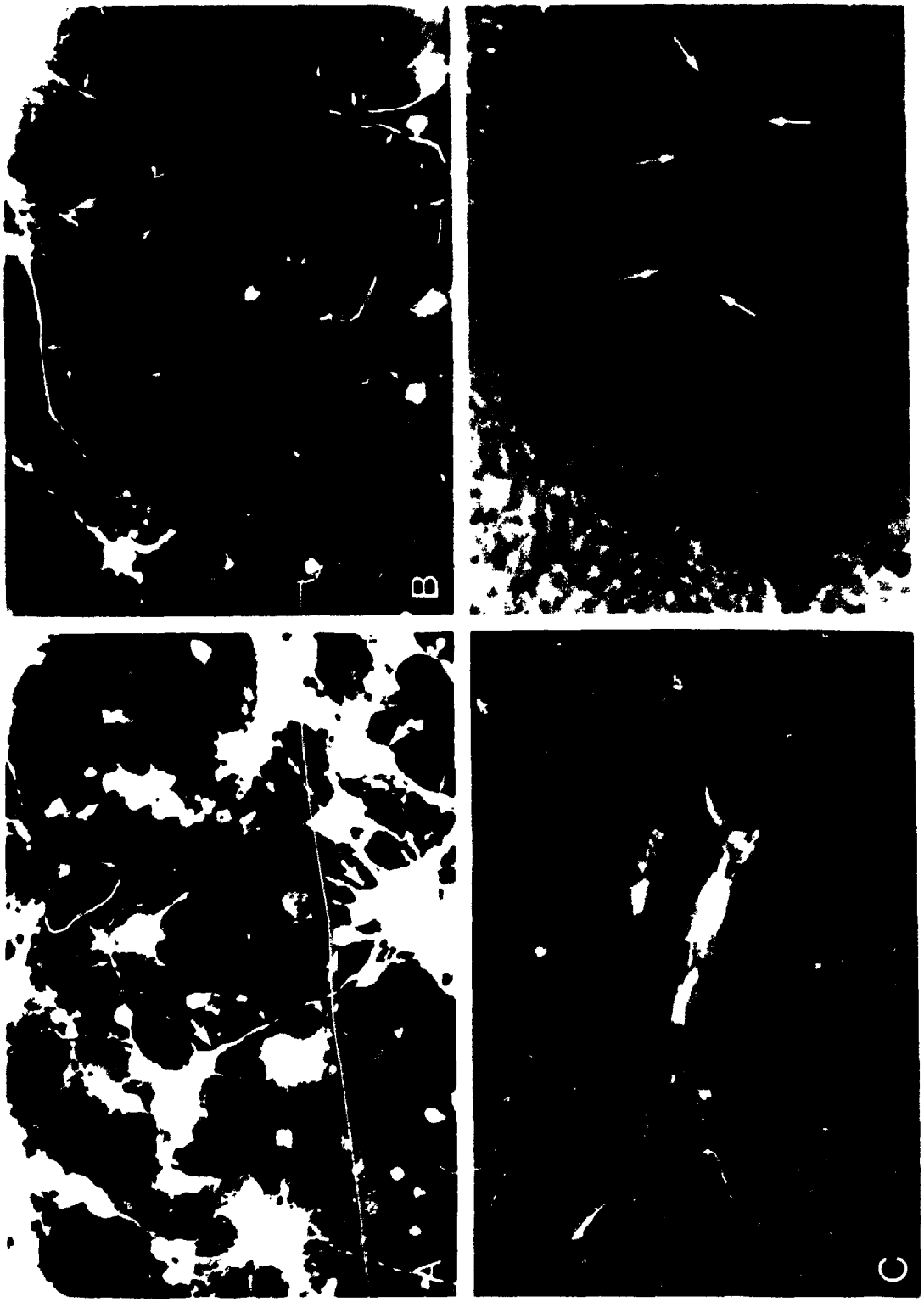
B
A
C

Table 2.1

Time Dependent Differentiation of O-2A Lineage Cells in Mixed Telencephalic Cultures Grown Under Serum-Free and Serum Supplemented Conditions*

	A2B5+		GC+	
Days in Culture	O1/T3	$DMEM_{10}$	O1/T3	$DMEM_{10}$
6 D.I.V./P6	23.1 ± 5.1	24.8 ± 10.7	4.2 ± 2.3	2.9 ± 2.3
8 D.I.V./P8	11.0 ± 3.5	19.6 ± 8.6	11.4 ± 6.0	8.9 ± 3.5
10 D.I.V./P10	4.0 ± 1.2	6.8 ± 3.3	10.4 ± 3.4	11.1 ± 2.5

*Mixed telencephalic cultures grown on 12 mm diameter glass coverslips in either O1/T3 or $DMEM_{10}$ were sampled at 6,8 and 10 D.I.V. for double labelling with A2B5 and anti-GC antibodies. $A2B5^+$ and GC^+ cells were then counted in 10 randomly picked 400x microscopic fields. Values are the means and standard deviations.

oligodendrocytes progressed to the point where membranous extensions were found in association with axons, indicative of potential myelination (Figure 2.4.B and C), as already described in primary telencephalic cultures by others (Muraoka and Takahashi, 1989).

These observations illustrate the dynamic nature of this culture system and indicated that the milieu of the culture medium influenced profoundly the survival of specific neural cell types, particularly neurons. Survival of neurons was in turn associated with differences in the histotypic organization that these cultures adopted, the development of which was likely contingent upon intercellular interactions and cellular differentiation.

2.3.2 Primary Mixed Telencephalic Cultures: Infection with JHMV.

To determine whether the differences observed in $DMEM_{10}$ and O1/T3 grown cultures influenced the ability to infect with JHMV, a series of mixed telencephalic cultures, grown in one or the other medium were inoculated at P10/10 D.I.V. at a m.o.i. of 1. The data in Figure 2.5 illustrate unequivocally that the culture milieu strongly influenced both the magnitude and longevity of virus production. In some experiments, cultures in O1/T3 inoculated at P10, remained productively infected for at least 6 weeks, yielding titers in the order of 1000 pfu/ml.

Connection between the acceleration of oligodendrocyte

Figure 2.4. Electron microscopy of selected cells in an uninfected telencephalic culture from neonatal WF rats preserved in situ at P15. Following explantation, the cultures were grown in $DMEM_{10}$ for 3 days then maintained in O1/T3 for 12 days. (A) Portion of a cell with neuronal morphology contains a central nucleus (N) with homogeneous karyoplasm, prominent Golgi membranes (G), numerous mitochondria (M) and bundles of microtubules (small arrows) inside the process. Numerous smaller processes in cross-section containing microtubules are also evident at the bottom right. (B) A smaller, dense cell, superimposed on the neuronal cell layer, possesses the fine-structure of an oligodendrocyte. (C) A portion of the cell as in (B), illustrates at a higher magnification a process from the adherent cell which partially surrounds the prominent neurite filled with microtubules (arrow). Bars = 0.5 μm.


A
M
M
M

Figure 2.5. JHMV replication in primary dissociated mixed telencephalic cultures derived from P0 WF rats. Cultures were grown continuously in $DMEM_{10}$, or switched at 3 D.I.V. to serum-free O1 with or without T_3 supplementation. $DMEM_{10}$ cultures receiving dbcAMP were treated 48 hours prior to, and 48 hours after inoculation with JHMV. All cultures were inoculated at 10 D.I.V./P10 with a m.o.i. of 1. The data are the mean titers ± SD from 4 identical experiments.

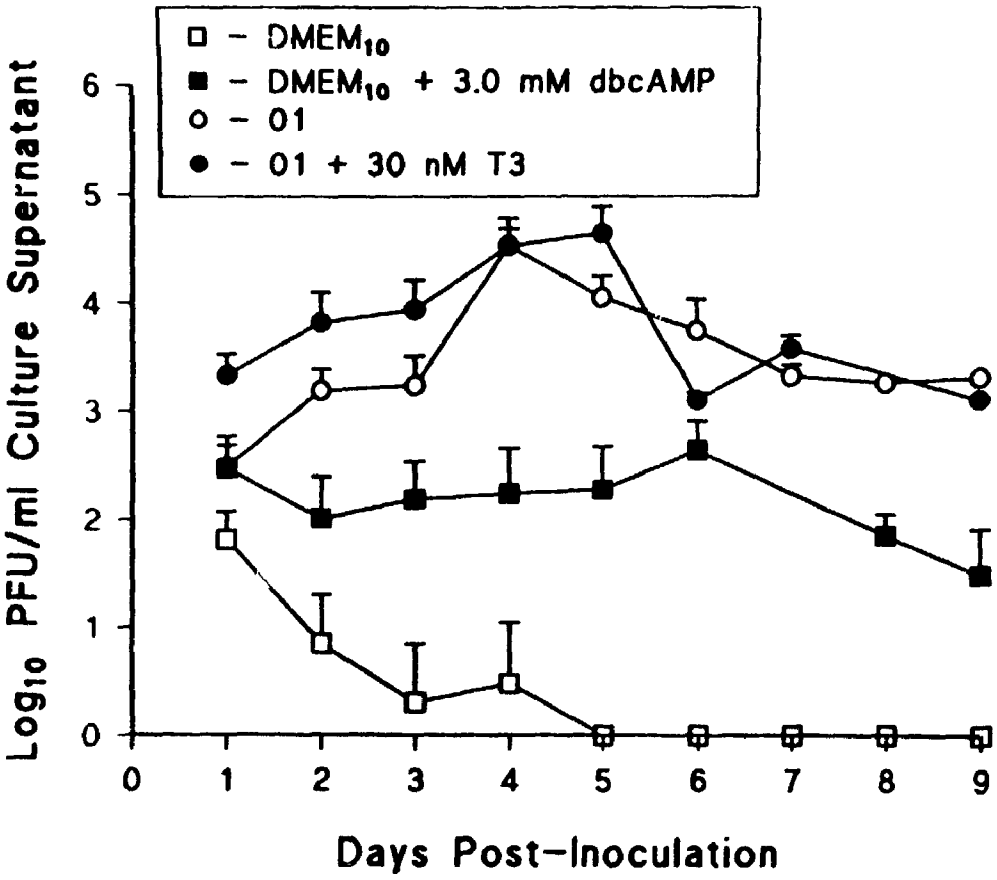
□ – DMEM10
■ – DMEM10 + 3.0 mM dbcAMP
○ – 01
● – 01 + 30 nM T3
Log10 PFU/ml Culture Supernatant
0
1
2
3
4
5
6
0
1
2
3
4
5
6
7
8
9
Days Post–Inoculation

differentiation and exposure to the cAMP analogue O2'-dibutyryladenosine 3':5'-cyclic monophosphate (dbcAMP) (McMorris, 1983; Beushausen and Dales, 1985; Raible and McMorris, 1989), or to activators of adenylate cyclase (Beushausen et al., 1987; Raible and McMorris, 1990), prompted us to assess the effects of pretreatment with dbcAMP. Previous work had shown that if cultures secondarily enriched for O-2A lineage cells were treated with compounds affecting adenylate cyclase metabolism before inoculation, subsequent establishment of JHMV infection was inhibited (Beushausen and Dales, 1985; Beushausen et al., 1987). The consequence of pretreatment of mixed telencephalic cultures grown in O1/T3 was of interest to us since these cultures contained O-2A lineage cells and neurons, both targets of JHMV in vivo (Sorensen and Dales, 1985). Treatment of O1/T3 cultures with 2.5 to 5.0 mM dbcAMP 72 hours prior to and 48 hours after inoculation with JHMV at P10 resulted in no adverse effects on virus production; to the contrary, dbcAMP frequently enhanced virus growth, which was most notable during the initial 5 day period post-inoculation. A similar dbcAMP-related enhancement, albeit very minor, was also observed occassionally in $DMEM_{10}$ cultures (Figure 2.5). The enhancement was attributed to cAMP per se since equimolar concentrations of sodium butyrate actually inhibited virus growth, resulting from the necrosis of cells of non-type-1 astrocytic phenotype (data not shown).

Addition of tri-iodothyronine (T_3), implicated in the process of postnatal oligodendroglial differentiation and

myelination (see appendix, Almazan et al., 1985; Nunez, 1984 for review) to cultures grown in serum-free medium had no effect on either the establishment of infection or long-term production of virus (Figure 2.5).

To ascertain whether the age of the culture influenced virus production, cultures grown in O1/T3 were inoculated with JHMV at a m.o.i. of 1 at 4 D.I.V./P4, 6 D.I.V./P6, 10 D.I.V./P10, 15 D.I.V./P15, and 21 D.I.V./P21. The influence of continuous treatment with 2.5 mM dbcAMP 48 hours prior to and 48 hours after inoculation was also assessed at P6, P10, P15, and P21. The results, summarized in Table 2.2, demonstrated first of all that an infection was most difficult to establish in very young P4 cultures, which contained a high frequency of bipotential O-2A progenitor cells and neurons elaborating an extensive network of neurites. Secondly, highest virus yields were obtained from cultures inoculated at P10, suggesting that the number and/or susceptibility of target cells is optimal at this stage. Thirdly, the enhancing effect of dbcAMP was most pronounced when inoculation occurred at P15 to P21. These differences on rates of JHMV replication led us to attempt further elucidation of the cell type(s) supporting the infection.

2.3.3 Primary Mixed Telencephalic Cultures: Identification of Virus Infected Cells.

Mixed telencephalic cultures established on glass coverslips were inoculated at P10 and monitored at 24 hour

Table 2.2

JHMV Replication in Primary Mixed Telencephalic Cultures Inoculated at Different Ages Postnatally[a]

Age at challenge	Treatment	Titer at the indicated day postinoculation: 1	2	3	4
P4	None (control)	ND[c]	0.4 ± 0.4	0.2 ± 0.07	5.6 ± 1.1
P6	None (control)	4.6 ± 0.6	24.0 ± 19.8	54.0 ± 13.4	340.0 ± 35.4
	dbcAMP	3.9 ± 0.5	7.4 ± 4.7	22.1 ± 21.1	197.5 ± 123.7
P10	None (control)	30.2 ± 11.7	116.8 ± 29.3	245.0 ± 99.0	250.0 ± 21.2
	dbcAMP	10.8 ± 3.2	52.0 ± 32.5	142.5 ± 60.1	272.5 ± 60.1
P15	None (control)	ND	4.1 ± 0.6	32.0 ± 0.7	10.0 ± 0
	dbcAMP	ND	53.8 ± 41.5	248.8 ± 136.8	109.0 ± 36.8
P21	None (control)	8.2 ± 0.7	11.0 ± 0.5	13.8 ± 6.7	18.0 ± 4.2
	dbcAMP	8.4 ± 1.0	48.8 ± 15.9	137.2 ± 19.4	217.5 ± 95.4

[a]Primary, mixed, dissociated telencephalic cultures were established using newborn WF rat pups. Duplicate cultures from each treatment were inoculated with JHMV at a m.o.i. of 1 at the ages indicated. Cultures in the control group were grown in O1/T3 medium beginning at 3 D.I.V. dbcAMP-treated cultures were exposed to 2.5 mM of this agent prior to inoculation with virus and continued for 48 hours postinoculation. Fresh dbcAMP was added daily during this period.

[b]All titers are the means of duplicate cultures and are expressed as 10^2 pfu/ml of culture supernatant.

[c]ND, not determined.

intervals for virus released into the supernatant. As anticipated, cultures maintained continuously in $DMEM_{10}$ which were devoid of neurons, determined as above, but contained numerous type-1 astrocytes and O-2A lineage cells, failed to produce infectious particles or viral N antigen, at 1,2, and 5 days postinoculation. In contrast, cultures maintained in O1/T3 commencing at 3 D.I.V. became efficient virus producers 24 hours postinoculation, expressing N antigen in both isolated individual cells and clusters of 4 to 5 cells. By 48 hours post-inoculation, the infected cell foci became larger. This was accompanied by the intensification of N antigen staining within the cytoplasm and spread along elongated processes radiating from the cell body as discrete, puncta (Figure 2.6). By simultaneous immunolabelling it was demonstrated that these cells were NSE^+, GC^- and $GFAP^-$, establishing their identity as forebrain neurons. It should be mentioned that co-labelling for NSE and N was evident only during the initial 24 hours post-inoculation, then became weaker and ultimately dissappeared. Simultaneous presence of $N^+/GFAP^+$ and N^+/GC^+ cells, which together comprised fewer than 1/4 of all those scored as N^+ within the initial 48 hours, revealed that cells of an astrocytic and oligodendrocytic phenotype had also been infected. By 5 days post-incculation, formation of syncytia, which were sometimes quite extensive, obliterated morphological details of the infected polykaryocytes. Nevertheless, prominent foci in the cell mass co-labelled for N and GFAP. Inoculations carried out at P6 and

Figure 2.6. Identification of JHMV infected cells in primary mixed telencephalic cultures propagated in medium O1/T3. (A) Following inoculation at P6 the culture was labelled at 3 dpi by reaction with MAb> JHMV N and FITC-conjugated goat> mouse IgG. Note the presence of N immunoreactivity in the soma and along the cell processes (arrows). (B) Another cell with comparable morphology and distribution of N, sampled 2 dpi in a culture inoculated at P10. Note that intense fluorescence of RITC-tagged GFAP of astrocytes is not completely suppressed by the FITC filter. (C) and (D) Culture inoculated at P6 sampled and labelled 1 dpi. In (C) the N^+ cell is identified as in (A); in (D) the same cell as in (C) (arrows) was co-labelled with rabbit> NSE and TR-conjugated goat> rabbit IgG. A and B x 1,250, C and D x 1,900

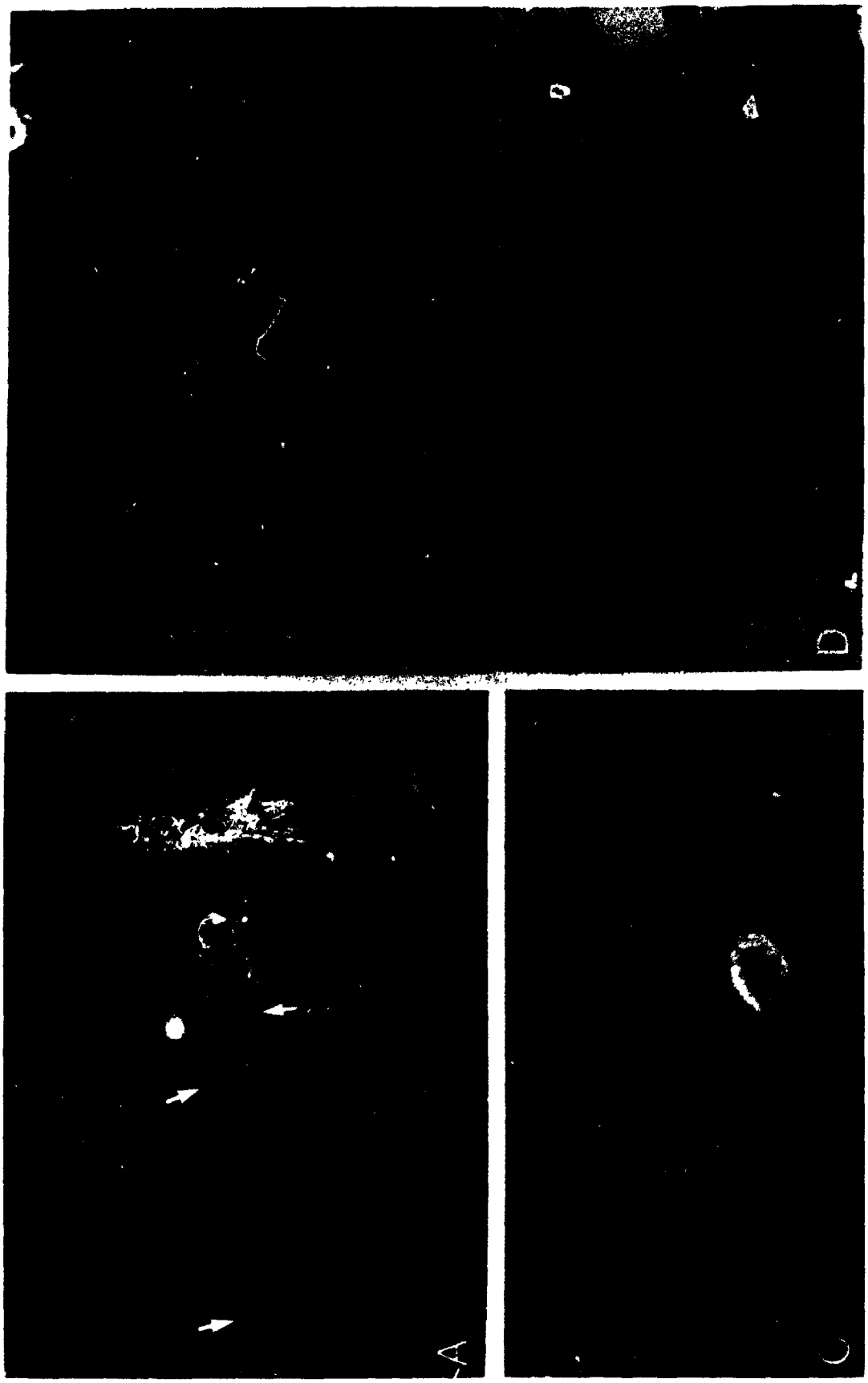
D
A
C

P17 resulted in similar labelling patterns. Consistent with above data from immunocytology and plaque assays we did not find any evidence of JHMV infection in $DMEM_{10}$ or $DMEM_{10}$ + dbcAMP cultures by electron microscopy, but observed cells containing coronavirus particles and inclusions of viral material in O1/T3 and O1/T3 + dbcAMP cultures (Figure 2.7). There was close correspondence in neuronal morphology of infected cells observed by light and electron microscopy with respect to the typical pyramidally shaped cell bodies extending long processes, presumably neurites, which were replete with microtubles (Figure 2.7). The prominent cytoplasmic inclusions consisted of aggregates of N previously identified by Massalski et al. (1982) in other host cells. In favourable orientations, the N component was regularly distributed along the microtubule arrays, extending from the soma into processes (Figure 2.7.B,C and E). Particles with morphology of coronavirions were readily found either as budding or free forms within endoplasmic reticulum (Figure 2.7.D), or at the surface.

To further identify the cell type(s) supporting replication of JHMV, we employed complement-mediated immune cytolysis. Binding of polyclonal> GC antibodies was used for eliminating cells of the oligodendrocytic phenotype, and MAb A2B5 was used to select neuronal (Eisenbarth et al., 1979), O-2A progenitor (Raff et al., 1983b), and type-2 astrocytic cells (Raff et al., 1983a). Immune lysis was carried out 24 hours following inoculation at P10 and the amounts of virus

Figure 2.7. Electron microscopy of selected examples of portions of neuronal type cells from a telencephalic explant culture infected and sampled as in Figure 2.4. (A) Portion of a cell with a prominent neurite and numerous dense cytoplasmic inclusions. In (B) to (E) the selected examples reveal a close association between microtubules (small arrows) and dense, granular, coronaviral nucleocapsid material (curved arrows), corresponding in structure to that described previously (Massalski et al., 1982). Individual JHM virions (large arrowheads) are evident inside cytoplasmic vacuoles near the nucleus in (D). Abreviations: N, the nucleus, M, mitochondria. Bars = 0.5 μm.

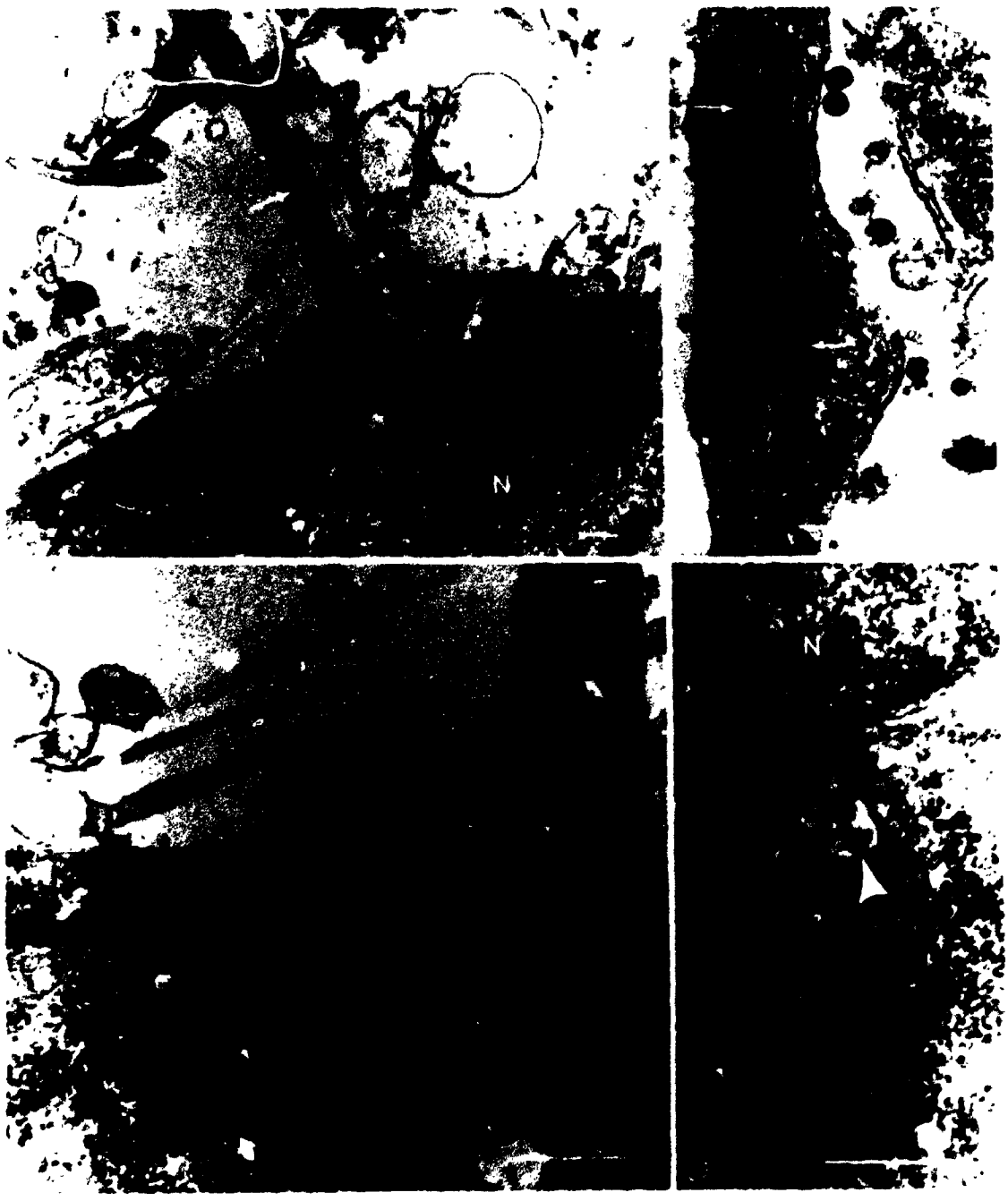
N
N

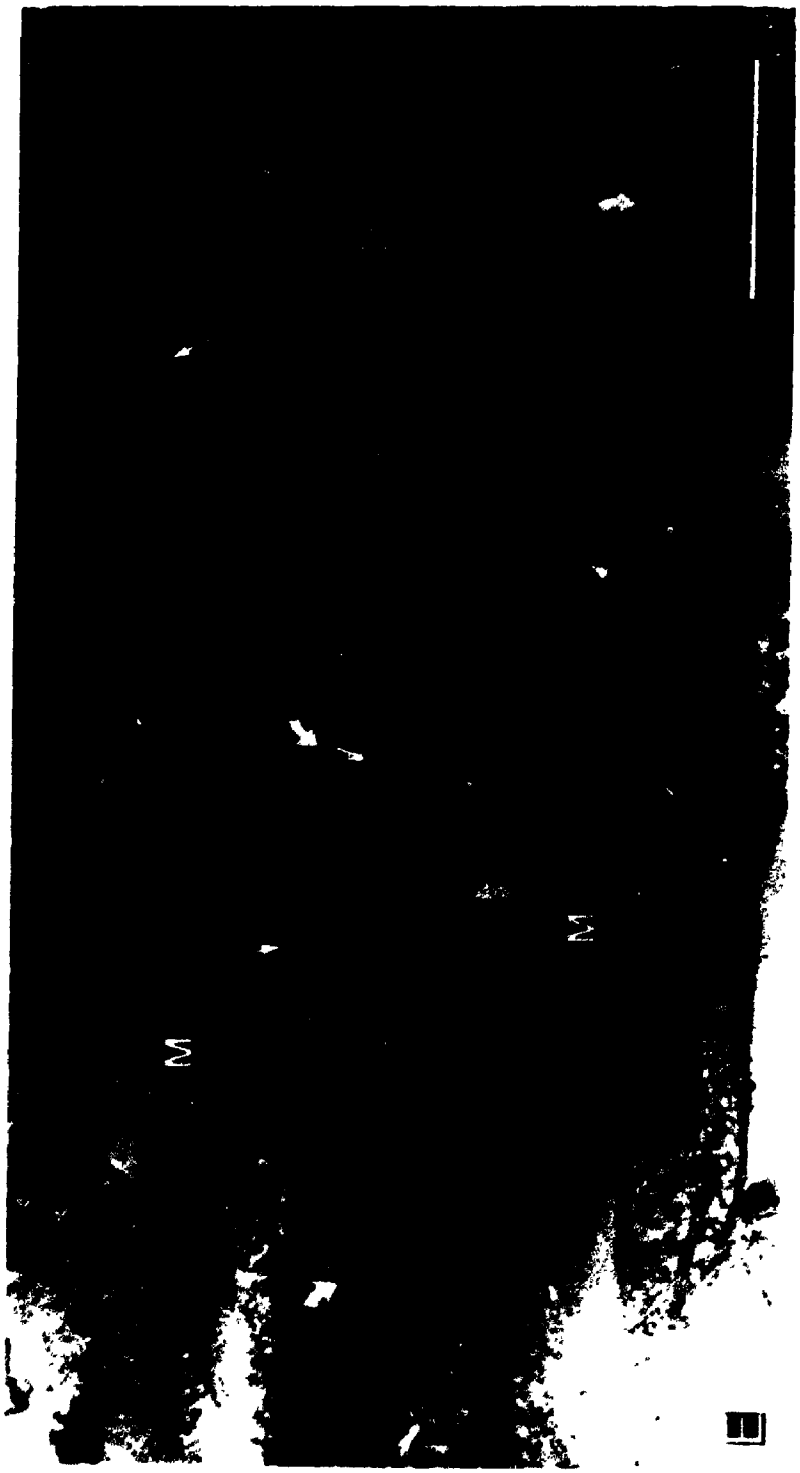
M
M

subsequently produced determined. As evident from the data in Table 2.3, cultures exposed to MAb A2B5 + complement produced virus an order of magnitude less than those left untreated or treated individually with A2B5 or complement. Application of antibodies> GC + complement reduced the virus titer marginally and at later times than observed with MAb A2B5 + complement. This was taken as suggestive evidence that $A2B5^+$ rather than GC^+ cells were the primary producers of JHMV, consistent with immunocytological and electron microscopic observations which implicated the neurons. However, some ambiguity remained as to the $A2B5^+$ cells affected, since MAb A2B5 can also recognize O-2A progenitors and type-2 astrocytes. It, therefore, became imperative to ascertain the role of glial cells in JHMV replication.

2.3.4 Secondary Glial Cultures: JHMV Replication in Type-1 Astrocytes and O-2A Lineage Cells.

Previous work in our laboratory identified the tropism of JHMV for rat cells within the O-2A lineage, and the lack of tropism for type-1 astrocytes. This is to be contrasted with the unambiguous tropism of a closely related coronavirus MHV3 for type-1 astrocytes (Beushausen and Dales, 1985). To account for the inefficient infection of O-2A lineage cells situated in mixed cultures grown in O1/T3 medium, and absence of virus growth by identically derived cultures grown in $DMEM_{10}$, epigenetic effects of the culture milieu were invoked. This idea was tested by infecting enriched type-1 astrocyte or O-2A

Table 2.3

Effects of Immune Lysis of GC$^+$ and A2B5$^+$ Cell Populations on the Replication of JHMV in Mixed Telencephalic Cultures*

Treatment of cultures	Days post-inoculation 2	3	4
O1/T3	6.8	9.1	12.6
O1/T3 + 2.5 mM dbcAMP	3.7	40.2	151.5
O1/T3 + anti-GC alone	16.5	13.5	36.2
O1/T3 + complement alone	6.9	17.8	23.5
O1/T3 + anti-GC + complement	7.4	10.0	17.0
O1/T3 + A2B5 alone	9.3	16.4	27.5
O1/T3 + A2B5 + complement	1.7	2.4	2.9

Note. All titers are the means of duplicate cultures and are expressed x10^2 pfu/ml culture supernatant.
*Mixed telencephalic cultures grown in 35 mm petri dishes were inoculated with JHMV at 10 D.I.V./P10 with a m.o.i. of 1. Cultures receiving dbcAMP treatment were given the agent on a daily basis 48 hours prior to and 48 hours following viral inoculation. Antibody and complement treatments were initiated 24 hours post-inoculation as described in Materials and Methods. The data is representative of 2 identical experiments.

lineage cultures grown under conditions similar to those found in the mixed culture environment.

Type-1 astrocytes possessed a flat epithelioid morphology when grown in the presence of serum supplement and a stellate morphology with fine processes in O1/T3. Process formation became even more accentuated upon the addition of dbcAMP, consistent with previous reports (Aizeman and deVellis, 1987; Gavaret et al., 1991). However, regardless of the culture conditions employed, type-1 astrocytes did not support JHMV replication, consistent with previously published results (Beushausen and Dales, 1985; Beushausen et al., 1987). This drew our attention to an apparent anomaly concerning JHMV expression in $GFAP^+$ cells, documented above.

Secondary cultures of O-2A lineage cells (~ 90% purity), were established at densities ranging from 1.25×10^5 to 2.5×10^5 cells/cm^2. Following 24 hours in $DMEM_{10}$, the cultures were grown for a further 48 or 72 hours in O1/T3, or O1/T3 mixed 1:1 with O1/T3 conditioned by exposure for 72 hours to either mixed telencephalic cultures (MTCM), or type-1 astrocyte cultures (ACM), then inoculated with JHMV at a m.o.i. of 1. In a number of experiments, O-2A lineage cells were also seeded directly onto a type-1 astrocyte bedlayer and the co-cultures grown for 48 to 72 hours in O1/T3 before inoculation. O-2A cultures grown in O1/T3 supported growth of JHMV; however, preexposure to MTCM or ACM inhibited JHMV replication, with virus yields that were only 1/10 to 1/100 of those from control cultures. Inhibition was even more

pronounced with O-2A lineage cells directly co-cultured with type-1 astrocytes (Figure 2.8). Since cell viability, assessed by trypan blue exclusion, was not altered under the above conditions, differences in virus production could not have been attributed to the loss of viable target cells. O-2A lineage enriched cultures were mitotically more active in MTCM or ACM than controls in O1/T3, consistent with previous reports (Richardson et al., 1988; Hunter and Bottenstein, 1989; Levine, 1989; Gard and Pfeiffer, 1990). In addition, cells tended to maintain bipolar to simple multipolar forms in conditioned media, but developed more complex forms typical of oligodendrocytes in unconditioned O1/T3. The suppressive effect on JHMV growth was evident in ACM diluted to 1:10 before disappearing, indicating that the activity was present at limiting concentrations. The suppression was specific to JHMV because VSV replicated equally well or better in O-2A cells grown in conditioned or un-conditioned O1/T3 (data not shown). Inhibition was also related specifically to cells of the O-2A lineage, because culture of L cells in O1/T3, MTCM or $DMEM_{10}$ for 72 hours prior to and after inoculation with JHMV did not influence virus growth (Table 2.4). Evidently, the factor(s) in conditioned media inhibiting JHMV infections act(s) specifically on the O-2A cell type.

2.3.5 Secondary Glial Cultures: Modulation of JHMV Replication in O-2A Cells by the Cytokines PDGF and bFGF.

The inhibition of virus production by O-2A cultures grown

Figure 2.8. Replication of JHMV in O-2A lineage enriched cultures derived from mixed glial cultures at 9 D.I.V./P9. (A) Cultures plated at 1.25 x 10^5 cells/cm^2 were grown in O1/T3 or MTCM for 48 hrs. prior to inoculating with JHMV at a m.o.i. of 1. The data, which are means of titers ± SD from triplicate cultures are representative of 3 independent experiments. (B) O-2A lineage cells, plated either directly onto the plasticware or a monolayer of type-1 astrocytes, were established at the same cell density as that in (A). After growth in O1/T3 or ACM for 48 hrs., they were inoculated with JHMV at a m.o.i. of 1, with compensation being made for O-2A/type-1 astrocyte co-cultures. Data are the means of titers from triplicate cultures and are representative of 3 independent experiments.

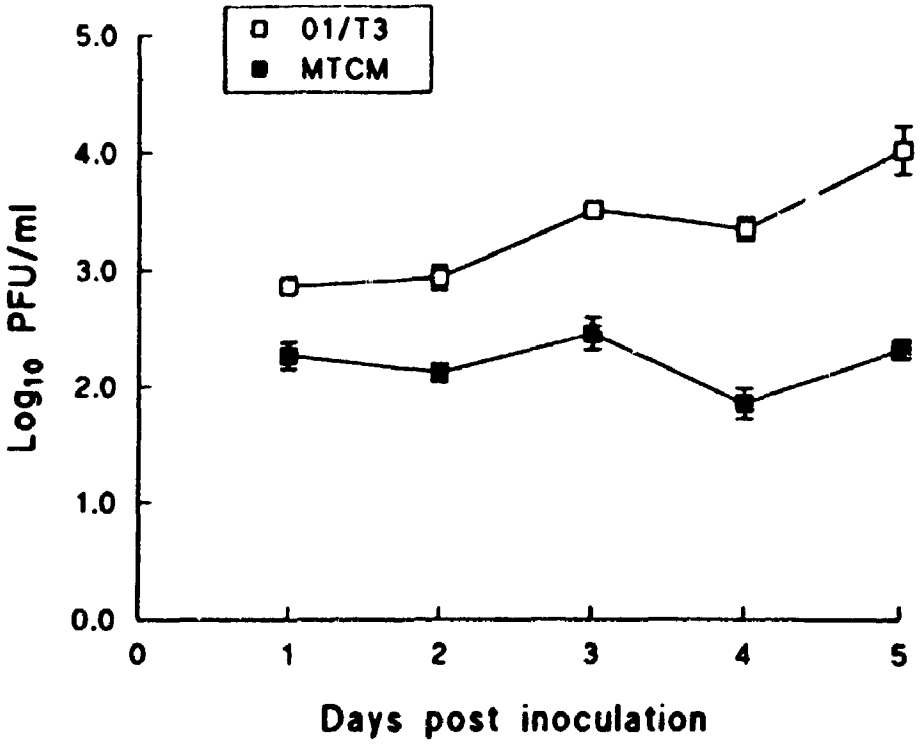
01/T3
MTCM
5.0
4.0
3.0
2.0
1.0
0.0
Log10 PFU/ml
0
1
2
3
4
5
Days post inoculation

A

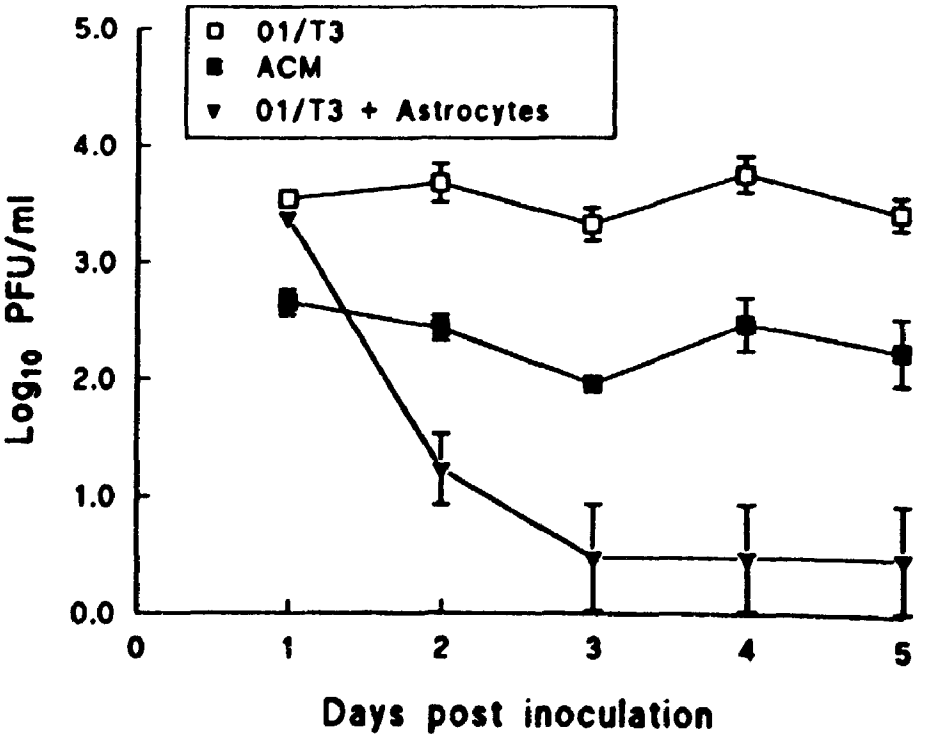
01/T3
ACM
01/T3 + Astrocytes
5.0
4.0
3.0
2.0
1.0
0.0
Log10 PFU/ml
0
1
2
3
4
5
Days post inoculation

B

Table 2.4
Effects of Cell and Virus Specificities and Culture Conditions on Virus Growth

Cell/virus system	Culture conditions	Titer (means ± SD) at indicated days postinoculation: 1	2	3	4
L cells[b]/JHMV (m.o.i. 0.1)	$DMEM_{10}$	21,000 ± 9,500			
	$DMEM_{10}$ + bFGF	23,000 ± 11,000			
	O1/T3	6,900 ± 2,700			
	O1/T3 + bFGF	6,700 ± 280			
	O1/T3 +bFGF+PDGF	7,000 ± 850			
	ACM	7,500 ± 1,200			
	MTCM	9,000 ± 1,400			
O-2A[c]/JHMV (m.o.i. 1)	O1/T3	ND[d]	10.7 ± 2.2	14.9 ± 8.9	30.8 ± 10.0
	O1/T3 +bFGF+PDGF	ND	0.2 ± 0.08	0 ± 0	0 ± 0
O-2A[c,e]/VSV (m.o.i. 1)	O1/T3	326.7 ± 20.8	33.3 ± 13.9		
	O1/T3 +bFGF+PDGF	513.3 ± 110.6	306.7 ± 81.4		

[a]All titers are expressed as 10^2 pfu/ml of culture supernatant.
[b]L-2 cell cultures were completely lysed by 18 hours post-inoculation.
[c]Enriched O-2A progenitor cultures derived from 5 D.I.V. and P5 mixed telencephalic cultures were established at a density of 1.25×10^5 cells per cm^2 and grown in O1/T3 supplemented with bFGF and PDGF (10 ng/ml each). At P9, half the cultures were switched to O1/T3 without cytokines and then inoculated at P13 with either JHMV or VSV.
[d]ND, not determined.
[e]O-2A cultures inoculated with VSV were completely lysed by 48 hours post-inoculation. Note that higher yields in cultures treated with O1/T3 + bFGF + PDGF correlated with higher cell densities.

under the conditions shown in Figure 2.8, suggested that modulation involved diffusable cellular factor(s), possibly of heterotypic origin. Since suppression of JHMV growth in O-2A cells cultured in MTCM or ACM was correlated with enhanced mitotic activity and retention of simpler cell morphologies, we assessed the effect on virus replication of PDGF and bFGF, two cytokines identified in effecting developmental control over cells of the O-2A lineage (Raff et al., 1988; Richardson et al., 1988; Bolger et al., 1990; McKinnon et al., 1990).

O-2A lineage cells isolated from mixed glial cultures at 9 D.I.V./P9 were grown for 72 hours with 10 ng/ml PDGF, 10 ng/ml bFGF, or in the presence of both factors, then were inoculated with JHMV at a m.o.i. of 2. The virus titers produced in presence and absence of cytokines are depicted in Figure 2.9. Culturing O-2A lineage cells in the presence of bFGF, PDGF, and bFGF+PDGF produced respectively a 3.1, 5.8, and 5.5 increase in cell number over a 4 day period relative to the control O1/T3 medium. Therefore, the rates of virus replication were inversely correlated with the mitotic activity. bFGF displayed a potent inhibitory effect on its own which disappeared at concentrations below 1 ng/ml (Figure 2.10). Interestingly, the continual presence of bFGF has been reported to inhibit the differentiation of O-2A progenitors into oligodendrocytes (McKinnon et al., 1990). No such inhibitory influence of PDGF and bFGF on virus production was evident with L-2 cell cultures allowed to grow to confluency under identical conditions prior to inoculation, demonstrating

Figure 2.9. Effects of bFGF and PDGF on the replication of JHMV in O-2A lineage enriched cultures. O-2A lineage cells derived from 9 D.I.V./P9 mixed glial cultures were plated at 2.5 x 10^5 cells/cm^2 and grown for 48 hrs. in O1/T3 or O1/T3 supplemented with 10 ng/ml bFGF, or PDGF, or bFGF + PDGF before inoculation with JHMV at a m.o.i. of 2. Data are the means of titers ± SD from triplicate cultures and are representative of 3 independent experiments.

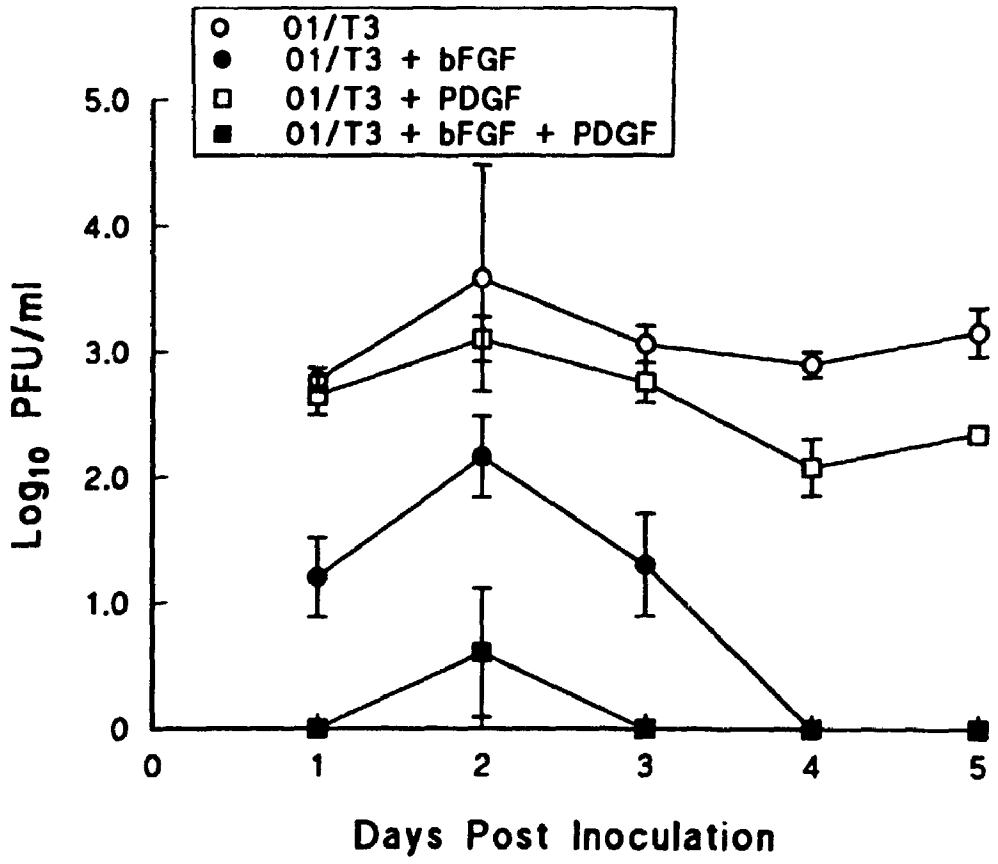
01/T3
01/T3 + bFGF
01/T3 + PDGF
01/T3 + bFGF + PDGF
5.0
4.0
3.0
2.0
1.0
0
Log10 PFU/ml
0
1
2
3
4
5
Days Post Inoculation

Figure 2.10. JHMV replication in O-2A lineage cell cultures in response to bFGF concentration. O-2A lineage cells derived from 8 D.I.V./P9 mixed glial cultures were plated at approximately 1.5 x 10^5 cells/cm^2 in 24 well culture dishes and grown for 24 hours in $DMEM_{10}$ before switching to medium O1/T3 or O1/T3 supplemented with the indicated concentrations of bFGF. Triplicate wells were employed for each condition tested. Fresh bFGF was added daily at the appropriate concentrations. After 48 hours growth under each condition, the cultures were inoculated with JHMV at a m.o.i. of 10. Data are the mean titers for each condition.

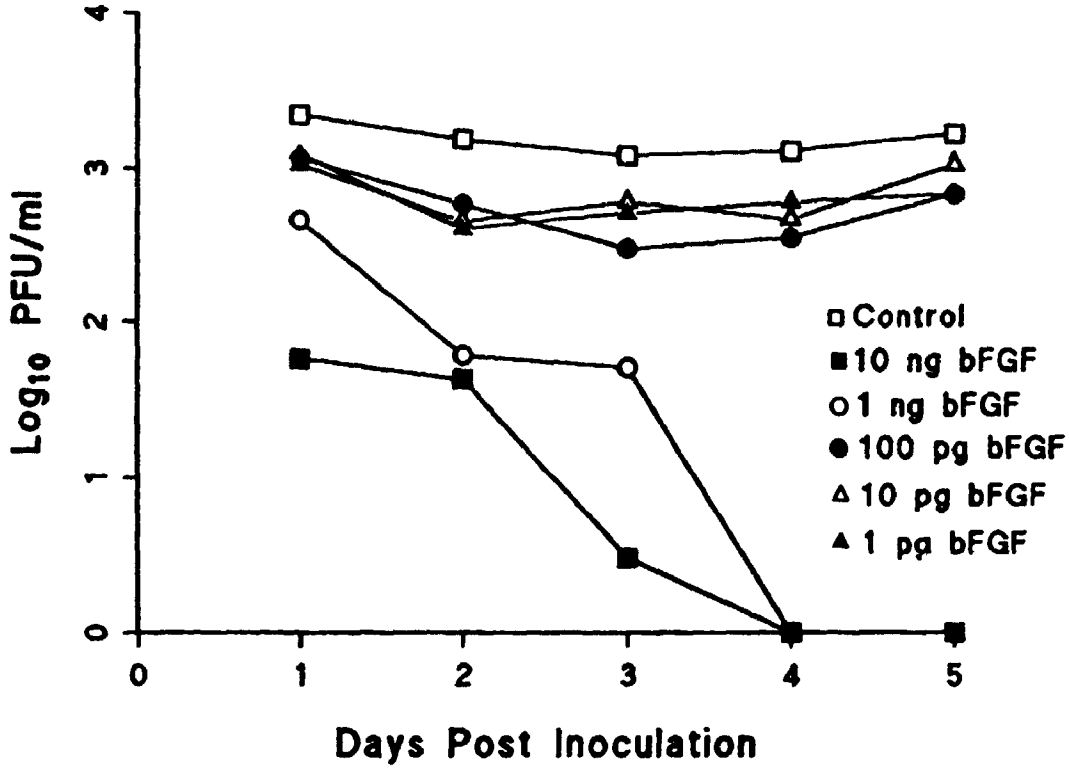
Log10 PFU/ml
0
1
2
3
4
0
1
2
3
4
5
Days Post Inoculation
Control
10 ng bFGF
1 ng bFGF
100 pg bFGF
10 pg bFGF
1 pg bFGF

that these cytokines affected the glia specifically (Table 2.4).

In order to better define the relationship between the virus inhibitory state and O-2A cell differentiation, mixed cultures at 5 D.I.V./P5 were used for isolating O-2A progenitor cells. At this stage the majority of surface adherent cells were bipolar or with few processes and had a $A2B5^+/GC^-$ phenotype (Table 2.1). After plating the released cells at 1.25×10^5 cells/cm^2 on glass coverslips coated with poly-L-lysine and fibronectin (1 μg fibronectin/cm^2), cultures were established in O1/T3 plus 10 ng/ml each of PDGF and bFGF [poly-L-lysine and fibronectin were used to enhance attachment and hence optimize survival of the O-2A cells after transfer from mixed cultures at a more juvenile stage, in accordance with Hunter and Bottenstein, (1990)]. Figure 2.11.A illustrates the appearance of a typical culture enriched for O-2A progenitors, 24 hours after plating. Approximately 90% of the cells were bipolar or of a simple multipolar morphology and were $A2B5^+/O4^-$. Only about 1% of the cells were GC^+, while the remainder were predominantly type-1 astrocytes. Some of these cultures enriched for progenitors were maintained continuously in the presence of PDGF and bFGF (replenished every 36 hours), while others were switched at intervals to O1/T3 devoid of cytokines. Inoculation with JHMV, at a m.o.i. of 1, was carried out at P6, 8, 9, and 13. Inoculation with VSV as the control virus, was carried out at identical time points. During continuous presence of combined PDGF and bFGF,

Figure 2.11. Growth factor regulation of oligodendrocyte differentiation from O-2A progenitors. O-2A progenitors were isolated from 5 D.I.V./P5 mixed glial cultures, seeded onto poly-L-lysine and fibronection coated glass coverslips and grown in medium O1/T3 supplemented with 10 ng/ml bFGF + PDGF. (A1) Phase contrast image of cultures highly enriched for O-2A progenitors 24 hours after plating demonstrating the typical bipolar morphology of the cells. (A2) Separate field and at higher magnification than in A1 demonstrating A2B5 immunoreactivity characteristic of O-2A progenitors. (B) Three to four days following the removal of bFGF + PDGF, most of the cells acquired a more complex, multipolar morphology and sulfatide expression on their surface membranes as determined on the basis of immunoreactivity against MAb O4. This stage has been referred to as the pro-oligodendrocyte. After 4 to 7 days of growth factor deprivation, cells acquire progressively more complex morphologies accompanied by GC immunoreactivity (C) followed by MBP immunoreactivity (D). A1 x 650, A2 x 950, B, C and D x 2,000.

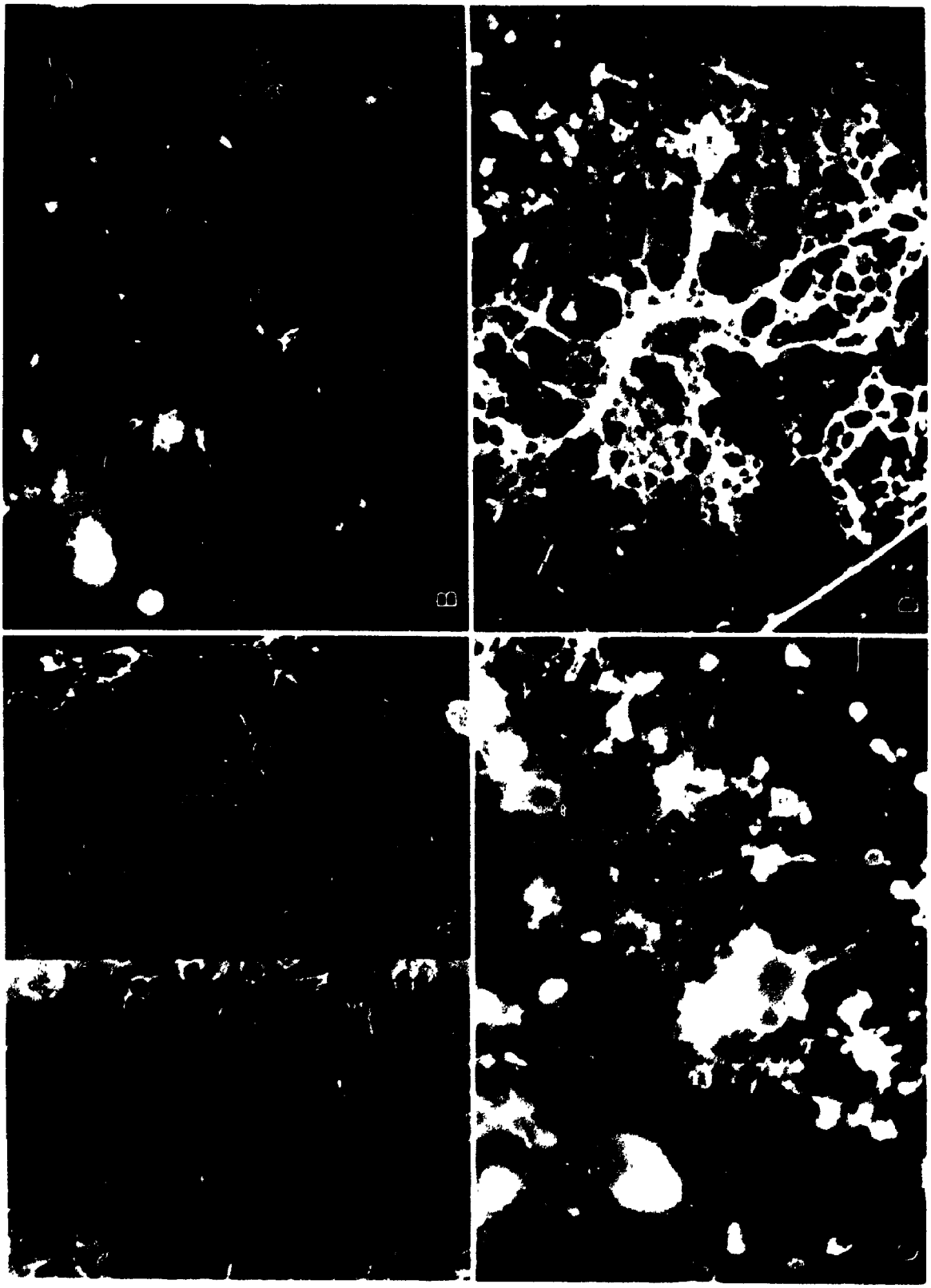

the O-2A progenitors continued to be mitotically active and possessed an A2B5$^+$/GC$^-$ phenotype as previously reported (Bolger et al., 1990; McKinnon et al., 1990), and concomitantly resisted infection by JHMV, as judged by absence of viral antigen and released virus. By contrast, replication of VSV was unaffected (Table 2.4), demonstrating, as in the case of MTCM and ACM, the specificity of cytokines in suppression of JHMV. Upon withdrawal of the cytokines only a small fraction of cells died. The surviving cells differentiated as determined by shifts in expression of stage specific phenotypic markers and acquisition of more complex morphologies (Figure 2.11.B to D). Four days after the removal of cytokines (P13), O-2A lineage cells were A2B5$^+$/O4$^+$ and weakly GC$^+$. By 7 days (P16), GC$^+$ and MBP$^+$ cells were present at 12.0 ± 4.1 and 15.4 ± 7.8 cells/500 x microscopic field respectively. It must be stressed however, that the progressive differentiation of O-2A cells induced by cytokine removal was by no means synchronous as has been reported by others (Temple and Raff, 1986; Goldman and Vaysse, 1991) and as illustrated in Figure 2.12. By contrast, the continuous presence of bFGF and PDGF prevented the appearance of GC and MBP as previously reported (Bolger et al., 1990; McKinnon et al., 1990), but not of membrane sulfatide recognized by MAb O4. Stellate GFAP$^+$ cells, some with A2B5 surface immunoreactivity, were also present in these cultures. This shift in phenotype was correlated with enhanced production of JHMV. This was most striking in cultures inoculated 4 days

Figure 2.12. Asynchrony of sulfatide and galacosyl cerebroside acquisition by O-2A progenitor cells following removal of bFGF + PDGF. Cultures enriched for O-2A progenitors were grown for 5 days in medium O1/T3 supplemented with bFGF + PDGF before switching to O1/T3 without cytokines. Three days following cytokine deprivation, differentiation of the progenitors was assessed on the basis of acquisition of membrane sulfatide and galactocerebroside. (A) Sulfatide expression was determined immunocytochemically using MAb O4 specific for sulfatide and FITC-conjugated secondary antibody. Note the heterogeneity in morphology of the $O4^+$ cells. (B) The identical field to that in panel A was immunocytochemically stained for GC using a rabbit polyclonal antiserum specific against galactosylcerebroside and Texas red-conjugated secondary antibody. Note that only a subset of the $O4^+$ positive cells are also GC^+ (arrows in panels A and B).
A and B x 1,800.

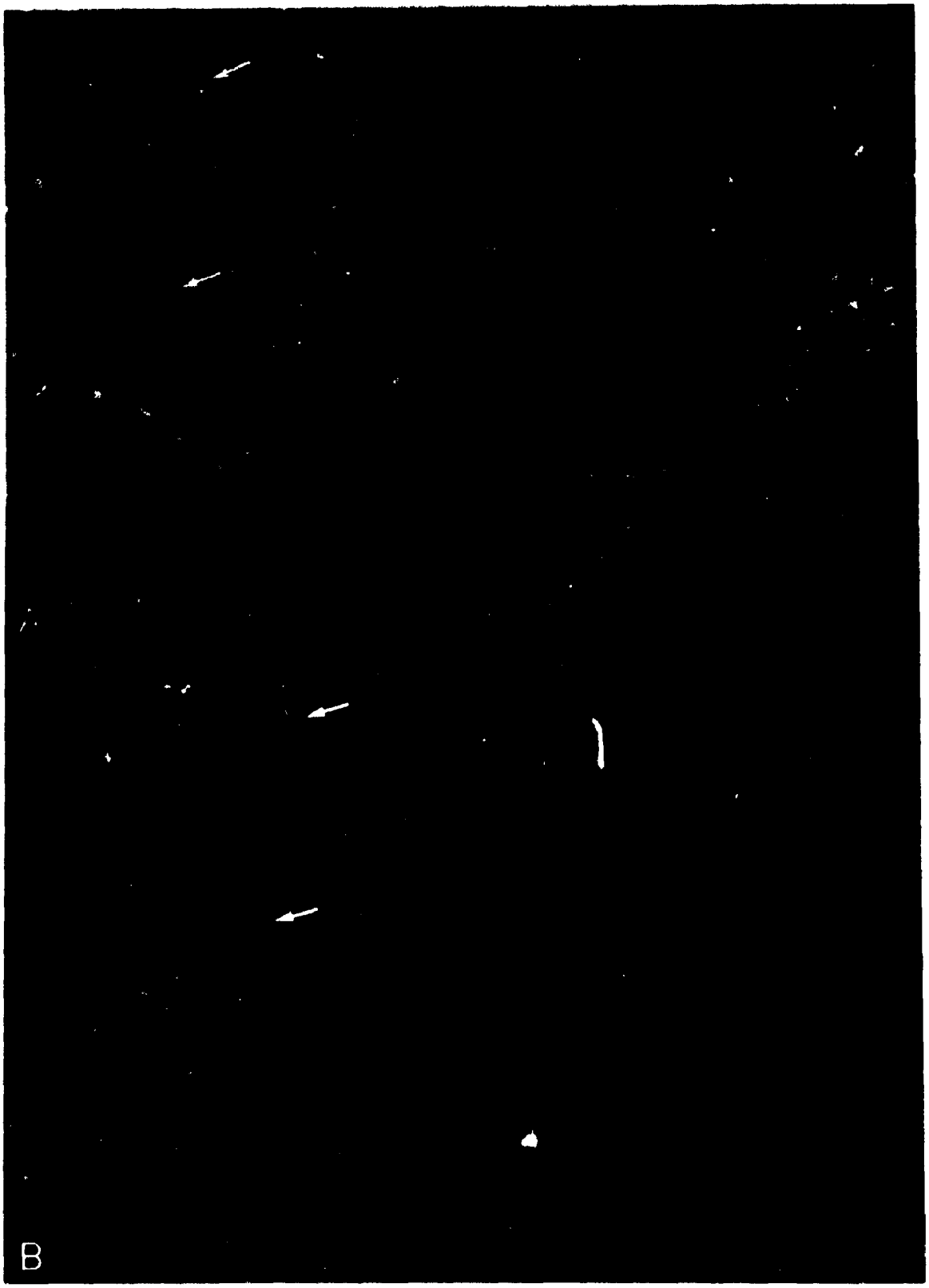
B

following removal of cytokines (Table 2.4). These cultures produced 3000 fold more virus than identically aged cultures continuously exposed to cytokines. Dual immunolabelling revealed that N antigen of JHMV was associated most frequently with GFAP$^+$ cells, and less frequently with GC$^+$ cells (Figure 2.13). Some of the JHMV N$^+$ cells were negative for both glial markers, as well as for the oligodendrocyte-specific MBP. Thus, repression of differentiation in O-2A progenitors was associated with a refractive state to JHMV infection, whereas progression towards more differentiated states correlated with enhanced permissiveness.

2.3.6 The Cellular Basis for Resistance of O-2A Progenitor Cells to Infection with JHMV.

The foregoing results prompted us to ask what cellular parameters make certain stages of the O-2A lineage more susceptible to infection with JHMV than others? Previous studies with terminally differentiated rat oligodendrocytes (Beushausen et al., 1987), rat C6 glioma (Van Dinter and Flintoff, 1987; Kooi et al., 1991) and African green monkey kidney or Vero cells (Kooi et al., 1991) suggested that the basis for JHMV resistance by these cells resulted from a defect involving the early stages of the infectious process. In all three cases the defect appeared to involve a stage subsequent to virus attachment but prior to the expression of viral genes. Experiments directed at addressing the possibility that JHMV resistance by O-2A progenitors might

Figure 2.13. JHMV infected cells in O-2A lineage enriched cultures. These cells were isolated from mixed glial cultures at 5 D.I.V./P5 as shown in Figure 2.11. They were then grown in O1/T3 supplemented with bFGF + PDGF until 9 D.I.V./P9, at which time they were switched to O1/T3 without cytokines and maintained for an additional 4 days before inoculation at P13 with JHMV. (A) N immunoreactivity in a cell 3 dpi with JHMV. (B) The same cell as in (A) reacted with rabbit> GC followed by TR-conjugated goat> rabbit IgG. (C) N immunoreactive cell 3 dpi with JHMV. (D) The same cell as in (C) demonstrating GFAP immunoreactivity by rabbit> GFAP followed by TR-conjugated goat> rabbit IgG. n are the nuclei in the same cells shown in (A) versus (B) and (C) versus (D). Arrows in (C) and (D) point towards a $N^+/GFAP^+$ cell. A, B, C and D x 2,000.

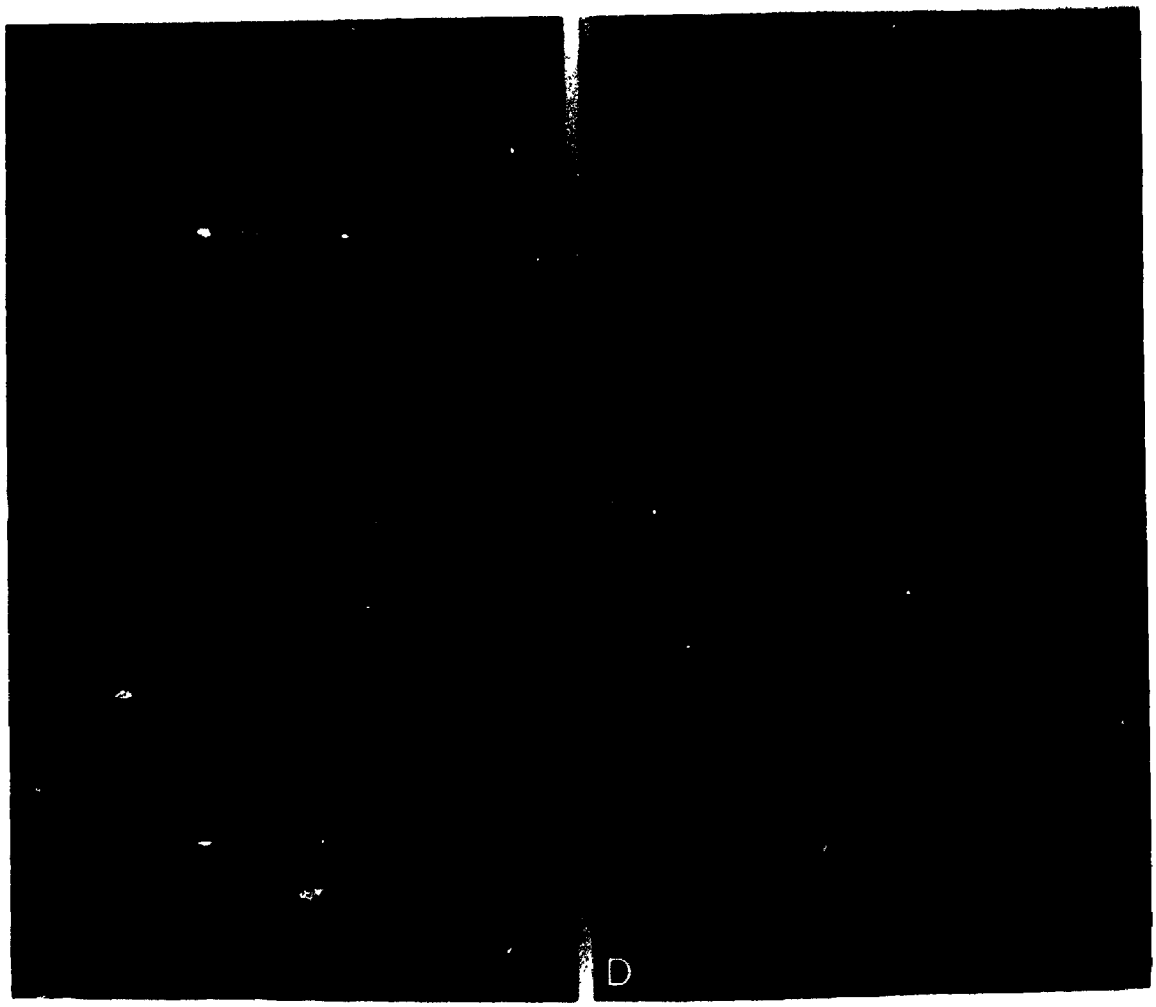
D

involve a similar stage or stages of virus-cell interactions were thus carried out.

O-2A progenitors grown in medium O1/T3 supplemented continuously with PDGF + bFGF or after 3 days of cytokine deprivation to allow differentiation of the progenitors to procede, were assessed for their ability to adsorb JHMV using isotopically labelled and unlabelled virus binding assays. Permissive L-2 and OBL21 neuronal cultures were used as positive controls. Roughly identical numbers of cells were used in test and control cultures. Adsorption was carried out at an m.o.i. of ~ 2 for 60 minutes at 4°C. A previous study demonstrated that these conditions resulted in saturated binding of both L-2 and C6 glioma cells by JHMV (Van Dinter and Flintoff, 1987). After the removal of non-specifically bound virus, binding was evaluated using the procedures described in section 2.2.12. As Table 2.5 illustrates, regardless of the assay employed, JHMV bound to all cell types with similar levels of saturation. Only 1 to 5% of the input virus was associated with virus-cell complexes, in agreement with previously published findings (Flintoff and Van Dinter, 1989), suggesting that this step is likely not the discriminating one responsible for JHMV resistance by O-2A progenitors. It should be further noted that in O-2A cultures permissive for JHMV, only ~ 1% of the total cell population is capable of forming infectious centers, indicating that the binding data are reasonably accurate.

Though controversy exists over the mode by which MHV

Table 2.5

Adsorption of JHMV to Permissive and Non-Permissive Cell Types[a]

Methodology	Cell type	Input inoculum	Adsorbed inoculum	Percentage adsorbed
Radiolabelled virus	O-2A +bFGF+PDGF	4380 cpm (~$2x10^6$ pfu)	27 cpm 22 cpm 33 cpm	0.6 ± 0.2%
	O-2A control	4380 cpm (~$2x10^6$ pfu)	38 cpm 60 cpm 56 cpm	1.2 ± 0.3%
	OBL21	4380 cpm (~$2x10^6$ pfu)	45 cpm 68 cpm 88 cpm	1.5 ± 0.5%
Unlabelled virus	O-2A +bFGF+PDGF	$4x10^6$ pfu $4x10^6$ pfu $3x10^6$ pfu	$9x10^4$ pfu $1x10^5$ pfu $9x10^4$ pfu	2.3 ± 0.1%
	O-2A control	$3x10^6$ pfu	$3x10^4$ pfu	1.0%
	L-2	$3x10^6$ pfu $3x10^6$ pfu $3x10^6$ pfu	$2x10^5$ pfu $2x10^5$ pfu $4x10^4$ pfu	4.9 ± 3.1%

[a] $2x10^6$ cells of each type situated in 35 mm petri dishes were exposed to JHMV. Input inoculum measured either in cpm's for [^{3}H]uridine labelled virus or in pfu's for unlabelled virus was adsorbed to the cells for 60 minutes at 4°C with continuous rocking. Cells were then washed to remove the unadsorbed inoculum and adsorbed virus quantitated on the basis of cell retained cpm's or pfu's.

penetrates target cells (Chapter 1, section 1.3), it was decided that an assay designed to evaluate the endocytic pathway of internalization could nevertheless prove informative. Hence, internalization of JHMV by the endocytic route in 1) O-2A cells grown in the presence of PDGF + bFGF, 2) O-2A cells grown after a period of cytokine deprivation, and 3) fully permissive L-2 cells was compared. Cultures containing identical numbers of cells of each type were exposed to JHMV, washed, incubated at 37°C for various periods of time to allow internalization of surface bound virus, treated with proteinase K to remove residual surface bound virus and then cells disrupted and assayed for infectious or nonuncoated virus. As Figure 2.14 illustrates, no discernible difference existed in the internalization of virus by the three cell types.

Since JHMV adsorption and endocytic internalization did not appear to differ among the cell types tested, it was decided to investigate whether viral RNA synthesis might be the discriminating step that distinguishes the permissive more differentiated from the non-permissive progenitor stages of the O-2A lineage. Hence, at 24, 48 and 72 hours after the inoculation of O-2A cultures, synthesis of JHMV-specific RNA was assessed by <u>in situ</u> hybridization. Comparison was made between O-2A cells grown in the continuous presence of PDGF + bFGF and after 3 days of cytokine deprivation. As Figure 2.15 shows, though some JHMV-specific RNA synthesis was evident in O-2A cells grown in the continuous presence of cytokines at 24

Figure 2.14. Internalization of JHMV into O-2A and L-2 cells. O-2A enriched cultures grown in the continuous presence of bFGF + PDGF (10 ng/ml), O-2A enriched cultures grown for 72 hours without cytokines, and L-2 cell cultures were inoculated with JHMV at a m.o.i. of approximately 2. Adsorption was carried out at 4 °C for 45 minutes before washing away the unattached virus with cold PBS and incubating the cultures at 37°C. After 0, 15, 30 and 60 minutes at 37°C, non-internalized virus was removed from the cell surfaces with proteinase K before disrupting the cells and assaying for proteinase K-resistant, non-uncoated, internalized virus by plaquing on L-2 cell monolayers.

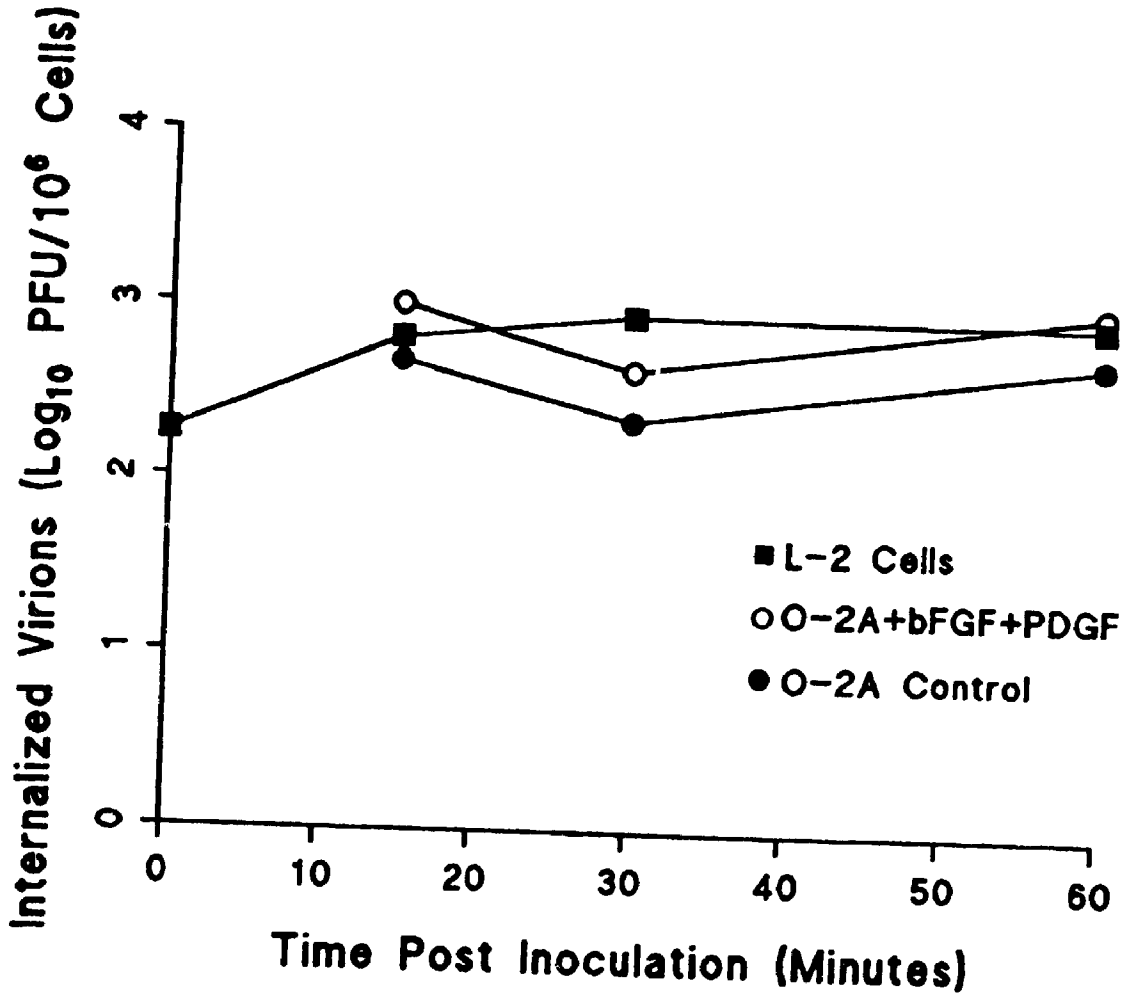
Internalized Virions (Log_{10} PFU/10^6 Cells)
0
1
2
3
4
0
10
20
30
40
50
60
Time Post Inoculation (Minutes)
L-2 Cells
O-2A+bFGF+PDGF
O-2A Control

Figure 2.15. JHMV-specific RNA synthesis in cytokine supplemented and control O-2A cultures. Cultures enriched for O-2A progenitor cells were established from 5 D.I.V./P5 mixed glial cultures. Half the cultures were grown in medium O1/T3 continuously supplemented with 10 ng/ml each of bFGF and PDGF, while the other half were deprived of these cytokines beginning 72 hours prior to inoculating with JHMV at a m.o.i. of approximately 5. At 24, 48 and 72 hours postinoculation, the cells were thoroughly washed with ice cold PBS, removed from the plasticware and then gently monodispersed in ice cold PBS before determing the cell concentration. Serial twofold dilutions of whole cell suspensions, beginning with 2 x 10^5 cells, were spotted onto nitrocellulose using a 96-well Schleicher & Schuell manifold filtering apparatus, followed by fixation and proteinase K digestion in preparation for *in situ* hybridization with ^{32}P-labelled pg344. This probe contains an 1800 bp MHV-A59 cDNA insert encoding genes 5 and 6 as well as the intergenic regions preceding genes 5, 6 and 7. Equivalent numbers of uninoculated cells were used as a negative control.

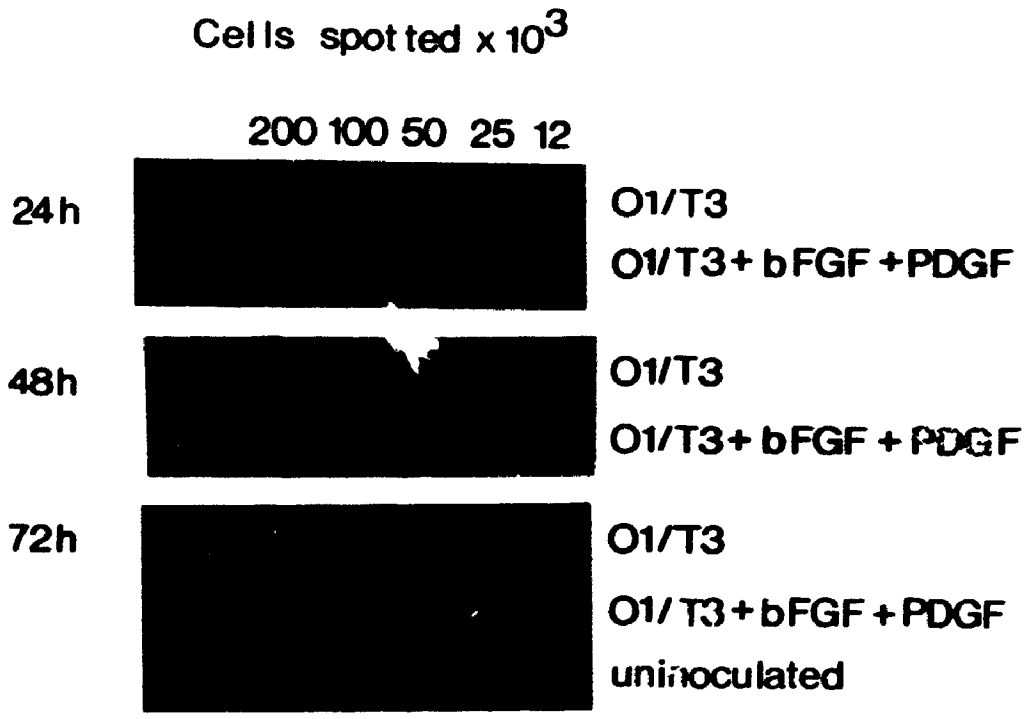
Cells spotted x 10^3
200 100 50 25 12
24h
48h
72h
O1/T3
O1/T3+bFGF+PDGF
O1/T3
O1/T3+bFGF+PDGF
O1/T3
O1/T3+bFGF+PDGF
uninoculated

hours post-inoculation, the level was only - 25% of that found in cells that had been cytokine deprived. Furthermore, JHMV-specific RNA expression was not maintained in cytokine treated cells beyond 24 hours post-inoculation whereas it was in cytokine deprived cells. These data suggest that JHMV non-permissiveness of O-2A progenitors may result from the infection being aborted at a stage just prior to or involving viral RNA synthesis.

In view of previous results demonstrating that cultured oligodendrocytes could be made JHMV non-permissive by accelerating their differentiation through pharmacologic manipulation of their cAMP secondary messenger system (Beushausen and Dales, 1985; Beushausen et al., 1987), the present findings imply that among O-2A lineage cells, susceptibility to JHMV may be restricted to discrete developmental stages. Furthermore, the basis for this resistance appears to involve a defect associated with the early steps in the interaction between virus and cell. These findings may be pertinent to the age-dependent induction of demyelinating disease by JHMV observed with suckling rats (Sorensen et al., 1980, 1982).

2.4 Discusssion.

This study describes an experimentally accessible, in vitro system potentially capable of providing further insight into the mechanisms by which JHMV induces demyelinating

disease in susceptible rats. It proved particularly useful in identifying initial CNS target cells, as well as subsequent virus-host interactions that may explain the observed temporal shift in disease character as a function of age at inoculation. Earlier studies (Beushausen and Dales, 1985; Beushausen et al., 1987) recognized oligodendrocyte differentiation as an important determinant controlling JHMV multiplication. Since differentiation likely entails an interplay between intrinsic cellular and extrinsic, epigenetic determinants involved in modulating a particular developmental program, use of a defined culture medium aided in the systematic evaluation of developmental factors potentially involved in regulating viral permissiveness in O-2A lineage cells.

Unexpectedly, serum-free culture conditions which enhanced the survival of neurons in mixed telencephalic cultures were also associated with enhanced JHMV replication, illuminating the importance of neurons in the establishment of JHMV infections under organotypic conditions. Immunocytochemical, electron microscopic, and immune-mediated cytolysis studies supported this contention. On the basis of cellular morphology and co-localization of viral N and neuron NSE antigens, it was evident that infection predominated in forebrain neurons within the first 24 to 48 hours post-inoculation. This was the case in cultures inoculated at P6, P10 or P17. Absence of NSE from infected neurons beyond 48 hours post-inoculation may have resulted from infection-

induced leakage, increased turnover and/or suppression of enzyme synthesis. Others have also documented negative effects of MHV on host macromolecular metabolism (S. Stohlman, personal communication). The clear and precise association between JHMV nucleocapsid material and the microtubules within neurites, revealed by electron microscopy, corroborated immunocytological observations. Such an interaction, not previously reported to our knowledge, may have important implications for understanding how JHMV is disseminated and contributes to neuropathogenesis in the CNS.

The resistance to JHMV infection evident with mixed telencephalic cultures grown continuously in $DMEM_{10}$, was unexpected since these cultures contain an abundance of O-2A lineage cells shown previously to be permissive targets for this virus (Beushausen and Dales, 1985). Curiously, to establish infection in these cells, it was necessary to separate them from the others present in mixed glial cultures. Furthermore, in dissociated telencephalic cultures maintained in defined medium, fewer than 25% of all cells manifesting an infection during the initial 24 to 48 hours were glia, suggesting that <u>in vitro</u>, a discrete albeit minor population of JHMV permissive O-2A lineage cells exists, among which virus susceptibility may somehow be connected with their state of differentiation. In this regard, MTCM and ACM which promoted mitogenesis and presumably blocked or delayed differentiation of O-2A cells, also caused a reduction of 10 to 100 fold in virus yields relative to those in unconditioned

O1/T3 medium. These findings are consistent with a brief mention (Van Berlo et al., 1989) of resistance to JHMV by A2B5$^+$ O-2A progenitors in primary dissociated cultures from Wistar rats. Our assumption that O-2A glia in mixed cultures are made non-permissive by factors released into the medium by other cell types, was supported by demonstrating that PDGF and bFGF while prolonging the mitotically active, undifferentiated state, also conferred reversible resistence to JHMV.

Besides maintenance of mitogenesis, treatment of O-2A lineage cells with PDGF or bFGF produces other phenotypic effects including: 1) induction of cerebroside sulfotransferase (CST) activity (Fressinaud et al., 1992) but inhibition of 2',3'-cyclic nucleotide 3'-phosphodiesterase (CNP) activity (Besnard et al., 1989) and myelin basic protein (MBP) expression (Besnard et al., 1989; McKinnon et al., 1990) by bFGF and 2) and induction of the migration of progenitors by PDGF (Noble et al., 1988; Armstrong et al., 1990).

In addition to PDGF and bFGF, a number of uncharacterized factors, produced by either primary neurons or neuronal cell lines have been also been shown mitogenic for O-2A progenitor cells (Hunter and Bottenstein, 1989, 1990; Levine, 1989; Gard and Pfeiffer, 1990). The rat CNS neuronal cell line B104 produces a soluble factor or factors shown to directly delay the differentiation and promote the proliferation of rat O-2A progenitors (Hunter and Bottenstein, 1989, 1990). Louis et al. (1992) reported that the mitogenic effects of B104 conditioned medium on a spontaneous O-2A progenitor-derived permanent cell

line, CG-4, could be fully substituted by the combination of bFGF and PDGF. Although the exact nature of the mitogenic factor(s) produced by this cell line remains unresolved, Thangnipon et al. (1989) indicated that the active fraction possessed an estimated molecular weight of 44 kDa as well as having heparin-binding activity. Levine (1989) and Gard and Pfeiffer (1990) both reported on the ability of medium conditioned by young cerebellar interneurons to promote the survival and proliferation of optic nerve derived O-2A cells. Antibodies to PDGF were reported to only partially block this mitogenic stimulus; moreover, the production of the factor(s) responsible for this effect was hypothesized to be developmentally regulated since older interneuron cultures appeared incapable of its production (Levine, 1989). Just as interesting, the data suggested that the targets for this neuronal-derived mitogen were not $A2B5^+/O4^-$ bipolar progenitors, but rather the $O4^+/GC^-$ immediate precursors to oligodendrocytes, implying that different stages of this lineage may respond to different mitogenic cues (Gard and Pfeiffer, 1990).

In light of the observed synergy between bFGF and PDGF driving the extended division of O-2A progenitor cells in vitro, and the apparent widespread distribution of these two growth factors within the CNS (Gonzalez et al., 1990; Sasahara et al., 1991; Yeh et al., 1991; Gomez-Pinilla et al., 1992; Woodward et al., 1992), one must ask what mechanisms permit O-2A progenitors to differentiate into oligodendrocytes? The

possibilities which have been proposed are: 1) mechanisms may exist for either down-regulating expression of bFGF, sequestering bFGF, or modulating the responsiveness of cells to bFGF (McKinnon et al., 1990) and 2) some as yet uncharacterized mechanism exists for inducing dividing progenitors to actively differentiate into oligodendrocytes at appropriate times (Bolger et al., 1990). Evidence actually exists to support both proposals. bFGF mRNA levels change with time in the developing rat CNS. The reports in this regard however, have been inconsistent. Ernfors et al. (1990) found that bFGF mRNA levels in rat brain were twice as high in the period beginning E16 through to the first postnatal week as compared with the second postnatal week through to adulthood. In contrast, Riva and Mocchetti (1991) found that bFGF mRNA levels were low in newborn rats but increased thereafter to reach peak levels around P21. Akio et al. (1991) examined the developmental expression of FGF-receptor mRNA in the rat at a number of embryonic and postnatal time points. During embryonic stages FGF-receptor mRNA was found predominantly within the ventricular zone, the birth place of mitotically active neuroepithelial precursors. Postnatally, receptor transcripts were localized primarily to specific neuronal populations which included hippocampal neurons, the deep cerebellar nuclei, the locus ceruleus and the trigeminal motor nucleus. Thus, down-regulation of FGF-receptor expression may occur in some cell populations subsequent to differentiation while being maintained in others. Proteoglycans which are

important extracellular matrix components and shown to be produced by cultured astrocytes (Ard and Bunge, 1988; Johnson-Green et al., 1991) bind and thereby modulate the effects of bFGF and other heparin-binding growth factors. Furthermore, Yayon et al. (1991) demonstrated that cell membrane heparan sulfate proteoglycan molecules or heparin was necessary for the binding of bFGF to its high affinity receptor (see Ruoslahti and Yamaguchi, 1991; Klagsbrun and Baird, 1991 for reviews). All of the above may prove important in modulating the effects of bFGF on O-2A progenitors.

Several extrinsic factors have been implicated in driving the developmental program of O-2A lineage precursors toward more differentiated phenotypes. One of these is insulin-like growth factor I (IGF-I) also known as somatomedin C (see appendix). Type I IGF receptors have been identified on oligodendrocytes and O-2A progenitors by [^{125}I]IGF-I binding and cross-linking studies (McMorris et al., 1986). Low concentrations of IGF-I (100 ng/ml) and high concentrations of insulin (50 μg/ml) are able to induce a 6 and 60 fold increase in GC$^+$ oligodendrocyte numbers in serum-supplemented and serum-free culture conditions respectively. The effect of insulin was explained by the ability to cross-react with type I IGF receptors at high concentrations. However, a subsequent report by Evercooren et al. (1991) indicated that at birth, O-2A lineage cells express both insulin and IGF-I receptor transcripts, but relatively more of the former. Thus, insulin and IGF-I may potentially modulate O-2A cell metabolism via

cognate as well as cross-reactive interactions. The mechanism by which either insulin or IGF-I increase oligodendrocyte numbers has been carefully analyzed. McMorris and Dubois-Dalcq (1988) found that in the absence of IGF-I, A2B5$^+$ O-2A progenitors growing in a chemically defined medium on a bedlayer of X-irradiated type-1 astrocytes, accumulated at the O4$^+$/GC$^-$ stage. The addition of IGF-I allowed transition to the O4$^+$/GC$^+$ stage suggesting direct involvement by this cytokine. Furthermore, IGF-I also appeared to increase the proliferative rate of these O4$^+$/GC$^-$ intermediate precursors. Mozell and McMorris (1991) also reported that IGF-I and high concentrations of insulin were able to increase the number of oligodendrocytes that developed and the amount of myelin that accumulated in rat brain aggregate cultures prepared from E16 rats. Evidence that IGF-I is important for normal myelination in vivo has recently been documented in a study which examined the expression of IGF-I and its receptor during remyelination following an episode of cuprizone-induced demyelination in mice (Komoly et al., 1992). In demyelinated white matter, IGF-I mRNA and protein were localized in situ to hypertrophic GFAP$^+$ astrocytes, while IGF-I receptor immunoreactivity was localized to O4$^+$ morpholcgically immature oligodendroglia.

Rat oligodendrocyte precursors express the cell surface receptor for reovirus type 3 (Cohen et al., 1990). O-2A lineage precursors express this receptor coincident with the expression of membrane sulfatide, (detected by the MAb O4) but prior to the expression of GC, the definitive phenotypic

marker for oligodendrocytes. $O4^+$ cells are capable of differentiating into either oligodendrocytes or type-2 astrocytes when grown under the appropriate culture conditions and therefore can still be considered bipotential (Trotter and Schachner, 1989). The reovirus type 3 receptor appears biochemically and antigenically similar to the β_2-adrenergic receptor (Ventimiglia et al., 1987). Treatment of rat optic nerve derived O-2A progenitors with anti-reovirus type 3 receptor antibodies induced GC and MBP expression along with the loss of the A2B5 marker after a period of exposure as short as 4 hours (Cohen et al., 1990 and 1991). The similarity between the reovirus type 3 and β_2-adrenergic receptors is theoretically a very interesting one. Vartanian et al. (1988) reported that sheep brain oligodendrocytes increased their expression of β-adrenergic receptors coupled to adenylate cyclase following adhesion to a poly-L-lysine coated substratum. Adhesion of oligodendrocytes to the substratum in turn led to the activation of diacylglycerol and cAMP secondary messenger systems resulting in the phosphorylation of MBP and CNPase by protein kinase A and C respectively. The cAMP second messenger system has also been demonstrated to play an important role in the differentiation of rat oligodendrocyte precursors (McMorris, 1983; Beushausen and Dales, 1985; Raible and McMorris, 1989; Raible and McMorris, 1990). The cAMP analogue dibutyryl cAMP (dbcAMP) inhibited DNA synthesis in $A2B5^+$ O-2A progenitors and accelerated their differentiation into oligodendrocytes (Raible and McMorris,

1989). Furthermore, immature oligodendrocytes have been shown to have a G protein-coupled adenylate cyclase system that can be pharmacologically modulated to accelerate oligodendrocyte differentiation (Raible and McMorris, 1990).

Levi et al. (1991) have presented evidence that a high molecular weight (>30 kDa) autocrine factor produced within high density O-2A cultures may be responsible for inducing the rapid differentiation of immature O-2A cells into oligodendrocytes. In this regard, Bansal et al. (1988) had earlier reported that treatment of mixed, E19-21, rat telencephalic cultures with the MAb O4, which reacts against cell surface sulfatide (Bansal et al., 1989) expressed on oligodendrocyte precursors (Dubois-Dalcq, 1987; Trotter and Schachner, 1989), induced aggregation and differentiation of oligodendrocytes. Time-course studies of CNPase specific activity and MBP expression demonstrated that the respective rate and accumulation were both significantly increased in response to O4 MAb treatment (Bansal et al., 1988). The authors proposed two models that could account for the observed effects. In the first model, the binding of MAb O4 to sulfatide was likened to a ligand:receptor interaction resulting in a signal transduction cascade within the cell. In support of this model, the binding of antibodies reactive against either GC (Dyer and Benjamins, 1990, 1991) or sulfatide (Dyer and Benjamins, 1991) have been shown to induce Ca^{++} influx in cultured mouse oligodendrocytes. Another glycosphingolipid, GM_1, has previously been shown to

participate in receptor and signal transduction events by virtue of its ability to couple cholera toxin binding with increased adenylate cyclase activity (Fishman, 1982). In the second model, MAb O4 may indirectly stimulate oligodendrocyte differentiation by virtue of its ability to induce aggregation of O-2A cells. Differentiation may result from the alteration of intracellular metabolism consequent to the cognate effects of homotypic cell aggregation, the exclusion of environmental factors which normally inhibit differentiation, or the increase in the local concentration of an autocrine factor which positively enhances differentiation. The foregoing should clearly emphasize the changing responsiveness of O-2A lineage cells to environmental cues, which in turn may have important consequences for virus-cell interactions.

Previous reports indicating that GFAP$^+$ cells in mixed brain cultures derived from perinatal Wistar Lewis rats were infected with JHMV (Massa et al., 1986; Massa et al., 1988; Van Berlo et al., 1989) may appear to be in conflict with earlier (Beushausen and Dales, 1985), and present documentation of resistance by purified type-1 astrocytes. Observations from the present study can account for this apparent discrepancy if one recognizes that type-1 astrocytes and O-2A lineage cells, from which type-2 astrocytes are derived, arise from two distinct cell lineages within the CNS (Raff et al., 1984; Raff, 1989 for review). Phenotypic plasticity, exemplified by the ability of cells of the O-2A lineage to co-express oligodendrocytic and astrocytic markers

has been documented *in vivo* and *in vitro* (Godfraind *et al.*, 1989; Ingraham and McCarthy, 1989; Kim, 1990; Lillien and Raff, 1990; Vaysse and Goldman, 1990). Therefore, the viral antigen$^+$/GFAP$^+$ cells may either be those expressing a type-2 astrocytic phenotype at the time of infection or, O-2A bipotential cells susceptible to JHMV at an interval between the proliferative and terminally differentiated states. This may explain why both oligodendrocytes and cells with an astrocytic phenotype were observed manifesting JHMV infection in O-2A enriched cultures as well as in primary mixed telencephalic cultures employed here and by others (Massa *et al.*, 1986, 1988). Since the conditions we imposed on O-2A lineage cells were not conducive to acquisition of a stable type-2 astrocytic phenotype (Lillien and Raff, 1990; Lillien *et al.*, 1990), it is possible that the infected GFAP$^+$ cells were expressing GFAP only transiently, or that the vary process of infection somehow induces GFAP expression perhaps by a manner similar to that of other *in vitro* environmental stimuli effecting the type-2 astrocytic phenotype (Lillien and Raff, 1990). Alternatively, the astrocytes supporting JHMV infection in these cultures may derive from a lineage that is distinguishable from type-1 and type-2 astrocytes. Fok-Seang and Miller (1992) have recently identified a process-bearing astrocyte whose progenitor possesses the morphologic, antigenic and migratory properties of bipotential O-2A progenitors. These progenitors proliferate in response to serum and PDGF but differentiate exclusively into astrocytes.

Though this astrocyte was identified in rat spinal cord cultures, cells with similar morphologic and antigenic characteristics have also been identified in rat cortical cultures (Vaysse and Goldman, 1992). Given the fact that attempts to infect highly enriched type-2 astrocyte cultures with JHMV were unsuccessful (data not shown), this explanation may be worthy of further consideration.

The previous demonstration that process-bearing O-2A lineage cultures become irreversibly non-permissive for JHMV when pretreated with dbcAMP, correlates with the accelerated terminal differentiation into oligodendrocytes (McMorris, 1983; Beushausen and Dales, 1985; Beushausen et al., 1987; Raible and McMorris, 1989). This irreversible effect of dbcAMP should be contrasted with present data showing reversibility to an infectable state upon removal of PDGF and bFGF from the medium of progenitor-enriched cultures. Thus neither the mitotically active O-2A progenitor nor terminally differentiated oligodendrocyte stages appear infectable, indicating that in this cell lineage, virus permissiveness occurs during a limited interim period.

The results of the present study support those from a number of previous ones where JHMV non-permissiveness was attributed to a defect involving early virus-cell interactions (Beushausen et al., 1987; Van Dinter and Flintoff, 1987; Kooi et al., 1988; Kooi et al., 1991). Though differences in virus adsorption and endocytic internalization were not observed between O-2A progenitor and more differentiated cultures,

differences in the magnitude and maintenance of viral RNA synthesis were. Recent evidence has suggested that virus internalization by the endocytic pathway does not necessarily lead to a productive infection (Kooi et al., 1991). Moreover, cell lines normally non-permissive for JMHV can be made JHMV-susceptible by polyethylene glycol (PEG) fusion of cell surface bound virus (Van Dinter and Flintoff, 1987; Kooi et al., 1991). PEG treatment was however unable to overcome JHMV resistance exhibited by O-2A progenitors (data not shown). This would further suggest that the defect in O-2A cells involves a post-penetration event.

Concerning JHMV-induced pathogenesis in the rat CNS, the following model is proposed. Present observations and previous in vivo studies (Sorensen et al., 1984; Sorensen and Dales, 1985; Parham et al., 1986), reveal that initial target cells are likely to be neurons, especially those in the hippocampus and cerebellum. Neurons may amplify the inoculum and possibly even act as a vehicle for dissemination to other target cells throughout the CNS. Demyelinating disease may ensue if O-2A lineage cells become infected at the susceptible stage of development, coinciding in vivo with the period when myelination is most active, during postnatal days 10 to 21 (Sorensen et al., 1982). Beyond 3 weeks of postnatal life, completion of myelination in the rat coincides with the onset of resistance to the demyelinating form of disease, even when immunosuppresive therapy is used. Immunosuppression introduced at this stage accentuates an acute encephalitic disease due to

fulminant neuronal infections (Zimmer and Dales, 1989, see appendix). Within the first week of postnatal life proliferating O-2A progenitor cells are migrating from subventricular zones to sites of future myelination (Levine and Goldman, 1988a and b; Hardy and Reynolds, 1991). The O-2A progenitors migrate in response to PDGF (Noble et al., 1988; Armstrong et al., 1990) produced by both type-1 astrocytes (Raff et al., 1988; Richardson et al., 1988) and neurons (Sasahara et al., 1991; Yeh et al., 1991). The synergistic effect of bFGF in extending the proliferative response due to PDGF is brought about by upregulation of the expression of PDGF receptors on progenitor cells (McKinnon et al., 1990). One may conclude from the present findings that the proliferative/migratory phase coincides with a state of resistance to JHMV. During the subsequent 2 weeks when mitogenesis of these migratory progenitors ceases, the differentiaton phase related to myelination commences (Hardy and Reynolds, 1991). This period may be associated with downregulation of bFGF (Ernfors et al., 1990) and and FGF-receptor (Aikio et al., 1991) mRNA levels within the rat brain, accentuating oligodendrocyte differentiation, and perhaps initiating a period of the greatest susceptibility of O-2A lineage cells to productive infection with JHMV. These events in turn may have important consequences regarding the induction of demyelinating lesions by this agent.

CHAPTER 3

JHMV INFECTIONS OF RODENT NEURONAL CELLS: REPLICATION AND TRAFFICKING OF STRUCTURAL PROTEINS AND PROGENY VIRIONS

3.1 Introduction.

In line with previous studies, the work presented here draws attention to the importance of neurons in the pathogenesis of both acute and chronic forms of MHV-induced neurologic disease. Following intranasal inoculation of mice, virus of A59 and JHM strains can invade the CNS by way of the olfactory and trigeminal nerves (Barthold, 1988; Lavi et al., 1988; Perlman et al., 1989). Accordingly, interneuronal spread was hypothesized to be the most likely mechanism involved in initial virus penetration of the CNS. Subsequent dissemination to other CNS regions was shown to also involve specific neuronal populations and tracts (Lavi et al., 1988; Perlman et al., 1990). Immunohistochemical and in situ hybridization methods have shown that in mice, MHV-A59 manifests tropism toward neurons of the olfactory nuclei, nuclei of the amygdala, central tegmental nucleus, entorhinal cortex, subiculum, claustrum, lateral habenular nucleus, subthalamic nucleus, basal ganglia, substantia nigra and septal nuclei in addition to other sites (Fishman et al., 1985; Lavi et al., 1988). In rats, JHMV was shown to have tropism for hippocampal and cerebellar Purkinje neurons (Sorensen and Dales, 1985; Parham et al., 1986; Matsubura et al., 1991). Although JHMV

inoculated rats can develop a delayed onset, demyelinating encephalomyelitis, without prior evidence of any acute encephalitis, histopathological and immunohistochemical studies have revealed that clinically inapparent neuronal involvement likely occurs and precedes development of the chronic, demyelinating form of disease (Koga et al., 1984; Zimprich et al., 1991). Apart from their potential to function in vectorial movement and spread of MHV and as host cell targets for active replication leading to cytopathic processes, neurons may serve as sites for viral persistence. The suggestion has been made that neurons may in fact be particularly well suited for this, due to insufficient expression of MHC class I molecules on their surfaces, thus enabling them to avoid recognition by virus specific cytotoxic T cells (Joly et al., 1991). From the above considerations it becomes evident that investigation of the interactions between neurotropic strains of MHV and neurons in vitro could be a potentially useful means of elucidating neuropathogenic phenomena occurring in vivo.

As stated in chapter 1, the assembly process of JHMV and MHV-A59 virions in fibroblastic cells occurs within the perinuclear region by budding at transitional reticulum vesicles positioned between the RER and Golgi apparatus (Massalski et al., 1982; Tooze et al., 1984). The time and location of progeny virion assembly is controlled by the kinetics of integral membrane glycoprotein (M) deposition on these transitional vesicles (Tooze et al., 1984). Similar

observations were made with MHV-infected AtT20 murine pituitary tumor cells in which progeny virions were shown to exit cells via the constitutive rather than the regulated, secretagogue enhancing exocytic pathway (Tooze et al., 1987). In the case of cultured mouse spinal cord neurons, JHM progeny virions become organized in close vicinity to the Golgi apparatus (Dubois-Dalcq et al., 1982).

The release of progeny virions to the outside in the above examples possibly involves a microtubule-dependent process. To understand virus assembly and release in neurons, one must consider the organization of these highly specialized and asymmetric cells. Each neuron possesses two types of neurites, dendrites and axons, each of which perform specialized functions. The axon is responsible for conducting electrical impulses away from the cell soma, while multiple dendrites serve to receive external signals. Polarization of impulse conductance by axons versus dendrites is inherent in the composition and fine-structure of these processes which differ with respect to their membrane proteins and cytoskeletal frameworks (Vallee and Bloom, 1991). Since biosynthetic functions of neurons are confined to the somato-dendritic domain, movement of materials to and from the apical or axonal domain, which may extend more than a meter in length, requires a highly efficient transport process. Axonal transport is accomplished by two microtubule-dependent processes: fast transport of membranous organelles and slow transport of cytosolic proteins, especially those of the

cytoskeleton (Vallee and Bloom, 1991). In the present study, I examined JHMV replication and trafficking of viral proteins and virions in cultured rat hippocampal neurons and a murine neuroblastoma, OBL21 cells (Ryder et al., 1990).

3.2 Materials and Methods.

3.2.1 Viruses.

The JHMV strain of MHV was propagated as previously described in Chapters 2. The JHMV variant AT11f cord and the MHV-4 variant V5A13 (88) were obtained from Dr. V. Morris of the University of Western Ontario and Dr. M.J. Buchmeier of the Scripps Clinic and Research Foundation, La Jolla, California respectively. The properties of these variants were mentioned in Chapter 1 and will be covered further in Chapter 4.

3.2.2 Culturing Hippocampal Neurons.

Embryonic day (E) 18 to 20 Wistar Furth rats were used for the preparation of dissociated hippocampal neuron cultures, following the procedures described by Goslin and Banker (1991) with minor modifications. Hippocampi were microscopically dissected from rat embryos and placed in ice cold plating medium consisting of a 1:1 mixture of DMEM and Ham's F12 supplemented with 10% (v/v) FBS, 15 mM hepes pH 7.3 and 10 µg/ml gentamycin. The tissue was washed with ice cold Ca^{++} and Mg^{++} free PBS pH 7.2, then digested with 1x

trypsin/EDTA (Sigma) at 37°C for 15 minutes. The tissue was washed twice with cold plating medium to inactivate the trypsin then gently dissociated by repeated passage through a fire-polished Pasteur pipette. The crude cell suspension which resulted was passed successively through 130 and 33 μm pore size nylon meshes (Nitex) to remove large cell clumps, then layered onto a cushion of FBS and centrifuged at 150 x g for 7 minutes. The cell pellet produced was resuspended in a small volume of cold plating medium and the viable cell numbers determined by counting the total and trypan blue excluding cells present. Cells were seeded at a density of 3 x 10^4 to 6 x 10^4 viable cells per cm^2 onto poly-L-lysine coated, 12 mm diameter glass coverslips, precleaned with concentrated HNO_3, or poly-L-lysine coated 35 mm plastic petri dishes. Following attachment to the substratum for 2 hours, the plating medium was exchanged for a serum-free neuronal medium consisting of a 1:1 mixture of DMEM and Ham's F12 supplemented with 100 μg/ml transferrin, 5 μg/ml bovine insulin, 100 μM putrescine, 20 nM progesterone and 30 nM sodium selenite (Bottenstein and Sato, 1979) with the addition of 1 mM Na pyruvate. To promote viability of hippocampal neurons, they were co-cultured in the presence of type-1 astrocytes which provided trophic support and countered the neurotoxic effects of the excitatory amino acid neurotransmitter glutamate. For co-culturing, astrocytes were attached to the surface of 60 mm petri dishes while neurons were placed on 12 mm diameter glass coverslips. Another procedure involved placing the astrocytes on 24.5 mm

diameter, collagen coated Costar transwell inserts with 0.4 μm pores (catalogue # 3425) and the neuronal cultures onto the surface of Costar 6 well cluster plates, as described by Walsh et al. (1992). The cells were maintained in a humidified atmosphere at 37°C with 5% CO_2. Approximately one-third of the culture medium was exchanged every third day.

3.2.3 Cultures of Neuroblastoma OBL21 Cells.

OBL21 cells (Ryder et al., 1990) were routinely grown on either poly-L-lysine coated, 12 mm diameter glass coverslips or 35 mm petri dishes (Nunc) in DMEM supplemented with 10% (v/v) FBS (Hybrimax, Sigma), 15 mM hepes, pH 7.3 and 10 μg/ml gentamycin. To enhance neurite outgrowth prior to inoculating with virus, dbcAMP was added to the culture medium to a final concentration of 2.5 mM. When indicated, vinblastine sulfate (David Bull Laboratories, Melbourne, Australia) was added to cultures to a final concentration of 10 μg/ml at either 24 or 36 hours following inoculation with JHMV.

3.2.4 Infection with JHMV and Variant Viruses.

Neurons growing on coverslips were removed from the dishes in which they were being co-cultured with type-1 astrocytes, transferred to new dishes and then inoculated with either wt JHMV, variant AT11f cord, or variant V5A13 (88) at m.o.i.'s between 5 and 30 pfu's per cell in 70 to 90 μl. Neurons growing on plastic in 35 mm dishes were inoculated with virus by first removing the transwell insert containing

the type-1 astrocytes, then aspiration of the culture medium and inoculating at m.o.i.'s as above in a volume of 400 µl. Adsorption was carried out for 60 minutes in a 5% CO_2 incubator at 37°C with intermittent, gentle rocking to facilitate the uniform spread of virus over the surface of the 35 mm dishes. Following virus attachment, cultures were washed twice with Hank's balanced salt solution then placed in neuronal medium described above and co-cultured with type-1 astrocytes.

3.2.5 Immunostaining of Neuronal Cultures.

The same procedures as those described in chapter 2 for immunocytochemically labelling primary neural cultures were employed for hippocampal neurons and OBL21 cells. In addition to the antibodies described in chapter 2, three additional preparations used were: rabbit> tau serum (Sigma) diluted 1:100, MAb 5B-170 ascites fluid specific for MHV-4 S protein diluted 1:9 (a generous gift from M.J. Buchmeier, Scripps Clinic and Research Foundation) and rabbit> tubulin serum (Nagayama and Dales,1972) diluted 1:40. Cells were either fixed in 4% paraformaldehyde in PBS for 5 minutes followed by permeabilizing by exposure for 30 seconds to acetone, or fixed in 4% paraformaldehyde plus 0.25% glutaraldehyde for 10 to 15 minutes followed by immersion in graded 50%, 70% and 95% ethanols before permeabilizing for 30 minutes in 95% ethanol as described by Caceres et al. (1986). Similar results were obtained with either method. Before adding any of the primary

antibodies, cells were thoroughly rinsed with PBS. Secondary antibodies were diluted with PBS and used as described in chapter 2.

3.2.6 Electron Microscopy of Monolayer Cultures.

The methods for preparing and examining primary hippocampal and OBL21 monolayer cultures were essentially the same as those described in chapter 2.

3.3 Results.

3.3.1 Growth Characteristics of Primary Hippocampal Neuronal Cultures.

Within 6 hours after plating, many of the neurons began to sprout neurites which continued to extend so that by 24 hours, most cells possessed several short and one long neurite emanating from their soma. The short processes have been previously been shown to be dendritic precursors and the single long ones to be the future axons (Banker and Cowan, 1979; Caceres et al., 1986). After 1 week in culture many of the neuronal cell bodies aggregated to form small clusters while the extended neurites formed a fine meshwork which covered the substratum. Fasiculation of axons was particularly prominent in cultures seeded at the higher cell densities (Figure 3.1.B). The number of contaminating astrocytes inevitably introduced along with neurons into these cultures varied between preparations, usually not exceeding 40% of the

Figure 3.1. Wistar Furth rat primary hippocampal neuronal cultures. Hippocampi were microscopically dissected from WF rats at embryonic day 18 to 20. The tissue was dispersed and cells plated at densities of 3 x 10^4 and 6 x 10^4 viable cells per cm^2. (A) Phase contrast micrograph of a low density culture at 10 D.I.V. Of the 5 neurons visible in this field, 3 have a distinctive pyramidal morphology. The arrows delineate a single long neurite of one of these cells. Phase lucent astrocytes are also visible. (B) A culture seeded at a higher density than the one shown in (A) but after an equivalent number of days *in vitro*. Immunocytochemistry using a MAb specific against the 160 kDa subunit of neurofilament and FITC-conjugated secondary antibody demonstrates the fine neuritic meshwork that has formed. The arrows point to a prominent axon fasicle that are common in cultures plated at 6 x 10^4 viable cells per cm^2. In (C) the same field as in (B) has been immunocytochemically labelled using a rabbit polyclonal antiserum specific against GFAP and Texas red-conjugated secondary antibody to demonstrate the presence of endogenous astrocytes routinely found in hippocampal neuronal cultures. A, B and C x 750.

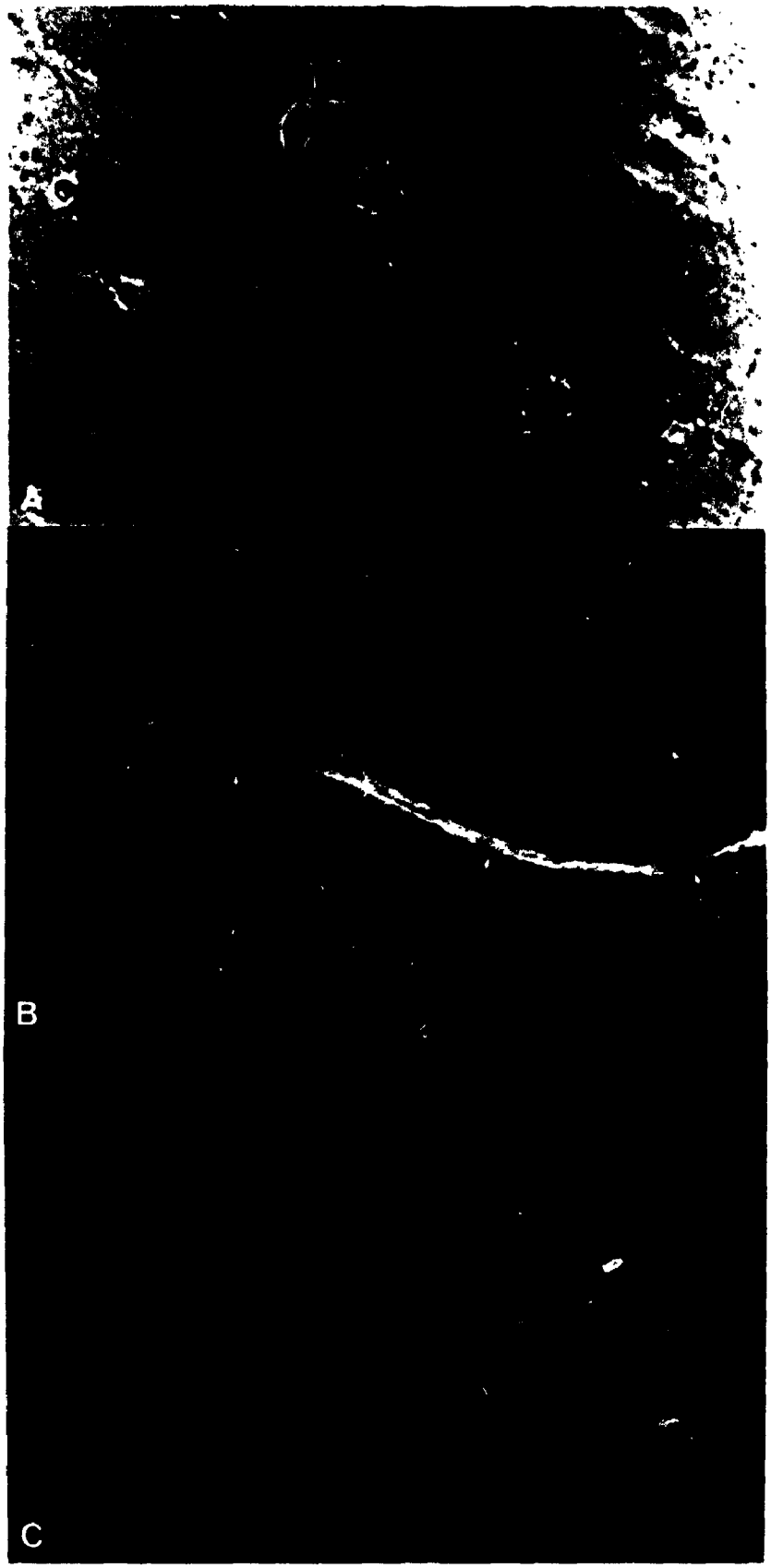
A
B
C

total cell population (Figure 3.1.C). Though these primary dissociated cultures were not pure for hippocampal neurons, they were nevertheless highly neuron enriched. Under these conditions, neuronal cell viability could be routinely maintained for longer than 2 weeks.

3.3.2 Growth of wt JHMV and Neuroattenuated S Deletion Variants in Hippocampal Neuron Cultures.

Hippocampal neurons were inoculated with JHMV at between 9 and 11 D.I.V. at m.o.i.'s between 5 and 30 pfu's per cell. At the time of virus challenge (Figure 3.1), most axons and dendrites were expected to have reached a mature state in terms of their organization, function and ability to form synapses (Goslin and Banker, 1991). For comparison with wt JHMV, two isolates with altered antigenic and pathogenic properties, ATllf cord and V5A13 (88), possessing overlapping deletions of 441 and 447 nucleotides respectively within the the S1 portion of the S gene (Parker et al., 1989; La Monica et al., 1991) were also tested. These variants were of particular significance in this work because of their reported attenuation in neurovirulence based on the shift in the pattern of disease they induced from one of fatal encephalomyelitis to chronic demyelination (Dalziel et al., 1986; Morris et al., 1989). This shift, moreover, was suggested to result from the loss of tropism for neurons but not glia (Dalziel et al., 1986). Consequently, this system provided an ideal opportunity to assess any changes in tropism

directly.

Cell density appeared to be a more important determinant than m.o.i. with respect to establishing and maintaining viral growth in hippocampal neuron cultures. In addition, although infection could be established with the three viruses employed, rates of replication were greater with the two variants (Table 3.1). Approximately 1% of the cells were scored by immunocytochemistry as virus antigen positive at 24 hours postinoculation (Figure 3.2.A), and although their number increased with time (Figure 3.2.B), infected cells were never in the majority, even after 5 days of infection. If virus-neuron interactions *in vitro* are close approximations of events occurring *in vivo*, it can be concluded from these data that deletions of gene sequences from the S glycoprotein did not cause a change in JHMV tropism for neurons. Furthermore, although our wt JHMV does express the HE glycoprotein (La Monica *et al.*, 1991), the two deletion variants are HE^- (La Monica *et al.*, 1991; M.J. Buchmeier, personal communication), suggesting that HE is not required for neuronal infections.

In some culture preparations, astrocytes which were present as a significant fraction of the cell population, did not usually manifest any infection until after 2 dpi (Figure 3.3.E and F), in agreement with previous observations (Pasick and Dales, 1991). When they did occur, infection of astroglia was usually evident in areas of syncytia formation (Figure 3.3.E and F). By contrast, neuronal infections did not promote syncytiogenesis (Figure 3.3.A to D).

Table 3.1

Growth of wt JHMV and S Deletion Variants in Dissociated Hippocampal Neuron Cultures

		PFU/ml of Culture Supernatant[a] Days Post-Inoculation				
		1	2	3	4	5
Experiment # 1[b]	wt JHMV	1.6 ±0.5	4.4 ±2.0	12.6 ± 8.0	47.0 ±12.7	55.5 ±17.7
	AT11f cord	3.1 ±0.1	33.0 ±12.1	116.0 ± 26.5	485.0 ± 57.3	239.7 ± 37.9
Experiment # 2[c]	wt JHMV	0.2 ±0.2	<0.1	0	0.6 ±1.0	1.4 ±2.4
	AT11f cord	1.6 ±1.0	3.3 ±1.2	2.1 ±1.0	15.8 ± 9.7	42.3 ± 2.3
	V5A13 (88)	4.1 ±1.1	12.0 ± 6.2	16.6 ± 6.1	48.7 ±22.6	79.0 ± 9.0

[a]Expressed as x 10^2

[b]In Experiment # 1 cells dispersed from E20 Wistar Furth rat hippocampi were seeded at a density of 60,000 viable cells/cm^2. At 11 D.I.V. cultures were inoculated with virus at a moi of 5 pfu/cell.

[c]In Experiment # 2 cells dispersed from E20 Wistar Furth rat hippocampi were seeded at a density of 30,000 viable cells/cm^2. At 10 D.I.V. cultures were inoculated with virus at a moi of 30 pfu/cell.

Figure 3.2. Spread of infection in primary hippocampal neuronal cultures. Dissociated hippocampal neuronal cultures plated at a density of 6 x 10^4 viable cells per cm^2 on 12 mm diameter glass coverslips, were inoculated with the ATl1f cord variant at 9 D.I.V. at a m.o.i. of approximately 10. Infected cells were identified using the MAb 4B6.2 specific against N and FITC-conjugated secondary antibody. (A) The density of infected cells shown here is typical for 1 dpi. At this stage, neurons accounted for approximately 75% of the virus infected cells. (B) By 3 dpi the number of virus infected cells increased with many of them found in clusters. By this stage, neuronal as well as astroglial involvement was evident. A and B x 400.


A
B

Figure 3.3. Identification of infected cells in rat hippocampal neuronal cultures. The identity of JHMV infected cells in high density, dispersed hippocampal cultures was determined by dual immunocytochemical labelling. Virus infected cells were identified using either MAb 4B6.2 specific against N, or MAb 5B-170 specific against S and FITC-conjugated secondary antibody. Infected astroglia were identified by dual labelling with a rabbit polyclonal antiserum specific against GFAP and Texas red-conjugated secondary antibody, while infected neurons were identified on the basis of morphology and absence of GFAP staining. A and B, C and D, and E and F form sets of identical microscopic fields in which virus infected cells are shown in panels A, C and E, while GFAP-labelled cells are identified in panels B, D and F. (A to D) Virus infected neurons identified on the basis of N (A) and S (C) immunolabelling are frequent at 1 dpi. Arrows in B and D demarcate the location of the neuronal cell body evident in A and C respectively. (E and F) By 3 dpi, the frequency of virus infected astrocytes has increased. A common feature of astroglial infections was the formation of multinucleated syncytia that was remarkably absent from infected neurons. A and B x 1,200, C,D,E and F x 3000.

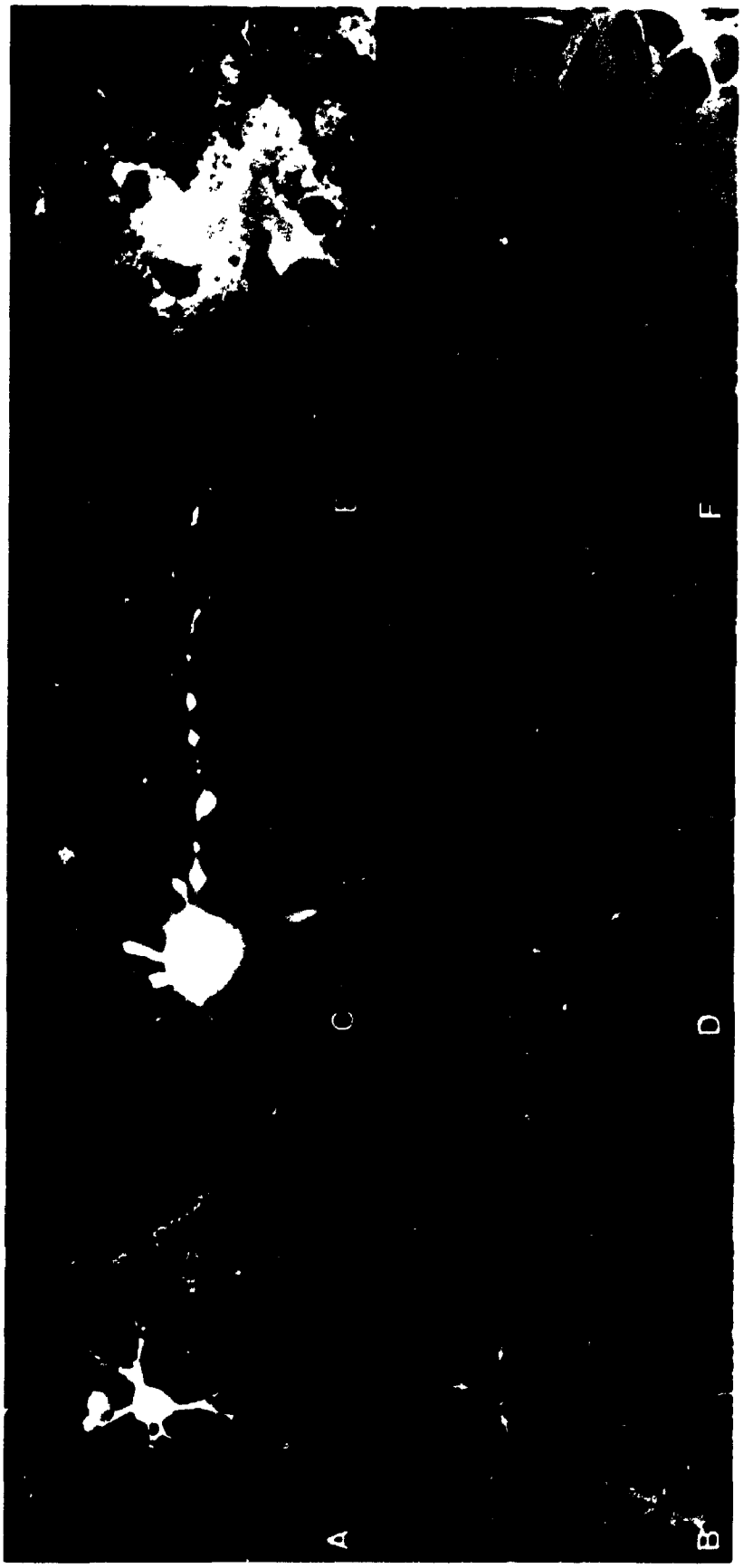
A
B
C
D
E
F

3.3.3 Localization of Viral N, S and Virions within Hippocampal Neurons.

Immunocytochemistry and EM studies of thinly sectioned neurons were used to localize JHMV particles and components. N and S antigens were present in tappering, dendritic-like neurites as well as in highly extended, fine axonal processes. Dual immunolabelling of viral and cytoskeletal antigens with antibodies specific for either N or S and tau, enabled localization of viral proteins in relation to the two cytoskeletal domains (Figure 3.4). Tau as well as MAP2 are microtubule-associated proteins which appear to form cross-bridges between adjacent microtubules (Goedert et al., 1990). In cultured rodent neurons, tau and MAP2 are segregated to predominantly axonal and somato-dendritic domains respectively (Kosik and Finch, 1987), corresponding to their distribution within the CNS (Binder et al., 1985). However, the topographical separation of tau and MAP2 is not entirely unambiguous in hippocampal neurons grown in culture. During the early stages of culture, MAP2 and tau immunoreactivity co-distribute within both axonal- and dendritic-like neurites (Caceres et al., 1986; Kosik and Finch, 1987); this may be because axons arise most commonly as a branch from the proximal segment of one of the dendrites, and not as a process emanating directly from the cell soma as occurs in vivo (Bartlett and Banker, 1984). In cultures in which neurons exhibited prominent fasciculation of their axons, co-

Figure 3.4. Localization of viral proteins to the two neuronal domains. E20 hippocampal neuronal cultures were inoculated with the V5A13 (88) variant at 10 D.I.V. and infected cells identified immunocytochemically at 1 dpi. (A) Two infected neurons are labelled with MAb 4B6.2 specific against N and FITC-conjugated secondary antibody. (B) Cells in the same field as A are labelled with a rabbit polyclonal antiserum specific against tau and Texas red-conjugated secondary antibody. (C) An infected neuron is identified using the MAb 5B-170 specific against S and FITC-conjugated secondary antibody. (D) The identical field to that shown in C demonstrates tau localization as described for B. The arrows point to the complementary neurites in panels A and B and panels C and D. Bars = 19 μm.

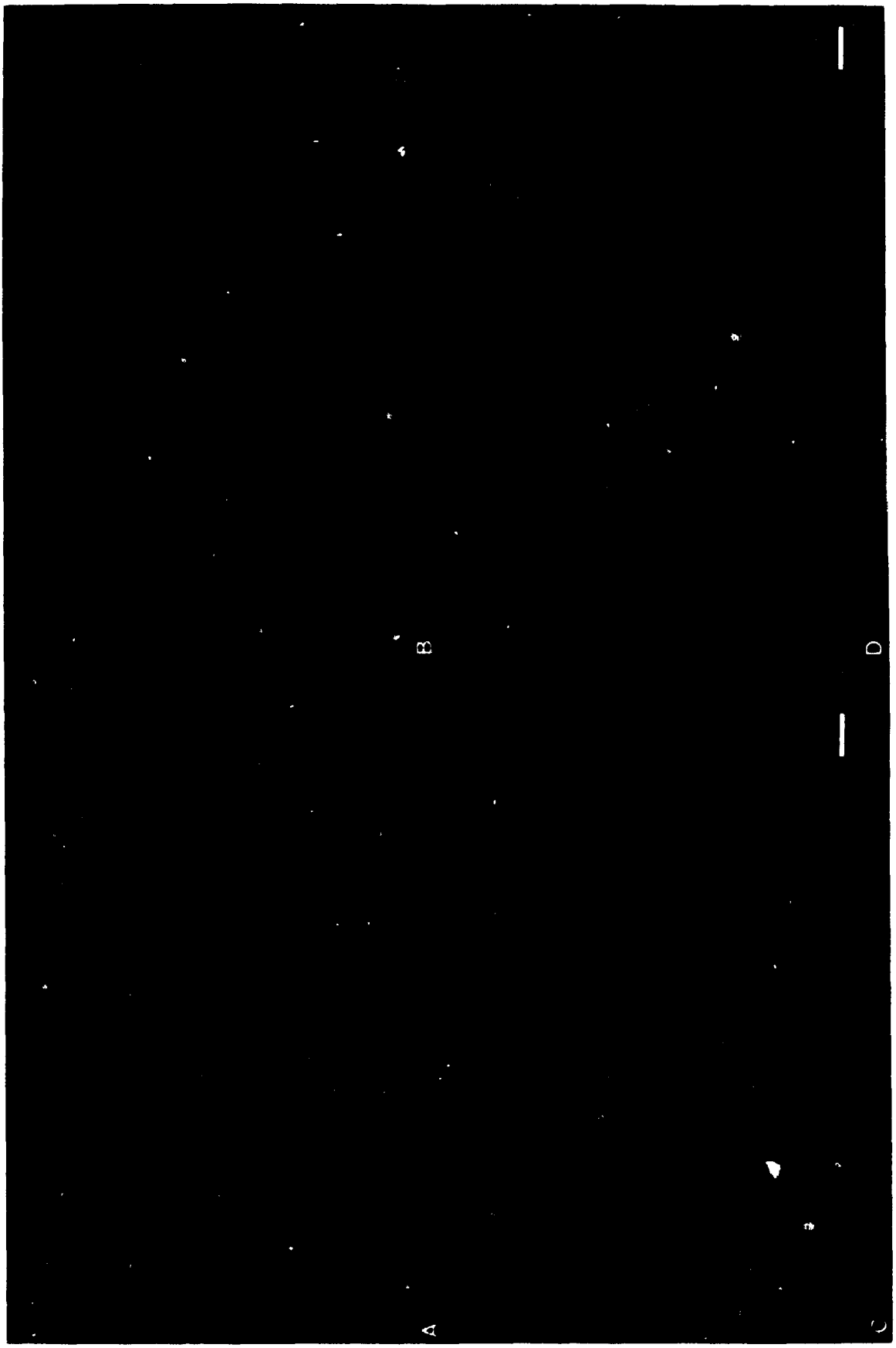
B
D
A
C

localization of N or S viral antigens with tau to axon bundles was observed (Figure 3.5), eliminating the ambiguity of whether viral proteins are trafficked to this domain. Electronmicroscopic examination of hippocampal cultures revealed concentrations of nucleocapsid helical cores of JHMV attached to bundles of microtubules, as reported for stratified, mixed telencephalic cultures in chapter 2 (Pasick and Dales, 1991). Occassionally whole virions were observed within neurites (Figure 3.6.A inset). An intriguing explanation for the attachment of nucleocapsids to neurite microtubules may come from the discovery of the protein sequence homology which exists between N and tau (Figure 3.7.A), in which the amino acid sequence similarity and identity are 42% and 20% respectively [this was found by Dr. Michael Clarke of the Department of Microbiology and Immunology, University of Western Ontario using the nucleotide sequence of N (Skinner and Siddel, 1983) to search the Gen Bank data base]. Optimal alignment of a putative tau microtubule binding motif (Goedert et al., 1991, for review) was found between amino acids 328 to 340 inclusive within the carboxy-terminal portion of N (Figure 3.7.B).

3.3.4 Compartmentalization of Virus Components and Whole Virions within OBL21 Neuronal Cells.

As a means of further assessing the putative importance of microtubules in movement and release of progeny virions to the cell exterior, the continuous neuronal cell line, OBL21,

Figure 3.5. JHMV-specific proteins are found within single, axon-like neurites, as well as within axon fasicles. Fasiculation or bundling of axon fibers, a prominent finding in high density hippocampal neuronal cultures, was used to help assess whether trafficking or distribution of viral proteins to the axonal or apical domain occurred. (A) Hippocampal neuronal culture labelled with a rabbit polyclonal antiserum specific against tau and Texas red-conjugated secondary antibody, one day following inoculation at 10 D.I.V. with the V5A13 (88) variant. The large arrows point to prominent axon fasicles while the small arrows point to fine, single, axon-like fibers. (B) The same field as in panel A only labelled with MAb 5B-170 specific against the spike protein and FITC-conjugated secondary antibody. The arrows in correspond with those in panel A. Note the co-localization of viral spike protein with axonal processes. A and B x 1,000.


A
B

Figure 3.6. Assessment of the compartmentalization of JHMV virions in OBL21 neuronal cells and primary hippocampal neurons by ultrastructural studies. Thin sections of infected OBL21 and primary hippocampal neuronal cultures were examined by electron microscopy to further assess JHMV maturation in these cells. (A) Linear arrays of progeny JHM virions found within cisternae of infected OBL21 cells were not uncommon. The solid arrows point to an immediately adjacent microtubule. The inset in panel A is from an infected primary hippocampal neuronal culture showing two virions within a neurite. (B) A higher resolution image of the area bracketed by the open arrows in panel A. The solid arrows point to microtubules. Bars = 0.5 μm.

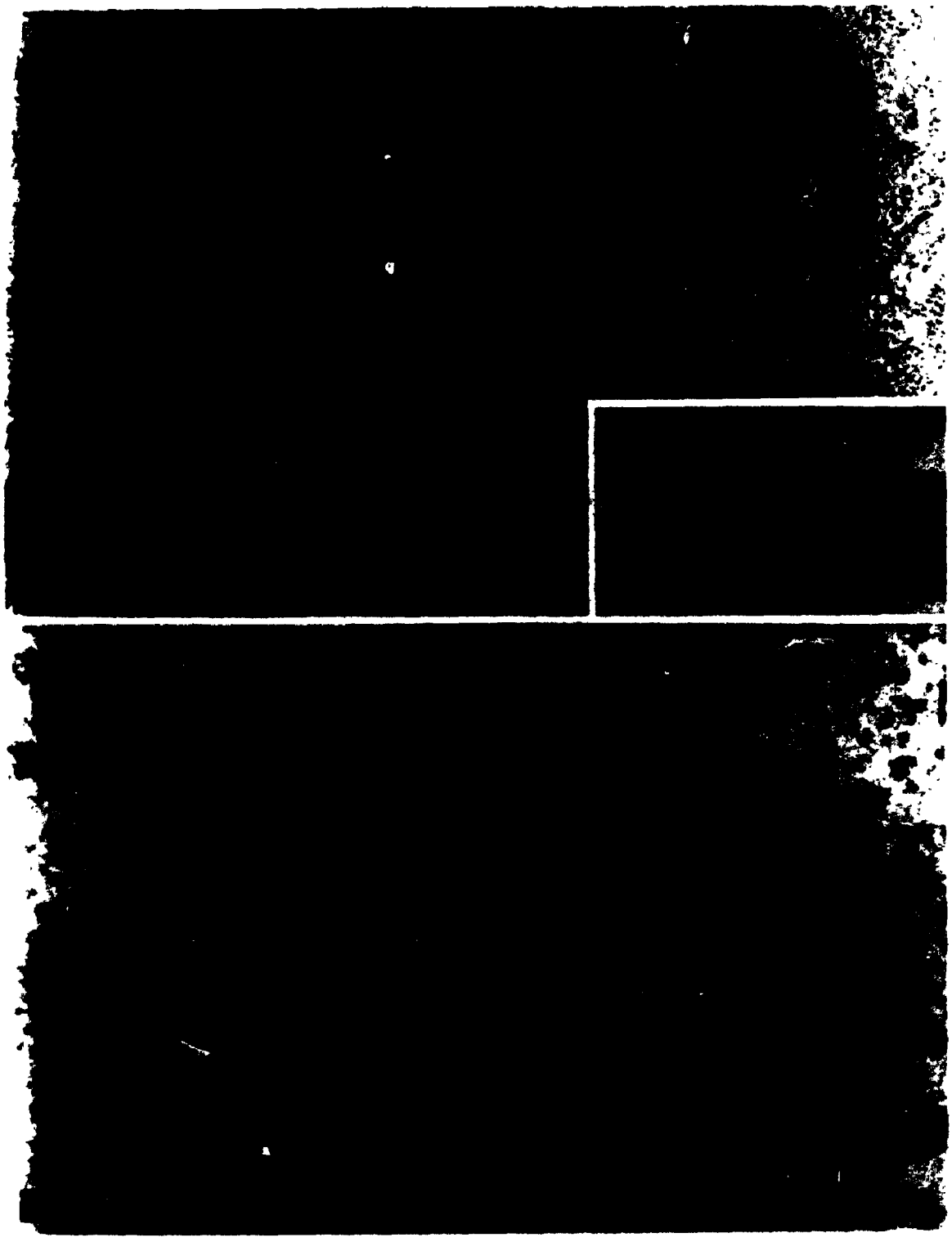

Figure 3.7. Comparison and alignment of the primary amino acid sequences of tau and the JHMV nucleocapsid protein. Dr. Michael Clarke of the Department of Microbiology and Immunology used the published nucleotide sequences of tau (Lee et al., 1988) and JHMV nucleocapsid protein (Skinner and Siddel, 1983) for translation into their primary amino acid sequences from which subsequent comparison and alignment operations were carried out. (A) Optimal amino acid sequence alignment between full length tau and N. The top sequence is tau while the bottom sequence is N. Identity is indicated by a vertical dashed line, while similarity is indicated by dots, with 2 dots meaning greater similarity than 1 dot. Overall, the two proteins showed amino acid similarity and identity of 42% and 20% respectively. The tandem repeat region of tau, involved in binding with microtubles, is boxed. (B) An invariant 12-mer that forms the supposed core of the microtubule binding motif of tau was optimally aligned within the carboxyterminal portion of N, involving residues 328 to 340 and demonstrated 30% identity.

A

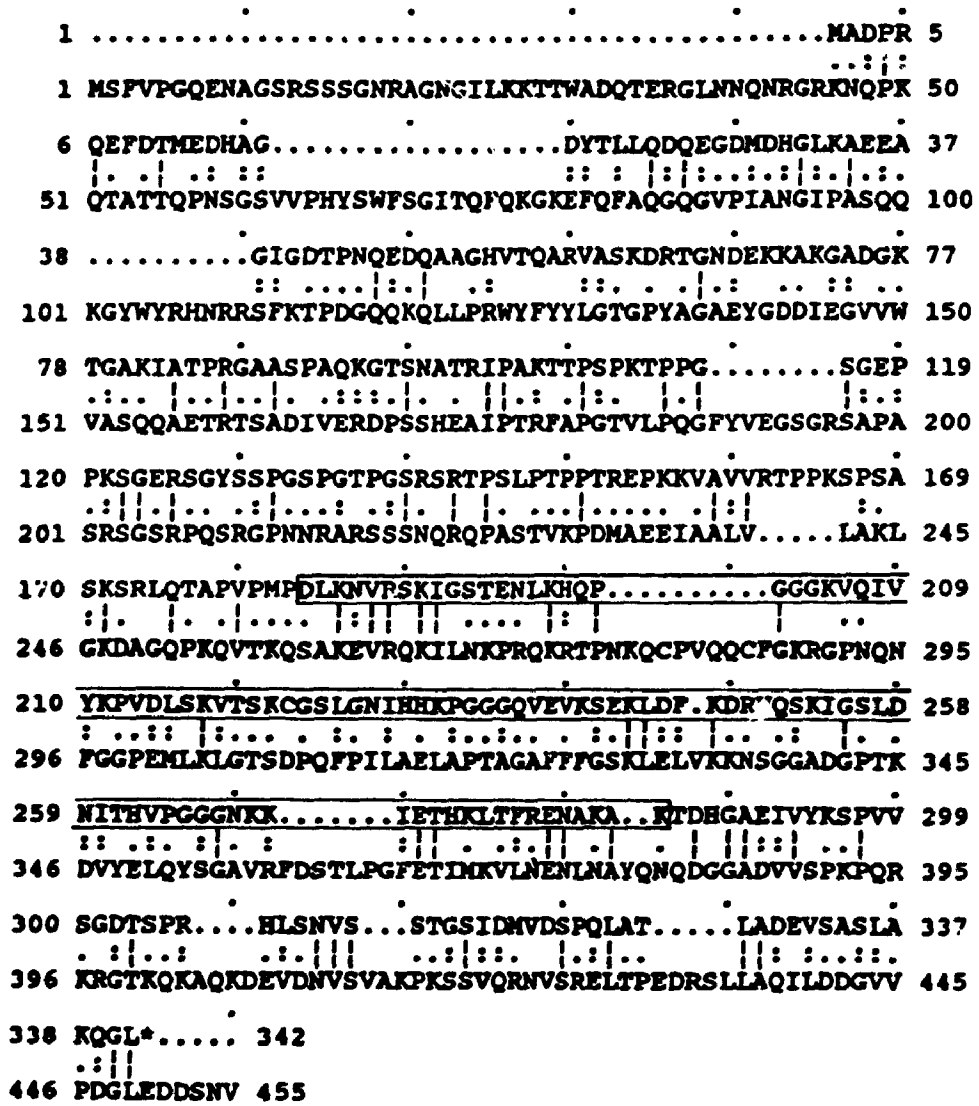

B

```
ProteinN  mlklgtsdpqfpilaelaptagafffgSKLELVKKNSGGAdgptldvyel   350
Tau       ---------------------------GSLDNIKHVPGGG----------   18
```

was employed. The OBL21 cell line was clonally derived from olfactory bulb cultures of CD.1 mice following immortalization by means of a replication-defective retrovirus vector encoding the avian myc gene (Ryder et al., 1990). Cells of the OBL21 line have exhibited a stable, homogeneous neurofilament$^+$ and GFAP$^-$ phenotype during culture in this laboratory. Electron microscopic and immunofluorescence analyses of JHMV infected OBL21 cells demonstrated the presence of nascent N and S components within neurite-like processes paralleling the findings on hippocampal neurons. Examination of thin sections often revealed nucleocapsid aggregates associated with microtubules as originally observed in infected primary neurons. Because the frequency of JHMV infections was much higher than in primary neurons, virions organized in precise linear arrays, evident within cisternae sometimes contiguous to microtubules, were found in favourably oriented thin sections (Figure 3.6.A and B). To identify the specificity of the virus-microtubule relationship more clearly, OBL21 cells infected with JHMV at a m.o.i. of 10 were treated with 10 μg/ml vinblastine beginning at 12 or 18 hours postinoculation then incubated for an additional 6 to 12 hours before sampling. Vinblastine is a mitotic inhibitor which also inhibits axonal transport by promoting the reorganization of tubulin, after microtubule depolymerization, into massive tubulin paracrystals (Dales et al., 1973). The observed collapse of the microtubule framework was accompanied by a concentrated accumulation of viral, cytosolic, nucleocapsid

aggregates and progeny virions within vesicles of the smooth endoplasmic reticulum and Golgi apparatus around contiguous tubulin paracrystals (Figure 3.8). Vinblastine treatment was also associated with 10-fold less virus being released into the culture supernatant as compared with control, infected cultures. These observations emphasize further the important role that microtubules appear to have in the intracellular distribution and perhaps transport of nascent viral material and progeny particles.

3.4 Discussion.

The JHMV S variants characterized by others as having a neuroattenuated phenotype *in vivo* do not exhibit diminished tropism for neurons when tested in the present system. It is possible however, that the neuroattenuated phenotype of these S variants is due to altered neuronal cytopathic effects like those evident with cell lines (Gallagher *et al.*, 1990). Two strains of Sindbis virus, one of high and the other of low neurovirulence were similarily shown to differ in their E2 glycoproteins which form the spikes that project from the surface of these virus particles and are responsible for mediating cell tropism and fusion. In this situation, the enhanced neurovirulence of the one strain was found to be due to increased efficiency of virus replication and cytopathic effects produced within neurons rather than to a fundamental change in cell tropism (Jackson *et al.*, 1988).

The disposition of JHMV components and progeny virions

Figure 3.8. The effects of microtubule depolymerization on the intracellular compartmentalization of viral components and progeny virions within infected OBL21 cells. JHMV inoculated OBL21 neuronal cultures were treated with 10 μg/ml vinblastine beginning at 18 hours postinoculation. Coverslip cultures destined for immunocytochemical analysis were incubated for an additional 6 hours before fixing and labelling. Cultures within plastic dishes destined for electron microscopic studies were incubated for an additional 12 hours before fixing and embedding. (A) Virus infected cells were identified using MAb 5B-170 specific against S and FITC-conjugated secondary antibody. Note the formation of syncytia by infected cells. Two important features of the S staining pattern include: fibers that project into the process (arrowheads) and rectangular-shaped areas that are devoid of staining (small arrows). (B) In the identical microscopic field shown in panel A, the tubulin staining pattern is demonstrated. The small arrows, which correspond to those in panel A, point to the rectangular-shaped tubulin paracrystals that are devoid of S staining evident in A. (C) Ultrastructural representation of the association between viral components and virions, and tubulin paracrystals. Large arrows outline a tubulin paracrystal, PC, around which core components, NC, and vesicles containing virions, V, have associated. Inset in C shows a Golgi stack containing a virion that is closely apposed to a paracrystal. Bar = 1 μm.

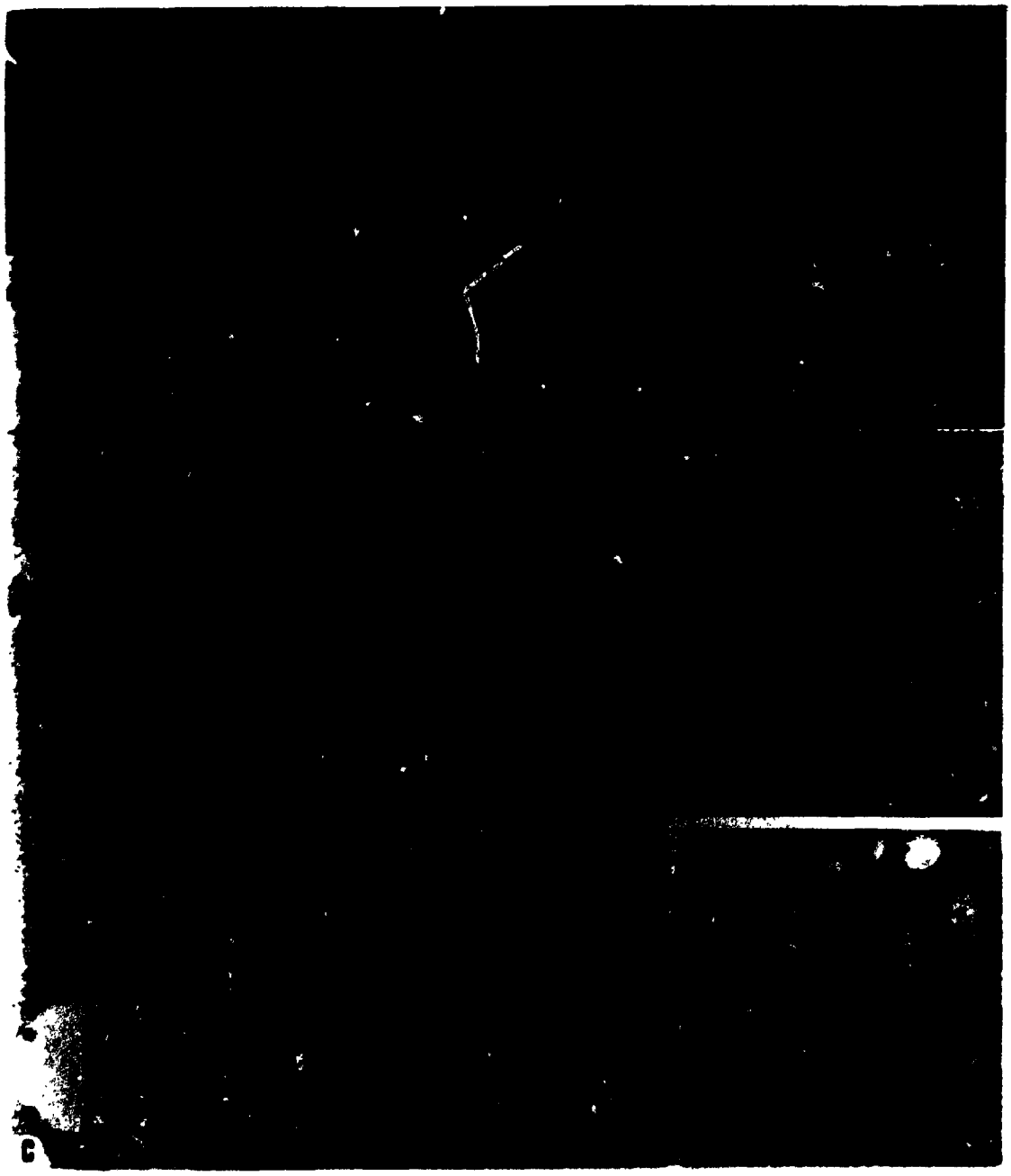
C

within primary hippocampal neurons and OBL21 cells is consistent with the idea that spread of the infection within the CNS is transneuronal. Concerning the specificity of JHMV externalization in infected polarized ependymal cells, progeny virions appear to exit the host cell baso-laterally as judged by the pattern of virus spread to adjacent ependyma and subependymal tissues (Wang et al., 1992). However, there are published arguments favouring also an apical site for exit of progeny JHMV from infected ependymal cells (Wang et al., 1992). From the pattern of distribution of N and S in hippocampal neurons, there are indications that trafficking can occur somato-dendritically as observed previously (Knobler et al., 1981; Dubois-Dalcq et al., 1982). This is conceivable because Golgi elements which are important for coronavirus assembly and transport are present within dendrites (Dotti and Simons, 1990). Axonal trafficking also appears to occur based on the distribution of viral N and S to tau^{+} axon bundles and to highly extended, fine, non-tapering neurites (Figure 3.4) which are the distinguishing features of axons. Therefore, coronaviruses may be disseminated from neurons at either basolateral and/or apical domains, in contrast to the situation prevailing among other enveloped RNA viruses which are released from polarized cells from one or the other domain (Rodriguez-Boulan and Pendergast, 1980; Kristensson et al., 1984; Dotti and Simons, 1990; Weclewicz et al., 1990). The observed presence of N and S in neurites presummed to be axons may be explained by the following: 1) trafficking of nascent

virus components into axons occurs by anterograde movement, 2) viruses released from the dendrites of one infected neuron are capable of crossing the synaptic cleft and being taken up at the synaptic terminal of a second synapsing neuron with subsequent transit in the retrograde direction, or 3) the flow of virus materials is bidirectional. In support of the third alternative are *in vivo* tracer studies which followed the temporally dependent progression of penetration and spread of JHMV within the murine CNS after intranasal inoculation of mice (Perlman *et al.*, 1989; Barnett and Perlman, in press). These studies concluded that JHMV moved along neural tracts in predominantly the retrograde, but also the antergrade direction.

The explanation concerning the electron microscopic evidence of an association between nucleocapsids and neuronal microtubules, established with mixed telencephalic cultures, described in chapter 2, and subsequently confirmed in hippocampal neurons and OBL21 cells, may be found in the amino acid sequence homology between N and tau (in this regard, it should be noted that N-specfic MAb 4B6.2 does not label uninfected hippocampal neurons). Tau-microtubule interaction occurs, in part, by means of a 31 or 32 amino acid sequence which is tandemly repeated 3 to 4 times within the carboxyterminal portion of the molecule (Lee *et al.*, 1988). Within each repeat is an 18-mer stretch, which as an isolated peptide, can bind to microtubules (Lee *et al.*, 1989). Out of the 18 residues, 12 are invariant among the repeats (Goedert

et al., 1991) and can be aligned optimally between residues 328 and 340 of N (Figure 3.7.B). Thus, attachment of N and tau to microtubules may occur through a closely homologous sequence, a hypothesis amenable to experimental verification. The relationship between N and microtubules may have further implications to the process of progeny virion assembly. One could invoke the N-microtubule association as a significant step in virion assembly, whereby cytosolic N, attached to microtubule surfaces, is relevantly positioned for subsequent interaction with the intergral membrane glycoprotein M during the process of budding into smooth vesicles and tubules. Such a sequence of events may account for the observed linear distribution of virions within membranous cisternae of OBL21 cells where adjacent microtubules are also evident. It remains to be established whether nucleocapsids not utilized for incorporation into progeny coronavirions are transferred into neurites by a slow axonal transport mechanism which is generally held to be responsible for the movement of cytoskeletal components into axons (Vallee and Bloom, 1991). This could explain the observed association between nucleocapsid cores and the extended microtubule arrays of neurites. Further understanding of these phenomena will likely contribute significantly to our understanding of coronavirus neuropathogenesis.

CHAPTER 4

THE VIRION'S SPIKE GLYCOPROTEIN AS A DETERMINANT OF NEUROPATHOGENESIS

4.1 Introduction.

Neurotropic strains of MHV can induce a fatal encephalitis in the majority of inbred mouse strains that have been tested (Stohlman and Frelinger, 1978; Knobler et al., 1981a). The genetic basis for the greater resistance of SJL/J mice to viral strains MHV-JHM (JHMV), MHV-4 and MHV-A59, has been attributed to a single recessive gene by Knobler et al. (1981a, 1984a) and Smith et al. (1984), or to at least two genes, one dominant and the other recessive by Stohlman and Frelinger (1978). Resistance was assessed according to the following criteria: 1) deficiency in establishing productive JHMV infections of primary spinal cord neuronal and peritoneal macrophage cultures (Knobler et al., 1981a; Knobler et al., 1984b; Smith et al., 1984); 2) the ability of an adherent macrophagic cell type from spleen or peritoneal exudates of naive, resistant, 12 week old mice, to adoptively transfer protection against JHMV to susceptible 6 week old recipients (Stohlman et al., 1980); 3) failure of JHMV to spread from the primary sites of infection within the nasal cavity to secondary targets in brain, intestine and liver (Barthold and Smith, 1987); and 4) absence of virus-binding to cell membranes of hepatocytes and enterocytes, attributed to a

deletion in or mutation of the virus-binding domain of a 110 to 120 kDa glycoprotein receptor (Boyle et al., 1987; Williams et al., 1990). Previous studies in our laboratory demonstrated however, that resistance of primary SJL/J glial cultures to JHMV could not be attributed to any deficiency in virus attachment, penetration, or early expression of viral genes, but was likely due to a failure in the cell-to-cell dissemination of the virus (Wilson and Dales, 1988). Consequently, the basis of SJL/J resistance, particularly as it relates to the number of determinants involved and to the presence or absence of functional receptors on target cells, has been the subject of some dispute.

The study by Wilson and Dales (1988) on JHMV resistance of primary SJL/J glial cells in culture, provided data which indicated that a defect existed in the cell-to-cell dissemination of the infection, and that S, the virion's major spike glycoprotein, was likely prominently involved. In this regard, S has been shown to function in virion attachment to target cells, mediation of syncytiogenesis and elicitation of a neutralizing antibody response (Collins et al., 1982; Sturman et al., 1985; Dalziel et al., 1986) and is believed to play a critical role in CNS pathogenesis. Certain isolates of MHV possess another less abundant envelope glycoprotein termed HE for hemagglutinin esterase, possessing both esterase and hemagglutinating activities. HE possesses sequence homology with the hemagglutinin of influenza C virus (Luytejes et al., 1988). Presence of HE varies among different isolates of JHMV,

indicating that this component provides an accessory and not absolutely necessary function for viral replication (Yokomori et al., 1991). By contrast, with bovine coronavirus, HE was shown to be essential for infectivity (Deregt and Babiuk, 1987). Therefore, the actual function of HE in MHV infections remains to be determined.

This study was undertaken to ascertain whether variant viruses bearing deletions within the coding sequences of the two surface glycoproteins, S and HE, possessed growth and neuropathological characteristics different from those of wt JHMV. Two experimental models were employed to address these questions: 1) SJL/J mice and primary neural cell cultures derived from them, and 2) suckling WF rats. By comparing the results obtained from resistant SJL/J mice and age susceptible WF rats, it was anticipated that some general conclusions could be made regarding the role of S in pathogenesis.

4.2 Materials and Methods.

4.2.1 Viruses.

MHV-JHM was obtained from the American Type Culture Collection (Rockville, Maryland) as indicated earlier. Details regarding the isolation and characterization of JHMV variants AT11f cord and AT11f brain as well as the MHV-4 variants V5A13 (88), V5A13.1 (86) and V4B11.3 (86) have been published previously (Morris et al., 1989; Parker et el., 1989; La

Monica et al., 1991). V5A13.1 (86) and V4811.3 (86), like V5A13 (88), were obtained as a gift from Dr. M. Buchmeier of the Scripps Clinic and Research Foundation, La Jolla, California. All viral strains were propagated on L-2 cell monolayers by inoculating at a moi of approximately 0.1. Membrane-associated inoculum prepared from combined culture supernatant and cell associated virus was titered on L-2 cell monolayers as described earlier in chapter 2.

4.2.2 Animals.

Inbred SJL/J and outbred CD.1 mice were obtained from the Jackson Laboratory, Bar Harbor, Maine. Inbred WF rats were obtained as breeding stock from Harlan Sprague Dawley. All animals were bred in-house as described previously (Sorensen et al., 1982), and have remained MHV free based on periodic serological testing (Institut Armand-Frappier, Laval, Quebec).

4.2.3 Primary Murine Neural Cultures.

Primary, dissociated, murine glial cultures were prepared as previously described (Wilson et al., 1986), with minor modifications. Briefly, mixed cultures consisting predominantly of astrocytes and cells of the oligodendrocytic lineage were derived from dissociated cerebral hemispheres of day old mice. Tissue culture plastic or 12 mm diameter, glass coverslips coated with poly-L-lysine were seeded at densities ranging from .18 to .36 cerebral hemispheres per cm^2 in Dulbecco's modified Eagle medium (DMEM-high glucose)

supplemented with 10% fetal bovine serum (Bocknek), 1.2 g per liter $NaHCO_3$, 15 mM Hepes pH 7.3 (Sigma) and 10 µg per ml gentamycin. A half medium change was made at day 4 *in vitro* and every third day thereafter.

Primary SJL/J hippocampal neuronal cultures were prepared from E20 hippocampi using the procedure described in chapter 3. Hippocampal neurons were grown on 12 mm diameter glass coverslips situated in 60 mm petri dishes with WF type-1 astrocytes that were adherent to the plastic surface. Co-cultures were grown in serum-free, chemically defined neuronal medium described in chapter 3 (Bottenstein and Sato, 1979).

4.2.4 Infection of Animals and Primary Neural Cultures.

Mice older than 2 weeks of age were lightly anesthetized with methoxyflurane before intracranially (ic) inoculating 30 to 40 µl of virus suspension using a 30 gauge needle. Uninfected L-2 cell lysate was used in control inoculations. Suckling WF rats were inoculated by an identical procedure which is described in more detail in the appendix. SJL/J mixed glial and hippocampal neuronal cultures were infected with a membrane-associated virus preparation at a multiplicity of infection of approximately 1 and 10 pfu's per cell. Virus was adsorbed for 60 minutes at 37°C, then unadsorbed inoculum was aspirated off, cultures washed twice with warm phosphate buffered saline (PBS), pH 7.2, nutrient medium was added and incubation resumed at 37°C in a humidified atmosphere containing 5% CO_2. The hippocampal neuronal cultures on

coverslips were returned to culture dishes where type-1 astrocyte cultures had been established.

4.2.5 Immunosuppression with Cyclosporin A.

Cyclosporin A (CsA) was obtained as Sandimmune (Sandoz Canada, Inc.) as a 50 mg per ml solution and diluted to a 2 mg per ml working concentration with PBS. Mice were weighed and injected intraperitoneally (ip) to deliver 25 mg per kg body weight (BW) per day. Treatment with CsA commenced either one day before or on the day of virus inoculation. After virus infection, daily CsA administration was continued for 5 to 10 days postinoculation, depending on the age at infection of the individual animal. In the case of mice inoculated at 11 weeks of age, CsA was given for 10 consecutive days postinoculation. Controls received only PBS.

4.2.6 Assay of Virus in Brain Tissue.

Animals were sacrificed *in extremis* or at predetermined time points following inoculation, the brains divided by a mid-sagittal incision and one half of the brain removed for virus titer determination. The tissue was weighed and placed into a suitable volume of ice-cold tissue culture medium supplemented with 10% FBS so that a 10% w/v tissue homogenate could be prepared. The homogentates were clarified by low speed centrifugation and the supernatants used to make 10-fold serial dilutions which were titered on L-2 cell monolayers.

4.2.7 Immunostaining of Primary Neural Cultures.

Primary murine neural cultures were immunostained using the techniques and reagents described in chapter 2.

4.2.8 Histology and Immunohistochemistry.

The half of the brain not used for virus titer determination, as well as the spinal cord, were isolated after sacrifice of animals and submersed in 10% neutral buffered formalin (10% formalin, 29 mM $NaH_2PO_4.H_2O$, 46 mM Na_2HPO_4) for several days at 4°C before dehydrating by sequential passage through graded ethanol solutions and chloroform in preparation for paraffin embedding. 10 μm sections were cut, then stained with hematoxylin and eosin for routine histopathology.

Virus N antigen was detected using MAb 4B6.2. Sensitivity was amplified employing biotin-anti-biotin conjugates coupled to alkaline phosphatase (AS/AP Plus immunostaining kit, BIO/CAN SCIENTIFIC) following the manufacturer's recommendations. Briefly, following deparaffinization, sections were digested in a 0.5% pepsin solution (Sigma) for 20 minutes at 37°C. MAb 4B6.2 as a tissue culture supernatant was then incubated overnight at room temperature at a 1:18 dilution prior to the amplification and chromogenic reactions. Specificity of the reaction was determined by testing tissues from uninoculated, control animals as well as by eliminating the primary antibody from infected tissues. Following the immunostaining reactions, the sections were briefly counterstained with hematoxylin.

4.2.9 In Situ Dot-Blot Analysis of JHMV RNA.

At 7 D.I.V. primary SJL/J glial cultures situated in 35 mm culture dishes were inoculated with wt JHMV, AT11f cord virus or AT11f brain virus at a moi of 1. At 24 and 48 hours post-inoculation, the culture supernatants were removed and the cultures thoroughly washed with ice-cold PBS. Cells were then gently scraped from the dishes and resuspended in PBS by aspiration through fire-polished Pasteur pipettes to produce a final concentration of 1 x 10^5 cells per ml. Suspended, intact cells were spotted onto a sheet of nitrocellulose using a Schleicher and Schuell "minifold" filtration apparatus and processed for in situ hybridization using the method outlined in chapter 2 (Paeratkul et al., 1988). The blot was probed at 42°C with nick-translated pg344 described in section 2.2.14 (Budzilowicz et al., 1985) isotopically labelled with ^{32}P. Blots were subjected to autoradiography on X-ray film using 24 to 48 hour exposures at -70°C.

4.2.10 Extraction of RNA from Virus Infected Cells.

RNA was prepared from cells infected with wt JHMV and the four spike protein deletion variants used in this study. Subconfluent, L-2 cell monlayers, grown in 150 cm^2, flatbottom T flasks were inoculated with virus at a m.o.i. of 0.1 as described in chapter 2. At 12 hours postinoculation, when approximately 90% of the cells were incorporatated into a multinucleated syncytium, total cellular RNA extracts were prepared by the method of Auffray and Rougeon (1980). Briefly,

each flask was washed twice with ice-cold PBS before adding 10 ml of a 6M urea/3M LiCl solution and scraping the cells from the plasticware using a rubber policeman. Lysates, produced by passing each suspension through a 23 gauge needle 4 times, were stored overnight at 4°C in parafilm covered corex tubes. The precipitates were pelleted by centrifuging at 12,000 rpm for 30 minutes at 0°C in a Beckman JS-13 rotor, resuspended by vortexing in 6M urea/3M LiCl, and then pelleted again by centrifugation. The pellets were dissolved in a proteolytic buffer consisting of 10 mM Tris HCl (pH 7.5), 0.5% (v/v) SDS and 50 μg/ml proteinase K (Boehringer Mannheim) and then incubated for 20 minutes at 37°C. The digestion products were extracted twice with phenol/chloroform and twice with chloroform. The RNA was precipitated from the aqueous phase by the addition of NaCl (0.1 M final concentration) and 2.5 volumes of 95% ethanol and incubating overnight at -20°C. The precipitated RNA was pelleted by centrifuging at 10,000 rpm for 60 minutes at 0°C in a Beckman JA-20 rotor, dissolved in diethylpyrocarbonate treated H_2O and concentration determined by measuring the absorbance at 260 nm in a spectrophotometer (1 OD_{260}= 42 μg of RNA/ml of solution).

4.2.11 Northern Hybridization.

Total cellular RNA from infected and uninfected L-2 cells was electrophoresed on a 1.1% agarose gel containing 10 mM sodium phosphate buffer (0.5 M NaH_2PO_4 and 0.5 M Na_2HPO_4) pH 7.0. RNA (20 μg of each sample) was denatured by mixing with

10 mM NaH_2PO_4, 10 mM Na_2HPO_4, 50% dimethyl sulfoxide and 1 M deionized glyoxal, final concentration, followed by heating to 50°C for 60 minutes. Samples were quenched on ice, loaded into the wells, and electrophoresed at 60 V for 18 hours. During this time, the running buffer was kept circulating by means of a perastaltic pump and the gel cooled by a cold water jacket. After electrophoresis, the gel was rinsed once with sterile H_2O before soaking in 50 mM NaOH for 20 minutes at room temperature to partially hydrolyze the RNAs. The gel was neutralized with 0.1 M Tris HCl pH 7.5, soaked briefly in 10 mM phosphate buffer and equilibrated in 20X SSC. The RNAs were transferred to a Hybond-N nylon membrane (Amersham #RPN.303N) in 20X SSC using the Vacugene blotting system. After completion of the transfer, the nylon membrane was briefly washed in 5X SSC before baking at 80°C for 2 hours under vacuum.

The membrane was prehybridized in annealing buffer (section 2.2.14) at 42°C for 16 hours. Hybridization with [α-^{32}P]dATP labelled pg344 (Budzilowcz *et al.*, 1985) was carried out in the same solution at 42°C for 48 hours. The blot was then washed as previously described and exposed to Kodak XAR-5 film at -70°C.

4.3 Results.

4.3.1 Comparison of the Replication of wt JHMV and S1 Deletion Variants in Primary Neural Cultures from SJL/J and CD.1 Mice.

Growth of wt JHMV and the AT11f cord variant was assessed on primary glial cultures derived from resistant SJL/J or susceptible CD.1 mice. The wt JHMV used in these experiments was shown to possess normal S and HE components after propagation under the present culture conditions (La Monica et al., 1991). S of the AT11f cord variant of JHMV (Morris et al., 1989) has a 441 nucleotide deletion in the middle 1/3 of the S1 fragment, as well as a 738 nucleotide deletion in the coding region of HE (La Monica et al., 1991). The AT11f cord variant is more fusogenic and capable of replicating to higher titers in G26-24 oligodendroglioma cells than wt JHMV (Morris et al., 1989).

Primary glial cultures from resistant SJL/J and susceptible CD.1 mice were infected with an m.o.i. of 1 at various times between 7 and 12 D.I.V. The challenged cultures contained a mixture of cell types including a bedlayer formed predominantly by astrocytes, on to which adhered cells of the oligodendrocytic lineage. As evident in Table 4.1, the AT11f cord variant was consistently produced in higher titers in SJL/J glial cultures than was wt JHMV. However, the magnitude of the difference in titer depended upon the method by which the virus inoculum was prepared. Inoculum made from a concentrated suspension of extracellular (ie released) virus as described in Wilson and Dales (1988), produced a 100 fold difference in growth between wt and variant virus (results of

Table 4.1

Comparison of the Replication of wt-JHMV and Selected Variants in Resistant SJL/J and Susceptible CD.1 Primary Glial Cultures

Strain of mouse	Days postinoculation	Titer of Culture Supernatnat[a]			
		wt-JHMV	AT11f brain	AT11f cord	V5A13 (88)
SJL/J	2	22.3 ± 6.8	21.1 ± 14.3	402.0 ± 28.3	476.0 ± 14.1
	3	30.0 ± 19.3	22.8 ± 11.7	311.0 ± 177.4	278.7 ± 5.5
	4	12.5 ± 7.6	26.6 ± 15.5	150.5 ± 61.5	127.3 ± 26.4
	6	10.1 ± 2.7	10.2 ± 4.4	22.8 ± 6.0	20.8 ± 3.3
CD.1	2	1,430 ± 380	3,100 ± 770	2,000 ± 1,300	1,850 ± 320

[a]Cultures were derived from the cerebral cortices of postnatal day 1 animals and grown in 24 well cluster dishes. At 7 D.I.V. the mixed glial cultures were inoculated with the indicated viruses at a m.o.i. of approximately 1 pfu/cell. The titers, which are the means ± SD of triplicate cultures are expressed as x 10^2 pfu/ml.

G.A.R. Wilson as reported in Pasick et al., 1992). However, with membrane-associated inocula prepared from disrupted cells, the difference in replication was usually only 10 fold (Table 4.1). In spite of the enhanced replication associated with the AT11f cord variant, growth in SJL/J cultures was still 1 to 2 orders of magnitude less than in CD.1 glial cultures (Pasick et al., 1992 and Table 4.1). At equivalent time points postinoculation, the syncytia observed in SJL/J cultures inoculated with wt JHMV were significantly smaller than those produced in AT11f cord infections. Polykaryons evident at 3 dpi in AT11f cord infected cultures contained 697 ± 245 (SD) nuclei versus 142 ± 118 (SD) nuclei in those induced by wt JHMV ($P < .001$, t test) (Figure 4.1 A,B). The syncytia contained predominantly $GFAP^+$ astrocytes while among the overlying oligodendrocytes there was ocassionally evidence of lysis (Figure 4.1 C,D,E,F). More rapid replication in CD.1 cells was accompanied by accelerated and more extensive syncytia formation, culminating in massive cell killing by 3 dpi (Pasick et al., 1992). By contrast, with SJL/J glial cultures the cytopathic effect due to AT11f cord virus involved no more than 30 to 40% of the culture area even at 10 dpi.

To ascertain whether specific sequences when deleted from S in the AT11f cord variant effected the enhanced efficiency of replication in SJL/J glial cultures, we compared growth of AT11f cord, V5A13 (88), AT11f brain and wt JHMV viruses. V5A13 (88) which possesses a 447 nucleotide deletion in the S coding

Figure 4.1. Comparison of infection at 8 D.I.V. and P8 of SJL/J primary glial cultures with wt JHMV or AT11f cord variant. (A) Foci of wt JHMV infected cells at 3 dpi identified by reaction with MAb against JHMV nucleocapsid (N) protein and FITC-conjugated goat anti-mouse IgG. (B) Foci of AT11f cord infected cells sampled and reacted as in (A). Note that the foci are about 5X larger in (B) than in (A). (C) Inoculated with AT11f cord and reacted for N as in (A). (D) Same field as in (C) reacted with rabbit anti-galactosyl cerebroside (GC) and Texas Red-conjugated goat anti-rabbit IgG to demonstrate oligodendrocytes. Arrows point to GC^+ disrupted cells. (E) Appearance of culture infected and reacted for N as in (B) at higher magnification. Note the absence of antigen from the nuclei. (F) The same field as in (E) demonstrating the co-localization of glial fibrillary acidic protein (GFAP) in astrocytes by reaction with rabbit anti-GFAP and TR-conjugated goat anti-rabbit IgG. A and B x 260, C and D x 360, E and F x 1850.

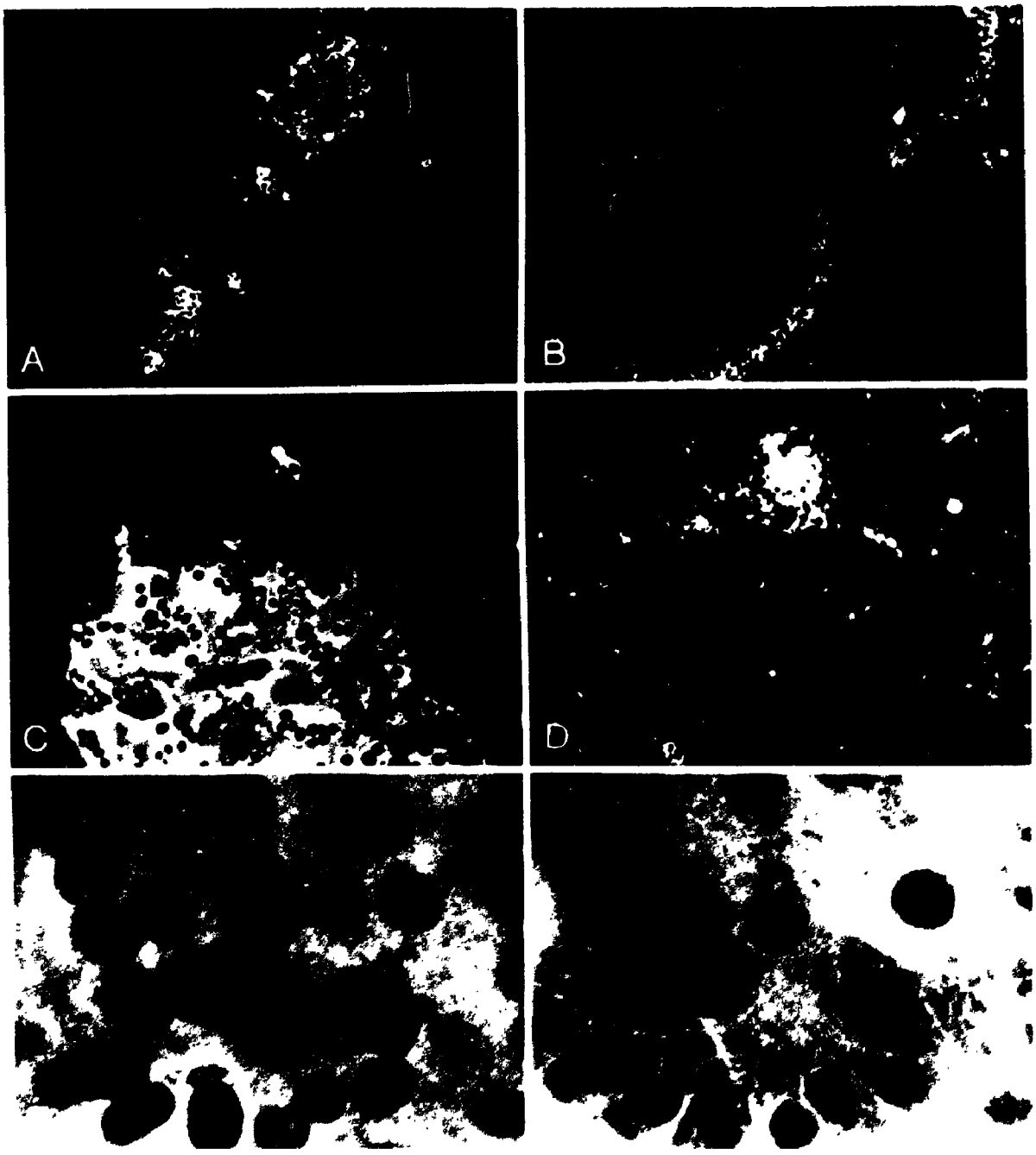
A
B
C
D

region (Parker et al., 1989) that overlaps the one present within AT11f cord (Figure 4.2), was selected in vitro from SAC- cells infected with wt virus on the basis of resistance to neutralization with MAb 5A13.5 (Parker et al., 1989) by the procedure originally described by Dalziel et al. (1986). This virus does not appear to express detectable levels of HE (M.J. Buchmeier, personal communication). The AT11f brain variant was another isolate from the same rat as AT11f cord virus (Morris et al., 1989) and carries the identical HE gene deletion as AT11f cord, but has no deletion within S (La Monica et al., 1991). For this reason, the AT11f brain variant provided a suitable control for assessing the significance of defective HE expression present in AT11f cord and V5A13 (88). It is evident from the data in Table 4.1, that SJL/J glial cultures infected with AT11f cord and V5A13 (88) variants produced approximately 10 times more virus than parallel cultures infected with AT11f brain virus or wt JHMV. Occassionally, AT11f brain virus grew about twice as efficiently as wt JHMV (data not shown). Together, these results indicate that more efficient growth of the AT11f cord variant can be attributed to the deletion in the S coding region, although a minor contributory role of the coincidental HE defect was not ruled out. The infection of SJL/J glial cells with all viral strains tested appeared self-limiting because it never progressed to where total destruction of the cultures was observed. Rather, there was a gradual decrease in virus produced with elapsing time postinoculation.

Figure 4.2. Diagramatic representation of the overlapping deletions in the S1 component of AT11f cord and V5A13 (88) variants of MHV-JHM and MHV-4 respectively. Deleted segments involve amino acids approximately between 430 and 590 located within the distal 1/3 of S1. Alignment of the deleted sequences was based on published sequence data (Parker et al., 1989; La Monica et al., 1991).

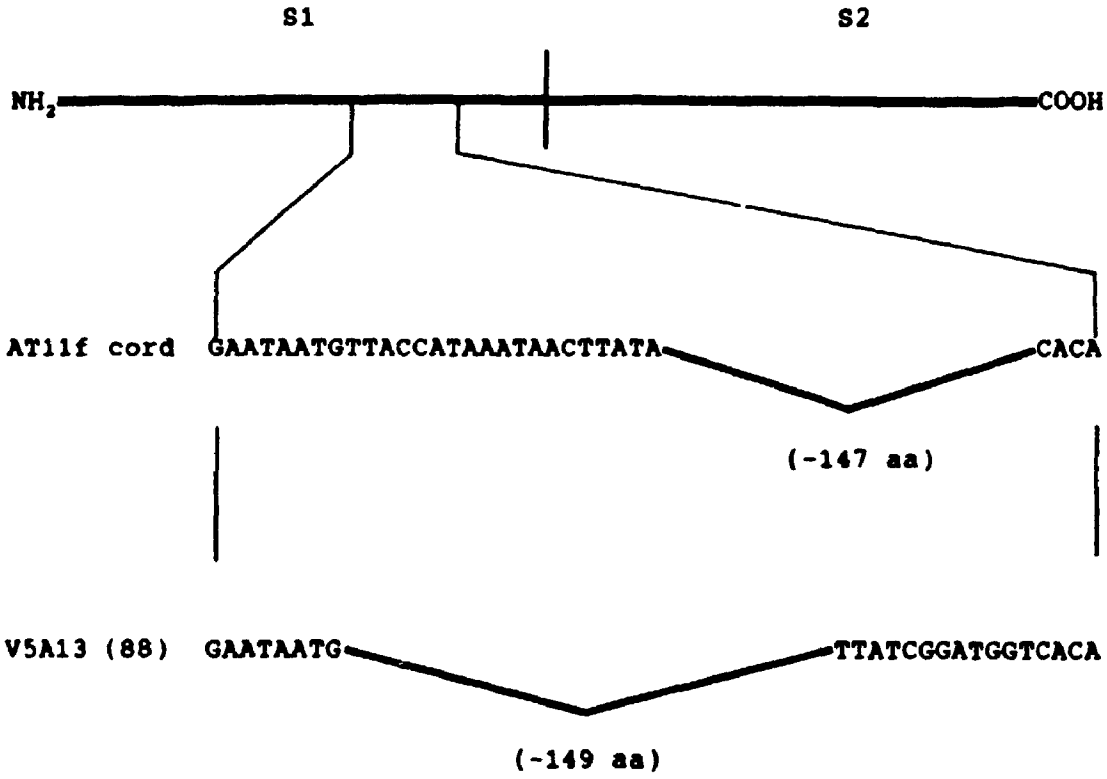
S1
S2
NH2
COOH
AT11f cord
GAATAATGTTACCATAAATAACTTATA
CACA
(-147 aa)
V5A13 (88)
GAATAATG
TTATCGGATGGTCACA
(-149 aa)

Comparative analysis of gene expression by wt JHM, AT11f brain and AT11f cord virus during infection of SJL/J glial cultures at 24 and 48 hours postinoculation, revealed that amounts of virus-specific RNA generated, reflected differences in the titers of progeny virus made and the extent of syncytia formed (Figure 4.3). Thus, synthesis of AT11f cord virus RNA was greater than that of AT11f brain virus RNA, which in turn was greater than that of wt JHMV RNA. However, the data do not allow us to identify the step(s) between virus and host affected by the S deletion, that in turn would explain the associated enhancement of growth.

To determine whether enhanced replication of JHMV variants in primary SJL/J glial cultures was a property general to neural cells, an investigation was made with primary SJL/J neurons. Furthermore, neuronal infections in vitro might provide data with important implications for the observed resistance in vivo. For this purpose, primary hippocampal neuronal cultures derived from E20 SJL/J mice were established and inoculated at 5 D.I.V. at a m.o.i. of 10 with wt JHMV or the AT11fcord variant. Immunocytochemistry was carried out at 1, 3 and 5 dpi to monitor virus expression. Experiments using two independent culture preparations demonstrated that SJL/J hippocampal neurons could be infected with both viruses, although infection with the the AT11f cord variant apppeared to involve more neurons than infection with wt. The pattern of viral N staining in infected SJL/J neurons was the same as that observed for infected rat hippocampal

Figure 4.3. In situ dot-blot analysis of MHV RNA present in infected SJL/J glial cultures. Primary SJL/J glial cultures were inoculated at 7 D.I.V. with JHMV, AT11f cord or AT11f brain virus using a m.o.i. of 1. At 24 and 48 hours post-inoculation, cells were washed and harvested by scraping into PBS. After resuspending the cells and adjusting to a final concentration of 1 x 10^6 cells per ml, 400, 200 and 100 x 10^3 cells per sample were spotted onto nitrocellulose and probed for MHV-specific RNA with ^{32}Plabelled pg344. Equivalent numbers of uninoculated cells were used as a negative control.

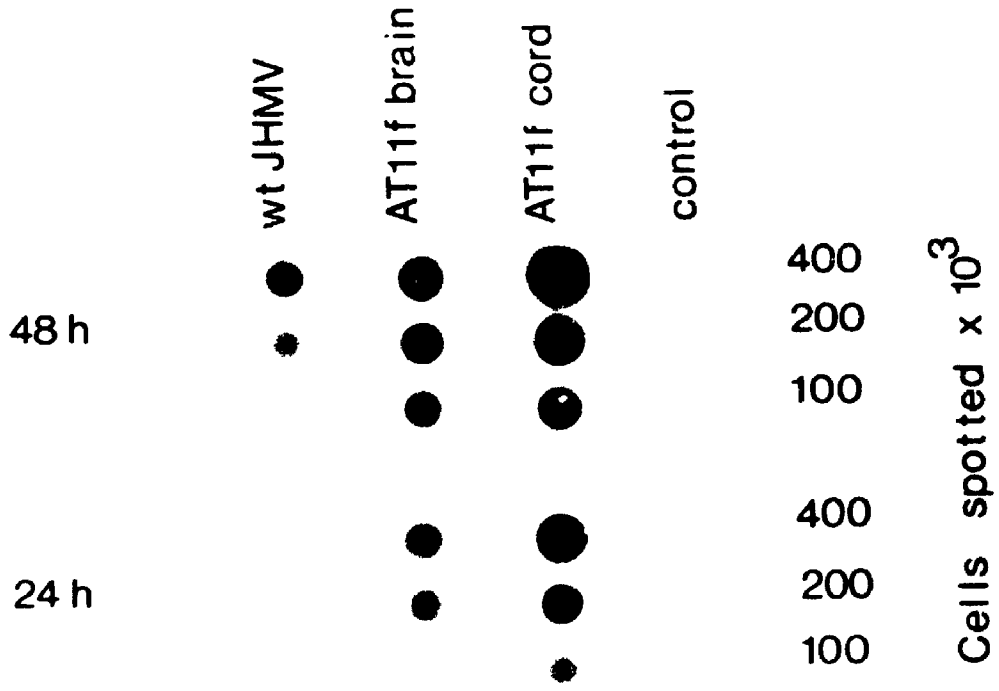
wt JHMV
AT11f brain
AT11f cord
control
48 h
24 h
400
200
100
400
200
100
Cells spotted x 10^3

neurons with antigen concentrated both in the cell body and neurites (data not shown). The infection involved more cells as time increased postinoculation. Thus, the enhanced efficieny of replication of the AT11f cord variant carrying a deletion in the spike protein occurred in both primary SJL/J neurons and glia.

4.3.2 Comparison of Replication Efficiency and the Disease Process in Resistant SJL/J and Susceptible CD.1 Mice Inoculated with wt JHMV and Variant AT11f Cord Virus.

In view of the enhanced replication obtained by AT11f cord virus in primary neural cultures, I decided to determine whether the CNS disease process might also be affected. To investigate the disease process, SJL/J mice were inoculated ic with varyir., doses of either wt JHMV or AT11f cord variant at 1, 2, 4, 5, 6, and 11 weeks of age. Comparison was made with age-matched, susceptible CD.1 mice as controls. The data, summarized in Table 4.2 demonstrated that in the case of SJL/J mice an age-related resistance developed. Thus at 1 and 2 weeks of age, SJL/J pups were completely susceptible and by 6 weeks uniformly resistant to both viruses. Some differences were evident between the wt and variant at 4 to 5 weeks of age when SJL/J mice demonstrated full resistance to wt JHMV and partial resistance to AT11f cord variant. This age-dependent development of resistance although similar to that previously reported (Stohlman et al., 1980) differs with respect to the exact ages at which the shift from susceptibility to

Table 4.2

Cumulative Data Obtained with Varying Doses of wt-JHMV and AT11fcord Following *In Vivo* Challenge of Resistant and Susceptible Strains of Mice

Strain of Animal	Age at Time of ic Challenge (weeks)	Size of Inoculum (pfu)	# animals dead or sacraficed *in extremis*/ # animals inoculated	
			wt-JHMV	AT11f cord
SJL/J	1	1×10^5	4/4	5/5
	2	1×10^5	4/4	4/4
	4	1×10^5	0/2	0/3
		1×10^6	0/4	1/5
	5	1×10^6	0/8	2/8
	6	1×10^3	--	0/3
		1×10^4	--	0/3
		1×10^5	0/2	0/2
		1×10^6	0/2	0/2
	11	1×10^6	0/4	0/4
CD.1[a]	3	1×10^4	3/3	3/3
		1×10^6	3/3	2/2
	4	1×10^5	5/5	5/5
		1×10^6	2/2	2/2
	6	1×10^6	2/2	2/2

[a]It was established (G.A.R. Wilson, unpublished results) that 2000 pfu of wt-JHMV were lethal for 100% of CD.1 mice challenged at 3 weeks of age.

resistance was observed. However, the data were virtually in complete agreement with those reported by another group (Barthold and Smith, 1987) where encephalitis was only observed in 1 week old SJL/J animals following intranasal inoculation with JHMV. As anticipated, CD.1 mice remained fully susceptible at all ages tested and their mean time to death ranged from 1.5 to 5.3 dpi depending on the age at inoculation, size of inoculum and virus used. Generally, equivalent doses of AT11f cord virus produced acute encephalitis in CD.1 mice in half the time required for that of wt JHMV. The rapidity of the disease process in CD.1 mice corresponded with the efficiency of virus replication in primary glial cultures (Table 4.1 and Pasick et al., 1992). Interestingly, it has been previously reported (Dalziel et al., 1986) that S deletion variants of JHMV behave as neuroattenuated agents in BALB/c mice judging by increased LD_{50}s and the propensity to induce chronic, demyelinating rather than acute, encephalitic disease. This however, has not been my experience using the doses of inoculum which were administered to CD.1 mice in the present studies.

Since even the more efficient S deletion variants of JHMV replicated in SJL/J glial cultures to titers that were at least one order of magnitude lower than those observed with CD.1 cells, I hypothesized that the host's immune response may, perhaps, control any differences in neuropathogenecity that might occur during growth in vivo. The role of the cellular immune responses on the outcome of the infection with

wt JHMV and AT11fcord variant were followed after administration of the immunosuppressant drug Cyclosporin A (CsA).

As evident from a comparison of the data in Table 4.2 versus Table 4.3, CsA treatment of animals following ic inoculation with either wt JHMV or AT11f cord variant led to a significant breakthrough of resistance in the 4 week old age group. Clinical signs consisted of lethargy and piloerection which progressed to irritability and seizures. The mean days to advanced disease was 8.1 ± 1.8 and 8.0 ± 2.6 dpi for wt and variant viruses respectively. This was longer than the development of advanced disease observed for age-matched CD.1 mice or 1 and 2 week old SJL/J mice, the latter of which succumbed to advanced disease in half this time. In the 5 week old age group, the AT11f cord variant produced a significantly higher incidence of encephalitis as compared with wt JHMV inoculants (P= 0.035, Fisher's exact test). Again, an age-related shift in resistance was observed despite CsA treatment, though not as pronounced as that observed in the non-CsA-treated group. Consistent with the observed growth of wt and variant virus in tissue culture, AT11f cord virus appeared to also replicate more efficiently <u>in vivo</u> than wt JHMV (Table 4.4). Examination of sectioned brain for histopathology revealed perivascular cuffing and mononuclear cell infiltration within the forebrain, loss of neurons within Ammon's horn of the hippocampus and vacuolation of the neuropil within the midbrain, as illustrated in Figure 4.4.

Table 4.3

Effect of Cyclosporin A on Disease and Mortality

Caused by wt-JHMV and AT11fcord Virus

in SJL/J Mice

Age at Time of ic Challenge (weeks)	Size of Inoculum (pfu)	# animals dead or sacraficed *in extremis*/# animals inoculated[a]	
		wt-JHMV	AT11f cord
4	1×10^6	9/14	14/16
5	1×10^6	0/7	4/7
6	1×10^3	-	0/3
	1×10^4	-	0/3
	1×10^6	0/2	0/2
11	1×10^6	0/4	1/4

[a]Cummulative data were obtained following ic inoculation at the times and virus concentrations indicated. Animals were treated with 25 mg/kg body weight CsA beginning either the day before or the day of inoculation with virus and continued for an additional 5 to 10 days following inoculation.

Table 4.4
Comparison of wt JHMV and AT11f cord Virus Growth in the Brains of SJL/J Mice Challenged at Different Ages

Age at time of ic inoculation (weeks)	Days post-inoculation	Viral Brain Titers[a] pfu/gram of brain tissue			
		wt-JHMV		AT11f cord	
		CsA^-	CsA^+	CsA^-	CsA^+
1	4	1.6×10^7(2)	ND	2.1×10^8(2)	ND
2	4	3.8×10^6(1)	ND	3.0×10^8(2)	ND
	5	7.0×10^7(2)	ND	5.8×10^8(1)	ND
4	4	ND	ND	2.6×10^6(2)[b]	3.0×10^6(2)[b]
	5	ND	ND	ND	6.4×10^7(2)
	6	ND	4.7×10^7(2)	ND	7.8×10^8(3)
	8	ND	3.3×10^6(2)	9.0×10^5(1)	2.9×10^7(2)
	13	ND	ND	2.9×10^6(1)[b]	2.5×10^3(1)
5	4	ND	ND	ND	6.2×10^5(2)
11	6	ND	ND	ND	2.6×10^4(1)

[a]Animals were sacrificed *in extremis* and either all or half the brain was homogenized in serum supplemented medium for virus titer determination. The data are from single animals or the averages of 2 or 3 animals, as indicated within the brackets
[b]Asyaptomatic ND Not Done.

Figure 4.4. Histology and immunohistochemistry of various brain regions from SJL/J mice inoculated with AT11f cord variant. (A) Hematoxylin-eosin stained section of the hippocampus at 13 dpi from an animal inoculated at 4 weeks of age and CsA treated. Arrows point to prominent mononuclear infiltrates within Ammon's horn (CA3 region). Note that the dentate gyrus (den) appears normal. (B) Adjacent section to that in A demonstrating large amounts of viral antigen in Ammon's horn detected by anti-N immunohistochemistry. (C) Hematoxylin-eosin stained section of the midbrain at 13 dpi from an animal inoculated at 4 weeks of age and CsA untreated. Note the perivascular cuffing, mononuclear infiltrates and vacuolation of the neuropil. (D) Adjacent section to that in C demonstrating intense nucleocapsid antigen staining in the area of vacuolation. (E) Hematoxylin-eosin stained section of the hindbrain at 9 dpi from an animal inoculated at 5 weeks of age and CsA untreated. Note the relatively normal histologic appearance. (F) Adjacent section to that illustrated in E demonstrating N^+ cells that are morphologically typical of glia. A, B, C and D x 75, E and F x 300.

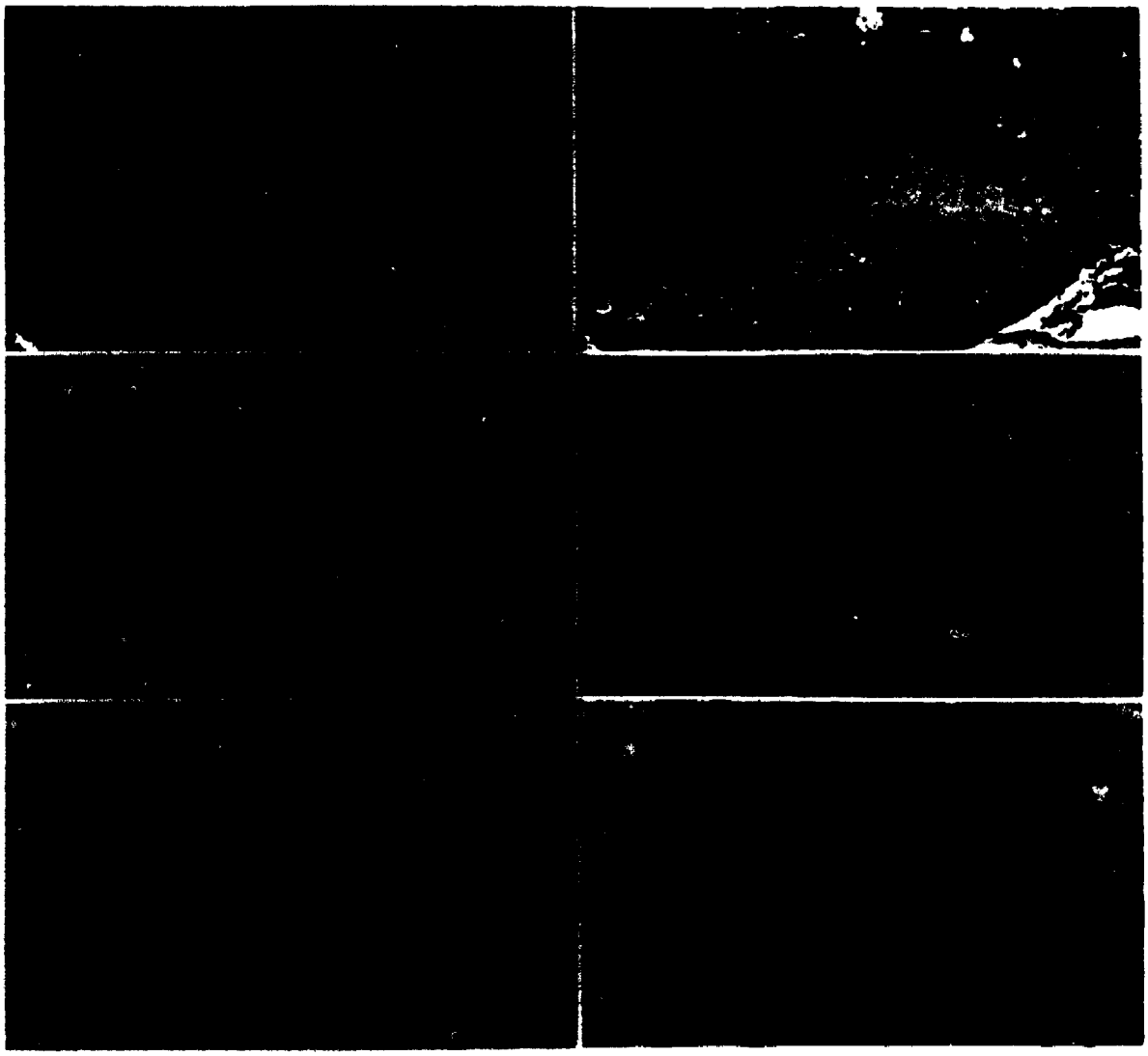

Viral antigen was confined primarily to cells possessing glial morphology, as well as to fiber tracts surrounding the hippocampal formation (Figure 4.4). Interestingly, in the mice which did not develop acute encephalitis, there was no subsequent development of chronic demyelinating disease, whether assessed clinically or histologically during a 60 day period following inoculation. Infectious virus was never recovered from the livers of mice that had developed signs of clinical disease. This information, combined with the above observations strongly implies that affected mice developed and were succumbing to an encephalitic disease process.

4.3.3 Comparison of the Neuropathology Caused in Suckling Wistar Furth Rats by wt JHMV and S Deletion Variants.

Comparison of the clinicopathologic disease induced by 4 variants of JHMV, possessing sizable deletions within a segment of S presumed to be hypervariable (Banner et al., 1990), was carried out among each other and with wt virus. Three variants originated from the MHV-4 isolates of Buchmeier and colleages while the fourth was from a rat infected with JHMV. It was originally assumed that parental MHV-4 and JHMV strains were identical. However, Parker et al. (1989) reported that the S gene sequence for MHV-4 differed from that originally described for JHMV (Schmidt et al., 1987) by the presence of an additional 423 nucleotides. It turned out that this additional sequence either constituted or spanned the hypervariable region found within S1. By contrast, the JHMV

strain employed in this study, which originated from the ATCC, contains the sequence present in MHV-4 (La Monica et al., 1991) but absent from the Wurzburg strain of JHMV (Schmidt et al., 1987). Thus, the strain of JHMV used in these studies can be considered equivalent to MHV-4, at least with respect to the spike protein. MHV-4 variants V5A13 (88), V5A13.1 (86) and V4B11.3 (86), which were independently selected on the basis of resistance to neutralization with MAbs, respectively possess 149, 142 and 159 overlapping amino acid deletions involving the hypervariable region of S1 (Parker et al., 1989). As indicated earlier, the AT11f cord variant derived from the ATCC isolate of JHMV, possesses a deletion within S that tightly overlaps the one existing in V5A13 (88) (Figure 4.2). To insure that the viruses being compared in this study possessed the genotypes described by others, Northern blot analysis of virus-specific RNAs from infected L-2 cell cultures was carried out. As Figure 4.5 demonstrates, the mRNA 3 for each of the S protein deletion variants migrated faster than that of wt JHMV as reported previously (Morris et al., 1989; Gallagher et al., 1990).

WF pups were inoculated with $1x10^5$ pfu's of the above panel of viruses at either P5 or later at between P10 and P13. The neurologic disease induced by these isolates was monitored and assessed according to incidence, time of onset, types of clinical signs presented at onset, viral titers in brains at the height of neurologic disease and examination of the histopathology. Table 4.5 summarizes the incidence and

Figure 4.5. Northern blot hybridization analysis of virus-specific RNAs from L-2 cell cultures infected with wt JHMV and spike protein deletion variants. L-2 cells were inoculated with the indicated viruses (or uninoculated in the case of the control lane) and the total cellular RNA extracted at 12 hours postinoculation. 20 μg of each RNA sample was electrophoresed through a 1.1% agarose gel after denaturation with glyoxal and dimethyl sulfoxide. The separated RNAs were blotted onto a nylon membrane and the virus-specific RNAs visualized following hybridization with ^{32}P-labelled pg344 which contains an 1800 base pair insert encoding genes 5 and 6 as well as the intergenic regions preceding genes 5, 6 and 7 of MHV-A59. Viral mRNAs 3 to 7 are labelled. The arrows point to the difference in mobility of mRNA 3, encoding the spike protein, between wt JHMV and the variants.

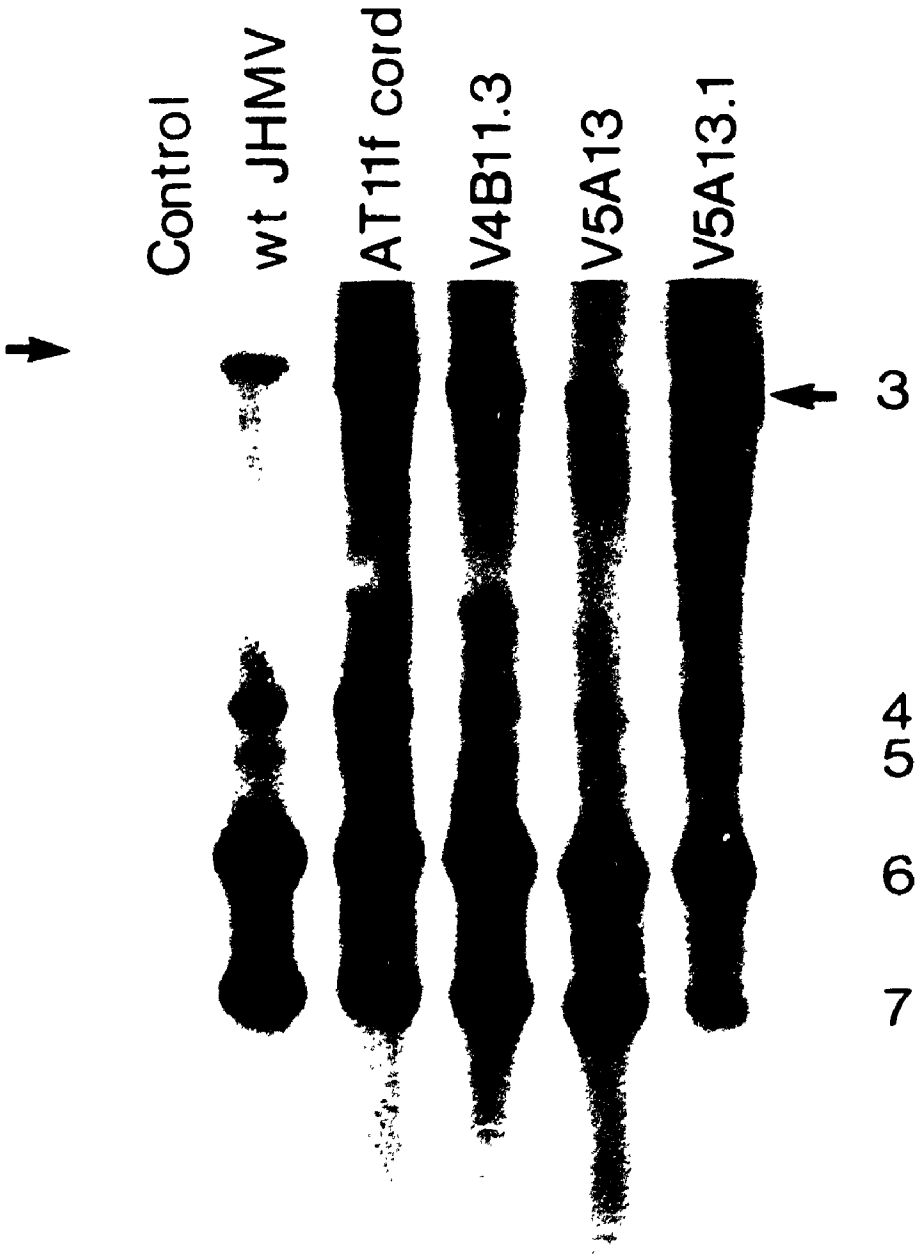
Control
wt JHMV
AT11f cord
V4B11.3
V5A13
V5A13.1
3
4
5
6
7

frequency distribution for development of clinical neurologic diseas for each virus. Note the reduction in incidence of clinical disease in animals inoculated at P10 to P13 versus those inoculated at P5 which is in agreement with the results originally reported by Sorensen et al. (1982). Inoculation at P5 with either wt JHMV or the variants produced an acute onset disease characterized by hunched posture, piloerection and irritability accompanied by marked cerebral cortical necrosis. Thus, with the challenge dose and age of animal tested here, no differences in neurovirulence were observed between wt JHMV and either AT11f cord or V5A13 (88). By contrast, in WF rats challenged between P10 and P13, the resulting disease was more delayed in its onset and was characterized most frequently by ataxia and paraparesis which would sometimes progress to paralysis. The clinical presentation evoked in rats challenged with all the S deletion variants was apparently the same and similar to the disease observed in animals challenged with wt virus. However, with wt JHMV, indications of acute encephalitis were sometimes also present, especially in animals that became ill within the first 13 days following inoculation.

Histopathologic examination of the CNS of rats challenged at P10 to P13 revealed the following: 1) animals challenged with variant viruses developed multifocal vacuolar and demyelinating lesions especially within the deep cerebellar white matter and adjacent areas of the medulla oblongata; 2) in addition to the above, a number of wt JHMV challenged

Table 4.5

Incidence and Temporal Distribution of Neurologic Disease Induced in Wistar Furth Rats by wt JHMV and Selected S Deletion Variants

Virus	Age when inoculated (Days)	Number inoculated	Clinical Neurologic Signs[a] Days Postinoculation			
			1-7	8-14	15-21	>21
wt JHMV	5	4	0	3	0	0
AT11f cord	5	5	0	5	0	0
V5A13 (88)	5	6	0	5	1	0
wt JHMV	10-13	30	2	4	6	0
AT11f cord	10-13	30	0	6	6	1
V5A13 (88)	10-13	18	0	5	3	0
V5A13.1 (86)	10-13	15	0	1	1	1
V4B11.3 (86)	10-13	19	0	2	4	1

[a]Rats that either died acutely or were sacrificed *in extremis*. WF rats were inoculated ic with $1x10^5$ pfu's of the indicated virus at either P5 or P10-P13 and observed daily for a minimum of 60 days for the development of clinical neurologic signs. Animals which developed disease were assigned to the indicated time intervals on the basis of when the signs became most pronounced.

animals also possessed lesions within the forebrain, which included varying degrees of hippocampal necrosis and neocortical rarefaction accompanied by mild perivascular cuffing and mononuclear and polymorphonuclear cell infiltration. In almost all cases, where vacuolation and demyelination of deep cerebellar white matter was present, there was an associated loss of neurons within the deep cerebellar nuclei. This was the case regardless of whether animals were challenged with wt JHMV or any of the variants. No significant differences were found in virus titers recovered from the CNS after infection by the strains tested. The titers recovered diminished progressively with increase in the time elapsing postinoculation in all cases (Table 4.6).

In summary, subtle qualitative differences were found to exist between wt JHMV versus S deletion variants, with respect to the type of disease and lesions they induced in WF rats. The disease process appeared to be highly controlled and differed according to the age of the animal at the time of challenge.

4.4 Discussion.

This study demonstrates the ways in which viral variants can be applied towards identifying important virus-host interactions. One of the conclusions reached as a consequence of this approach agrees with an earlier one (Wilson and Dales, 1988) that SJL/J resistance to JHMV is complex and likely contingent on more than one virus or host determinant.

Table 4.6

Comparison of Viral Growth Between wt JHMV and Selected S Deletion Variants in Wistar Furth Rat Brain

Virus	Age at time of ic inoculation	Days postinoculation	Viral Brain Titers[a] pfu/gram of brain tissue
wt JHMV	10	7	4.0×10^6
		13	1.0×10^6
		14	6.2×10^5
		20	1.2×10^2
AT11f cord	5	10	1.2×10^7
	10	15	2.3×10^5
		16	1.2×10^6
		19	4.1×10^4
		20	1.1×10^6
V5A13 (88)	5	10	5.5×10^7
	10	12	1.3×10^6
		19	2.6×10^5
V5A13.1 (86)	10	12	8.2×10^5
		15	3.0×10^4
		23	0
V4B11.3 (86)	10	15	1.4×10^6
		18	1.4×10^4
		20	2.1×10^3

[a] WF pups were inoculated ic with 1×10^5 pfu's of virus, then sacrificed at the times indicated when animals were *in extremis*. Brains were subsequently removed for viral titer determination. The data are from individual animals.

Previous work had demonstrated that the genetic resistance observed in SJL/J mice to JHMV was already inherent in primary glial cultures derived from neonates (Wilson and Dales, 1988). Glia appear to be targets for JHMV in susceptible C57BL/6 mice during both acute encephalomyelitis and delayed demyelinating disease (Perlman et al., 1987). It is possible that glial infections may play an important role in the pathogenesis of the subacute, demyelinating as well as acute encephalitic forms of disease, especially when one considers the important supportive role that astrocytes have in maintaining normal neuronal functions. Characterization of virus-glial interactions in vitro has the potential to provide insight into pathogenesis in vivo. The observation that both AT11f cord and V5A13 (88) variants possessed growth advantages over wt JHMV in primary glial cultures was, in turn, reflected by enhanced growth and ability to induce disease in vivo. The enhanced growth of AT11f cord virus correlated with increased viral gene expression and the ability of the variant to incorporate greater numbers of cells into syncytia, a phenomenon that is most likely attributable to the fusogenic properties of S. The fact that cultured hippocampal neurons, like the glia, were able to support infection of both wt and variant viruses suggests that resistance is likely not associated with any defect involving interactions with neurons of this type. It also confirms the conclusions reached in the previous chapter, that the attenuated neurovirulence of the S deletion variants cannot be attributed to a loss in neuronal

tropism, contrary to the supposition of Dalziel et al. (1986).

Comparing the distribution pattern for resistance to MHV among strains of recombinant-inbred mice, Knobler et al. (1984a) demonstrated that the susceptibilty of peritoneal macrophages for MHV-4 was linked to the Svp-2 locus on the proximal end of mouse chromosome 7. Interestingly, these authors alluded to the fact that several loci on this chromosome encode trypsin-like proteases and molecules involved in secretory processing. These correlations fit with the hypothesis that resistance of SJL/J glia to JHMV may involve a defect in cell-to-cell spread, which in turn may be intimately dependent upon syncytiogenesis. This hypothesis, originally advanced by Wilson and Dales (1988), further proposed that resistance by SJL/J glia may be associated with defective processing of S necessary for optimal syncytiogenesis and thus spread of infection.

Previously, an infectious centers assay suggested that the restriction of growth of wt JHMV in primary SJL/J glial cultures was associated with defective cell-to-cell spread from initially infected foci (Wilson and Dales, 1988). Both resistant SJL/J and susceptible CD.1 glial cultures adsorbed and sequestered the inoculum with equal efficiency (Wilson and Dales, 1988). In the current study, a small but progressive increase in size of infected foci was observed during the initial 3 to 4 days following inoculation with the AT11f cord variant. Thus a combination of present and previous results favours the hypothesis that greater replication efficiency of

S deletions variants over wt JHMV in SJL/J glial cultures is likely due to enhanced spread of the infection rather than to differences in numbers of cells initially infected or the replication rates within individual cells. However, one cannot rule out the possibility that yields of virus per infected cell may differ between wt and variant viruses, an explanation advanced to account for greater titers obtained with MHV-4 S deletion variants in delayed brain tumor (DBT) cells (Gallagher et al., 1990). The higher yields of these variants compared with those of wt MHV-4 in DBT cells were concluded to be the result of decreased fusogenicity of the truncated versions of S. This is consistent with attenuated cytopathogenicity whereby the growth cycle of the variants is prolonged compared with that of wt MHV-4. Contradicting this concept are observations that with G26-24 cells (a murine oligodendroglioma) V5A13 (88) and AT11f cord viruses are both more fusogenic than wt JHMV (V. Morris, personal communication) indicating that the attribute of fusogenicity may be host cell as well as virus regulated (Frana et al., 1985).

As outlined in chapter 1, S is a 180 kDa glycoprotein that becomes cotranslationally glycosylated in the endoplasmic reticulum, and reportedly undergoes trimerization prior to assembly into virions (Delmas and Laude, 1990). Virions assemble by budding into a smooth membrane compartment between transitional elements of the Golgi stack (Tooze et al., 1988) and are released from the cell via constitutive exocytosis

(Tooze et al., 1987). Spike glycoprotein that is produced in excess and not incorportated into virions, is transported to the cell exterior and anchored to the plasma membrane where it can induce cell-to-cell fusion from within (Vennema et al., 1990). Proteolytic cleavage of the 180 kDa S precursor to 90 kDa N-terminal S1, and C-terminal S2 products is mediated by host proteases; the extent of this reaction varying according to the host cell involved (Frana et al., 1985). Proteolytic cleavage of S was originally thought to be a necessary prerequisite for virus-induced cell fusion and was reported to occur just prior to the release of virions from infected cells (Sturman et al., 1985). Recent reports have indicated however that fusogenicity is not absolutely dependent on the proteolytic cleavage of S, though it can apparently be enhanced by it (Stauber et al., in press; Taguchi et al., in press; Heijnen et al., in press). Although the molecular mechanism by which S induces host cell-to-cell fusion is not known, specific determinants within both S1 and S2 have been implicated (Makino et al., 1987; Routledge et al., 1991) along with associated conformational changes involving S1 and S2 subunits (Sturman et al., 1990; Weismiller et al., 1990). Neutralizing epitopes, as well as fusogenic and neurovirulence determinants also appear to be associated with a multiplicity of sites along the S molecule (Takase-Yoden et al., 1990; Routledge et al., 1991; Wang et al., 1992), indicating that the basis for a number of the spike protein's biological functions are complex and dependent on interactions between S1

and S2 subunits.

The basis for the resistance of SJL/J neural cells to JHMV presented here, is in contrast to the explanation proposed by others, specifically, the lack of functional receptors on target tissues of SJL/J mice. This presumption derived from a comparison of virus binding to isolated heptocyte and intestinal brush border membranes from resistant SJL/J and susceptible BALB/c mice (Boyle et al., 1987; Williams et al., 1990). MHV bound to a 110 to 120 kDa glycoprotein present on the membranes of susceptible BALB/c hepatocytes and enterocytes that was apparently absent or non-functional in identical membrane preparations from resistant SJL/J mice (Boyle et al., 1987; Williams et al., 1990). The gene for this receptor glycoprotein was eventually cloned and identified as a member of the carcinoembryonic antigen (CEA) family in the immunoglobulin superfamily (Williams et al., 1991). As conclusive proof that this protein was indeed a functional MHV receptor, resistant human and hamster cell lines were rendered MHV-susceptible following transfection and expression of the cloned gene (Dveksler et al., 1991). Despite this, the inability to detect this molecule in the brain and spinal cord of susceptible BALB/c mice (Williams et al., 1991) suggested that CNS infections likely involved another receptor molecule and that conclusions drawn from work on enterocytes and hepatocytes should not be used as the basis for explaining SJL/J resistance to JHMV CNS infections. Involvement of alternate receptor(s) for binding JHMV to cells of the CNS was

implied in a report by Barthold and Smith (1987). They showed that JHMV could replicate equally well in BALB/c and SJL/J brains following intranasal inoculation of 1 week old mice. By contrast, BALB/c intestine and liver would support virus growth, while SJL/J intestine and liver would not. Very recently, Yokomori and Lai (1992) have demonstrated that a related CEA family member is expressed within the CNS and can serve as a functional MHV receptor. In fact, this second receptor referred to as mmCGM2, is very likely related to the first receptor or mmCGM1, by alternative mRNA splicing (Yokomori and Lai, 1992). Perhaps more intriguing is, that when mmCGM1 or mmCGM2 that have been cloned from resistant SJL/J mice are expressed in resistant Cos7 cells, conversion to a MHV-susceptibile phenotype results. Evidently, some other factor other than the receptor is involved in determining the resistance of SJL/J cells to JHMV, supporting the original conclusions of Wilson and Dales (1989) that resistance by SJL/J glia does not result from inadequate virus attachment. Yokomori and Lai (1992) have further alluded that resistance of SJL/J cells to JHMV likely involves a step early in the infections cycle but still requires the participation of the spike protein.

Control over virus multiplication and related disease processes by cellular immunity was clear from the work with immunosuppressants. The fact that CsA treatment could accentuate the CNS disease due to both wt JHMV and variants, suggests that cellular immunity confers protection against

disease by limiting virus replication and spread. CsA is known to inhibit the activation of T lymphocytes by antigen (Sevach, 1985) apparently by specifically inhibiting the function of nuclear proteins important for the transcriptional activation of the genes for IL-2, the IL-2 receptor, IL-4 and γIFN (Emmel et al., 1989). Although the primary site of CsA action may be directly on T cells, particularly $CD4^+$ cells, the drug may also affect functions of B cells and macrophages. The lethality of JHMV infections of C57BL/6 mice may be prevented by adoptively transferring virus specific T cell clones implicated in a local DTH response. Interestingly, the protection afforded does not result in the inhibition of virus replication (Stohlman et al., 1986, 1988). In this study, no difference in virus titers was evident at 4 dpi between CsA-treated and control mice inoculated with AT11f cord virus at 4 weeks of age. In this age group, maximal viral brain titers occurred at 6 dpi (Table 4.4), which preceded the mean onset of advanced disease by 2 days. The single CsA untreated mouse which did succumb to encephalitis at 8 dpi had a brain virus titer which was an order of magnitude less than found in CsA treated mice at the same number of dpi. Such a difference in titer was not observed in CsA treated versus control mice examined at 13 dpi. Clearance of JHMV from the CNS has been shown to be T cell mediated and likely requires both $CD4^+$ and $CD8^+$ phenotypes (Sussman et al., 1989; Williamson and Stohlman, 1980; Williamson et al., 1991; Yagamuchi et al., 1991). The reason that CsA immunosuppression was unable to

abrogate resistance to either wt or variant JHMV in mice challenged at 11 weeks of age, is not known, but might be attributed to some age related maturation event of neural targets. One previously discussed possibilty (Dveksler et al., 1991; Yokomori and Lai, 1992) takes the developmental regulation of CEA expression (Huang et al., 1990) into account by proposing that the level of MHV-receptor expression may be higher in newborn than adult SJL/J mice. Alternatively, in 11 week old mice, CsA may not interfere with the function of macrophage-like cells shown previously to be protective against JHMV in older animals (Stohlman et al., 1980), or with function of natural killer cells which are potentially important in suppressing the virus within the CNS (Williamson et al., 1991).

The above data demonstrate that resistance of SJL/J mice to JHMV-induced neurologic disease cannot be attributed to regulation by a single factor, but appears to involve at least two factors. This is consistent with observations from crossbreeding analyses on SJL x B10.S F1 hybrids and F1 backcrosses which gave evidence against control by a single gene but in favour of mediation by at least two genes (Stohlman and Frelinger, 1978). Current data are consistent with the notion that a defect in cell-to-cell spread of the infection, as well as to protective functions of the immune response are responsible for mediating resistance.

Previous studies conducted with mice (Dalziel et al., 1986) and rats (Morris et al., 1989; Matsubara et al., 1991)

led to the conclusion that JHMV variants are neuroattenuated when their spike glycoproteins carry a large deletion. Results from the present study on WF rats generally confirmed the above conclusions for animals inoculated between P10 and P13, but not for rats challenged earlier in life at P5, in contrast with an earlier report (Morris et al., 1989). The cability of the S variants to induce acute encephalitis with prominent grey matter involvement in P5-challenged WF rats, in addition to their ability to productively infect rat and mouse hippocampal neurons in culture, strongly implies that neuroattentuation is not related to a loss in neuronal tropism. The above contradictions, coupled with the enhanced neurovirulence observed when the AT11f cord variant infects young or immunosuppressed SJL/J mice, point out the important role in neurovirulence and pathogenesis played by the spike glycoprotein and the modulating influence of host factors such as cellular immunity.

CHAPTER 5

SUMMARY AND CONCLUSIONS

The age and strain of the rodent host markedly influence the outcome of CNS infections with MHV. The intent of this thesis was to identify, or characterize further, factors which may lie at the root of these contingencies. The question from which this work began, asked whether the developmental determinants that control postnatal CNS myelination in rats, also influence the susceptibility of this host to the demyelinating form of JHMV-induced neurologic disease. CNS myelination is a complex process under the control of many factors. The decision of which factor to study and hence the approach used to test the hypothesis that the state of CNS myelination influences the pathogenesis of the demyelinating form of JHMV disease, was a problem in itself. Preliminary studies directed at establishing whether a link existed between thyroid hormone's known influence on postnatal CNS myelination and the pathogenesis of the demyelinating disease form of JHMV disease yielded inconclusive results which did not warrant further pursuit (see appendix for details). Hence, an <u>in vitro</u> approach was implemented for the purpose of testing this hypothesis.

Primary dissociated neural cultures, which have become powerful models for investigating developmental events and cell-cell interactions within the intact CNS, were likewise

equally useful in addressing questions pertaining to viral pathogenesis. O-2A cells, the myelin forming cells of the CNS, were shown to be semi-permissive for infection with JHMV in a differentiation dependent mannner. By growing O-2A enriched cultures in the presence of bFGF + PDGF, oligodendrocyte differentiation was prevented and JHMV replication concomitantly inhibited. By contrast, withdrawing the growth factors initiated oligodendrocyte differentiation and resulted in a proportion of the cells becoming permissive for JHMV. These findings, coupled with those of Beushasen and Dales (1985) and Beushausen et al. (1987), which demonstrated the non-permissive nature of terminally differented oligodendrocytes, led to the hypothesis that the interval for induction of demyelinating encephalomyelitis in postnatal rats may be explained, to some extent, by a differential, stage-dependent susceptibilty of O-2A cells to infection with JHMV. In other words, the factors that contribute to histogenesis and myelinogenesis of the CNS, may also indirectly influence the type of disease induced by JHMV. In attempting to identify the cellular parameters that make certain stages of the O-2A lineage more permissive for JHMV than others, the conclusion that the block against infection involved an early event(s) in the interaction between virus and cell was reached. Permissivity appeared to depend on an event(s) occurring after virus adsorption-penetration, but before or involving the expression of viral genes. The details surrounding the nature of this block will obviously require further work.

The use of primary neural cultures to study virus-cell interactions provided other insights into the process of neuropathogenesis. The involvement of neurons as the initial target cell population in organotypic, rat, telencephalic cultures, as well as the studies dealing with the trafficking of viral proteins and progeny virions in primary hippocampal neuronal and OBL21 cultures, indicated that this class of cell may play a major role in both acute and chronic forms of JHMV-induced neurologic disease. Due to the vast diversity of neurons that exists within the CNS, one must ask whether all types are equally susceptible to infection with JHMV. The fact, that in mice, JHMV appears to infect a wider range of neurons than the less neurotropic MHV-A59 strain (Lavi et al., 1990), coupled with more recent findings that JHMV appears to preferably infect neurons within many of the cholinergic pathways (Barnett and Perlman, in press), suggests that viral and host factors are both involved in determining neuronal tropism. Spread along specific neurotransmitter pathways of the brai could significantly influence the overall pattern of lesion formation within the CNS and hence, the clinical presentation of the disease. This might explain the noted predispositon for occurance of demyelinating lesions within the deep cerebellar white matter of rats.

The third population of cells observed to be infected with JHMV were astrocytes. Therefore, their participation in the process of pathogensis must also be considered. Previous studies also demonstrated that astrocytes can serve as hosts

for JHMV, however, further clarification of this matter will be necessary in order to adequately understand its significance in the process of pathogenesis. Purified rat type-1 astrocyte cultures resist infection with JHMV, which is in sharp contrast to the noticeable astroglial involvement observed after infecting mixed telencephalic cultures, O-2A lineage enriched cultures and hippocampal neuronal cultures. The reason for this discrepancy is still not known but two possibilities may account for it. In the first, astroglial subpopulations may possess differential susceptibility toward direct infection with JHMV. In this regard, astroglial heterogeneity has been fairly well documented (Wilkin et al., 1990). Some of this heterogeneity may be explained on the basis of multiple astrocyte lineages (Goldman and Vaysse, 1991; Miller and Szigeti, 1991; Fok-Seang and Miller, 1992; Vaysse and Goldman, 1992). It is possible that only certain lineages give rise to astrocytes that are permissive for JHMV. In the second, infection of astrocytes may depend on the presence of other infected cell types. In this regard, Gallagher et al. (1992) have recently shown that JHMV can spread to cells lacking a specific MHV-receptor by a process involving membrane fusion. Therefore, infection may be transmitted to astrocytes by fusion with another cell type. Astrocytes are a potentially important target cell from the standpoint of pathogenesis since they participate in the formation and maintenance of the blood-brain barrier (Risau and Wolburg, 1990) and as antigen presenting cells in the CNS

(Fontana et al., 1984). Infection of astrocytes with JHMV could potentially compromise the blood-brain barrier resulting in demyelination by an indirect mechanism, which has been proposed (Compston et al., 1991), and was based on the inherent susceptibility of oligodendrocytes to be lysed by homologous complement in the absence of specific antibody (Wren and Noble, 1989). Lastly, murine astrocytes release a soluble factor in response to MHV-A59 infections that induces the expression of class I MHC molecules on the surfaces of oligodendrocytes and astrocytes (Suzumura et al., 1986,1988), allowing these cells to participate in cell-mediated immune reactions against the virus. This may be of particular importance, since the suggestion has been made that JHMV-induced demyelination does not primarily result from the direct lysis of virus infected oligodendrocytes, but rather from an immunologically mediated mechanism (Wang et al., 1990). Viral target cells and their interrelationships are diagramatically summarized in Figure 5.1.

In accordance with other studies, the spike glycoprotein of the virus was shown to constitute an important pathogenic determinant. Paradoxically, variants shown previously to possesses neuroattenutated characteristics in susceptible strains of mice, possessed enhanced neuropathologic potentials in resistant SJL/J mice. The phenomenon of variation, particularly among viruses with RNA genomes has led to the concept of the quasispecies, which is a population of viral genomes that are closely related to, yet different from one

Figure 5.1. The anatomical and functional interrelationships existing among neurons, oligodendrocytes and astrocytes within the CNS. Oligodendrocytes are depicted as being primarily involved in the formation of myelin sheaths around axons. Perineuronal oligodendrocytes or "satellite cells" are not shown, in part, because their functions are unknown. The roles of astrocytes include: compartmentation of the neuropil, particularly at the nodes of Ranvier, neuronal processes and synapses, regulation of material exchange between capillaries and neurons, trophic support of neurons and possibly other cell types, and regulation of extracellular ionic and neurotransmitter concentratons. The spatiotemporal development of oligodendroytes, which begins in the late embryonic period and continues into the first 3 or more weeks of postnatal life, is portrayed at the bottom half of the figure along with changes that take place in the expression of a number of antigenic markers. Solid lines indicate expression, whereas broken lines the absence or loss of expression of each marker. Neuronal and astrocytic influences on this development scheme are not shown (see Figure 2.1). Pathogenesis of neurologic disease induced by JHMV should be viewed in the context of the determinants influencing viral tropism for each of these cell populations, as well as how infection might consequently influence their functions and interrelationships.

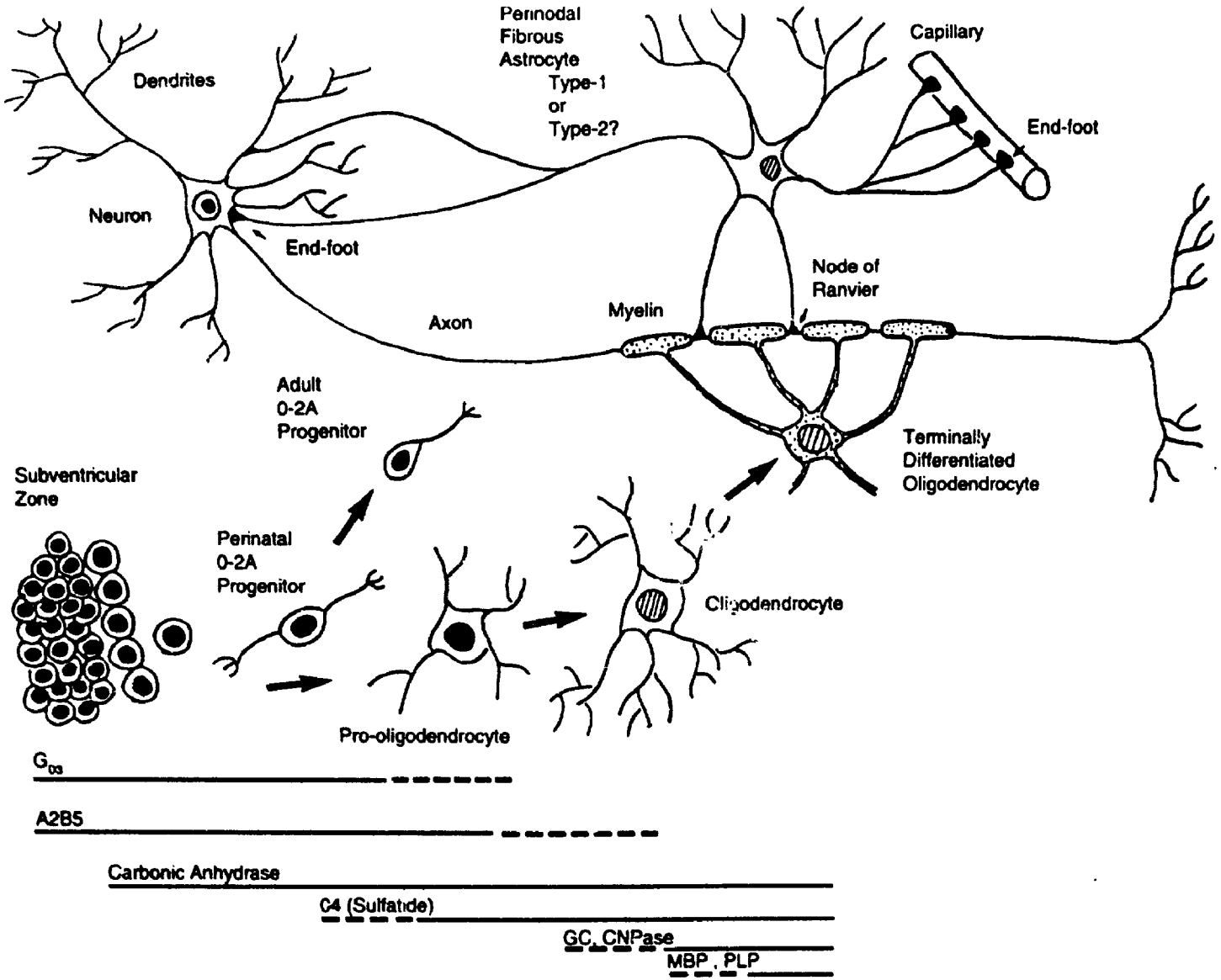
Perinodal
Fibrous
Astrocyte
Type-1
or
Type-2?
Capillary
Dendrites
End-foot
Neuron
End-foot
Node of
Ranvier
Myelin
Axon
Adult
0-2A
Progenitor
Terminally
Differentiated
Oligodendrocyte
Subventricular
Zone
Perinatal
0-2A
Progenitor
Oligodendrocyte
Pro-oligodendrocyte
G_{o3}
A2B5
Carbonic Anhydrase
C4 (Sulfatide)
GC, CNPase
MBP, PLP

another (Steinhauer and Holland, 1987). In addition to the obvious advantages that genetic variation has on population survival, the evolution of variants likely also plays an important role in pathogenesis. Further work is required to determine if generation and amplification of variants over the course of an infection is necessary for the pathogenesis of the chronic forms of neurologic disease induced by this agent.

Lastly, I have only lightly touched on the importance of the immunologic response to JHMV as a determinant in disease outcome. This was best exemplified by the need for immunosuppressive intervention in abrogating resistance to both wt virus and S deletion variants in SJL/J mice. Thus, in this model of virus-induced neurologic disease, many factors appear to contribute to the outcome of infection. Demyelination in particular, should likely be viewed as a complex, multistep process which may be sensitive to a number of conditions.

APPENDIX

RELATIONSHIP BETWEEN INFLUENCE OF THYROID HORMONE ON CNS DEVELOPMENT AND ACQUISITION OF RESISTANCE TO JHMV-INDUCED DEMYELINATING ENCEPHALOMYELITIS IN POSTNATAL RATS

Introduction.

Sorensen et al. (1980, 1982) originally demonstrated the variation in susceptibility among different strains of inbred rats to JHMV. Rats of the inbred Wistar Lewis (WL) strain were found to be completely resistant to JHMV-induced neurologic disease, brought on by the intracranial inoculation of 10^4 to 10^5 pfu of virus, by P10, in contrast to inbred Wistar Furth (WF) rats which did not become completely resist until P21. Interestingly, the resistant state was achieved progressively with associated changes in disease incidence and clinicopathologic character. WF pups inoculated during the first week of postnatal life typically developed a fulminant encephalitis involving forebrain grey matter 7 to 10 days following challenge, whereas animals inoculated during the subsequent two weeks of postnatal life developed neurologic disease that was lower in frequency, more delayed in its onset, and characterized clinically by paraparesis which progressed to paralysis and pathologically by multi-focal demyelination of white matter within the brainstem and spinal cord (Sorensen et al., 1980, 1982). Onset of resistance in both WL and WF rats can be due in part to the ability of a

maturing cellular immune system to suppress the infection, evident from experiments demonstrating the nullifying effects of immunosuppressive drugs (Sorensen et al., 1982; Zimmer and Dales, 1989). However, after abrogation of cellular immunity with cyclosporin A (CsA), or in its absence as with athymic, nude rats, JHMV induced a predominantly grey matter disease with minimal involvement of white matter that was more like the encephalitic disease of neonates (Sorensen et al., 1987; Zimmer and Dales, 1989). This evidence suggested that induction of primarily demyelinating disease may involve determinants other than the cellular immune responses. Myelination might be one determinant because the period for optimal induction of demyelinating encephalomyelitis coincides with an interval when developmental events related to myelinogenesis in the rat are maximal.

It has long been known that thyroid hormone can influence development and maturation of the CNS: an association between myelin formation and thyroid hormone status has been particularly well recognized (reviewed by Nunez, 1984). Thyroid hormone can either stimulate or repress gene expression by a mechanism similar to that for steroid hormones. The receptor for tri-iodothyronine (T_3) which is the product of the c-erb-A proto-oncogene (Sap et al., 1986; Weinberger et al., 1986) is localized to the nucleus of thyroid hormone responsive cells. This receptor has three functional domains: hormone or ligand binding, DNA binding and transcriptional regulatory. DNA binding and transcriptional

regulatory functions are apparently activated by the binding of T_3 to the receptor (Evans, 1988).

Stimulation of myelination by thyroid hormone could invoke both direct and indirect mechanisms. Myelin-forming oligodendrocytes are probably directly responsive to T_3, as indicated by studies employing rat glial and reaggregating brain cell cultures in which T_3 increased oligodendrocyte number, sulfolipid synthesis, 2':3' cyclic nucleotide-3'-phosphohydrolase (CNPase) activity and myelin basic protein (MBP) accumulation in a dose-dependent mannner (Almazan et al., 1985; Koper et al., 1986). In fact, rat oligodendrocytes, like astrocytes and neurons, do possess intranuclear T_3 receptors (Yusta et al., 1988).

Hypomyelination associated with hypothyroidism may also be a secondary consequence of neuropile hypoplasia resulting from reduced length and branching of neurites (Nunez, 1984), or could be due to the growth hormone deficiency that prevails in hypothyroid rats (Coulombe et al., 1980; Walker and Dessault, 1980; DeGennaro et al., 1988). The latter is presummed to be a direct consequence of down regulation of the T_3-dependent growth hormone gene (Lavin et al., 1988). During growth hormone deficiency, glial precursor cell migration from the subventricular zone becomes retarded and accumulation of myelin membrane components is diminished (Pelton et al., 1977). The above sequelae may in turn be mediated through a deficiency in the secondarily induced trophic factor, insulin-like growth factor type I (IGF-I).

At birth, rats are constitutively hypothyroid then begin producing T_3 and T_4 until peak levels are reached at around postnatal days 14 and 26 respectively as a direct consequence of the maturation of the hypothalamo-pituitary-thyroid axis (Dussault and Labrie, 1975; Dubois and Dussault, 1977). Since peak T_3 and T_4 concentrations appear at the period of maximal myelination, when susceptibility to JHMV-induced demyelination is greatest, a possible connection between the above cited processes was investigated.

Materials and Methods.

Animals.

Inbred Wistar Furth (WF) and Wistar Lewis (WL) rats were obtained from Harlan Sprague Dawley and bred in house as previously described by Sorensen et al. (1982). Animals within the colony have remained MHV free based on periodic serologic testing (Armand-Frappier, Laval, Quebec).

Virus Inoculation into Animals.

Suckling rats were inoculated through an intracranially inserted 30 gauge needle, with 1 x 10^5 pfu of JHMV (unless indicated otherwise) contained within a 30 μl volume. The needle was introduced at a 45° angle along the midline of the skull, just posterior to the orbits to a depth of approximately 3 to 4 mm. Animals older than 14 days of age

(P14) were lightly anesthetized with methoxyflurane before carrying out this procedure. Control animals were inoculated by the same procedure with an uninfected L-2 cell lysate.

Induction of Hypothyroidism in Suckling Rats.

Hypothyroidism was induced in litters of suckling WL rats by the addition of 0.05% propylthiouracil (PTU) to the dam's drinking water beginning 5 days before parturition. This treatment was continued until weaning. Hypothyroidism in the pups results from the presence of PTU secreted in the dam's milk. To counteract decreased water consumption due to the bitter taste associated with PTU, the water was sweetened with sucrose. Effects of PTU on thyroid function were assessed indirectly by comparing the growth rates of animals from treated versus control litters. For this purpose pups were weighed daily. The connection between thyroid hormone levels and growth were reported by Kawada et al. (1988) where lowered serum T_4 levels and retarded growth correlated directly with low CNPase activities in cerebral tissue. In the present study, the effects of PTU on thyroid gland microstructure, cerebellar external granule cell migration and thickness of myelin cover were ascertained by means of histological and immunohistochemical procedures.

Thyroxine Adminstration to Suckling Rats.

L-thyroxine or T_4 (Sigma) was administered daily for 10 to 14 days to WF rat pups beginning on P1. Each animal

received 3.0 μg T_4/g body weight (BW) subcutaneously. Control animals within the same litter received injections of physiologic saline by the same route. The effects of exogenous thyroxine were evaluated by comparing the growth curves and age when eyes first opened between treated and control animals.

Virus Titration of Brain Tissue.

JHMV inoculated animals were sacrificed *in extremis* , the brains were divided by a mid-sagittal incision and one half of the brain was then aseptically removed for virus titer determination. The tissue was weighed and placed into a suitable volume of ice-cold tissue culture medium supplemented with 10% FBS so that a 10% w/v tissue homogenate could be prepared. The homogenates were clarified by low speed centrifugation and the supernatants used to make serial 10-fold dilutions which were titered on L-2 cell monolayers.

Histological and Immunohistochemical Examination of CNS Tissues.

The half of the brain not used for virus titer determination, as well as the spinal cord, were isolated after sacrifice of animals and submersed in 10% neutral buffered formalin (10% formalin, 29 mM $NaH_2PO_4.H_2O$, 46 mM Na_2HPO_4) for several days at 4°C before dehydrating by sequential passage through graded ethanol solutions and chloroform in preparation for paraffin embedding. 10 μm sections were cut, then stained

with hematoxylin and eosin for routine histopathology. Myelin thickness and demyelinating lesions were assessed by staining with luxol fast blue. Virus N antigen was detected using the MAb 4B6.2, kindly provided by Dr. M. Buchmeier of the Scripps Clinic and Research Foundation. Sensitivity was amplified employing biotin-anti-biotin conjugates coupled to alkaline phosphatase (AS/AP Plus immunostaining kit, BIO/CAN SCIENTIFIC). Briefly, following deparaffinization, sections were digested in a 0.5% pepsin solution (Sigma) for 20 minutes at 37°C. MAb 4B6.2 as tissue culture supernatant was then incubated overnight at room temperature at a 1:18 dilution prior to the amplification and chromogenic reactions. Following the immunostaining reactions, the sections were briefly counterstained with hematoxylin. MBP immunohistochemistry using a rabbit polyclonal antiserum to guinea pig MBP (Beushausen and Dales, 1985) diluted 1:100 and alkaline phosphatase conjugated secondary antibody (AS/AP immunostaining kit, BIO/CAN SCIENTIFIC) were also employed for the evaluation of myelin thickness.

Results.

Effects of PTU on Pre-Weanling WL Rats and Thyroxine on WF Rats.

The original reports of Sorensen *et al*. (1980, 1982) indicated that suckling WL rats acquire resistance to JHMV-

induced demyelination sooner than WF rats. If thyroid hormone is involved in resistance, then one would predict that WL rats made hypothyroid will have retarded development of resistance. Conversely, administration of thyroxine to WF rats should shorten the interval for development of resistance to JHMV related disease. To test these hypotheses, WL sucklings were rendered hypothyroid by PTU and WF sucklings relatively 'hyperthyroid' by administration of thyroxine (T_4) before challenging with JHMV.

PTU is one of the thiourea antithyroid compounds which inhibit thyroid hormone biosynthesis by blocking iodide oxidation, a necessary prerequisite for its incorporation into mono- and di-iodotyrosine precursors. As a consequence of PTU treatment, thyroid follicles do not accumulate thyroglobulin, which is the obligatory substrate for T_3 and T_4 formation. As Figure 1 illustrates, the effect of treatment of WL pups with PTU, on growth, was manifested before P10, and became progressively more pronounced until termination at P21, in agreement with a previously published report (Nathaniel et al., 1988). PTU treated animals also consistently opened their eyes 3 to 4 days later than controls. The effect of PTU on growth has been attributed to a reduction in growth hormone levels by Coulombe et al. (1980), Walker and Dessault (1980) and DeGennaro et al. (1988). Histologic examination of the thyroid glands from age-matched PTU treated and control animals revealed clear cut differences. As expected, in treated rats there was follicular epithelial cell hyperplasia

Figure 1. The effect of PTU treatment on body growth of Wistar Lewis rats. The growth of preweanling WL rats receiving PTU treatment via the dam's milk beginning at birth and continuing until P21, was compared with that of untreated controls. (A) Growth curves for PTU treated and control animals. The points are the means and standard deviations of body weights from a representative control (11 pups) and PTU treated (10 pups) litters. (B) Comparison of the sizes of age-matched control (top) and PTU treated (bottom) animals at P18.

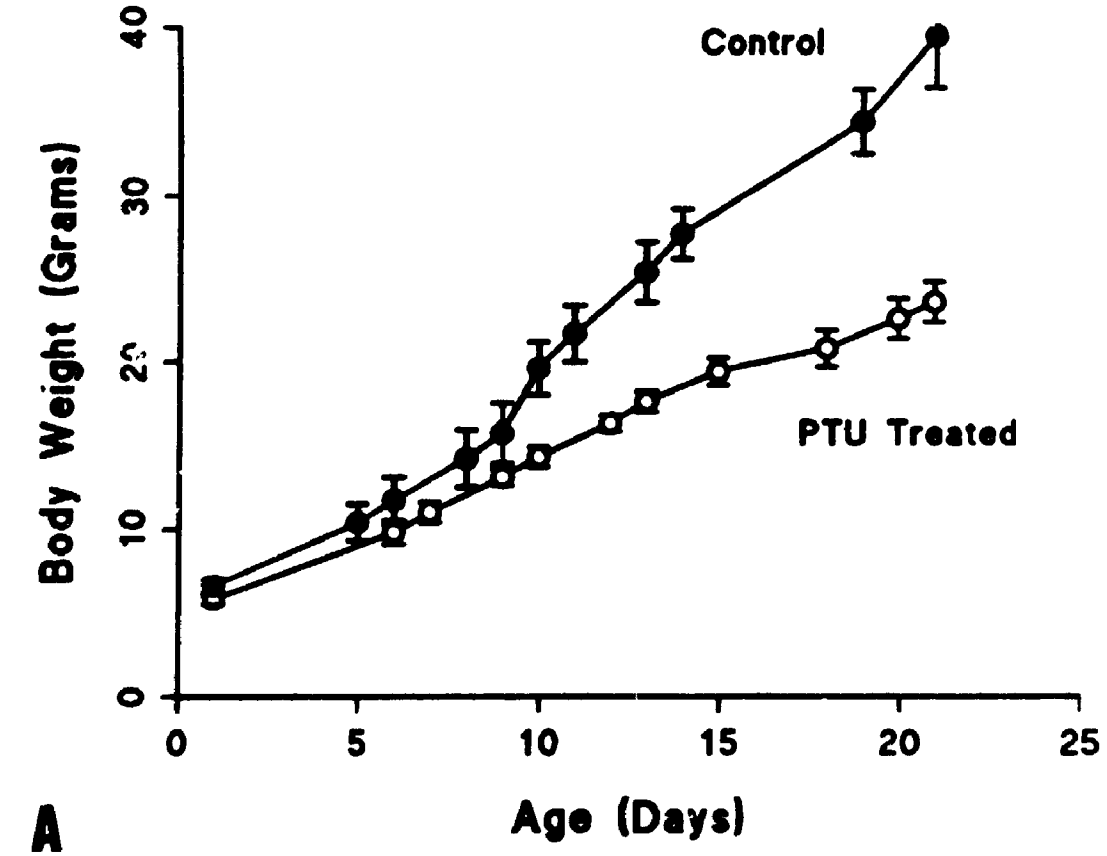
Control
PTU Treated
Body Weight (Grams)
0
10
20
30
40
0
5
10
15
20
25
Age (Days)

A

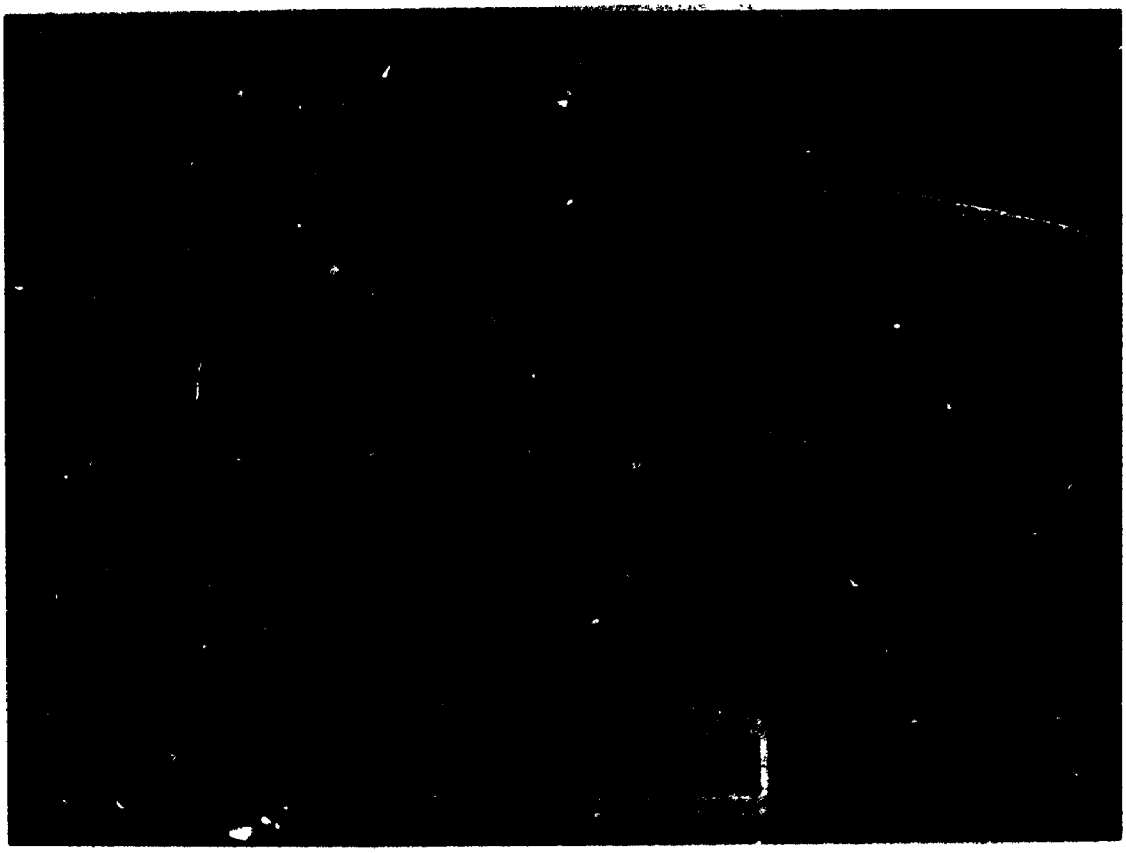

and absence or paucity of colloid in the follicles, whereas in controls, follicles were large and filled with colloid and the epithelium was of normal size (data not shown). These results confirmed the effectiveness of PTU on thyroid hormone metabolism of weanlings. PTU treatment produced more subtle but nevertheless consistent effects on brain development. This was concluded from a qualitative histological assessment of the inward movement of the neuronal external granule cell layer in the cerebellum and of myelin deposition. As evident in Figure 2, by P15, the inward migration of the external granule cell layer of the cerebellum in PTU treated animals, was retarded to the point where it was 3 to 4 days behind that found in controls. Hypothyroidism has also been shown to depress neuronal migration in other areas of the brain where postnatal neurogenesis takes place (Patel et al., 1979). At P15, discernable differences were also obvious in the amount of myelin deposition, as determined by luxol fast blue staining (Figure 2.A and B) and MBP immunohistochemistry (data not shown), however, these differences became less apparent by P21. Taken together, these data show that induction of hypothyroidism in WL rat pups by administration of PTU caused retardation in growth and brain development.

The daily administration of L-thyroxine (T_4) beginning at birth was previously reported to markedly increase the CNPase activity [μmol/hr/mg protein] (Patel et al., 1988), and accelerate the developmental program for myelinogenesis (Walters and Morell, 1981) in normal rats. Daily subcutaneous

Figure 2. Comparison of external granular cell layer thickness and myelin deposition in PTU treated and control WL rats. CNS tissues from PTU treated and control WL rats were examined histologically following hematoxylin-eosin and luxol fast blue-neutral red staining reactions, as well as by MBP immunohistochemistry. Comparisons were made at P15, P18 and P21. The typical appearance of the cerebellum of a P15 control rat in panel A as compared with that from an age-matched, PTU treated animal in panel B demonstrates obvious differences in the thickness of the external granular cell layer (EGL and arrows) and myelin deposition within the white matter (W). Abreviations: IGL, internal granular cell layer; M, molecular layer. Luxol fast blue-neutral red staining. A and B x 170


M
E
M

injections of WF rats with 3.0 g per gram of BW of T_4 between P1 and P10 to P14 caused a significant reduction in body weight which became evident by P7-8 (Figure 3), consistent with a previous report (Walters and Morell, 1981). The T_4 treated animals were leaner, generally more active and opened their eyes 3 to 4 days ahead of the controls. These effects were compatible with an accelerated maturation resulting from the administration of T_4. These results in turn were consistent with previous studies demonstrating promotion of differentiation and functional development in biochemical terms of the rat brain by thyroid hormone (Balazs et al., 1975; Patel et al., 1988; Walters and Morell, 1981). Although my studies on the effects of PTU-induced hypothyroidism on WL rat brain and T_4 on WF rat brain were somewhat limited, the results obtained, together with those from previous studies by others, revealed clear differences compared with developing control rats. Consequently, it seemed appropriate to pursue looking at any possible relationship existing between control of development by thyroid hormone and time of onset of resistance to JHMV-induced demyelinating disease in preweanling rats.

Characterization of the Neurologic Disease Induced by JHMV in Control and Hypothyroid WL Rats.

In a previous report, Sorensen et al. (1982) indicated that WL rats become fully resistant to the induction of clinically apparent neurologic disease by JHMV at about P10.

Figure 3. The effect of thyroxine supplementation on body growth of Wistar Furth rats. Growth of WF sucklings given daily injections of 3.0 μg thyroxine per gram of body weight, commencing at P1 and continuing until P10 to P14, was compared with saline injected control animals. The points are the means and standard deviations of body weights of thyroxine injected (13 pups) and control (13 pups) animals.

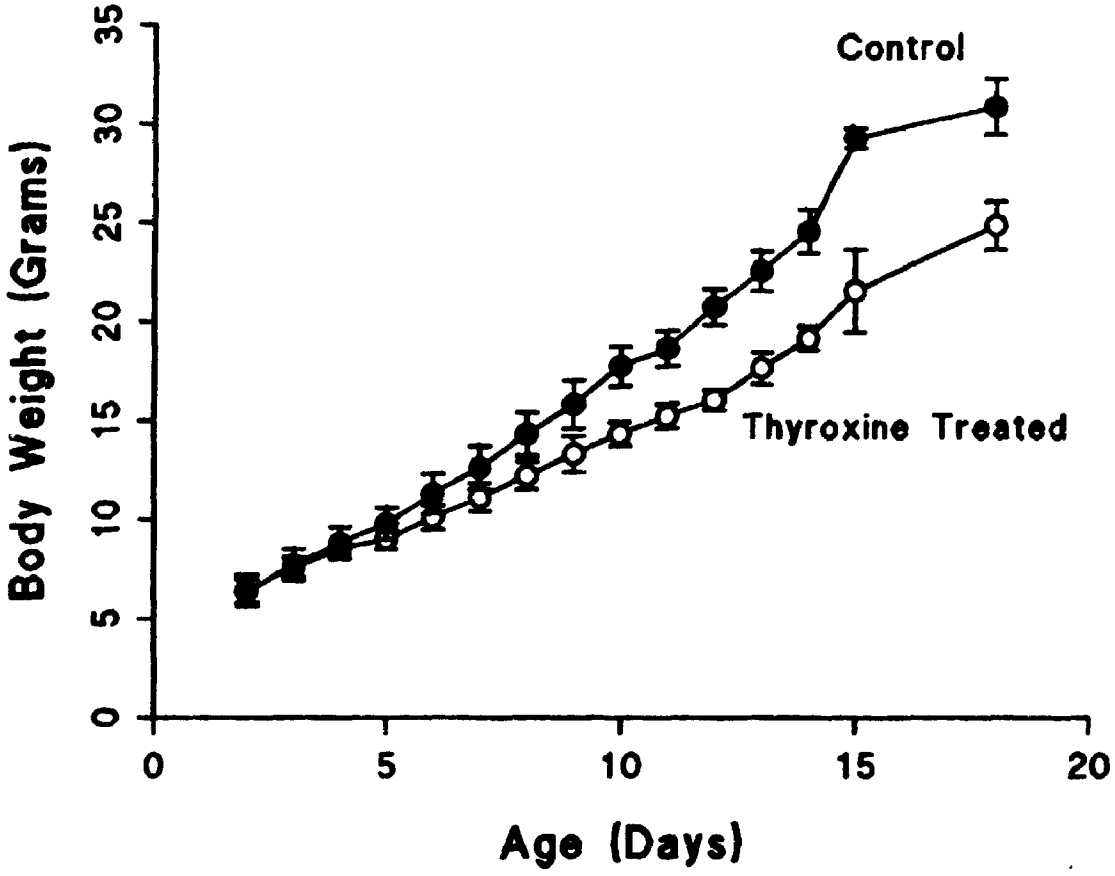
Body Weight (Grams)
0
5
10
15
20
25
30
35
0
5
10
15
20
Age (Days)
Control
Thyroxine Treated

To test whether hypothyroidism delayed the onset of resistance, PTU treated WL rats were challenged ic with $1x10^5$ pfu's of JHMV at P9 or P10 and P13 or P15, while controls were inoculated at P9 or P10 and P15. Forty-three animals were used in total; 34 received virus and 9 received an uninfected L-2 cell lysate. Animals were monitored at least once daily for a minimum of 60 days for the appearance of neurologic disease, and those with signs were sacrificed in extremis and the CNS sampled for histopathology and determination of virus titer. As Table 1 shows, no striking differences between control and PTU treated groups in the overall incidence or time interval for onset of clinical neurologic disease were apparent. The average number of days to advanced disease for controls and PTU treated animals challenged at P9 or P10 was 7.6 and 9 days respectively, while the interval for controls challenged at P15 and PTU treated rats challenged at P13 or P15 was 18.3 and 19.7 days respectively. In addition, the clinicopathologic picture presented was dependent more on the age at the time of inoculation and the time interval elapsing between inoculation and onset of clinical signs, rather than on PTU treatment. Thus, animals that were challenged at P9 or P10 generally developed acute encephalitis, characterized by cerebral cortical and/or hippocampal necrosis, while those inoculated at either P13 or P15 manifested paralytic disease with demyelinating lesions involving the brain stem and spinal cord (Figure 4). However, the late onset disease was not entirely confined to the white matter. Neuronal loss, especially

Figure 4. CNS lesions in clinically affected Wistar Lewis rats following inoculation with JHMV. PTU treated and control WL sucklings were challenged with JHMV by ic inoculation at P9 or P10 and P13 or P15, and the pathological changes evoked at the time of maximal neurological signs was assessed histologically. Panel A demonstrates marked necrosis and rarefaction of the cerebral cortex, 9 days following the inoculation of a PTU treated rat at P10. Clinically, this animal was irritable with a hunched posture and ruffled hair coat. The underlying hippocampus (H) appears normal. Abreviations: pcl, pyramidal cell layer; CA1 to CA4, subfields of the pyramidal cell layer; gl, granular layer of the dentate gyrus. Hematoxylin-eosin. x 170

Panel B demonstrates a focus of demyelination involving the deep cerebellar white matter (bracketed by arrows), 18 days following the inoculation of a PTU treated rat at P10. Vacuolation (asterisk) and neuronal loss involving one of the deep cerebellar nuclei (DCN) is also apparent.

Luxol fast blue-neutral red. x 170


CAT
H

Table 1

Effects of Hypothyroidism on the Susceptibility of Inbred WL Rats to JHMV-Induced Neurologic Disease

Treatment	Age when inoculated (Days)	Number inoculated	Clinical Neurologic Signs[a] Days Postinoculation			
			1-7	8-14	15-21	>21
PTU treated	9-10	9	0	6	1	0
	13-15	10	0	2	1	4
Control untreated	9-10	6	1	3	0	1
	15	9	0	0	4	1

[a]Rats that either died or were sacrificed *in extremis*.
PTU treated, WL rats were inoculated ic with $1x10^5$ pfu's of JHMV at P9-P10 and P13-P15, while controls were inoculated at P9-P10 and P15. Animals were observed daily for a minimum of 60 days and assigned to the above time intervals on the basis of when clinical neurologic signs became most pronounced. Out of a total of 9 animals inoculated ic with an unifected L-2 cell lysate, none developed any signs of illness.

involving the deep cerebellar nuclei, was frequently associated with contiguous demyelinating lesions (Figure 4.B). Likewise, JHMV replication within the CNS was not appreciably different in control versus PTU treated rats (Table 2), both showing progressively lower titres the greater the time elapsing between inoculation and development of clinically apparent disease. In summary then, induction of hypothyroidism in suckling WL rats did not seem to discernibly affect the outcome of JHMV challenge. Moreover, these experiments demonstrated a greater sensitivity to JHMV-induced neurologic disease by P15 WL rats than was previously reported (Sorensen et al., 1982).

Characterization of Neurologic Disease Induced by JHMV in Control and Thyroxine Treated WF Rats.

Administration of thyroxine to suckling WF rats prior to challenge with JHMV also did not effect the resistance to or nature of disease provoked, as shown in Table 3, which contains a summary of the time course of disease presentation among thyroxine treated an control WF rats which were inoculated at P10. The time elapsing before evidence of advanced disease was 12.3 ± 5.2 days for thyroxine treated and 14.1 ± 5.2 days for the control animals. In both groups, panencephalitis was the most common outcome of virus challenge. Animals that became ill before 14 dpi frequently demonstrated cerebral cortical necrosis, hippocampal necrosis and cerebellar vacuolation. Animals that developed clinical

Table 2

Comparison of JHMV Growth in the Brains of PTU Treated and Control WL Rats Challenged at Different Ages

Age at time of ic inoculation	Days postinoculation	Viral Brain Titers[a] pfu/gram of brain tissue	
		Control	PTU treated
P9	9	$9x10^6$ (1)	$5x10^6$ (3)
P13	12	ND	$3x10^6$ (1)
	17	ND	$1x10^6$ (1)
	24	ND	$3x10^4$ (1)
	26	ND	$2x10^3$ (1)
P15	16	$2x10^4$ (1)	ND
	20	$2x10^2$ (1)	ND

[a]WL pups were inoculated ic with $1x10^5$ pfu's of JHMV at the indicated ages. Animals were sacrificed *in extremis* and the brains removed then homogenized in serum supplemented medium for virus titer determination. The data are from single animals or the average of 3 animals, as indicated within the brackets.
ND, No data.

Table 3

E Effects of Thyroxine Treatment on the Susceptibility of Inbred WF Rats to JHMV-Induced Neurologic Disease

Treatment	Age when inoculated (Days)	Number inoculated	Clinical Neurologic Signs[a] Days Postinoculation			
			1-7	8-14	15-21	>21
Thyroxine treated	10	12	2	3	5	0
Control untreated	10	11	1	6	2	1

[a]Rats that either died or were sacrificed in extremis
Thyroxine supplemented and control WF rats were inoculated ic with $1x10^5$ pfu's of JHMV at P10. Animals were observed daily for a minimum of 60 days and assigned to the above time intervals when clinical neurologic signs became most pronounced. Out of a total of 7 animals inoculated ic with an uninfected L-2 cell lysate, none developed any signs of illness.

neurologic disease after 14 dpi, tended to show less necrosis of forebrain grey matter and more demyelinating lesions within the brain stem and spinal cord, in agreement with previously published findings of Sorensen et al. (1982). Virus titers in brain tissue were variable from one animal to another irrespective of thyroxine treatment. However, there appeared to exist a concordance between decrease in pfu's and time elapsing postinoculation (Table 4) as observed with WL rats. Therefore, like PTU, though thyroxine supplementation appeared to affect development of WF preweanlings, it did not significantly alter the nature or course of progression of JHMV-induced disease.

The Effects of Cyclosporin A Treatment on JHMV-Induced Neurologic Disease in WL Rats.

Data from the present study demonstrate that in WL preweanlings, the age at inoculation determines whether a grey matter or white matter disease is manifested, irrespective of the thyroid hormone status and related CNS maturation phenomena. Since resistance to JHMV-induced disease can be abrogated in WL rats even at P3' 'y use of very high doses of viru: inoculum or administration of immunosuppressants such as cyclosporin A (Zimmer and Dales, 1989), I decided to examine the influence of the cellular immune system on onset of the resistance in hypothyroid and euthyroid animals. For this purpose, 14 hypothyroid and 12 euthyroid control WL rats were challenged with 5 x 10^4 pfu's of JHMV at P22.

Table 4

Comparison of JHMV Growth in the Brains of Thyroxine Treated and Control WF Rats

Age at time of ic inoculation	Days postinoculation	Viral Brain Titers[a] pfu/gram of brain tissue Control	Thyroxine treated
10	5	ND	$4x10^3$ (1)
	7	$4x10^6$ (1)	$8x10^5$ (1)
	9	$2x10^5$ (1)	ND
	10	ND	$9x10^4$ (1)
	11	ND	$3x10^6$ (2)
	13	$1x10^6$ (2)	ND
	14	$6x10^5$ (2)	ND
	16	ND	$3x10^4$ (2)
	17	$1x10^3$ (1)	ND
	18	ND	$4x10^4$ (3)
	24	$2x10^3$ (1)	ND

[a]WF pups were inoculated ic with $1x10^5$ pfu's of JHMV at P10. Animals were sacrificed *in extremis* and the brains removed then homogenized in serum supplemented medium for virus titer determination. The data are from single animals or the average of 2 or 3 animals, as indicated within the brackets.
ND, No data.

Immunosuppression begun at P18 in 7 of the PTU treated, and 6 of the control animals by intraperitoneally (ip) injecting 25 mg of Cyclosporin A (CsA) per kg of BW. The control group received saline injections ip. CsA treatment was continued until day 4 postinoculation (P26) then was stopped for 12 days and resumed on day 16 postinoculation (P38). This protocol was based on a previous study (Zimmer and Dales, 1989) demonstrating the effectiveness of this time course of CsA treatment in abrogating resistance to production of CNS disease. I found that 90% of the CsA treated, hypothyroid and euthyroid animals developed neurologic disease between 4 and 26 days postinoculation ($d_{\epsilon}i$). The majority of these animals presented with a peracute to acute onset disease which in 3 out of 9 animals died suddenly. By contrast, only 30% of CsA untreated rats from both hypothyroid and control groups manifested a slowly progressive paralytic disease at 15 to 28 dpi. In CsA treated animals that had succumbed peracutely, immunohistochemical analysis for presence of JHMV N protein revealed widespread distribution in both neurons and glia throughout the CNS (Figure 5.A and B). By comparison, in CsA negative controls undergoing the chronic, paralytic form of disease, N expression was confined to glia of the hindbrain (Figure 5.C). In summary, thyroid hormone status appeared to have no influence of virus-induced disease or replication in immunosuppressed postweanlings. Furthermore, the cellular immune response appears to play a crucial role in controlling the spread of infection in neurons and thus the severity of

Figure 5. Immurohistochemical staining of JHMV infected neural cells in cyclosporin A treated and control Wistar Lewis rats. PTU treated (hypothyroid) and control (euthyroid) WL rats were inoculated with JHMV at P22. Half of the animals from each group were treated with CsA beginning 4 days before virus challenge and continued for an additional 4 days following challenge. Treatment with CsA was then halted and resumed 12 days later at 16 dpi. Animals from CsA treated/$PTU^{+/-}$ and CsA untreated/$PTU^{+/-}$ groups which subsequently went on to develop clinical neurologic disease, had their CNS tissues sampled and subjected to hematoxylin-eosin and immunoenzyme staining using the N-specific MAb 4B6.2. Panels A and B show viral N^+ neural cells from a CsA treated/PTU^- rat that developed acute neurologic disease at 15 dpi. Neurons within the cerebral cortex (A) and cervical spinal cord grey matter (large arrows in B) as well as intrafasicular oligodendrocytes (small arrows in inset within B) are stained for N. Abreviations; W, white matter; G, grey matter.

Panel C shows viral N^+ cells, most of which appear to possess glial morphology, from the medulla oblongata of a CsA untreated/PTU^+ animal that developed hind-end paresis at 27 dpi. A x 135, B and C x 750.

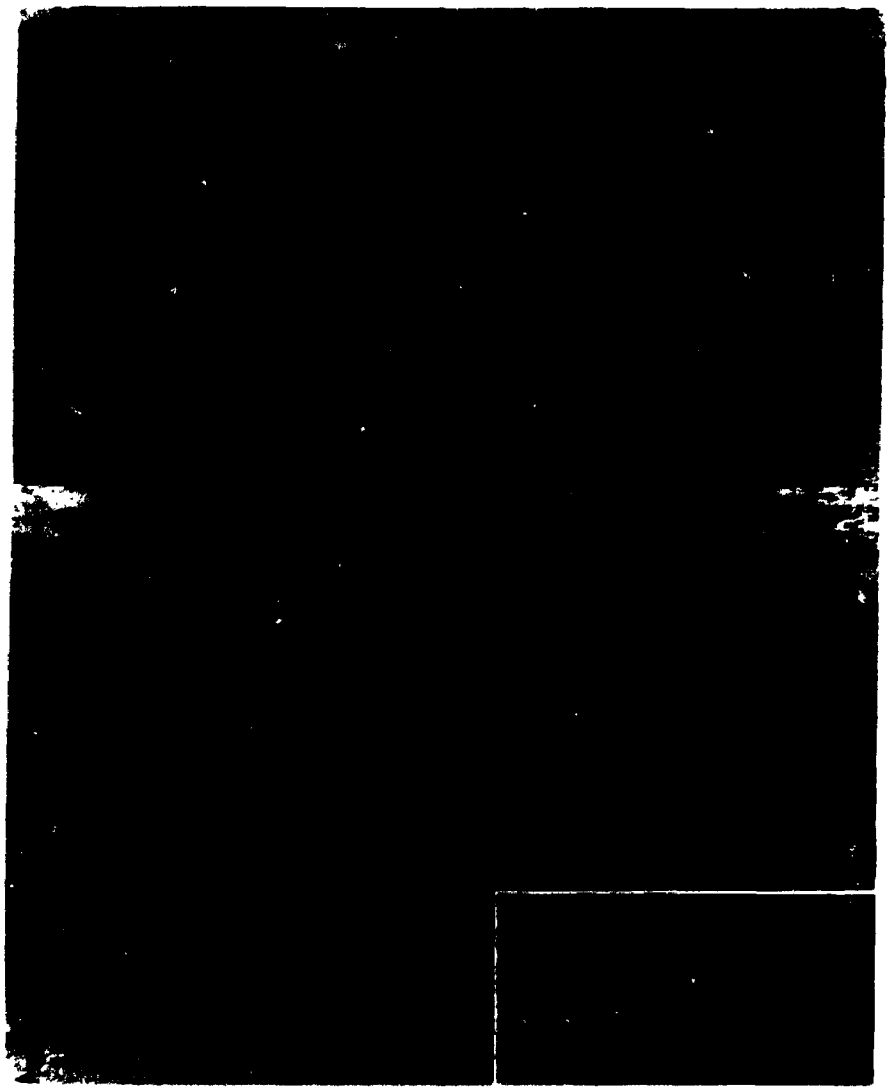

the disease in rats, as concluded previously by Zimmer and Dales (1989).

Discussion.

JHMV disease of rats is a useful paradigm for identifying determinants important in virus-induced, CNS demyelination. Of particular interest is the relationship that exists between the age of the animal at the time of virus challenge and the type of disease evoked. In general, challenge of neonates evokes an acute encephalitis, which shifts to a chronic, demyelinating encephalomyelitis for animals which are inoculated during the second and third weeks of postnatal life. Eventually a disease resistant state is reached by the time animals reach weaning age. The shift from the acute grey matter to chronic white matter form of disease occurs during a period in postnatal development when many events, having potential relevance to the processes of pathogenesis and resistance acquisition, are taking place. Among these are: maturation of the immune response, postnatal neurogenesis, neurite outgrowth and synaptogenesis, and myelinogenesis. I was especially interested in what influence the stage of myelination had on the character of disease evoked by JHMV. The reasons for considering this relationship as potentially important were based on the earlier findings of Beushausen and Dales (1985), who showed that infection of cultured rat oligodendrocytes with JHMV was dependent on their state of

differentiation. More specifically, it was shown that terminally differentiated oligodendrocytes would not support JHMV infection while earlier stages would. This, as well as the observed pattern for development of resistance *in vivo*, suggested that the stage of myelination or oligodendrocyte differentiation, may be an important determinant by which virus replication and disease production within white matter could be controlled. In addition, previous observations demonstrating that abrogation of resistance with immunosuppressants, in P35 challenged WL rats, resulted in a disease in which neuronal involvement predominated over that of white matter (Zimmer and Dales, 1989), further suggested that induction of the demyelinating form of disease may be restricted to a critical postnatal time period. Since thyroid hormones have been shown to significantly influence a number of processes critical to normal brain development, in particular myelination (Nunez, 1984), it was decided to investigate whether a relationship between thyroid hormone's effects on myelination and susceptibility to JHMV-induced demyelinating encephalomyelitis existed.

The rationale for inducing hypothyroidism in WL sucklings and T_4 supplementing WF sucklings before challenging with virus was to slow the onset of resistance to the demyelinating form of disease in the WL strain, while accelerating the onset of resistance in the WF strain. Though both treatments effected growth and CNS maturation which was in agreement with the more extensive studies of others (Balazs *et al.*, 1975;

Patel et al., 1979; Coulombe et al., 1980; Walker and Dessault, 1980; DeGennaro et al., 1988; Patel et al., 1988), they did not significantly influence the outcome of JHMV challenge. As it turned out, the age of the animal at the time of virus challenge and the host's immunologic status continued to influence the outcome of infection, regardless of thyroid hormone status. Earlier studies have also signified the importance of the immune response to the acquisition of resistance (Sorensen et al., 1982; Zimmer and Dales, 1989). The cellular immune response in particular, has been shown important in curtailing virus spread (Dorries et al., 1991) as well as in clearing virus from the CNS (Sussman et al., 1989; Williamson and Stohlman, 1990; Williamson et al., 1990; Yamaguchi et al., 1991).

Unexpectedly, WL rats showed greater susceptibility to JHMV than was previously reported (Sorensen et al., 1982). The reasons for this are not known but possibilities include: genetic differences between the animals used in the present and previous studies, qualitative differences in inocula, prior exposure to MHV, rat coronavirus or other agents and unknown environmental factors.

Although this study does not support a role for thyroid hormone in the pathogenesis of JHMV-induced demyelinating disease of rats, it does not allow me to rule out involvement either. It should be noted that thyroid hormone has been implicated in the pathogenesis of Border disease, which is a pestivirus-induced, congenital, hypomyelination disorder of

lambs. Newborn lambs with Border disease have significantly lower serum T_3 and T_4 concentrations which has been associated with noncytolytic, Border disease virus (BDV) infection of thyroid follicular epithelial cells (Anderson et al., 1987). This association led to the suggestion that hypomyelination in Border disease may result as an indirect effect of the depressed circulating thyroid hormones levels. However, BDV is also present in morphologically normal oligodendrocytes, astrocytes and neurons of lambs with hypomyelination (Jeffrey et al., 1990) indicating that factors in addition to virus-induced hypothyroidism likely participate in the pathogenesis of this disease.

In summmary, alternative approaches may be required to identify putative, non-immunologic, host developmental factors involved in controlling the outcome of JHMV infections of rats. Furthermore, approaches that exclude the influence of the viral immune response could be reasoned as being potentially advantageous.

REFERENCES

Abney, E.R., B.P. Williams, and M.C. Raff. 1983. Tracing the development of oligodendrocytes from precursor cells using monoclonal antibodies, fluorescence-activated cell sorting, and cell culture. Dev. Biol. 100:166-171.

Agresti, C., F. Aloisi, and G. Levi. 1991. Heterotypic and homotypic cellular interactions influencing the growth and differentiation of bipotential oligodendrocyte-type-2 astrocyte progenitors in culture. Dev. Biol. 144:16-29.

Aizenman, Y., J. de Vellis. 1987. Synergistic action of thyroid hormone, insulin and hydrocortisone on astrocyte differentiation. Brain. Res. 414:301-308.

Akio, W., E.M. Johnson, Jr., and J. Milbrandt. 1990. Localization of FGF receptor mRNA in the adult rat central nervous system by in situ hybridization. Neuron 5:267-281.

Al-Ali, S.Y., A.G.H. Al-Zuhair, and B. Dawod. 1988. Ultrastructural study of phagocytic activities of young astrocytes in injured neonatal rat brain following intracerebral injection of colloidal carbon. Glia 1:211-218.

Almazan, G., P. Honegger, and J.M. Matthieu. 1985. Triiodotyronine stimulation of oligodendroglial differentiation and myelination. Dev. Neurosci. 7:45-54.

Anderson, C.A., R.J. Higgins, M.E. Smith, and B.I. Osburn.

1987. Border disease: virus-induced decrease in thyroid hormone levels with associated hypomyelination. Lab. Invest. 57:168-175.

Armstrong, R.C., L. Harvath, and M. Dubois-Dalcq. 1990. Type 1 astrocytes and oligodendrocyte-type-2 astrocyte progenitors migrate toward distinct molecules. J. Neurosci. Res. 27:400-407.

Armstrong, J., H. Niemann, S. Smeekens, P. Rottier, and G. Warren. 1984. Sequence and topology of a model intracellular membrane protein, E1 glycoprotein, from a coronavirus. Nature (Lond.) 308:751-752.

Araujo, D.M., and C.W. Cotman. 1992. Basic FGF in astroglial, microglial, and neuronal cultures: characterization of binding sites and modulation of release by lymphokines and trophic factors. J. Neurosci. 12:1668-1678.

Ard, M.D., and R.P. Bunge. 1988. Heparin sulfate proteoglycan and laminin immunreactivity on cultured astrocytes: relationship to differentiation and neurite outgrowth. J. Neurosci. 8:2844-2858.

Auffray, C., and F. Rougeon. 1980. Purification of mouse immunoglobulin heavy-chain messenger RNAs from total myeloma tumor RNA. Eur. J. Biochem. 107:303-314.

Bailey, O.T., A.M. Pappenheimer, F.S. Cheever, and J.B. Daniels. 1949. A murine virus (JHM) causing disseminated encephalomyelitis with extensive destruction of myelin. II. Pathology. J. Exp. Med. 90:195-231.

Balazs, R., P.D. Lewis, and A.J. Patel. 1975. Effects of

metabolic factors on brain development, in: "Growth and Development of the Brain." M.A.B. Brazier, ed. pp83-115. Raven Press, New York.

Banker, G., and K. Goslin. 1991. Rat hippocampal neurons in low density culture, in: "Culturing Nerve Cells," G. Banker and K. Goslin, eds., MIT Press, Cambridge, Mass.

Banker, G.A., and M. Cowan. 1977. Rat hippocampal neurons in dispersed cell culture. Brain Res. 126:397-425.

Banker, G.A., and M. Cowan. 1979. Further observations on hippocampal neurons in dispersed cell culture. J. Comp. Neur. 187:469-494.

Banner, L.R., J.G. Keck, and M.M.C. Lai. 1990. A clustering of RNA recombination sites adjacent to a hypervariable region of the peplomer gene of murine coronavirus. Virol. 175:548-555.

Bansal, R., A.L. Gard, and S.E. Pfeiffer. 1988. Stimulation of oligodendrocyte differentiation in culture by growth in the presence of a monoclonal antibody to sulfated glycolipid. J. Neurosci. Res. 21:260-267.

Bansal, R., A.E. Warrington, A.L. Gard, B. Ranscht, and S.E. Pfeiffer. 1989. Multiple and novel specificities of monoclonal antibodies O1, O4, and R-mAb used in the analysis of oligodendrocyte development. J. Neurosci. Res. 24:548-557.

Baric, R.S., G.W. Nelson, J.O. Fleming, R.J. Deans, J.G. Keck, N. Casteel, and S.A. Stohlman. 1988. Interactions between coronavirus nucleocapsid protein and viral RNAs:

implications for viral transcription. J. Virol. 62:4280-4287.

Baric, R.S., S.A. Stohlman, M.K. Razavi, and M.M.C. Lai. 1985. Characterization of leader-related small RNAs in coronavirus-infected cells: further evidence for leader-primed mechanism of transcription. Virus Res. 3:19-33.

Barnett, E., and S. Perlman. Mouse hepatitis virus and herpes simplex virus move along different CNS pathways after intranasal inoculation. Adv. Exp. Med. Biol. In press.

Barthold, S.W. 1988. Olfactory neural pathway in mouse hepatitis virus nasoencephalitis. Acta Neuropath. 76:502-506.

Barthold, S.W., and A.L. Smith. 1987. Response of genetically susceptible and resistant mice to intranasal inoculation with mouse hepatitis virus JHM. Virus Res. 7:225-239.

Behar, T., F.A. McMorris, J.L. Novotny, J.L. Barker, and M. Dubois-Dalcq. 1988. Growth and differentiation properties of O-2A progenitors purified from rat cerebral hemispheres. J. Neurosci. Res. 21:168-180.

Berry, M., and A.W. Rogers. 1965. The migration of neuroblasts in the developing cerebral cortex. J. Anatom. 99:691-709.

Besnard, F., F. Perraud, M. Sensenbrenner, and G. Labourdette. 1989. Effects of acidic and basic fibroblast growth factors on proliferation and maturation of cultured rat oligodendrocytes. Int. J. Dev. Neurosic. 7:401-409.

Beushausen, S., and S. Dales. 1985. In vivo and in vitro models of demyelinating disease XI. tropism and

differentiation regulate the infectious process of coronaviruses in primary explants of the rat CNS. Virology 141:89-101.

Beushausen, S., S. Narindrasorasak, B.D, Sanwal, and S. Dales. 1987. In vivo and in vitro models of demyelinating disease: activation of the adenylate cyclase system influences JHM virus expression in explanted rat oligodendrocytes. J. Virol. 61:3795-3803.

Binder, L.I., A. Frankfurter, and L.I. Rebhun. 1985. The distribution of tau in the mammalian central nervous system. J. Cell Biol. 101:1371-1378.

Bogler, O., D. Wren, S.C. Barnett, H. Land, and M. Noble. 1990. Cooperation between two growth factors promotes extended self-renewal and inhibits differentiation of oligodendrocyte-type-2 astrocyte (O-2A) progenitor cells. Proc. Natl. Acad. Sci. USA 87:6368-6372.

Bottenstein, J.E. 1986. Growth requirements in vitro of oligodendrocyte cell lines and neonatal rat brain oligodendrocytes. Proc. Natl. Acad. Sci. USA 83:1955-1959.

Bottenstein, J.E., and G.H. Sato. 1979. Growth of a rat neuroblastoma cell line in serum-free supplemented medium. Proc. Natl. Acad. Sci. USA 76:514-517.

Boyle, J.F., D.G. Wesmiller, and K.V. Holmes. 1987. Genetic resitance to mouse hepatitis virus correlates with absence of virus-binding activity on target tissues. J. Virol. 61:185-189.

Boursnell, M.E.G., T.K.D. Brown, I.J. Foulds, P.F. Green, F.M. Tomley, and M.M. Binns. 1987. Completion of the sequence of the genome of the coronavirus avian bronchitis virus. J. Gen. Virol. 68:57-77.

Brayton, P.R., R.G. Ganges, and S.A. Stohlman. 1981. Host cell nuclear function and murine hepatitis virus replication. J. Gen. Virol. 56:457-460.

Buchmeier, M.J., R.G. Dalziel, M.J.M. Koolen. 1988. Coronavirus-induced CNS disease: a model for virus-induced demyelination. J. Neuroimmunol.20:111-116.

Buchmeier, M.J., H.A. Lewicki, P.J. Talbot, and R.L. Knobler. 1984. Murine hepatitis virus-4 (strain JHM)-induced neurologic disease is modulated in vivo by monoclonal antibody. Virol. 132:261-270.

Budzilowicz, C.J., S.P. Wilczynski, and S.R. Weiss. 1985. Three intergenic regions of coronavirus mouse hepatitis virus strain A59 genome RNA contain a common nucleotide sequence that is homologous to the 3' end of the viral mRNA leader sequence. J. Virol. 53:834-840.

Burks, J.S., B.L. DeVald, L.D. Jankovsky, J.C. Gerdes. 1980. Two coronaviruses isolated from central nervous system tissue of two multiple sclerosis patients. Science 209:933-934.

Caceres, A., G.A. Banker, and L. Binder. 1986. Immunocytochemical localization of tubulin and microtubule-associated protein 2 during the development of hippocampal neurons in culture. J. Neurosci. 6:714-

722.

Cheever, F.S., J.B. Daniels, A.M. Pappenheimer, and O.T. Bailey. 1949. A murine virus causing disseminated encephalomyelitis with extensive destruction of myelin I. Isolation and biological properties of the virus. J. Exp. Med. 90:181-194.

Cohen, J.A. W.V. Williams, H.M. Geller, and M.I. Greene. 1991. Anti-reovirus receptor antibody accelerates expression of the optic nerve oligodendrocyte developmental program. Proc. Natl. Acad. Sci. USA 88:1266-1270.

Cohen, J.A., W.V. Williams, D.B. Weiner, H.M. Geller, and M.I. Greene. 1990. Ligand binding to the cell surface receptor for reovirus type 3 stimulates galactocerebroside expression by developing oligodendrocytes. Proc. Natl. Acad. Sci. USA 87:4922-4926.

Collins, A.R., R.L. Knobler, H. Powell, and M.J. Buchmeier. 1982. Monoclonal antibodies to murine hepatitis virus-4 (strain JHM) define the viral glycoprotein responsible for attachment and cell-cell fusion. Virol. 119:358-371.

Compston, A., N. Scolding, D. Wren, and M. Noble. 1991. The pathogenesis of demyelinating disease: insights from cell biology. Trends Neurosci. 14:175-182.

Compton, S.R., D.B. Rogers, K.V. Holmes, D. Fertsch, J. Remenick, and J.J. McGowan. 1987. In vitro replication of mouse hepatitis virus strain A59. J. Virol. 61:1814-1820.

Coulombe, P., J. Ruel, and J.H. Dussault. 1980. Effects of

neonatal hypo- and hyperthyroidism on pituitary growth hormone content in the rat. Endocrin. 107:2027-2033.

Dales, S. and H. Hanafusa. 1972. Penetration and intracellular release of the genomes of avian RNA tumor viruses. Virology 50:440-458.

Dales, S., K.C. Hsu, and A. Nagayama. 1973. The fine structure and immunological labelling of the achromatic mitotic apparatus after disruption of cell membranes. J. Cell Biol. 59:643-655.

Dalziel, R.G., P.W. Lampert, P.J. Talbot, and M.J. Buchmeier. 1986, Site-specific alteration of murine hepatitis virus type 4 peplomer glycoprotein E2 results in reduced neurovirulence. J. Virol. 59:463-471.

David-Ferreira, J.F., and R.A. Manaker. 1965. An electron microscope study of the development of a mouse hepatitis virus in tissue culture cells. J. Cell Biol. 24:57-78.

De Gennaro, V., S.G. Cella, M. Bassetti, R. Rizzi, D. Cocchi, and E.E. Muller. 1988. Impaired growth hormone secretion in neonatal hypothyroid rats: hypothalamic versus pituitary component. Proc. Soc. Exp. Biol. Med. 187:99-106.

De Groot, R.J., W. Luytjes, M.C. Horzinek, B.A.M. van der Zeijst, W.J.M. Spaan, J.A. Lenstra. 1987. Evidence for a coiled-coil structure in the spike proteins of coronaviruses. J. Mol. Biol. 196:963-966.

Delmas, B., and H. Laude. Assembly of coronavirus spike protein into trimers and its role in epitope expression.

J. Virol. 64:5367-5375.

Denison, M.R., and S. Perlman. 1986. Translation and processing of mouse hepatitis virus virion RNA in a cell-free system. J. Virol. 60:12-18.

Denison, M.R., and S. Perlman. 1987. Identification of putative polymerase gene product in cells infected with murine coronavirus A59. Virol. 157:565-568.

Denison, M., T. Ross, and J. Gombold. Mouse hepatitis virus A59 intracellular RNA synthesis is inhibited by leupeptin. Adv. Exp. Med. Biol. In press.

Denison, M.R., P.W. Zoltick, S.A. Hughes, B. Giangreco, A.L. Olson, S. Perlman, J.L. Leibowitz, and S.R. Weiss. 1992. Intracellular processing of the N-terminal ORF 1a proteins of the coronavirus MHV-A59 requires multiple proteolytic events. Virol. 189:274-284.

Dension, M.R., P.W. Zoltick, J.L. Leibowitz, C.J. Pachuk, and S.R. Weiss. 1991. Identification of polypeptides encoded in open reading frame 1b of the putative polymerase gene of the murine coronavirus mouse hepatitis virus A59. J. Virol. 65:3076-3082.

Deregt, D., and L.A. Babiuk. 1987. Monoclonal antibodies to bovine coronavirus: characteristics and topological mapping of neutralizing epitopes on the E2 and E3 glycoproteins. Virol. 161:410-420.

Dorries, R., S. Schwender, H. Imprich, and H. Harms. 1991. Population dynamics of lymphocyte subsets in the central nervous system of rats with different susceptibility to

coronavirus-induced demyelinating encephalitis. Immunol. 74:539-545.

Dotti, C.G. and K. Simons. 1990. Polarized sorting of viral glycoproteins to the axon and dendrites of hippocampal neurons in culture. Cell 62:63-72.

Dubois, J.D., and H. Dussault. 1977. Ontogenesis of thyroid function in the neonatal rat. Thyroxine (T_4) and triiodothyronine (T_3) production rates. Endocrin. 101:435-441.

Dubois, C., J.C. Manuguerra, B. Hauttecoeur, J. Maze. 1990. Monoclonal antibody A2B5, which detects cell surface antigen, binds to ganglioside G_{T3} ($II^3(NeuAc)_3$ LacCer) and to its 9-O-acetylated derivative. J. Biol. Chem. 265: 2797-2803.

Dubois-Dalcq, M. 1987. Characterization of a slowly proliferative cell along the oligodendrocyte differentiation pathway. EMBO J. 6:2587-2595.

Dubois-Dalcq, M., E.W. Doller, M.V. Haspell, and K.V. Holmes. 1982. Cell tropism and expression of mouse hepatitis viruses (MHV) in mouse spinal cord cultures. Virol. 119:317-331.

Dussault, J.H., and F. Labrie. 1975. Development of the hypothalamic-pituitary-thryroid axis in the neonatal rat. Endocrin. 97:1321-1324.

Dutly, F., and M.E. Scwab. 1991. Neurons and astrocytes influence the development of purified O-2A progenitor cells. Glia 4:559-571.

Dveksler, G.S., M.N. Pensiero, C.B. Cardellichio, R.K. Williams, G.-S. Jiang, K.V. Holmes, and C.W. Dieffenbach. 1991. Cloning of the mouse hepatitis (MHV) receptor: expression in human and hamster cell lines confers susceptibility to MHV. J. Virol. 65:6881-6891.

Dyer, C.A., and J.A. Benjamins. 1990. Glycolipids and transmembrane signaling: antibodies to galactocerebroside cause an influx of calcium in oligodendrocytes. J. Cell Biol. 111:625-633.

Dyer, C.A., and J.A. Benjamins. 1991. Galactocerebroside and sulfatide independently mediate Ca^{2+} responses in oligodendrocytes. J. Neurosci. Res. 30:699-711.

Eisenbarth, G.S., F.S. Walsh, M. Nirenberg. 1979. Monoclonal antibody to a plasma membrane antigen of neurons. Proc. Natl. Acad. Sci. USA 76:4913-4917.

Emmel, E.A., C.L. Verweij, D.B. Durand, K.M. Higgins, E. Lacy, and G.R. Crabtree. 1989. Cyclosporin A specifically inhibits the function of nuclear proteins involved in T cell activation. Science 246:1617-1620.

Ernfors, P., P. Lonnerberg, C. Ayer-LeLievre, H. Perrson. 1990. Developmental and regional expression of basic fibroblastic growth factor mRNA in the rat central nervous system. J. Neurosci. Res. 27:10-15.

Evans, R.M. 1988. The steroid and thyroid hormone receptor superfamily. Science 240:889-894.

Evercooren, A. B.-V., C. Olichon-Berthe, A. Kowlaski, G. Visciano, and E. Van Obberghen. 1991. Expression of IGF-

I and insulin receptor genes in the rat central nervous system: a developmental, regional, and cellular analysis. J. Neurosci. Res. 28.244-253.

Ferrara, N., F. Ousley, and D. Grospodarowicz. 1988. Bovine brain astrocytes express basic fibroblastic growth factor, a neurotropic and angiogenic mitogen. Brain Res. 462:223-232.

Fishman, P.H. 1982. Role of membrane gangliosides in the binding and action of bacterial toxins. J. Membrane Biol. 69:85-97.

Fishman, P.S., J.S. Gass, P.T. Swoveland, E. Lavi, M.K. Highkin, and S.R. Weiss. 1985. Infection of the basal ganglia by a murine coronavirus. Science 229:877-879.

ffrench-Constant, C., and M.C. Raff. 1986. The oligodendrocyte-type-2 astrocyte lineage is specialized for myelination. Nature (Lond) 323:335-338.

Fleming, J.O., R.A. Shubin, M.A. Sussman, N. Casteel, and S.A. Stohlman. 1989. Monoclonal antibodies to the matrix (E1) glycoprotein of mouse hepatitis virus protect mice from encephalitis. Virol. 168:162-167.

Fleming, J.O., M.D. Trousdale, J. Bradbury, S.A. Stohlman, and L.P. Weiner. 1987. Experimental demyelination induced by coronavirus JHM (MHV-4): molecular identification of a viral determinant of paralytic disease. Microbial Path. 3:9-20.

Fleming, J.O., M.D. Trousdale, F.A.R. El-Zaatari, S.A. Stohlman, and L.P. Weiner. 1986. Pathogenicity of

antigenic variants of murine coronavirus JHM selected with monoclonal antibodies. J. Virol. 58:869-875.

Flintoff, W.F., and S. Van Dinter. 1989. Several rat cell lines share a common defect in their ability to internalize murine coronaviruses efficiently. J. Gen. Virol. 70:1713-1724.

Fok-Seang, J., and R.H. Miller. 1992. Astrocyte precursors in neonatal rat spinal cord cultures. J. Neurosci. 12:2751-2764.

Fontana, A., W. Fierz, and H. Wekerle. 1984. Astrocytes present myelin basic protein to encephalitogenic T-cell lines. Nature (Lond.) 307:273-276.

Frana, M.F., J.N. Behnke, L.S. Sturman, and K.V. Holmes. 1985. Proteolytic cleavage of the E2 glycoprotein of murine coronavirus: host-dependent differences in proteolytic cleavage and cell fusion. J. Virol. 56:912-920.

Fressinaud, C., L.L. Sarlieve, D. Dalencon, and G. Labourdette. 1992. Differential regulation of cerebroside sulfotransferase and 2',3'-cyclic nucleotide 3'-phosphodiesterase by basic fibroblast growth factor in relation to proliferation in rat oligodendrocyte cultures. J. Cell. Physiology. 150:34-44.

Gallagher, T.M., M.J. Buchmeier, and S. Perlman. 1992. Cell receptor-independent infection by a neurotropic murine coronaviurs. Virol. 191:517-522.

Gallagher, T.M., C. Escaramis, and M.J. Buchmeier. 1991. Alteration of the pH dependence of coronavirus-induced

cell fusion: effect of mutations in the spike glycoprotein. J. Virol. 65:1916-1928.

Gallagher, T.M., S.E. Parker, and M.J. Buchmeier. 1990. Neutralization-resistant variants of a neurotropic coronavirus are generated within the amino-terminal half of the spike glycoprotein. J. Virol. 64:731-741.

Gard, A.L., and S.E. Pfeiffer. 1989. Oligodendrocyte progenitors isolated directly from developing telencephalon at a specific phenotypic stage: myelinogenic potential in a defined environment. Development 106:119-132.

Gard, A.L., and S.E. Pfeiffer. 1990. Two proliferative stages of oligodendrocyte lineage ($A2B5^{+}O4^{-}$ and $O4^{+}GalC^{-}$) under different mitogenic control. Neuron 5:615-625.

Gavaret, J.M., D. Toru-Delbauffe, P. Baghdassarian-Chalage, M. Pomerance, and M. Pierre. 1991. Thyroid hormone action: induction of morphological changes and protein secretion in astroglial cell cultures. Develop. Brain. Res. 58:43-49.

Gilad, G.M., G. Shanker, D. Dahl, and V.H. Gilad. 1990. Dibutyryl cyclic AMP-induced changes in neuron-astroglia interactions and fibronectin immunocytochemistry in dissociated rat cerebellar cultures. Brain Res. 508:215-224.

Gilbert, S.F. 1988. Early vertebrate development: neurulation and ectoderm, in "Development Biology." pp 152-167. Sinauer Associates, Inc., Sunderland. Mass.

Godfraind, C., V.L. Friedrich, K.V. Holmes, and M. Dubois-Dalcq. 1989): In vivo analysis of glial cell phenotypes during viral demyelinating diseases in mice. J. Cell. Biol. 109:2405-2416.

Goedert, M., R.A. Crowther, and C.C. Garner. 1991. Molecular characterization of microtubule-associated proteins tau and MAP2. Trends Neurosci. 14:193-199.

Goldman, J.E., and P. J.-J. Vaysse. 1991. Tracing glial cell lineages in the mammalian forebrain. Glia 4:149-156.

Gomez-Pinilla, F., J.W.-K. Lee, and C.W. Cotman. 1992. Basic FGF in adult rat brain: cellular distribution and response to entorhinal lesion and fimbria-fornix transection. J. Neurosci. 12:345-355.

Gonzalez, A.-M., M. Buscaglia, M. Ong, and A. Baird. 1990. Distribution of basic fibroblastic growth factor in the 18-day rat fetus: localization in the basement membranes of diverse tissues. J. Cell Biol. 110:753-765.

Hardy, R., and R. Reynolds. 1991. Proliferation and differentiation potential of rat forebrain oligodendroglial progenitors both in vitro and in vivo. Devlop. 111:1061-1080.

Hart, I.K., W.D. Richardson, S.R. Bolsover, and M.C. Raff. 1989a. PDGF and intracellular signaling in the timing of oligodendrocyte differentiation. J. Cell Biol. 109:3411-3417.

Hart, I.K., W.D. Richardson, C.-H. Heldin, B. Westermark, and M.C. Raff. 1989b. PDGF receptors on cells of the

oligodendrocyte-type-2 astrocyte (O-2A) cell lineage. Develop. 105:595-603.

Haspel, M.V., Lampert, P.W., and M.B.A. Oldstone. 1978. Temperature-sensitive mutants of mouse hepatitis virus produce a high incidence of demyelination. Proc. Natl. Acad. Sci. USA 75:4033-4036.

Hatten, M.E., M. Lynch, R.E. Rydel, J. Sanchez. J. Joseph-Silverstein, D. Moscatelli, and D.B. Rifkin. 1988. In vitro neurite extension by granule neurons is dependent upon astroglial-derived fibroblast growth factor. Develop. Biol. 125:280-289.

Heijnen, L., W. van Haren, and W.J.M. Spaan. Mutagenesis of the mouse hepatitis virus spike protein: cleavage is not strictly necessary for induction of cell fusion. Adv. Exp. Med. Biol. In press.

Herndon, R.M., D.E. Griffin, U. McCormick, and L.P. Weiner. 1975. Mouse hepatitis virus-induced recurrent demyelination. Arch. Neurol. 32:32-35.

Hofmann, M.A., P.B. Sethna, and D.A. Brian. 1990. Bovine coronavirus mRNA replication continues throughout persistent infection in cell culture. J. Virol. 64:4108-4114.

Holmes, K.V., C. Yeager, G.S. Dveksler, R.K. Williams, M.N. Pensiero, C.B. Cardellichio, R.T. Ashum, L. Shapiro, T. Barnett, S. Gagneten, A.T. Look, and C.W. Dieffenback. Comparative studies on receptor recognition by human and rodent coronaviruses. Adv. Exp. Med. Biol. In press.

Huang, J.Q., C. Turbide, E. Daniels, S. Jothy, and N. Beauchemin. 1990. Spatiotemporal expression of murine carcinoembryonic antigen (CEA) gene family members during mouse embryogenesis. Develop. 110:573-588.

Hunter, S.F., and J.E. Bottenstein. 1989. Bipotential glial progenitors are targets of neuronal cell line-derived growth factors. Develop. Brain Res. 49:33-49.

Hunter, S.F., and J.E. Bottenstein. 1990. Growth factor responses of enriched bipotential glial progenitors. Develop. Brain Res. 54:235-248.

Ingraham, C.A., and K.D. McCarthy. 1989. Plasticity of process-bearing glial cell cultures from neonatal rat cerebral cortical tissue. J. Neurosci. 9:63-69.

Jackson, A.C., T.R. Moench, B.D. Trapp, and D.E. Griffin. 1988. Basis of neurovirulence in Sidbis virus encephalomyelitis of mice. Lab. Invest. 58:503-509.

Jeffrey, M., G.A.H. Wells, A.W. Bridges, and J.J. Sands. 1990. Immunocytochemical localization of Border disease virus in the spinal cord of fetal and newborn lambs. Neuropath. Appl. Neurobiol. 16:501-510.

Johnson-Green, P.C., K.E. Dow, and R.J. Riopelle. 1991. Characterization of glycosaminoglycans produced by primary astrocytes in vitro. Glia 4:314-321.

Joly, E., L. Mucke, and M.B.A. Oldstone. 1991. Viral persistence in neurons explained by lack of major histocompatibility class I expression. Science 253:1283-1285.

Kawada, J., H. Mino, M. Nishida, and Y. Yoshimura. 1988. An appropriate model for congenital hypothyroidism in the rat induced by neonatal treatment with propylthiouracil and surgical thyroidectomy: studies on learning ability and biochemical parameters. Neuroendocrin. 47:424-430.

Keck, J.G., G. Matsushima, S. Makino, J.O. Fleming, D.M. Vannier, S.A. Stohlman, and M.M.C. Lai. 1988a. In vivo RNA-RNA recombination of coronavirus in mouse brain. J. Virol. 62:1810-1813.

Keck, J.G., L.H. Soe, S. Makino, S.A. Stohlman, and M.M.C. Lai. 1988b. RNA recombination of murine coronaviruses: recombination between fusion-positive mouse hepatitis virus A59 and fusion-negative mouse hepatitis virus 2. J. Virol. 62:1989-1998.

Kersting, G., and E. Pette. 1956. Zur pathohistologie und pathogenese der experimentellen JHM-virusencephalomyelitis des affen. Deutsche Zeitschrift f Nervenheilkunde Bd. 174:283-304.

Kim, S.U. 1990. Neurobiology of human oligodendrocytes in culture. J. Neurosci. Res. 27:712-728.

Klagsbrun, M., and A. Baird. 1991. A dual receptor system is required for basic fibroblast growth factor activity. Cell 67:229-231.

Knobler, R.L., M. Dubois-Dalcq, M.V. Haspel, A.P. Claysmith, P.W. Lampert, and M.B.A. Oldstone. 1981a. Selective localization of wild type and mutant mouse hepatitis virus (JHM strain) antigens in CNS tissue by

fluorescence, light and electron microscopy. J. Neuroimmunol. 1:81-97.

Knobler, R.L., M.V. Haspel, and M.B.A. Oldstone. 1981b. Mouse hepatitis virus type 4 (JHM strain)-induced fatal central nervous system disease I. genetic control and the murine neuron as the susceptible site of disease. J. Exp. Med. 153:832-843.

Knobler, R.L., P.W. Lampert, and M.B.A. Oldstone. 1982. Virus persistence and recurring demyelination produced by a temperature-sensitive mutant of MHV-4. Nature (Lond.) 298:279-298.

Knobler, R.L., B.A. Taylor, M.K. Woodel, W.G. Beamer, and M.B.A. Oldstone. 1984a. Host genetic control of mouse hepatitis virus type-4 (JHM strain) replication. Expl Clin. Immunogenet. 1:217-222.

Knobler, R.L., L.A. Tunison, and M.B.A. Oldstone. 1984b. Host genetic control of mouse hepatitis virus type 4 (JHM strain) replication.I. restriction of virus amplification and spread in macrophages from resistant mice. J. Gen. Virol.65:1543-1548.

Koga, M., H. Wege, and V. ter Meulen. 1984. Sequence of murine coronavirus JHM induced neuropathological changes in rats. Neuropath. Appl. Neurobiol. 10:173-184.

Komoly, S., L.D. Hudson, H.D. Webster, and C.A. Bondy. 1992. Insulin-like growth factor I gene expression is induced in astrocytes during experimental demyelination. Proc. Natl. Acad. Sci. USA 89:1894-1898.

Kooi, C., M. Cervin, and R. Anderson. 1991. Differentiation of acid-pH-dependent and -nondependent entry pathways for mouse hepatitis virus. Virol. 180:108-119.

Kooi, C., L. Mizzen, C. Alderson, M. Daya, and R. Anderson. 1988. Early events of importance in determining host cell permissiveness to mouse hepatitis virus infection. J. Gen. Virol. 69:1125-1135.

Koper, J.W., R.C. Hoeben, F.M.H. Hochstenbach, L.M.G. van Golde, and M. Lopes-Cardozo. 1986. Effects of triiodothyronine on the synthesis of sulfolipids by oligodendrocyte-enriched glial cultures. Biochem. Biophys. Acta 887:327-334.

Kosik, K.S., and E.A. Finch. 1987. MAP2 and tau segregate into dendritic and axonal domains after the elaboration of morphologically distinct neurites: an immunocytochemical study of cultured rat cerebrum. J. Neurosci. 7:3142-3153.

Kristensson, K., B. Lundh, E. Norrby, L. Payne, and C. Orvell. 1984. Asymmetric budding of viruses in ependymal and choroid plexus epithelial cells. Neuropath. Appl. Neurobiol. 10:209-219.

Kyuwa, S., K. Yamaguchi, Y. Toyoda, and K. Fujiwara. 1991. Induction of self-reactive T cells after murine coronavirus infection. J. Virolo. 65:1789-1795.

Lai, M.M.C., R.S. Baric, P.R. Brayton, and S.A. Stohlman. 1984. Characterization of leader RNA sequences on the virion and mRNAs of mouse hepatitis virus, a cytoplasmic RNA virus. Proc. Natl. Acad. Sci. USA 81:3626-3630.

La Monica, N., L.R. Banner, V.L. Morris, and M.C. Lai. 1991. Localization of extensive deletions in the structural genes of two neurotropic variants of murine coronavirus JHM. Virol. 182:883-888.

Lampert, P.W., J.K. Sims, and A.J. Kniazeff. 1973. Mechanism of demyelination in JHM virus encephalomyelitis: electronmicroscopic studies. Acta Neuropath. 24:76-85.

Lavi, E., P.S. Fishman, M.K. Highkin, and S.R. Weiss. 1988. Limbic encephalitis after inhalation of a murine coronavirus. Lab. Invest. 58:31-36.

Lavi, E., E.M. Murray, S. Makino, S.A. Stohlman, M.M.C. Lai, and S.R. Weiss. 1990. Determinants of coronavirus MHV pathogenesis are localized to 3' portions of the genome as determined by ribonucleic acid-ribonucleic acid recombination. Lab. Invest. 62:570-578.

Lavi, E., A. Suzumura, M. Hirayama, M.K. Highkin, D.M. Dambach, D.H. Silberberg, and S.R. Weiss. 1987. Coronavirus mouse hepatitis virus (MHV)-A59 causes a persistent, productive infection in primary glial cell cultures. Microbial Path. 3:79-86.

Lavi, E., A. Suzumura, E.M. Murray, D.H. Silberberg, and S.R. Weiss. 1989. Induction of MHC class I antigens on glial cells is dependent on persistent mouse hepatitis virus infection. J. Neuroimmunol. 22:107-111.

Lavin, T.N., J.D. Baxter, and S. Horita. 1988. The thyroid hormone receptor binds to multiple domains of the rat growth hormone 5'-flanking sequence. J. Bio. Chem.

263:9418-9426.

Lee, H.-J., C.-K. Shieh, A.E. Gorbalenya, E.V. Koonin, N. La Monica, J. Tuler, A. Bagdzhadzhyan, and M.M.C. Lai. 1991. The complete sequence (22 kilobases) of murine coronavirus gene 1 encoding the putative proteases and RNA polymerase. Virol. 180:567-582.

Lee, G., N. Cowan, and M. Kirschner. 1988. The primary structure and heterogeneity of tau protein from mouse brain. Science 239:285-288.

Lee, G., R.L. Neve, and K.S. Kosik. 1989. The microtubule binding domain of tau protein. Neuron 2:1615-1624.

Leibowitz, J.L., K.C. Wilhelmsen, and C.W. Bond. 1981. The virus-specific intracellular RNA species of two murine coronaviruses: MHV-A59 and MHV-JHM. Virol. 114:39-51.

Lerea, L.S., and K.D. McCarthy. 1989. Astroglial cells in vitro are heterogenous with respect to expression of the α_1-adrenergic receptor. Glia 2:135-147.

Levi, G., C. Agresti, D. D'Urso, and F. Aloisi. 1991. Is the oligodendrocyte differentiation of bipotential oligodendrocyte-type 2 astrocyte progenitors promoted by autocrine factors? Neurosci. Lett. 128:37-41.

Levi, G., V. Gallo, and M.T. Ciotti. 1986. Bipotential precursors of putative fibrous astrocytes and oligodendrocytes in rat cerebellar cultures express distinct surface features and "neuron-like" γ-aminobutyric acid transport. Proc. Natl. Acad. Sci. USA 83:1504-1508.

Levi, G., F. Aloisi, and G.P. Wilkin. 1987. Differentiation of cerebellar bipotential glial precursors into oligodendrocytes in primary culture: developmental profile of surface antigens and mitotic activity. J. Neurosci. Res. 18:407-417.

Levine, J.M. 1989. Neuronal influences on glial progenitor cell development. Neuron 3:103-113.

LeVine, S.M., and J.E. Goldman. 1988a. Embryonic divergence of oligodendrocytes and astrocyte lineages in developing rat cerebrum. J. Neurosci. 8:3992-4006.

LeVine, S.M., and J.E. Goldman. 1988b. Spatial and temporal patterns of oligodendrocyte differentiation in rat cerebrum and cerebellum. J. Comp. Neurol. 277:441-455.

Lillien, L.E., and M.C. Raff. 1990. Analysis of the cell-cell interactions that control type-2 astrocyte development in vitro. Neuron 4:525-534.

Lillien, L.E., M. Sendtner, and M.C. Raff. 1990. Extracellular matrix-associated molecules collaborate with ciliary neurotrophic factor to induce type-2 astrocyte development. J. Cell. Biol. 111:635-644.

Lillien, L.E., M. Sendtner, H. Rohrer, S.M. Hughes, and M.C. Raff. 1988. Type-2 astrocyte development in rat brain cultures is initiated by a CNTF-like protein produced by type-1 astrocytes. Neuron 1:485-494.

Lomniczi, B. 1977. Biological properties of avian coronavirus RNA. J. Gen. Virol. 36:531-533.

Louis, J.C., E. Magal, D. Muir, M. Manthorpe, and S. Varon.

1992. CG-4, a new bipotential glial cell line from rat brain, is capable of differentiating in vitro into either mature oligodendrocytes or type-2 astrocytes. J. Neurosci. Res. 31:193-204.

Lucas, A., M. Coulter, R. Anderson, S. Dales, and W. Flintoff. 1978. In vivo and in vitro models of demyelinating diseases II. Persistence and host regulated thermosensitivity in cells of neural derivation infected with mouse hepatitis and measles viruses. Virology 88: 325-337.

Luytjes, W., P.J. Bredenbeek, A.F. Noten, M.C. Horzinek, and W.J. Spaan. 1988. Sequence of mouse hepatitis virus A59 mRNA 2: indications for RNA-recombination between coronavirus and influenza C virus. Virol. 166:415-422.

Luytjes, W., L.S. Sturman, P.J. Bredenbeek, J. Charite, B.A.M. van der Zeijst, M.C. Horzinek, and W.J.M. Spaan. 1987. Primary structure of the glycoprotein E2 of coronavirus MHV-A59 and identification of the trypsin cleavage site. Virol. 161:479-487.

Machamer, C.E., and J.K. Rose. 1987. A specific transmembrane domain of a coronavirus E1 glycoprotein is required for its retention in the Golgi region. J. Cell Biol. 105:1205-1214.

Makino, S., J.O. Fleming, J.G. Keck, S.A. Stohlman, and M.C. Lai. 1987. RNA recombination of coronaviruses: localization of neutralizing epitopes and neuropathogenic determinants on the carboxyl terminus of peplomers. Proc.

Natl. Acad. Sci. USA 84:6567-6571.

Makino, S., J.G. Keck, S.A. Stohlman, and M.M.C. Lai. 1986. High-frequency RNA recombination of murine coronaviruses. J. Virol. 57:729-737.

Massa, P.T., H. Wege, V. Ter Meulen. 1986. Analysis of murine hepatitis virus (JHM strain) tropism toward Lewis rat glial cells in vitro. Lab. Invest. 55:318-327.

Massa, P.T., H. Wege, V. Ter Meulen. 1988. Growth pattern of various JHM coronavirus isolates in primary rat glial cell cultures correlates with differing neurotropism in vivo. Virus Res. 9:133-144.

Massalski, A., M. Coulter-Mackie, R.L. Knobler, M.J. Buchmeier, and S. Dales. 1982. In vivo and in vitro models of demyelinating diseases V. Comparison of the assembly of mouse hepatitis virus, strain JHM, in two murine cell lines. Intervirol. 18:135-146.

Matsubara, Y., R. Watanabe, and F. Taguchi. 1991. Neurovirulence of six different murine coronavirus JHMV variants for rats. Virus Res. 20:45-58.

McCarthy, K.D., and J. deVellis. 1980. Preparation of separate astroglial and oligodendroglial cell cultures from rat cerebral tissue. J. Cell. Biol. 85:890-902.

McIntosh, K. 1974. Coronaviruses: a comparative review. Curr. Top. Microbiol. Immunol. 63:85-129.

McKinnon, R.D., T. Matsui, M. Dubois-Dalcq, and A. Aaronson. 1990. FGF modulates the PDGF-driven pathway of oligodendrocyte development. Neuron 5:603-614.

McMorris, F.A. 1983. Cyclic AMP induction of the myelin enzyme 2',3'-cyclic nucleotide 3'-phosphohydrolase in rat oligodendrocytes. J. Neurochem. 41:506-515.

McMorris, F.A., and M. Dubois-Dalcq. 1988. Insulin-like growth factor I promotes cell proliferation and oligodendrocyte commitment in rat glial progenitor cells developing in vitro. J. Neurosci. Res. 21:199-209.

McMorris, F.A., T.M. Smith, S. DeSalvo, and R.W. Furlanetto. 1986. Insulin-like growth factor I/somatomedin C: a potent inducer of oligodendrocyte development. Proc. Natl. Acad. Sci. 83:822-826.

Merenmies, J., and H. Rauvala. 1990. Molecular cloning of the 18-kDa growth-associated protein of developing brain. J. Bio. Chem. 265:16721-16724.

Miller, R.H., and V. Szigeti. 1991. Clonal analysis of astrocyte diversity in neonatal rat spinal cord cultures. Develop. 113:353-362.

Misson, J.-P., T. Takahashi, and V.S. Caviness. 1991. Ontogeny of radial and other astroglial cells in murine cerebral cortex. Glia 4:138-148.

Mizzen, L., A. Hilton, S. Cheley, and R. Anderson. 1985. Attenuation of murine coronavirus infection by ammonium chloride. Virol. 142:378-388.

Mobley, J., G. Evans, M.O. Dailey, and S. Perlman. 1992. Immune response to a murine coronavirus: identification of a homing receptor-negative $CD4^+$ T cell subset that responds to viral glycoproteins. Virol. 187:443-452.

Morris, V.L., C. Tieszer, J. MacKinnon, and D. Percy. 1989. Characterization of coronavirus JHM variants isolated from Wistar Furth rats with a viral-induced demyelinating disease. Virology 169:127-136.

Mozell, R.L., and F.A. McMorris. 1991. Insulin-like growth factor I stimulates oligodendrocyte development and myelination in rat brain aggregate cultures. J. Neurosci. Res. 30:382-390.

Muraoka, S., and T. Takahashi. 1989. Primary dissociated cell culture of fetal rat central nervous tissue. II. Immunocytochemical and ultrastructural studies of myelinogenesis. Dev. Brain Res. 49:63-74.

Murray, R.S., B. Brown, [illegible]orian, and G.F. Cabirac. 1992a. Detection of coronavirus RNA and antigen in multiple sclerosis brain. Ann. Neurol. 31:525-533.

Murray, R.S., G.-Y. Cai, K. Hoel, J.-Y. Zhang, K.F. Soike, and G.F. Cabirac. 1992b. Coronavirus infects and causes demyelination in primate central nervous system. Virol. 188:274-284.

Nagashima, K., H. Wege, R. Meyermann, and V. Ter Meulen. 1978. Coronavirus induced subacute demyelinating encephalomyelitis in rats: a morphological analysis. Acta Neuropath. 44:63-70.

Nagayama, A., and S. Dales. 1970. Rapid purification and immunological specificity of mammalian microtubular paracrystals possessing and ATPase activity. Proc. Natl. Acad. Sci. USA 66:464-471.

Nathaniel, E.J.H., D.R. Nathaniel, L.M. Nathaniel, S. Burt, and F. Panfili. 1988. Effect of thyroxine replacement therapy on the growth patterns of body, brain, and cerebellum in the neonatal hypothyroid rat. Exp. Neurol. 101:1-16.

Noble, M., K. Murray, P. Stroobant, M.D. Waterfield, and P. Riddle. 1988): Platelet-derived growth factor promotes division and motility and inhibits premature differentiation of the oligodendrocyte/type-2 astrocyte progenitor cell. Nature (Lond.) 333:560-562.

Nunez, J. 1984. Effects of thyroid hormones during brain differentiation. Mol. Cell. Endocrinol. 37:125-132.

Paeratakul, U., P.R. De Stasio, and M.W. Taylor. 1988. A fast and sensitive method for detecting specfic viral RNA in mammalian cells. J. Virol. 62:1132-1135.

Parham, D., A. Tereba, P.J. Talbot, D.P. Jackson, and V.L. Morris. 1986. Analysis of JHMV central nervous system infections in rats. Arch. Neurol. 43:702-708.

Parker, S.E., T.M. Gallagher, and M.J. Buchmeier. 1989. Sequence analysis reveals extensive polymorphism and evidence of deletions within the E2 glycoprotein gene of several strains of murine hepatitis virus. Virol. 173:664-673.

Pasick, J.M.M., and S. Dales. 1991. Infection of coronavirus JHM of rat neurons and oligodendrocyte-type-2 astrocyte lineage cells during distinct developmental stages. J. Virol. 65:5013-5028.

Pasick, J.M.M., G.A.R. Wilson, V.L. Morris, and S. Dales. 1992. SJL/J resistance to mouse hepatitis virus-JHM-induced neurologic disease can be partially overcome by viral variants of S and host immunosuppression. Microbial Path. 13:1-15.

Patel, A.J., P.D. Lewis, R. Balazs, P. Bailey and M. Lai. 1979. Effects of thyroxine on postnatal cell acquistion in the rat brain. Brain Res. 172:57-72.

Patel, A.J., M. Hayashi, and A. Hunt. 1988. Role of thyroid hormone and nerve growth factor in the development of choline acetyltransferase and other cell-specific marker enzymes in the basal forebrain of the rat. J. Neurochem. 50:803-811.

Pelton, E.W., R.E. Grindeland, E. Young, and N.H. Bass. 1977. Effects of immunologically induced growth hormone deficiency on myelinogenesis in developing rat cerebrum. Neurol. 27:282-288.

Perlman, S., G. Jacobsen, and A. Afifi. 1989. Spread of a neurotropic murine coronavirus into the CNS via the trigeminal and olfactory nerves. Virol. 170:556-560.

Perlman, S., G. Jacobsen, and S. Moore. 1988. Regional localization of virus in the central nervous system of mice persistently infected with murine coronavirus JHM. Virol. 166:328-338.

Perlman, S., G. Jacobsen, A.L. Olson, and A. Afifi. 1990. Identification of the spinal cord as a major site of persistence during chronic infection with a murine

coronavirus. Virol. 175:418-426.

Perlman, S., and D. Ries. 1987. The astrocyte is a target cell in mice persistently infected with mouse hepatitis virus, strain JHM. Microbial Path. 3:309-314.

Perlman, S., R. Schelper, E. Bolger, and D. Ries. 1987. Late onset, symptomatic encephalomyelitis in mice infected with MHV-JHM in the presence of maternal antibody. Microbial. Path. 2:185-194.

Perry, V.H., and S. Gordon. 1988. Macrophages and microglia in the nervous system. Trends Neurosci. 11:273-277.

Pfleiderer, M., E. Routledge, G. Herrler, and S.G. Siddell. 1991. High level transient expression of the murine coronavirus haemagglutinin-esterase. J. Gen. Virol. 72:1309-1315.

Price, J., and L. Thurlow. 1988. Cell lineage in the rat cerebral cortex: a study using retroviral-mediated gene transfer. Develop. 104:473-482.

Privat, A., and C.P. Lebond. 1972. The subependymal layer and neighbouring region in the brain of the young rat. J. Comp. Neurol. 146:277-302.

Raff, M.C. 1989. Glial cell diversification in the rat optic nerve. Science 243:1450-1455.

Raff, M.C., E.R. Abney, J. Cohen, R. Lindsay, and M. Noble. 1983a. Two types of astrocytes in cultures of developing rat white matter: Differences in morphology, surface gangliosides, and growth characteristics. J. Neurosci. 3:1289-1300.

Raff, M.C., E.R. Abney, and J. Fok-Seang. 1985. Reconstitution of a developmental clock in vitro: a critical role for astrocytes in the timing of oligodendrocyte differentiation. Cell 42:61-69.

Raff, M.C., E.R. Abney, and R.H. Miller. 1984. Two glial cell lineages diverge prenatally in rat optic nerve. Devlop. Biol. 106:53-60.

Raff, M.C., L.E. Lillien, W.D. Richardson, J.F. Burne, and M.D. Noble. 1988. Platelet-derived growth factor from astrocytes drives the clock that times oligodendrocyte development in culture. Nature (Lond.) 333:562-565.

Raff, M.C., R.H. Miller, and M. Noble. 1983b. A glial progenitor cell that develops in vitro into an astrocyte or an oligodendrocyte depending on culture medium. Nature (Lond) 303:390-396.

Raible, D.W., and F.A. McMorris. 1989. Cyclic AMP regulates the rate of differentiation of oligodendrocytes without changing the lineage commitment of their progenitors. Develop. Biol. 133:437-446.

Raible, D.W., and F.A. McMorris. 1990. Induction of oligodendrocyte differentiation by activators of adenyl cyclase. J. Neurosci. Res. 27:43-46.

Rauvala, H. 1989. An 18-kd heparin-binding protein of developing brain that is distinct from fibroblast growth factors. EMBO J. 8:2933-2941.

Reddy, U.R., and D. Pleasure. 1992. Expression of platelet-derived growth factor (PDGF) and PDGF receptor genes in

the developing rat. J. Neurosci. Res. 31:670-677.

Richardson, W.D., N. Pringle, M.J. Mosley, B. Westermark, and M. Dubois-Dacq. 1988. A role for platelet derived growth factor in normal gliogenesis in the central nervous system. Cell 53:309-319.

Risau, W., and H. Wolburg. 1990. Development of the blood-brain barrier. Trends Neurosci. 13:174-178.

Riva, M.A., and I. Mocchetti. 1991. Developmental expression of the basic fibroblast growth factor gene in rat brain. Dev. Brain Res. 62:45-50.

Robb, J.A., and C.W. Bond. 1979a. Pathogenic murine coronaviruses. I. Characterization of biological behavior in vitro and virus-specific intracellular RNA of strongly neurotropic JHMV and weakly neurotropic A59V viruses. Virol. 94:352-370.

Robb, J.A., C.W. Bond, and J.L. Leibowitz. 1979b. Pathogenic murine coronaviruses. III. Biological and biochemical characterization of temperature-sensitive mutants of JHMV. Virol. 94:385-399.

Rothfels, K.H., A.A. Axelrad, L. Siminovitch, E.A. McCulloch, and R.C. Parker. 1959. The origin of altered cell lines from mouse, monkey and man as indicated by chromosome and transplantation studies. Canad. Cancer Conf. 3:189-214.

Routledge, E., R. Stauber, M. Pfleiderer, and S.G. Siddell. 1991. Analysis of murine coronavirus surface glycoprotein functions by using monoclonal antibodies. J. Virol.

65:254-262.

Ruoslahti, E., and Y. Yamaguchi. 1991. Proteoglycans as modulators of growth factor activities. Cell 64:867-869.

Ryder, E.F., E.Y. Snyder, and C.L. Cepko. 1990. Establishment and characterization of multipotent neural cell lines using retrovirus vector-mediated oncogene transfer. J. Neurobiol. 2:356-375.

Sap, J., A. Munoz, K. Damm, Y. Goldberg, J. Ghysdael, A. Leutz, H. Beug, and B. Vennstrom. 1986. The c-erb-A protein is a high-affinity receptor for thyroid hormone. Nature (Lond.) 324:635-640.

Sasahara, M., J.W.U. Fries, E.W. Raines, A.M. Gown, L.E. Westrum, M.P. Frosch, D.T. Bonthron, R. Ross, and T. Collins. 1991. PDGF B-chain in neurons of the central nervous system, posterior pituitary, and in a transgenic model. Cell 64:217-227.

Sato, Y., P.R. Murphy, R. Sato, and H.G. Friesen. 1989. Fibroblastic growth factor release by bovine endothelial cells and human astrocytoma cells in culture is density dependent. Mol. Endocrin. 3:744-748.

Sawicki, S.G., and D.L. Sawicki. 1986. Coronavirus minus-strand RNA synthesis and effect of cyclohemimide on coronavirus RNA synthesis. J. Virol. 57:328-334.

Sawicki, S.G., and D.L. Sawicki. 1990. Coronavirus transcription: subgenomic mouse hepatitis virus replicative intermediates function in RNA synthesis. J. Virol. 64:1050-1056.

Schmidt, I., M. Skinner, and S. Siddel. 1987. Nucleotide sequence of the gene encoding the surface projection glycoprotein of coronavirus MHV-JHM. J. Gen. Virol. 68:47-56.

Schochetman, G., R.H. Stevens, and R.W. Simpson. 1977. Presence of infectious polyadenylated RNA in the coronavirus avian infectious bronchitis virus. Virol. 77:772-782.

Schwender, S., H. Imprich, and R. Dorries. 1991. The pathogenic role of virus-specific antibody-secreting cells in the central nervous system of rats with different susceptibility to coronavirus-induced demyelinating encephalitis. Immunol. 74:533-538.

Sethna, P.B., M.A. Hoffman, and D.A. Brian. 1991. Minus-strand copies of replicating coronavirus mRNAs contain antileaders. J. Virol. 65:320-325.

Sethna, P.B., S.-L. Hung, and D.A. Brian. 1989. Coronavirus subgenomic minus-strand RNAs and the potential for mRNA replicons. Proc. Natl. Acad. Sci. USA 86:5626-5630.

Shevach, E.M. 1985. The effects of cyclosporin on the immune system. Ann. Rev. Immunol. 3:397-423.

Shieh, C.-K., H.-J. Lee, K. Yokomori, N. La Monica, S. Makino, and M.M.C. Lai. 1989. Identification of a new transcriptional initiation site and the corresponding functional gene 2b in the murine coronavirus RNA genome. J. Virol. 63:3729-3736.

Siddell, S. 1983. Coronavirus JHMV: coding assignments of

subgenomic mRNAs. J. Gen. Virol. 64:113-125.

Skinner, M.A., and S.G. Siddell. 1983. Coronavirus JHM: nucleotide sequence of the mRNA that encodes nucleocapsid protein. Nucleic Acids Res. 11:5045-5054.

Skoff, R.P., and P. Knapp. 1991. Division of astroblasts and oligodendroblasts in postnatal rodent brain: evidence for separate astrocyte and oligodendrocyte lineages. Glia 4:165-174.

Smith, M.S., R.E. Click, and P.G.W. Plagemann. 1984. Control of mouse hepatitis virus replication in macrophages by a recessive gene on chromosome 7. J. Immunol. 133:428-432.

Soe, L.H., C.-K. Shieh, S.C. Baker, M.-F. Chang, and M.M.C. Lai. 1987. Sequence and translation of the murine coronavirus 5'-end genomic RNA reveals the N-terminal structure of the putative RNA polymerase. J. Virol. 61:3968-3976.

Sommer, I., and M. Noble. 1986. Plasticity and commitment in oligodendrocyte development. Soc. Neurosci. Abstrs. 2:1585.

Sommer, I., and M. Schachner. 1981. Monoclonal antibodies (O1 and O4) to oligodendrocyte cell surfaces: an immunocytochemical study in the central nervous system. Develop. Biol. 83:311-327.

Sommer, I., and M. Schachner. 1982. Cells that are O4 antigen-positive and O1 antigen-negative differentiate into O1 antigen-positive oligodendrocytes. Neurosci. Lett.

29:183-188.

Sorensen, O., M.B. Coulter-Mackie, S. Puchalski, and S. Dales. 1984. In vivo and in vitro models of demyelinating disease IX. Progression of JHM virus infection in the central nervous system of the rat during overt and asymptomatic phases. Virology 137:347-357.

Sorensen, O., and S. Dales. 1985. In vivo and in vitro models of demyelinating disease: JHM virus in the rat central nervous system localized by in situ cDNA hybridization and immunofluourescent microscopy. J. Virol. 56:434-438.

Sorensen, O., R. Dugre, D. Percy, and S. Dales. 1982. In vivo and in vitro models of demyelinating disease: endogenous factors influencing demyelinating disease caused by mouse hepatitis virus in rats and mice. Infect. Immun. 37:1248-1260.

Sorensen, O., D. Percy, and S. Dales. 1980. In vivo and in vitro models of demyelinating diseases III. JHM virus infection of rats. Arch. Neurol. 37:478-484.

Sorensen, O., A. Saravani, and S. Dales. 1987. In vivo and in vitro models of demyelinating disease. XVII. The infectious process in athymic rats inoculated with JHM virus. Microbial Path. 2:79-90.

Stauber, R., M. Pfleiderer, and S.G. Siddell. Proteolytic cleavage of the murine hepatitis coronavirus JHM glycoprotein S is not required for its fusogenic activity. Adv. Exp. Med. Biol. In press.

Steinhauer, D.A., and J.J. Holland. 1987. Rapid evolution of

RNA viruses. Ann. Rev. Microbiol. 41:409-433.

Stohlman, S.A., R.S. Baric, G.Y. Nelson, L.H. Soe, L.M. Welter, and R.J. Deans. 1988a. Specific interaction between coronavirus leader RNA and nucleocapsid protein. J. Virol. 62:4288-4295.

Stohlman, S.A., and J.A. Frelinger. 1978. Resistance to fatal central nervous system disease by mouse hepatitis virus. Immunogenet. 6:277-281.

Stohlman, S.A., J.A. Frelinger, and L.P. Weiner. 1980. Resistance to fatal central nervous system disease by mouse hepatitis virus, strain JHM. J. Immunol. 124:1733-1739.

Stohlman, S.A., S. Kyuwa, M. Cohen, C. Bergmann, J.M. Polo, J. Yeh, R. Anthony, and J.G. Keck. 1992. Mouse hepatitis virus nucleocapsid protein-specific cytotoxic T lymphocytes are L^d restricted and specific for the carboxy terminus. Virol. 189:217-224.

Stohlman, S.A., G.K. Matsushima, N. Casteel, and L.P. Weiner. 1986. In vivo effects of coronavirus-specific T cell clones: DTH inducer cells prevent a lethal infection but do not inhibit virus replication. J. Immunol. 136:3052-3056.

Stohlman, S.A., M.A. Sussman, G.K. Matsushima, R.A. Shubin, and S.S. Erlich. 1988b. Delayed-type hypersensitivity response in the central nervous system during JHM virus infection requires viral specificty for protection. J. Neuroimmunol. 19:255-268.

Stohlman, S.A., and L.P. Weiner. 1981. Chronic central nervous system demyelination in mice after JHM virus infection. Neurol. 31:38-44.

Sturman, L.S., and K.V. Holmes. 1977. Characterization of a coronavirus. II. Glycoproteins of the viral envelope: tryptic peptide analysis. Virol. 77:650-660.

Sturman, L.S., K.V. Holmes, and J. Behnke. 1980. Isolation of coronavirus envelope glycoproteins and interaction with the viral nucleocapsid. J. Virol. 33:449-462.

Sturman, L.S., C.S. Ricard, and K.V. Holmes. 1985. Proteolytic cleavage of the E2 glycoprotein of murine coronavirus: activation of cell-fusing activity of virions by trypsin and separation of two different 90K cleavage fragments. J. Virol. 56:904-911.

Sturman, L.S., C.S. Ricard, and K.V. Holmes. 1990. Conformational change of the coronavirus peplomer glycoprotein at pH 8.0 and 37°C correlates with virus aggregation and virus-induced cell fusion. J. Virol. 64:3042-3050.

Sussman, M.A., R.A. Shubin, S. Kyuwa, and S.A. Stohlman. 1989. T-cell-mediated clearance of mouse hepatitis virus strain JHM from the central nervous system. J. Virol. 63:3051-3056.

Suzumura, A., E. Lavi, S. Bhat, D. Murasko, S.R. Weiss, and D.H. Silberberg. 1988. Induction of glial cell MHC antigen expression in neurotropic coronavirus infections. Characterization of the H-2-inducing soluble factor

elaborated by infected brain cells. J. Immunol. 140:2068-2072.

Suzumura, A., E. Lavi, S.R. Weiss, and D.H. Silberberg. 1986. Coronavirus infection induces H-2 antigen expression on oligodendrocytes and astrocytes. Science 232:991-993.

Taguchi, F., T. Ikeda, K. Saeki, H. Kubo, and T. Kikuchi. Fusogenic properties of uncleaved spike protein of murine coronavirus JHMV. Adv Exp. Med. Biol. In press.

Taguchi, F., P.T. Massa, and V. ter Meulen. 1986. Characterization of a variant virus isolated from neural cell culture after infection of mouse coronavirus JHMV. Virol. 155:267-270.

Taguchi, F., S.G. Siddell, H. Wege, and V. ter Meulen. 1985. Characterization of a variant virus selected in rat brains after infection by coronavirus mouse hepatitis virus JHM. J. Virol. 54:429-435.

Takase-Yoden, S., T. Kikuchi, S.G. Siddel, and F. Taguchi. 1990. Localization of major neutralizing epitopes on the S1 polypeptide of the murine coronavirus peplomer glycoprotein. Virus Res. 18:99-108.

Talbot, P.J., and M.J. Buchmeier. 1985. Antigenic variation among murine coronaviruses: evidence for polymorphism on the peplomer glycoprotein E2. Virus Res. 2:317-328.

Talbot, P.J., A.A. Salmi, R.L. Knobler, and M.J. Buchmeier. 1984. Topographical mapping of epitopes on the glycoproteins of murine hepatitis virus-4 (strain JHM): correlation with biological activities. Virol. 132:250-

260.

Tanaka, R., Y. Iwasaki, and H. Koprowski. 1976. Ultrastructural studies of pervascular cuffing cells in multiple sclerosis brain. J. Neurolog. Sci. 28:121.

Temple, S. 1989. Division and differentiation of isolated CNS blast cells in microculture. Nature (Lond.) 340:471-473.

Temple, S., and M.C. Raff. 1986. Clonal analysis of oligodendrocyte development in culture: evidence for a developmental clock that counts cell divisions. Cell 44:773-779.

Thangnipon, W., G.H. Frost, and J.E. Bottenstein. 1989. Heparin-binding growth factors in CNS neuronal cell line conditioned medium stimulate proliferation of O-2A glial progenitors. Soc. Neurosci. Abstr. 15:328.

Tooze, J., S.A. Tooze, and S.D. Fuller. 1987. Sorting of progeny coronavirus from condensed secretory proteins at the exit from the trans-Golgi network of AtT20 cells. J. Cell Biol. 105:1215-1226.

Tooze, J., S. Tooze, and G. Warren. 1984. Replication of coronavirus MHV-A59 in sac$^-$ cells: determination of the first site of budding of progeny virions. Eur. J. Cell Biol. 33:281-293.

Tooze, S.A., J. Tooze, and G. Warren. 1988. Site of addition of N-acetyl-galactosamine to the E1 glycoprotein of mouse hepatitis virus-A59. J. Cell Biol. 106:1475-1487.

Torelli, S., P. Dell'Era, M.G. Ennas, V. Sogos, F. Gremo, G. Ragnotti, and M. Presta. 1990. Basic fibroblastic growth

factor in neuronal cultures of human fetal brain. J. Neurosci. Res. 27:78-83.

Trotter, J., and M. Schachner. 1989. Cells positive for the O4 surface antigen isolated by cell sorting are able to differentiate into astrocytes or oligodendrocytes. Dev. Brain Res. 46:115-122.

Vallee, R.B., and G.S. Bloom. 1991. Mechanisms of fast and slow axonal transport. Ann. Rev. Neurosci. 14:59-92.

Van Berlo, M.F., R. Warringa, G. Wolswijk, and M. Lopes-Cardozo. 1989. Vulnerability of rat and mouse brain cells to murine hepatitis virus (JHM-strain): studies in vivo and in vitro. Glia 2:85-93.

Van Dinter, S., and W.F. Flintoff. 1987. Rat glial C6 cells are defective in murine coronavirus internalization. J. Gen. Virol. 68:1677-1685.

Vartanian, T., T.J. Sprinkle, G. Dawson, and S. Szuchet. 1988. Oligodendrocyte substratum adhesion modulates expression of adenylate cyclase-linked receptors. Proc. Natl. Acad. Sci. USA 85:939-943.

Vaysse, P.J.-J., and J.E. Goldman. 1990. A clonal analysis of glial lineages in neonatal forebrain development in vitro. Neuron 5:227-235.

Vaysse, P.J.-J., and J.E. Goldman. 1992. A distinct type of CD3+, flat astrocyte in rat CNS cultures. J. Neurosci. 12:330-337.

Vennema, H., L. Heijnen, A. Zijderveld, M.C. Horznek, and W.C. Spaan. 1990. Intracellular transport of recombinant

coronavirus spike proteins: implications of virus assembly. J. Virol. 64:339-346.

Ventimiglia, R., M.I. Greene, and H.M. Geller. 1987. Localization of B-adrenergic receptors on differentiated cells of the central nervous system in culture. Proc. Natl. Acad. Sci. USA 84:5073-5077.

Walker, P., and J.H. Dussault. 1980. Hypothalamic somatostatin and pituitary and serum growth hormone concentrations during postnatal development in rats exposed chronically to a propylthiouracil or a low iodine diet. J. Dev. Physiol. 2:111-117.

Walsh, E., Y. Ueda, H. Nakanishi, and K. Yoshida. 1992. Neuronal survival and neurite extension supported by astrocytes co-cultured in transwells. Neurosci. Lett. 138:103-106.

Walters, S.N., and P. Morell. 1981. Effects of altered thyroid states on myelinogenesis. J. Neurochem. 36:1792-1801.

Wang, F.-I., J.O. Fleming, and M.C. Lai. 1992a. Sequence analysis of the spike protein gene of murine coronavirus variants: study of genetic sites affecting neuropathogenecity. Virology 186:742-749.

Wang, F.-I., D.R. Hintin, W. Gilmore, M.D. Trousdale, and J.O. Fleming. 1992b. Sequential infection of glial cells by the murine hepatitis virus JHM strain (MHV-4) leads to a characteristic distribution of demyelination. Lab. Invest. 66:744-754.

Wang, F.-I., S.A. Stohlman, and J.O. Fleming. 1990.

Demyelination induced by murine hepatitis virus JHM strain (MHV-4) is immunologically mediated. J. Neuroimmunol. 30:31-41.

Warf, B.C., J. Fok-Seang, and R.H. Miller. 1991. Evidence for the ventral origin of oligodendrocyte precursors in the rat spinal cord. J. Neurosci. 11:2477-2488.

Watanabe, R., H. Wege, and V. ter Meulen. 1983. Adoptive transfer of EAE-like lesions from rats with coronavirus-induced demyelinating encephalomyelitis. Nature (Lond.) 305:150-153.

Weclewicz, K., K. Kristensson, and C. Orvell. 1990. Segregation of viral structural proteins in cultured neurons of rat spinal ganglia and cord. Neuropath. Appl. Neurobiol. 16:357-364.

Wege, H., R. Watanabe, and V ter Meulen. 1984. Relapsing subacute demyelinating encephalomyelitis in rats during the course of coronavirus JHM infection. J. Neuroimmunol. 6:325-336.

Wege, H., J. Winter, H. Korner, E. Flory, F. Zimprich, and H. Lassmann. 1990. Coronavirus induced demyelinating encephalomyelitis in rats: immunopathological aspects of viral persistence. Adv. Exp. Med. Biol. 276:637-645.

Wege, H., J. Winter, and R. Meyermann. 1988. The peplomer protein E2 of coronavirus JHM as a determinant of neurovirulence: definition of critical epitopes by variant analysis. J. Gen. Virol. 69:87-98.

Weinberger, C., C.C. Thompson, E.S. Ong, R. Lebo, D.J. Gruol,

and R.M. Evans. 1986. The c-erb-A gene encodes a thyroid hormone receptor. Nature (Lond.) 324:641-646.

Weiner, L.P. 1973. Pathogenesis of demyelination induced by a mouse hepatitis virus. Arch. Neurol. 28:298-303.

Weismiller, D.G., L.S. Sturman, M.J. Buchmeier, J.O. Fleming, and K.V. Holmes. 1990. Monoclonal antibodies to the peplomer glycoprotein of coronavirus mouse hepatitis virus identify two subunits and detect a conformational change in the subunit released under mild alkaline conditions. J. Virol. 64:3051-3055.

Wilkin, G.P., D.R. Marriott, and A.J. Cholewinski. 1990. Astrocyte heterogeneity. Trends Neurosci. 13:43-46.

Williams, R.K., G.-S. Jiang, S.W. Snyder, M.F. Frana, and K.V. Holmes. 1990. Purification of the 110-kilodalton glycoprotein receptor for mouse hepatitis virus (MHV)-A59 from mouse liver and identification of a nonfunctional, homologous protein in MHV-resistant SJL/J mice. J. Virol. 64:3817-3823.

Williams, R.K., G.-S. Jiang, and K.V. Holmes KV. 1991. Receptor for mouse hepatitis virus is a member of the carcinoembryonic antigen family of glycoproteins. Proc. Natl. Acad. Sci. USA 88:5533-5536.

Williams, B.P., J. Read, and J. Price. 1991. The generation of neurons and oligodendrocytes from a common precursor cell. Neuron. 7:685-693.

Williamson, J.S.P., and S.A. Stohlman. 1990. Effective clearance of mouse hepatitis virus from the central

nervous system requires both $CD4^+$ and $CD8^+$ T cells. J. Virol. 64:4589-4592.

Williamson, J.S.P., K.C. Sykes, and S.A. Stohlman. 1991. Characterization of brain-infiltrating mononuclear cells during infection with mouse hepatitis virus strain JHM. J. Neuroimmunol. 32:199-207.

Wilson, G.A.R., S. Beushausen, and S. Dales. 1986. In vivo and in vitro models of demyelinating diseases XV. Differentiation influences the regulation of coronavirus infection in primary explants of mouse CNS. Virology 151:253-264.

Wilson, G.A.R., and S. Dales. 1988. In vivo and in vitro models of demyelinating disease: effeciency of virus spread and formation of infectious centers among glial cells is genetically determined by the murine host. J. Virol. 62:3371-3377.

Woodward, W.R., R. Nishi, C.K. Meshul, T.E. Williams, M. Coulombe, and F.P. Eckenstein. 1992. Nuclear and cytoplasmic localization of basic fibroblast growth factor in astrocytes and CA2 hippocampal neurons. J. Neurosci. 12:142-152.

Wren, D.R., and M. Noble. 1989. Oligodendrocytes and oligodendrocyte/type-2 astrocyte progenitor cells of adult rats are specifically susceptible to the lytic effects of complement in absence of antibody. Proc. Natl. Acad. Sci. USA 86:9025-9029.

Yamaguchi, K., N. Goto, S. Kyuwa, M. Hayami, and Y. Toyoda.

1991. Protection of mice from a lethal coronavirus infection in the central nervous system by adoptive transfer of virus-specific T cell clones. J. Neuroimmunol. 32:1-9.

Yayon, A., M. Klagsbrun, J.D. Esko, P. Leder, and D.M. Ornitz. 1991. Cell surface, heparin-like molecules are required for binding of basic fibroblastic growth factor to its high affinity receptor. Cell 64:841-848.

Yeh, H.J., K.G. Ruit, Y.X. Wang, W.C. Parks, W.D. Snider, and T.F. Deuel. 1991. PDGF A-chain gene is expressed by mammalian neurons during development and in maturity. Cell 64:209-216.

Yokomori, K., S.C. Baker, S.A. Stohlman, and M.M.C. Lai. 1992. Hemagglutinin-esterase-specific monoclonal antibodies alter the neuropathogenicity of mouse hepatitis virus. J. Virol. 66:2865-2874.

Yokomori, K., L.R. Banner, and M.C. Lai. 1991. Heterogeneity of gene expression of the hemagglutinin-esterase (HE) protein of murine coronaviruses. Virol. 183:647-657.

Yokomori, K., N. La Monica, S. Makino, C.-K. Shieh, and M.M.C. Lai. 1989. Biosynthesis, structure, and biological activities of envelope protein gp65 of murine coronavirus. Virol. 173:683-691.

Yokomori, K., and M.M.C. Lai. 1992. Mouse hepatitis virus utilizes two carcinoembryonic antigens as alternative receptors. J. Virol. 66:6194-6199.

Yoshida, K., and F.H. Gage. 1991. Fibroblast growth factors

stimulate nerve growth factor synthesis and secretion by astrocytes. Brain Res. 538:118-126.

Yusta, B., F. Besnard, J. Ortiz-Carlo, A. Pascual, A. Aranda, and L. Sarlieve. 1988. Evidence for the presence of nuclear 3,5,3'-triiodothyronine receptors in secondary cultures of pure rat oligodendrocytes. Endocrin. 122:2278-2284.

Zimmer, M.J., and S. Dales. 1989. In vivo and in vitro models of demyelinating diseases XXIV. The infectious process in cyclosporin A treated Wistar Lewis rats inoculated with JHM virus. Microbial Path. 6:7-16.

Zimprich, E., J. Winter, H. Wege, and H. Lassmann. 1991. Coronavirus induced primary demyelination: indications for the involvement of a humoral immune response. Neuropath. Appl. Neurobiol. 17:469-484.